MARINE ZOOPLANKTON COMMUNITY RESPONSES TO ANTHROPOGENIC INFLUENCES

Dissertation

zur Erlangung des Doktorgrades

- Dr. rer. nat. -

der Mathematisch-Naturwissenschaftlichen Fakultät

der Christian-Albrechts-Universität zu Kiel

Vorgelegt von

Carsten Spisla

Kiel, Dezember 2021

GEOMAR
Helmholtz-Zentrum für Ozeanforschung Kiel

C|A|U
Christian-Albrechts-Universität zu Kiel

1. Gutachter:	Prof. Dr. Ulf Riebesell
2. Gutachter:	Prof. Dr. Maarten Boersma
Tag der Disputation:	28.03.2022
Zum Druck genehmigt:	28.03.2022

CONTENTS

SUMMARY

Continued anthropogenic carbon dioxide (CO_2) emissions lead to a persistent intensification of current levels of ocean acidification (OA) and have already had measurable impacts on life in the world's oceans.

Even if greenhouse gas emissions, including those of CO_2, immediately ceased, a deliberate anthropogenic removal of CO_2 from the atmosphere via so-called 'negative emission technologies' (NETs) is inevitable in order to reach the 2015 Paris Agreement goal of maximum 2°C global warming. Little is known, however, about possible side-effects of particularly ocean based NETs and potential interdependencies with ongoing climate change, which could affect plankton communities, marine ecosystems, and ecosystem services like fisheries.

In the present thesis, the response of pelagic ecosystems was investigated under the influence of the environmental stressor OA and one of the ocean-based NETs that is under consideration, artificial upwelling. In this NET nutrient rich deep-water is admixed into nutrient depleted surface waters in order to enhance productivity and sequester carbon via the biological carbon pump. My work focused on the responses of plankton community composition, trophic level interactions, and productivity of the impacted zooplankton community. All of which are regulating factors that are important for the overall production of organic matter in an ecosystem.

In a first step to assess these factors, I evaluated in a large scale mesocosm experiment, how the overall function and structure of a natural plankton community is affected by extreme OA conditions. The experiment revealed pronounced positive and negative treatment effects on the species composition, abundance and biomass of various species within the plankton community in the mesocosms, emerging shortly after the CO_2 manipulation. These OA effects were visible in all trophic levels of the planktonic food web as well as the elemental stoichiometry of organic matter. The results imply that a variety of indirect and direct OA effects led to an increase in secondary consumer biomass and enhanced top-down control in the food web, yet with unknown consequences for the productivity of the ecosystem.

Intrigued by the clear effects of OA on higher trophic levels (fish larvae and hydrozoans) in the aforementioned mesocosm study, a more detailed analysis was carried out in a separate study. Here, I focused on the drivers and implications of the observed changes on the top predators in the enclosed plankton community. The findings of this study indicate that an observed decrease in Hydrozoa predation pressure and higher fish larvae survival at the top of the food chain were indirectly mediated by OA affecting lower trophic levels (phyto-,

micro-, mesoplankton) as well as the predator - prey relationship between fish larvae and hydrozoans. The immediate consequences these indirect OA effects had on the top predators could entail extensive alterations also for ecosystem services.

In a final step, I assessed the possible application of artificial upwelling for enhancing productivity and the efficiency of carbon transfer in an oligotrophic plankton community. A large scale mesocosm experiment simulating different upwelling modes and intensities was conducted. The results revealed an increase in primary and secondary production as well as the carbon transfer efficiency in the food web. The corresponding effect size of this increase was closely linked to temporal frequency and intensity of upwelling as well as the species and size composition of the zooplankton/ copepod community and its access to food in different qualities.

Altogether, this dissertation revealed two distinct findings on the stressor and application of potential NET of artificial upwelling. Firstly, intensifying OA under a business-as-usual scenario could lead not only to a pronounced restructuring of zooplankton populations, but also entire plankton communities, including substantial changes in the predator-prey coupling of higher trophic levels, e.g. Hydrozoa and fish larvae. On the other hand, the application of artificial upwelling caused distinct changes in the productivity of the affected zooplankton community, which, under certain circumstances, supports the potential of this technique to create efficient food webs with considerable biomass output. In conclusion, these findings make clear that more focus has to be put on ocean-based climate change solutions like artificial upwelling in order to counteract direct effects of future environmental stressors to plankton communities.

ZUSAMMENFASSUNG

Die steigenden anthropogenen Emissionen des Treibhausgases Kohlenstoffdioxid (CO_2) führen zu einem steten Vorantreiben der Ozeanversauerung und haben damit das Leben in den Weltmeeren bereits messbar beeinträchtigt. Nichtsdestotrotz wurde 2015 im Pariser Klimaabkommen das Ziel einer maximalen globalen Erwärmung um 2°C formuliert, welches selbst in Anbetracht des Szenarios eines sofortigen Herunterfahrens aller Treibhausgasemissionen nicht einzuhalten wäre. Um dieses Ziel dennoch erreichen zu können, sind sogenannte „Negative Emissions-Technologien“ (NET) unabdingbar. Welche Auswirkungen gerade NET, die im Ozean angewandt werden sollen, auf marine Planktongemeinschaften, Ökosysteme und Ökosystemdienstleistungen wie Fischerei haben, und welche Wechselwirkungen es mit bereits bestehenden Auswirkungen des Klimawandels geben könnte, ist dabei bisher nicht oder nur wenig erforscht.

Daher soll die hier vorliegende Dissertation die Auswirkungen auf pelagische Ökosysteme von 1.) Ozeanversauerung als prominenten Stressfaktor für den Ozean und 2.) künstlichem Auftrieb als möglicher Lösungsansatz für die Folgen des Klimawandels untersuchen. Bei künstlichem Auftrieb handelt es sich dabei um eine NET, die nährstoffreiches Tiefenwasser in nährstoffarmes Oberflächenwasser einmischt und somit die Produktivität des Ökosystems und dessen Fähigkeit erhöht, Kohlenstoff über die biologische Kohlenstoffpumpe aufzunehmen und zu sequestrieren.

Im Fokus meiner Arbeit lagen hier insbesondere die Auswirkungen von Ozeanversauerung auf Zooplanktongemeinschaften und Beziehungen zwischen den trophischen Ebenen einer Planktongesellschaft, sowie der Effekt des künstlichen Auftriebs auf die Produktivität der untersuchten Zooplanktongemeinschaften.

Dazu habe ich zunächst innerhalb eines großskaligen Mesokosmen-Experimentes untersucht, wie sich die Simulation einer extremen Ozeanversauerung auf die generelle Struktur und Funktionalität einer natürlichen Planktongemeinschaft auswirkt. Dabei haben sich im Experiment bereits kurz nach der CO_2 Manipulation des Systems negative und positive Effekte der Versauerung auf Artenzusammensetzung, sowie Abundanzen und Biomasse verschiedener Arten der Planktongemeinschaft herauskristallisiert. Diese Effekte traten auf allen trophischen Ebenen des planktonischen Nahrungsnetzes auf, sowie in der elementaren Stöchiometrie der partikulären, in der Wassersäule vorhandenen, organischen Materialen. Diese Ergebnisse implizieren, dass verschiedene indirekte und direkte Ozeanversauerungseffekte zu einer Zunahme der Biomasse von sekundären Konsumenten,

sowie der Top-Down Kontrolle im Ökosystem geführt haben; mit noch unklaren Folgen für die Produktivität des Systems.

Aufgrund der deutlichen Effekte, die Ozeanversauerung in diesem Experiment auf die höheren trophischen Ebenen des Nahrungsnetzes hatte (Fischlarven und Hydrozoen), wurde in einer anschließenden Studie genauer untersucht, welche Ursachen und Folgen diese Effekte für die eingeschlossene Planktongemeinschaft haben könnten. Dabei deuten die gewonnenen Erkenntnisse daraufhin, dass es direkte Effekte der Versauerung sowohl auf die unteren trophischen Ebenen des Nahrungsnetzes (Phyto-, Mikro-, Mesoplankton), als auch auf die Räuber-Beute-Beziehung zwischen Fischlarven und Hydrozoen gab. Diese waren maßgeblich für die Abnahme des Fraßdruckes der Hydrozen und eine gesteigerte Überlebensrate der Fischlarven an der Spitze der Nahrungskette verantwortlich. Dass diese indirekten Versauerungseffekte solch unmittelbare Konsequenzen für die Top-Prädatoren in dem untersuchten Ökosystem hatten, lässt zudem den Schluss zu, dass sich hieraus auch weitreichende Veränderungen für Ökosystemdienstleistungen wie Fischerei ergeben könnten.

Die Auswirkungen und die potentielle Anwendbarkeit von künstlichem Auftrieb als Mittel zur Steigerung der Produktivität und Kohlenstoff-Transport-Effizienz einer oligotrophen Planktongesellschaft in den Ozeanen wurde in einer abschließenden Studie bewertet. Dazu wurden in einem großskaligen Mesokosmen-Experiment verschiedenen Auftriebsmodi und -intensitäten von künstlichem Auftrieb simuliert und deren Auswirkungen auf die betroffenen Planktongemeinschaften untersucht. Dabei ließ sich ein deutlicher Anstieg sowohl von Primär- und Sekundärproduktion, als auch der Effizienz, mit der Kohlenstoff im Nahrungsnetz transportiert wird, feststellen. Wie stark der Anstieg in diesen Parametern ausfiel, stand hierbei eng im Zusammenhang mit der jeweiligen Frequenz und Intensität des künstlichen Auftriebs, der Artenzusammensetzung und Größenklassenverteilung in der vorhandenen Zooplankton-/ Ruderfußkrebsgemeinschaft, sowie Unterschieden in der Qualität des für diese zugänglichen Nahrungsangebotes.

Damit lassen sich zusammenfassend zwei klare Ergebnisse aus dieser Dissertation ableiten: Einerseits zeigte sich, dass im Rahmen des Kontinuitätsszenarios (‚business-as-usual') die zunehmende Ozeanversauerung durchaus das Potential hat, nicht nur das Zooplankton, sondern eine gesamte Planktongemeinschaft umfassend umzustrukturieren, inklusive wesentlicher Veränderungen in der Räuber-Beute-Beziehung zwischen höheren trophischen Ebenen wie Hydrozoen und Fischlarven. Andererseits haben deutliche Veränderungen in der Produktivität der Zooplanktongemeinschaft in unserer Simulation von künstlichem

Auftrieb gezeigt, dass die Anwendung dieser Technik unter bestimmten Voraussetzungen durchaus das Potential besitzt, effektive, ertragreiche Nahrungsnetze zu erschaffen. Daraus wird klar, dass mehr Fokus auf ozeanbasierende Lösungen des Klimawandels wie den künstlichen Auftrieb gelegt werden muss, um den zukünftigen direkten Effekten von Ökosystemstressoren auf Planktongemeinschaften zu begegnen.

I. GENERAL INTRODUCTION

1. Global climate change

The atmospheric concentrations of greenhouse gases have reached values "that are unprecedented in at least the last 800,000 years" (IPCC, 2021), thus causing a multitude of anomalies throughout the earth's climate system, summarized under the term "climate change". Out of the different greenhouse gases, carbon dioxide is considered to be the main driver of climate change, as it makes up for about two-thirds of all the emitted greenhouse gases (Ritchie & Roser, 2020). Nearly all of this anthropogenically emitted CO_2 is produced via fossil fuel combustions (81%) and land use change (19%, see Friedlingstein *et al.* (2020)). In numbers, these emissions correspond to a total of 1650 gigatons of carbon dioxide (Gt CO_2) that have been emitted by the year 2019, with 1420 Gt CO_2 (≈ 86%) in the past 70 years alone, compared to 230 Gt CO_2, which were emitted in the first 200 years of industrial revolution until 1950 (Ritchie and Roser (2020), see **Fig. 1A**). Consequently, the global mean atmospheric CO_2 concentration constantly increased from preindustrial values of around 280 ppm to currently 412 ppm in September 2021 (see **Fig. 1B**), and according to the intergovernmental panel on climate change (IPCC) are predicted to further increase in the future (IPCC, 2021).

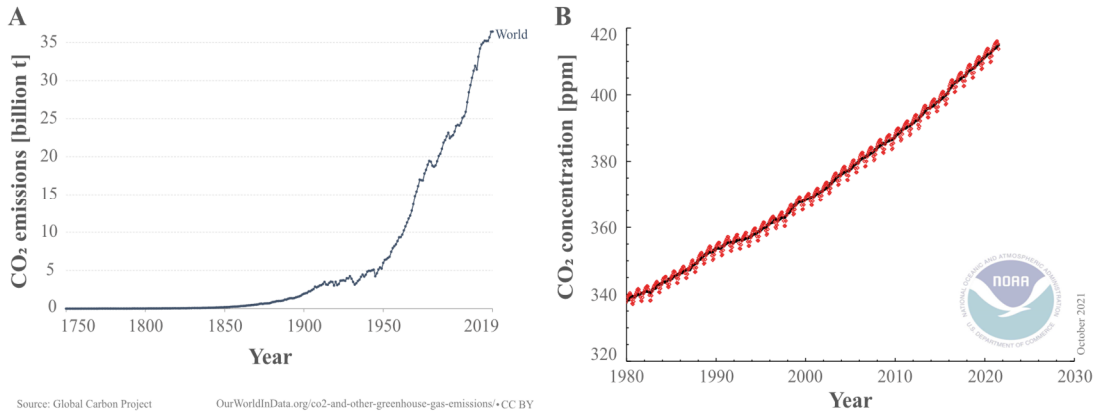

Figure 1: (A) Global annual CO_2 emissions from fossil fuel combustion in billion tons (t) of CO_2. Land use change not included. Obtained and modified after source and link given in the figure. Accessed on 23rd October 2021 **(B)** Global monthly mean atmospheric carbon dioxide (CO_2) averaged over marine surface sites from 1980 to 2021. The data is expressed as the number of molecules carbon dioxide divided by the entirety of molecules in air (including CO_2) in parts per million (ppm). The dashed red line as well as the black line represent monthly mean values, however values on the black line are corrected for the average seasonal cycle. Obtained and modified after Ed Dlugokencky and Pieter Tans, NOAA/GML (gml.noaa.gov/ccgg/trends/), accessed on 23rd October 2021. See website for further information on calculation and correction of the mean values.

The IPCC assesses future climate change scenarios based on five "Shared Socio-economic Pathways" (SSPs) of ongoing anthropogenic greenhouse gas emissions and their consequences for the earth's climate system (IPCC, 2021). Overall, they differentiate between five scenarios of further increasing emissions. Under SSP5-8.5 and SSP3-7.0, a doubling of annual CO_2 emissions by the year 2050 and 2100 is estimated, respectively. Under SSP2-4.5 emissions are projected to be similar to current levels until 2050 and decrease thereafter, and under SSP1-2.6 and SSP1-1.9 "net-negative" annual emissions are expected, characterized by anthropogenic removal of atmospheric CO_2 exceeding the emissions. In general, projections of annual CO_2 emissions by the year 2100 range from over 120 Gt CO_2 y^{-1} (SSP5-8.5) to a net negative value of about 10 Gt CO_2 y^{-1} (SSP1-1.9, IPCC (2021)) in these scenarios. Irrespective of the projected emission scenarios, atmospheric CO_2 concentrations will further increase to at least 500 ppm even under net negative conditions, or exceed the value of 1300 ppm approximated under SSP5-8.5 by the year 2100 (IPCC, 2021).

The accumulation of CO_2 in the atmosphere would be even more pronounced without the earth's ability to transform and bind large parts of the anthropogenically emitted CO_2 into biomass on land and in the world's oceans (Friedlingstein *et al.*, 2001). Despite being an indispensable component against climate change, this sequestration of CO_2 also entails certain negative consequences, which are especially eminent for the world's oceans. The oceans absorb extensive amounts of carbon dioxide via gas exchange with the atmosphere, thereby acting as a carbon sink. In doing so, they have taken up approximately 30% of all anthropogenic CO_2 emission between 1800 and 2007 (Gruber *et al.*, 2019). Over the past decade (2010-2019), the amount of anthropogenic CO_2 taken up by the ocean has almost doubled (Friedlingstein *et al.*, 2020). This substantial uptake results in a continuously enhanced dissolution of CO_2 in seawater, and subsequently an increased formation of carbonic acid, which leads to a decrease of the average seawater pH. This process is generally referred to as ocean acidification (OA) (Caldeira & Wickett, 2003; Emerson & Hedges, 2008).

2. Ocean acidification and its consequences for marine life

OA describes the formation of carbonic acid (H_2CO_3) from the reaction of atmospheric carbon dioxide (CO_2) and water (H_2O), and its dissociation into hydrogen and bicarbonate ions (Eq. 1).

$$[CO_2]+[H_2O]\Leftrightarrow[H_2CO_3]\Leftrightarrow[HCO_3^-]+[H^+] \quad \text{(Eq. 1)}$$

Naturally, CO_2 dissolved in seawater is present as aqueous CO_2 (including H_2CO_3; ~ 1%), as CO_3^{2-} (~ 8%), and to a much larger extent as HCO_3^- (~ 91%, Raven *et al.* (2005), see **Fig. 2**). When additional H^+ from enhanced dissolution of atmospheric CO_2 is formed through dissociation of H_2CO_3, the natural buffer capacity of the seawater carbonate system binds the hydrogen ions to a certain extent by forming HCO_3^- as seen in Eq. 2. This buffering capacity, however, is limited, and the concentration of H^+ and H_2CO_3 increases substantially with increasing amounts of CO_2 diffusing in the oceans, thereby lowering seawater pH (Emerson & Hedges, 2008).

$$[H^+]+[CO_3^{2-}]\Leftrightarrow[HCO_3] \quad \text{(Eq. 2)}$$

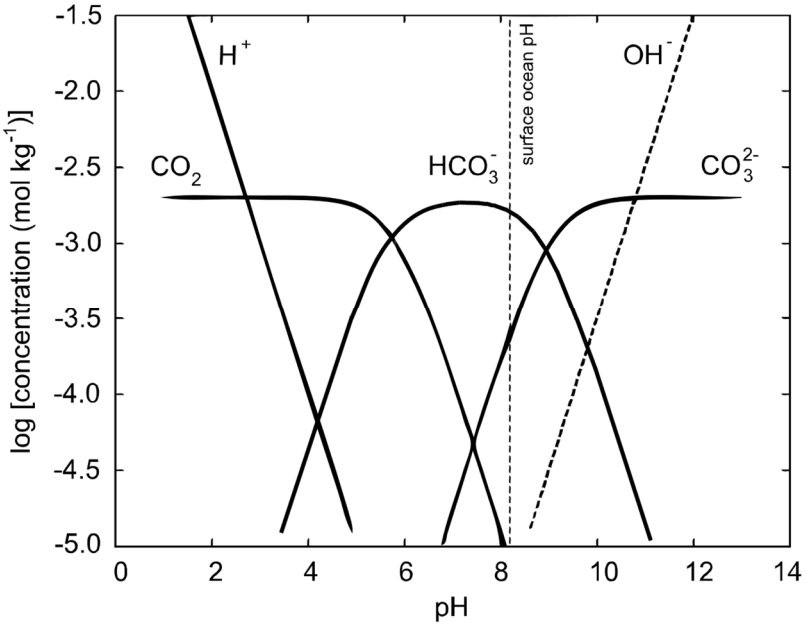

Figure 2: Bjerrum plot of the logarithmic concentration of the dissolved carbonate types as well as hydrogen and hydroxide ions in seawater as a function of pH. Dashed vertical line depicts the global average sea surface pH at the time of the publication (2015). Obtained from Roberts (2015).

Thus, OA already led to a decrease in global mean seawater surface pH of between 0.017 - 0.027 units per decade since the 1980s, and is projected to cause a further decline ranging between 0.036 - 0.042 (SSP1-1.9) and 0.287 - 0.291 (SSP5-8.5) pH units by the end of the 21st century. Ultimately, this would result in lowering the mean seawater surface pH from present-day values of about 8.05 down to 8.0 or below 7.7, for SSP1-2.6 and SSP5-8.5, respectively (IPCC, 2021). Besides the purely chemical alterations of the system in terms of pH and carbonate chemistry of seawater, also the organisms inhabiting the world's oceans

are already and will be even further affected by the present and future OA conditions (Bindoff *et al.*, 2019).

Consequences of ocean acidification for marine biota

To date, the effects of OA are visible in a broad variety of organisms ranging from photoautotrophic primary producers (phytoplankton) to a variety of heterotrophic consumers (zooplankton) (Kroeker *et al.*, 2013). Within this range, it is apparent that the most pronounced effects of OA are displayed in smaller sized individuals of both, phyto- and zooplankton, e.g. in the size range of small calcifying algae like coccolithophorids up to small crustaceans like copepods or ichthyoplankton, i.e. eggs and larvae of fish (Pörtner *et al.*, 2005).

Some of the most severe consequences of OA are caused by the decrease in carbonate ion concentrations, leading to a substantial inhibition of biogenic calcification, i.e. the formation of calcium carbonate ($CaCO_3$) from carbonate and calcium (Ca^{2+}). Moreover, lower pH leads to enhanced dissolution of existing $CaCO_3$ (see Eq. 2). Especially in its most widespread forms of calcite and aragonite, calcium carbonate is an important structural material for calcareous, shell-forming phytoplankton taxa such as coccolithophorids, as well as for a multitude of zooplankton species, e.g. gastropods, mollusks or corals. Consequently, the predicted $CaCO_3$ undersaturation of seawater or a shift to corrosive conditions induced by OA is expected to have extensive effects on such 'calcifiers': Under present day pH and under pH values predicted for the year 2100, several species belonging to corals, coccolithophores, echinoderms, gastropods and mollusks were found to be significantly inhibited in their ability to build up their calcareous shell as well as in their growth, abundance and survival (Kroeker *et al.*, 2010; Lischka *et al.*, 2011).

Besides these prominent effects of OA on calcifying organisms, changes in seawater carbonate chemistry can also affect various other zooplankton taxa that do not depend on calcite or aragonite as structural material. The decrease in seawater pH can also lead to lower pH in the tissues and body fluids of marine organisms, a process termed acidosis, which can propagate into two major metabolic disruptions: Firstly, the affected organism will try to restore its pH *status quo* via acid-base regulation performed by high energy consuming ion pumps. This forces the animal to increase its metabolic rate, i.e. energy input, resulting in an essential demand for sufficient food availability (Wittmann & Pörtner, 2013). Secondly, if the pH regulation mechanism fails, the decrease of pH in body fluids might

lead to a decreased oxygen transport by pH sensitive pigments. The subsequent lower oxygen transport efficiency causes a hypercapnia that could result in metabolic depression and inefficient oxygen supply to body tissues if not compensated by an increase in metabolic rate, i.e. energy intake (Pörtner *et al.*, 2005; McNeil & Sasse, 2016). In accordance with that, Pörtner *et al.* (2005) found a general trend of lower survival and growth of affected organisms under OA and in combination with natural food densities, while substantial changes in respiration and ingestion rates were shown by Cripps *et al.* (2016) and Thor and Oliva (2015) for copepods with enhanced food availability. Additionally, it was shown that the hypercapnia related decrease in oxygen transport efficiency in vertebrates such as fish larvae, can significantly lower survival by damaging body tissue (Frommel *et al.*, 2012) or inducing cardiac failure (McNeil & Sasse, 2016).

These direct OA effects on individual species, however, can cause a variety of indirect OA induced changes among species directly connected to the initially affected organism, e.g. as competitors or predators. These indirect effects, in turn, can propagate further throughout the food web of an ecosystem, ultimately leading to a potential restructuring of large parts of the prevailing planktonic community (see **Fig. 3** and e.g. Taucher *et al.* (2017), Sunday *et al.* (2017)). More specifically, a decrease in abundance of a direct negatively influenced phytoplankton species at the bottom of the food web could hamper the population of zooplankton organisms grazing on it, such as copepods. A decrease in copepod numbers in turn, would reduce the food availability for higher trophic levels like fish larvae, thus further reinforcing their OA related metabolic stress. Besides, a negatively influenced phytoplankton species could also open up its ecological niche for a competitor that possibly constitutes a more nutritional food source for the adherent zooplankton species, ultimately leading to an increase in abundance or biomass of higher trophic levels. Such indirect OA effects are, however, not only triggered by direct effects at the bottom of the food web, but can also be caused at higher trophic levels via increasing or decreasing predatory pressure on the subordinate links of the food chain.

In addition to the food web alterations caused by such top-down induced OA effects, direct OA effects on higher trophic levels get particularly eminent when affecting the early life stages, and thus the recruitment, of economically important fish species such as Atlantic cod (*Gadus morhua*, Stiasny *et al.* (2016)), Senegalese sole (*Solea senegalensis*, Pimentel *et al.* (2014)), or Yellowfin tuna (*Thunnus albacares*, Frommel *et al.* (2016)). Because such effects on fish recruitment could intensify under future increasing OA scenarios, the

consequences for important fishing grounds might be severe (see e.g. Hänsel *et al.* (2020)). Not only could OA directly and substantially lower productivity in high fishery yielding regions, but with the decreased competitiveness of the fish, due to the direct metabolic disruptions, competitors and/ or predators such as jellyfish could be capable of suppressing fish as top predators and impede their recovery even further (Daskalov & Mamedov, 2007).

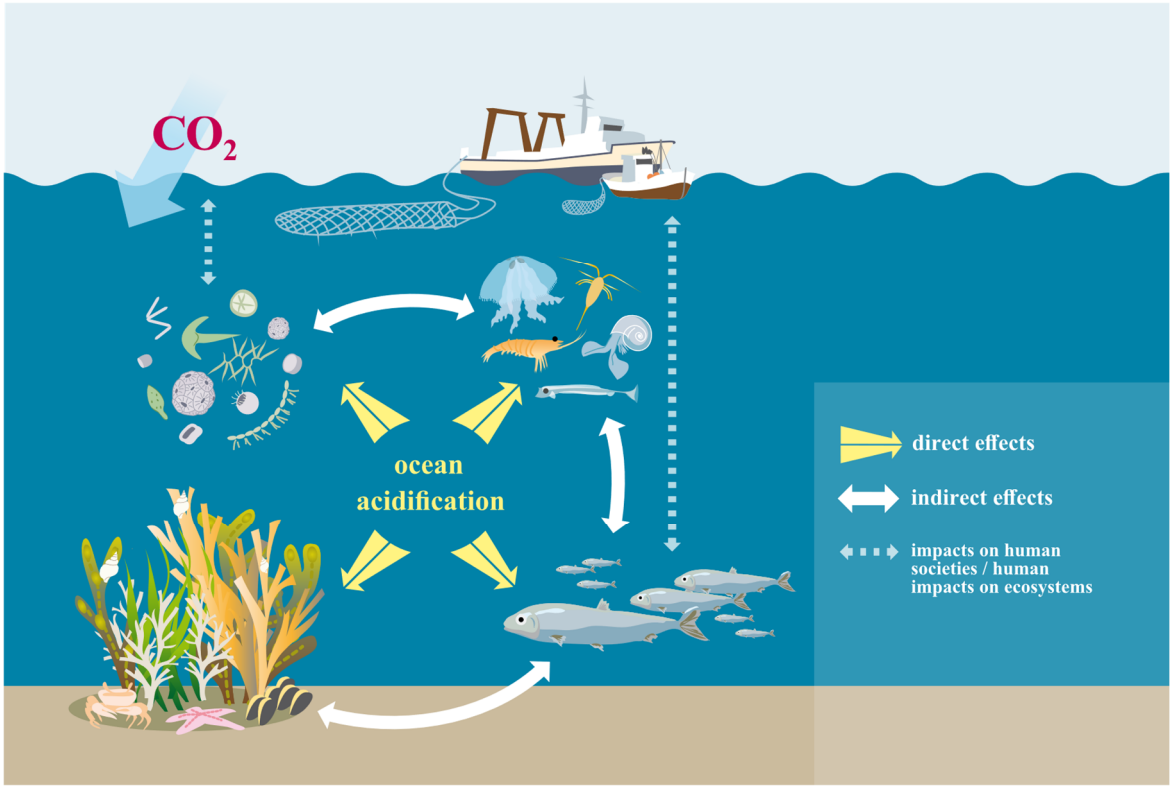

Figure 3: Ecosystem perspective on the interplay of direct and indirect ocean acidification (OA) effects caused by CO_2 dissolution in seawater. Depicted are direct OA effects (yellow arrows) on plankton organisms living on the seafloor (benthic zone, lower left), phytoplankton (upper left) and small zooplankton (upper right) in the water column, and fish stocks (lower right). White arrows symbolize the reciprocal indirect OA effects between all these organisms, triggered by the direct OA effects. Reworked original artwork of Rita Erven, © GEOMAR Helmholtz Centre for Ocean Research Kiel

Overall, the entirety of these complex interactions shows that not only the direct effects of OA need to be assessed (e.g. in single species laboratory experiments), but that the interaction of both, direct and indirect OA effects is decisively forming the overall response of an ecosystem to a stressor such as OA. Nevertheless, testing and evaluating whole ecosystem responses over different trophic levels is still an underrepresented section in the field of OA, due to the large logistical effort and complexity necessary for experiments targeting whole ecosystems. Consequently, the research conducted in this direction so far, is rather performed under laboratory than under open ocean conditions (e.g. Berge *et al.* (2010); Nielsen *et al.* (2010); Rossoll *et al.* (2013)) or solely focuses on the basis or key

species of the food web (Calbet *et al.*, 2014; Thomson *et al.*, 2016; Bach *et al.*, 2017). In addition to that, research on the responses of a variety of trophic levels in a complex zooplankton community are especially scarce for OA levels in the range of the SSP5-8.5 predictions or those that are predicted beyond the Year 2100, even though some oceanic regions already experience values in such a range or will experience those in the near-future (Fassbender *et al.*, 2011; McNeil & Sasse, 2016; Bindoff *et al.*, 2019).

3. Ocean based carbon dioxide removal

In order to minimize the consequences of future climate change and its effects on marine life, and to reach the Paris agreement goals of keeping global warming well below 2°C, it is becoming obvious that it is not sufficient to reduce anthropogenic CO_2 emissions alone, but that actively removing CO_2 from the Earth's atmosphere is obligatory (Rogelj *et al.*, 2016; GESAMP, 2019; IPCC, 2021). Techniques focusing on these negative emission technologies (NETs) include both land- and ocean-based solutions. Land-based negative emission techniques such as reforestation and bioenergy combined with point source carbon capture and geological storage have often been discussed and assessed in the last years (IPCC, 2014). Within these assessments, however, it became apparent that their feasibility and potential is limited. If carried out in a sufficiently large scale to effectively remove atmospheric CO_2, these technologies would interfere with human activities, mainly as competition for land (Smith *et al.*, 2019). The ocean on the other side covers the majority of the Earth's surface area and hence comprises large areas available for possible implementation of NETs, not interfering with human activities (GESAMP, 2019). Such ocean NETs are in general dealing with chemical, physical or biological solutions that could lead to an enhanced uptake and storage of atmospheric CO_2 in the oceans. They cover a wide-range of approaches, but can be categorized into ocean fertilization, carbon storage in the ocean, ocean pumping, enhancing ocean alkalinity, methane capture and degradation, increasing ocean albedo/ reflectivity, and others such as ocean thermal energy conversion (OTEC) or deep-water source cooling (GESAMP (2019), see **Fig. 4**).

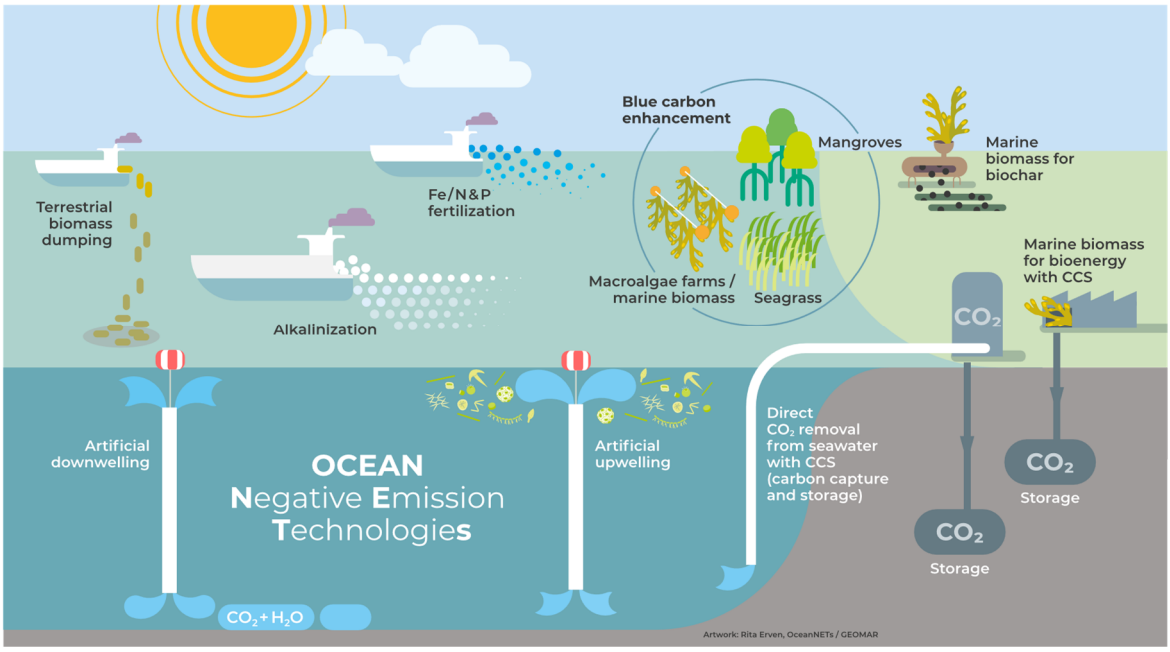

Figure 4: Overview over various ocean negative emission technologies and closely related land-based approaches, as presented by the project OceanNETs (for details see: https://www.oceannets.eu/). Original artwork by Rita Erven, © GEOMAR Helmholtz Centre for Ocean Research Kiel

Particularly interesting among these approaches, especially in light of the formerly mentioned consequences of OA to marine ecosystems, is a concept termed "artificial upwelling" within the "ocean pumping" NETs. This approach involves the artificial injection of water from deeper ocean layers to the surface (Lovelock & Rapley, 2007), thereby stimulating primary production and enhancing oceanic uptake of CO_2 via the formation and subsequent export of new biomass in an oligotrophic system, i.e. increasing the oceanic biological carbon pump (Kirke, 2003). Controversially discussed is the potential scale of this carbon sequestration (e.g. Oschlies *et al.* (2010)). Despite nutrients, upwelled deep-water will also bring up additional dissolved CO_2 to surface waters, and besides autotrophic organisms fixing CO_2 to create biomass, heterotrophic organisms produce CO_2 via respiration. Although this might limit the sequestration potential of artificial upwelling, all these factors are also still highly depending on location, technical implementation, flow rate or ultimately the local community composition of the area in which artificial upwelling should be applied (Pan *et al.*, 2016).

In addition to the carbon sequestration potential the enhanced primary production evoked by artificial upwelling is imitating a naturally occurring process that creates the most productive regions in the world's ocean, particularly in eastern boundary upwelling areas off Peru, California or Namibia as well as open-ocean regions along the equator (Chavez &

Messié, 2009). In these regions the distinct stratification between warm surface and colder deep-water layers, caused by the temperature, salinity, and pressure depended density of salt water, is overcome by ocean and wind currents, naturally bringing up nutrient rich deep-water to the surface. This nutrient enrichment of surface waters causes a significant enhancement of phytoplankton primary production, which can then be utilized by subsequent trophic levels of micro- and mesozooplankton organisms. Over time, this upwelling process transformed these regions into hotspots of phyto-, zoo-, and ichthyoplankton (Kirke, 2003; Kämpf & Chapman, 2016).

Productive regions like these, however, only cover a small proportion of the oceans (< 1%). In the majority of the oceans' waters, stratification prevents surface waters from admixing of deep-water, which is enriched with bioavailable inorganic nutrients (e.g. nitrate, phosphate, silicate, iron) essential for the growth and biomass accumulation of autotrophic primary producers at the bottom of the food web (Sakka Hlaili *et al.*, 2006; Sigman & Hain, 2012; Moore *et al.*, 2013). These regions are mostly located in the low- and mid-latitude subtropical gyres, and are predicted to further expand with climate change and rising sea surface temperature (Polovina *et al.*, 2008; Irwin & Oliver, 2009; Li *et al.*, 2020). Artificial upwelling could counteract the extension of these so called "ocean deserts". By artificially enriching nutrient depleted surface waters with nutrient rich deep-water via a pumping device, the subsequent biomass build up could ultimately create sustainably harvestable ecosystem-based fishing grounds, if successfully transferred to higher trophic levels like fish larvae and fish (see **Fig. 5**, and e.g. GESAMP (2019), Giraud *et al.* (2016), Kirke (2003)).

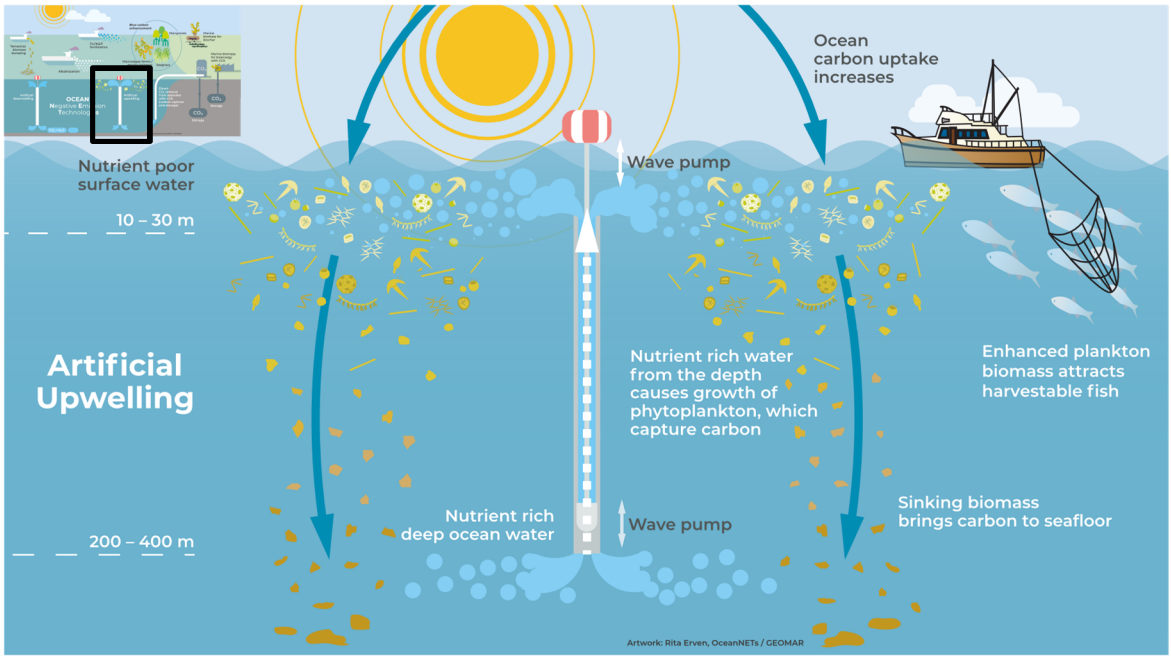

Figure 5: Mechanistic overview of a wave pump operated artificial upwelling system, as part of the OceanNETs (marked by the black box in the overview figure in the upper left corner). Original artwork of Rita Erven, © GEOMAR Helmholtz Centre for Ocean Research Kiel (see bottom of the figure), reworked with symbols taken from "Courtesy of the Integration and Application Network, University of Maryland Center for Environmental Science (ian.umces.edu/symbols/)", accessed 10.10.2021.

Furthermore, the expected increase in food availability for the different organisms within the former oligotrophic system could additionally provide an opportunity for them to better cope with the expected negative impacts of OA (see **Section I.2.**). For instance, by supplying the affected organisms with more available food, possibly even of higher quality, the metabolic depression caused by OA could be dampened by meeting the adherent higher energy demand of the organisms.

Artificial upwelling and zooplankton

While the theoretical considerations suggest that artificial upwelling may lead to beneficial effects on the entire food-web, little empirical work has been conducted on this topic. In order to achieve and increase the harvestable amounts of fish, enhancing primary production via nutrient enrichment is only a first step. A potential bottleneck is that biomass created by primary producers has to be transformed into secondary/ tertiary biomass in adequate amounts for the adjacent trophic levels. Therefore, the phyto- and zooplankton community formed through artificial upwelling has to be composed in a way that allows efficient transfer of biomass from primary to secondary production and up to fish, i.e. with minimal loss of biomass from one trophic level to the next. That means, the rearranged plankton community should include very little potential "dead ends" in the food chain, e.g. toxic

phyto-/ microplankton or jellyfish, but rather produce a phytoplankton community suitable for consumers such as copepods that serve as main prey for many early stages of different fish species (Pauly & Christensen, 1995; Støttrup, 2003; Castonguay *et al.*, 2008; Tommasi *et al.*, 2017). Traditionally, observations in natural upwelling systems suggest that such a phytoplankton community would be dominated by diatoms, as they can directly be preyed upon by copepods, and with that create a short and efficient food web (Cushing, 1989). However, it was also found that a higher species diversity in the phytoplankton community composition is, besides increased phytoplankton biomass in general, essential for the formation of productive upwelling regions, e.g. in the Galician upwelling system (Otero *et al.*, 2020). In the upwelling area off Chile, Medellín-Mora *et al.* (2019) also found that mean size of the phytoplankton community can influence species composition as well as the overall biomass production of the subsequent zooplankton trophic level substantially. They furthermore reported, along with several other studies, that the zooplankton community should be dominated by small crustaceans, i.e. copepods, and preferably in small to medium sizes, as these organisms are not only the most abundant metazoans in the world's oceans, but especially vital for highly productive regions (Turner, 2004; Escribano *et al.*, 2016; Valdés *et al.*, 2017).

Despite this theoretical claim, it is still a fairly open question how exactly a plankton community adapted to oligotrophic conditions is altered by artificial upwelling. Although some research was already conducted in this field of ocean-based solutions, most of the science focused on different possibilities of technical implementations (e.g. overview by Pan *et al.* (2016) or concept Pan *et al.* (2019)), the carbon sequestration potential (see Oschlies *et al.* (2010)), or the temporal and spatial mode in which artificial upwelling pumps should be operated (Fan *et al.*, 2016). In terms of how the plankton community is affected by artificial upwelling, the few studies conducted so far only investigated the direct nutrient effect on phytoplankton primary production, revealing that the artificial nutrient input can indeed enhance primary production. However, its effect size largely depends on the technical approach that is chosen (Masuda *et al.*, 2010; Maruyama *et al.*, 2011).

In conclusion, there still remain essential open questions that need to be addressed in the field of artificial upwelling, especially regarding the composition of the zooplankton community that develops in the manipulated ecosystem:

1) If and to what extent is enhanced primary production transferred to the secondary and/ or tertiary consumers in the zooplankton?
2) Is the effect size of secondary/ tertiary biomass output also affected by different technical or methodological upwelling approaches?
3) Along with increasing zooplankton numbers, is there an increase in population sizes of potentially detrimental species like jellyfish, which are capable of intercepting the biomass transfer to fish larvae and fish?

How can zooplankton production be quantified?

Besides the design of suitable experiments to tackle these comprehensive ecosystem related questions, another methodological hurdle is that in order to answer these questions it is crucial to accurately measure and quantify primary, secondary and higher trophic level production and consumption as well as energy and biomass fluxes in between these different trophic levels. Quantifying such a variety of production and growth rates, however, still constitutes a major methodological challenge, especially under *in situ* conditions and for zooplankton organisms like copepods. So far, production rates of zooplankton, and copepods in particular, were usually indirectly assessed e.g. from egg production (Sekiguchi *et al.*, 1980; Kiørboe *et al.*, 1988), molting rates (Peterson *et al.*, 1991), bioenergetic balance and temperature approaches (Huntley & Lopez, 1992), biochemical methods (e.g. Sastri and Roff (2000)) or computer models (e.g. EcoPath, Christensen and Walters (2004)). In general, these laboratory methods often have to make use of a few, easy to handle key species inhabiting the investigated ecosystem, which first need to be relocated from their natural *in situ* environmental conditions (Yáñez *et al.*, 2018). These approaches have the disadvantage of considerably varying in their output, making the extrapolation from the results back to open-ocean plankton communities difficult.

One approach that could overcome the constraints of all these traditional methods and efficiently quantify the fate of biomass production within a food web, is stable isotope (SI) labeling (Van den Meersche *et al.*, 2011; Middelburg, 2014). Although SIs are mostly and traditionally analyzed with regards to their natural abundance in order to reconstruct diets or allocate species to trophic positions within food webs (Boecklen *et al.*, 2011), natural isotope abundances can also be enriched to "label" specific components within an ecosystem and subsequently trace the fate of the enriched isotope through the food web (Boschker & Middelburg, 2002). The heavier carbon isotope ^{13}C in that context is particularly suitable to assess primary and secondary production rates. In the form of ^{13}C

bicarbonate or carbonate it can be easily utilized to enrich the natural ^{13}C dissolved inorganic carbon (DIC) pool of an enclosed experimental design (e.g. de Kluijver *et al.* (2013)). It is subsequently traceable throughout the entire food web, due to the amount of ^{13}C in the organism of a consumer after a certain time reflecting the combined amount of ^{13}C of its resources (Zanden & Rasmussen, 1999; Post, 2002; Middelburg, 2014). As a result, biomass fluxes and production rates could be calculated via a sampling strategy that permits to measure a consumer's standing stock biomass ($C_{consumer}$), its ^{13}C signature ($^{13}C_{consumer}$) as well as the ^{13}C signature of its food ($^{13}C_{food}$) over time (timepoint $(t)_{-1}$ until t), and set this into relation as seen in Eq. 3, after Hama *et al.* (1993). These measured values could be obtained, for instance, by isotope ratio mass spectrometry (IRMS) of phytoplankton 'food', i.e. dissolved inorganic carbon (DIC, e.g. from a water sample), of phytoplankton itself in the form of suspended particulate organic carbon (POC, e.g. collected by filtering water), and defined numbers of zooplankton organisms picked from net hauls samples.

$$\text{Production rate} = \frac{(^{13}C_{consumer(t)} - ^{13}C_{consumer(t-1)})}{(^{13}C_{food(t)} - ^{13}C_{consumer(t-1)})} \times \frac{biomass_{consumer(t)}}{t} \qquad \text{(Eq. 3)}$$

Elaborated to this extent, SI labeling could provide an important insight in to the carbon fluxes and production rates of an ecosystem, particularly in combination with experiments designed to explore possible influences of artificial upwelling from a whole-ecosystem perspective. This combination might substantially help to improve our understanding of how artificial upwelling could influence mesozooplankton communities in particular, as they are a link to higher trophic levels like fish. The approach could provide a major step towards the necessary future global focus of solution orientated, active management against climate change.

4. Motivation for this work and thesis outline

Despite the high complexity of conducting experiments designed to answer research questions from a natural, whole ecosystem perspective, it is inevitable to do so when dealing with comprehensive environmental changes like OA or artificial upwelling. That is, because the strong dynamics within the plankton community of an ecosystem in terms of inter- and intraspecific interactions as well as the variable consequences of the interplay of direct and indirect effects of environmental stressors cannot be conclusively extrapolated from small scale laboratory experiments.

As already pointed out beforehand, it is uncertainties regarding these complex plankton community responses that are the cause for important knowledge gaps in the research field of OA and especially artificial upwelling. Consequently, the here presented thesis was designed with the aim of filling some of these gaps present for complex ecosystems, particularly regarding changes in functionality and structure of natural zooplankton communities under the influence of future OA and artificial upwelling conditions. In the context of these anthropogenic influences, this thesis aims on: (A) assessing direct and indirect effects of OA on community composition and trophic level interactions, especially within the zooplankton and up to trophic levels like fish larvae. (B) quantification of the change in productivity and efficiency of carbon fluxes within a zooplankton community via SI-labeling, particularly in dependence of the upwelling conditions (time of appliance, amount and nutrient content of upwelled water), and with regard to the possibility of high fishery yield.

Ultimately, the results of the here presented thesis are meant to provide valuable information for linking the projections of future climate change pathways closer to zooplankton community changes in terms of OA, and improve our understanding of the usability, zooplankton community side-effects, and possible food web efficiency enhancement of artificial upwelling.

Chapter 1 evaluates how a natural plankton community is influenced by extreme pH values. Such values are scarcely targeted by OA research, because they are only projected for the surface ocean under a "business as usual" pathway or worse toward the end of the century. But, there is a high probability of substantially low pH values to be reached under more moderate pathways by the year 2150. In order to simulate such OA conditions, and to assess its effects on the functionality and structure of a complex ecosystem, a large scale mesocosm experiment was carried out under pCO_2 levels of around 2000 µatm. Results are presented that stem from closely monitoring OA-induced changes in the enclosed phyto-, micro-, and mesoplankton community structure during nutrient limited post-bloom conditions.

Chapter 2 highlights results from the in Chapter 1 conducted experiment with regards to OA affecting particularly higher trophic level predatory organisms in the enclosed plankton community. There are still substantial knowledge gaps on how OA is affecting predatory plankton, in this case Hydrozoa and fish larvae, and their interaction in complex natural communities. OA induced changes to this higher tropic level interaction, however, may have significant consequences for marine food webs and ecosystem services. In the

presented study, the effects of OA were investigated by monitoring the development and interactions of fish larvae introduced to the mesocosms, and an already established Hydrozoa population. The influence of OA on the Hydrozoa - fish relationship was evaluated by comparing control and treatment mesocosm regarding survival and growth of fish larvae at the end of the experiment in combination with Hydrozoa abundances and biomass as well as changes in the phyto-, micro-, and mesoplankton community over time.

Chapter 3 shows results from a large scale mesocosm experiment assessing the effect of different simulated upwelling modes and intensities of artificial upwelling on the productivity and trophic transfer efficiency of a natural plankton community in subtropical oligotrophic waters. These nutrient-depleted areas of the world's oceans in general are of low biological productivity and expanding with ongoing climate change. Artificial upwelling could increase the productivity of such "ocean deserts" via nutrient enrichment, however, it remains fairly unclear how oligotrophic plankton communities react to simulated upwelling, and under which modes and intensities primary and secondary production could be enhanced to what extent. In the presented study, artificial upwelling was simulated in two different modes and four different intensities by adding natural deep-water to the mesocosms. The plankton community responses were monitored over time, and production rates as well as trophic transfer efficiencies were assessed via addition and tracing of the stable isotope ^{13}C.

The thesis closes with a synthesis, which sets the results of the different chapters comprehensively into relation with current knowledge on natural zooplankton community responses under OA and artificial upwelling. In addition to that, current scientific perception complemented by the insights of the presented experiments is used to elaborate an outlook of how zooplankton communities could be shaped by artificial upwelling and ongoing ocean acidification.

II. THESIS CHAPTERS

First author publications

Chapter 1:

Spisla, C., Taucher, J., Bach, L. T., Haunost, M., Boxhammer, T., King, A. L., Jenkins, B. D., Wallace, J. R., Ludwig, A., Meyer, J., Stange, P., Minutolo, F., Lohbeck, K. T., Nauendorf, A., Kalter, V., Lischka, S., Sswat, M., Dörner, I., Ismar-Rebitz, S. M. H., Aberle, N., Yong, J. C., Bouquet, J.-M., Lechtenbörger, A. K., Kohnert, P., Krudewig, M. and Riebesell, U. (2021): Extreme Levels of Ocean Acidification Restructure the Plankton Community and Biogeochemistry of a Temperate Coastal Ecosystem: A Mesocosm Study. *Frontiers in Marine Science,* **7.**

Idea and experimental design: U. Riebesell, L. T. Bach, J. Taucher, C. Spisla, M. Haunost, T. Boxhammer, M. Sswat, K. T. Lohbeck, A. Ludwig, P. Stange, S. Lischka
Experimental work: C. Spisla, J. Taucher, L. T. Bach, M. Haunost, T. Boxhammer, A. K. Lechtenbörger, B. D. Jenkins, J. R. Wallace, A. Ludwig, J. Meyer, P. Stange, F. Minutolo, K. T. Lohbeck, A. Nauendorf, V. Kalter, S. Lischka, M. Sswat, I. Dörner, S. M. H. Ismar-Rebitz, J. C. Yong, J.-M. Bouquet, P. Kohnert, M. Krudewig, U. Riebesell
Sample analysis: C. Spisla, J. Taucher, L. T. Bach, T. Boxhammer, B. D. Jenkins, J. R. Wallace, A. Ludwig, J. Meyer, P. Stange, F. Minutolo, K. T. Lohbeck, A. Nauendorf, V. Kalter, S. Lischka, M. Sswat, I. Dörner, S. M. H. Ismar-Rebitz, J. C. Yong, J.-M. Bouquet, A. K. Lechtenbörger
Data analysis: C. Spisla, J. Taucher, L. T. Bach, T. Boxhammer, K. T. Lohbeck, V. Kalter, I. Dörner, S.-M. Ismar-Rebitz, J. C. Yong
Manuscript preparation: C. Spisla, with comments of U. Riebesell, L. T Bach, J. Taucher, M. Haunost, T. Boxhammer, M. Sswat, K. T. Lohbeck, S. Lischka, A. K. Lechtenbörger, A. L. King, F. Minutolo, V. Kalter, S. M. H- Ismar-Rebitz, N. Aberle, J.-M. Bouquet

Chapter 2:

Spisla, C., Taucher, J., Sswat, M., Wunderow, H., P. Kohnert, C. Clemmesen, Riebesell, U. (2021): Ocean Acidification Alters the Predator – Prey Relationship between Hydrozoa and Fish Larvae. Submitted to *Frontiers in Marine Science*

Idea and experimental design: U. Riebesell, J. Taucher, C. Spisla
Experimental work: C.Spisla, M. Sswat
Sample analysis: C. Spisla, P. Kohnert
Data analysis: C.Spisla
Manuscript preparation: C. Spisla with comments of all co-authors

Chapter 3:

C. Spisla, J. Taucher, M. Sswat, J. Ortiz, N. Smith-Sanchez, K. G. Schulz, U. Riebesell: Assessing the Influence of Artificial Upwelling on Zooplankton Secondary Production and Trophic Transfer Efficiency of an Oligotrophic Plankton Community via ^{13}C labeling

Idea and experimental design: U. Riebesell, J. Taucher, C. Spisla, K. G. Schulz
Experimental work: C.Spisla, J. Taucher, J. Ortiz, N. Smith-Sanchez, K. G. Schulz
Sample analysis: C. Spisla, K. G. Schulz
Data analysis: C.Spisla,
Manuscript preparation: C. Spisla with comments of all co-authors

CHAPTER 1

Extreme Levels of Ocean Acidification Restructure the Plankton Community and Biogeochemistry of a Temperate Coastal Ecosystem: A Mesocosm Study

C. Spisla[1*], J. Taucher[1], L. T. Bach[1], M. Haunost[1], T. Boxhammer[1], A.L. King[2], B.D. Jenkins[3], J.R. Wallace[3], A. Ludwig[1], J. Meyer[1], P. Stange[1], F. Minutolo[1], K. T. Lohbeck[1,4], A. Nauendorf[1], V. Kalter[5], S. Lischka[1], M. Sswat[1], I. Dörner[1], S. M. H. Ismar-Rebitz[1], N. Aberle[6], J. C. Yong[1], J.-M. Bouquet[7], A. K. Lechtenbörger[1], P. Kohnert[1], M. Krudewig[1], U. Riebesell[1]

[1]*GEOMAR, Helmholtz Centre for Ocean Research Kiel, Biological Oceanography, Kiel, Germany*
[2]*Norwegian Institute for Water Research, Department of Marine Biogeochemistry and Oceanography, Bergen, Norway*
[3]*Department of Cell and Molecular Biology, University of Rhode Island, Rhode Island, RI, United States of America*
[4]*Limnological Institute, University of Konstanz, Konstanz, Germany*
[5]*Department of Ocean Sciences, Memorial University of Newfoundland, Newfoundland, NL, Canada*
[6]*Department of Biology, Norwegian University of Science and Technology, Trondheim, Norway*
[7]*Department of Biology, SARS International Centre for Marine Molecular Biology, University of Bergen, Bergen, Norway*

***Correspondence:**
Carsten Spisla
cspisla@geomar.de

Frontiers of Marine Science:
Submitted 28th September 2020, revised 14th December 2020, accepted 23rd December 2020, published 25th January 2021

Abstract

The oceans' uptake of anthropogenic carbon dioxide (CO_2) decreases seawater pH and alters the inorganic carbon speciation - summarized in the term ocean acidification (OA). Already today, coastal regions experience episodic pH events during which surface layer pH drops below values projected for the surface ocean at the end of the century. Future OA is expected to further enhance the intensity of these coastal extreme pH events. To evaluate the influence of such episodic OA events in coastal regions, we deployed eight pelagic mesocosms for 53 days in Raunefjord, Norway, and enclosed 56 - 61 m^3 of local seawater containing a natural plankton community under nutrient limited post-bloom conditions. Four mesocosms were enriched with CO_2 to simulate extreme pCO_2 levels of 1978 - 2069 µatm while the other four served as untreated controls. Here, we present results from multivariate analyses on OA-induced changes in the phyto-, micro-, and mesozooplankton community structure. Pronounced differences in the plankton community emerged early in the experiment, and were amplified by enhanced top-down control throughout the study period. The plankton groups responding most profoundly to high CO_2 conditions were cyanobacteria (negative), chlorophyceae (negative), auto- and heterotrophic microzooplankton (negative), and a variety of mesozooplankton taxa, including copepoda (mixed), appendicularia (positive), hydrozoa (positive), fish larvae (positive), and gastropoda (negative). The restructuring of the community coincided with significant changes in the concentration and elemental stoichiometry of particulate organic matter. Results imply that extreme CO_2 events can lead to a substantial reorganization of the planktonic food web, affecting multiple trophic levels from phytoplankton to primary and secondary consumers.

INTRODUCTION

The world oceans currently absorb 2.5 ± 0.5 Gt C y^{-1} of the total 11.5 ± 0.9 Gt C yr^{-1} anthropogenic CO_2 emissions (2009 - 2018, Friedlingstein *et al.* (2019)). The uptake of CO_2 by the oceans reduces global warming, but CO_2 dissolution in seawater results in the formation of carbonic acid, whose dissociation decreases average seawater pH – a process generally termed ocean acidification (OA) (Caldeira & Wickett, 2003; Emerson & Hedges, 2008). Realistic emission scenarios project that the pH of ocean surface waters will further decline by at least 0.2 units to about 7.9 by the end of the century (IPCC scenario RCP4.5, Pörtner *et al.* (2014)). The effects of this alteration in the carbonate systems of the oceans on the inherent marine organisms has already been targeted by a variety of different experiments and approaches (Gattuso & Hansson, 2011). Within these studies, the observed consequences for marine plankton communities are diverse, indicating that the increased CO_2/ decreased pH might put some marine species at advantage (e.g. diatoms) and others at disadvantage (e.g. calcifiers such as gastropods, molluscs) (Orr *et al.*, 2005; Kroeker *et al.*, 2013; Wittmann & Pörtner, 2013). In addition, recent studies have shown that consequences of an elevated partial pressure of CO_2 (pCO_2) also vary strongly between different oceanic regions as well as between planktonic communities (Fabricius *et al.*, 2011; Riebesell *et al.*, 2013a; Paul *et al.*, 2015; Gazeau *et al.*, 2017; Taucher *et al.*, 2017). What they have in common, however, is that although the studies cover plankton communities in e.g., the Baltic Sea, the north western Mediterranean, the eastern subtropical North Atlantic or the Artic, they all discovered OA effects in similar trophic positions. Riebesell *et al.* (2013a) and Paul *et al.* (2015) both discovered predominantly positive effects of an OA simulation on pico- and nanophytoplankton organisms, along with corresponding changes in chl *a* or particulate organic matter (POM). Taucher *et al.* (2017), additionally, observed a pronounced reorganization of the whole plankton community under elevated pCO_2, still suspected to be driven by phytoplankton, but contrary to the other studies also affecting micro- and mesozooplankton organisms (Algueró-Muñiz *et al.*, 2019).

In contrast to open ocean environments, coastal regions already experience seasonal/ temporal pH conditions as low as or even lower the 7.9 projected for the RCP4.5 end of the century scenario (Feely *et al.*, 2008; Fassbender *et al.*, 2011; Hofmann *et al.*, 2011; McNeil *et al.*, 2011). For example, Feely *et al.* (2008) found pH values of 7.75 and below at the coast line of western North America from central Canada to northern Mexico, and Fassbender *et al.* (2011) reported pH values as low as 7.6, with pCO_2 exceeding 1100 µatm,

at the coast of California during upwelling events. These near shore pCO_2 values were nearly three times higher than those found off shore. Extreme pH events like the one monitored here in the California upwelling region occur episodically in short- or medium-term intervals (days to weeks), and result in substantial changes in carbonate chemistry, including increasing pCO_2, dissolved inorganic carbon (DIC), and calcite/ aragonite corrosiveness of the seawater. Coastal plankton communities may harbor species that are well adapted to cope with these extreme conditions, while others may be living on the verge of their physiological capacities. This issue is especially eminent when considering that the scales and frequency of such pH events could increase in the future due to intensification of coastal upwelling, concurrent with end-of-the-century climate change projections (Hofmann *et al.*, 2011; Sydeman *et al.*, 2014). Although a lot of studies have already been targeting OA and its impacts on marine organisms, experiments suitable to assess the consequences of enhanced extreme pH events on coastal ecosystems and their plankton community structures are rare. When investigating community-level changes, the majority of studies focused on pCO_2 values within the IPCC RCP4.5 end of the century projections or such that were just slightly exceeding them (see Lischka *et al.* (2017), Bach *et al.* (2016) or meta-analysis by Kroeker *et al.* (2010)). When higher pCO_2 values were applied, experiments were often either conducted in laboratory setups (e.g. Berge *et al.* (2010); Nielsen *et al.* (2010); Rossoll *et al.* (2013)), focused on lower trophic level dynamics in natural settings (Calbet *et al.*, 2014; Thomson *et al.*, 2016; Bach *et al.*, 2017) or on specific ecosystem key taxa such as calcifiers or appendicularians (see Thomsen *et al.* (2010); Lischka *et al.* (2011); Bouquet *et al.* (2018)). Apart from that, even these large-scale experiments still stayed beneath the pCO_2 values presumed here for future coastal areas that could reach a drop in pH of 0.4 units under a RCP8.5 scenario (Pörtner *et al.*, 2014), thus leaving unclear, how coastal plankton communities might cope with future extreme pH events. To approach this uncertainty, we conducted a large-scale *in-situ* mesocosm experiment enclosing a natural coastal plankton community in Raunefjord, Norway, and tested the two hypotheses of **(1)** plankton community composition/ structure will change under extreme pH values, and **(2)** extreme pH will accordingly influence the biogeochemistry in the enclosed ecosystem.

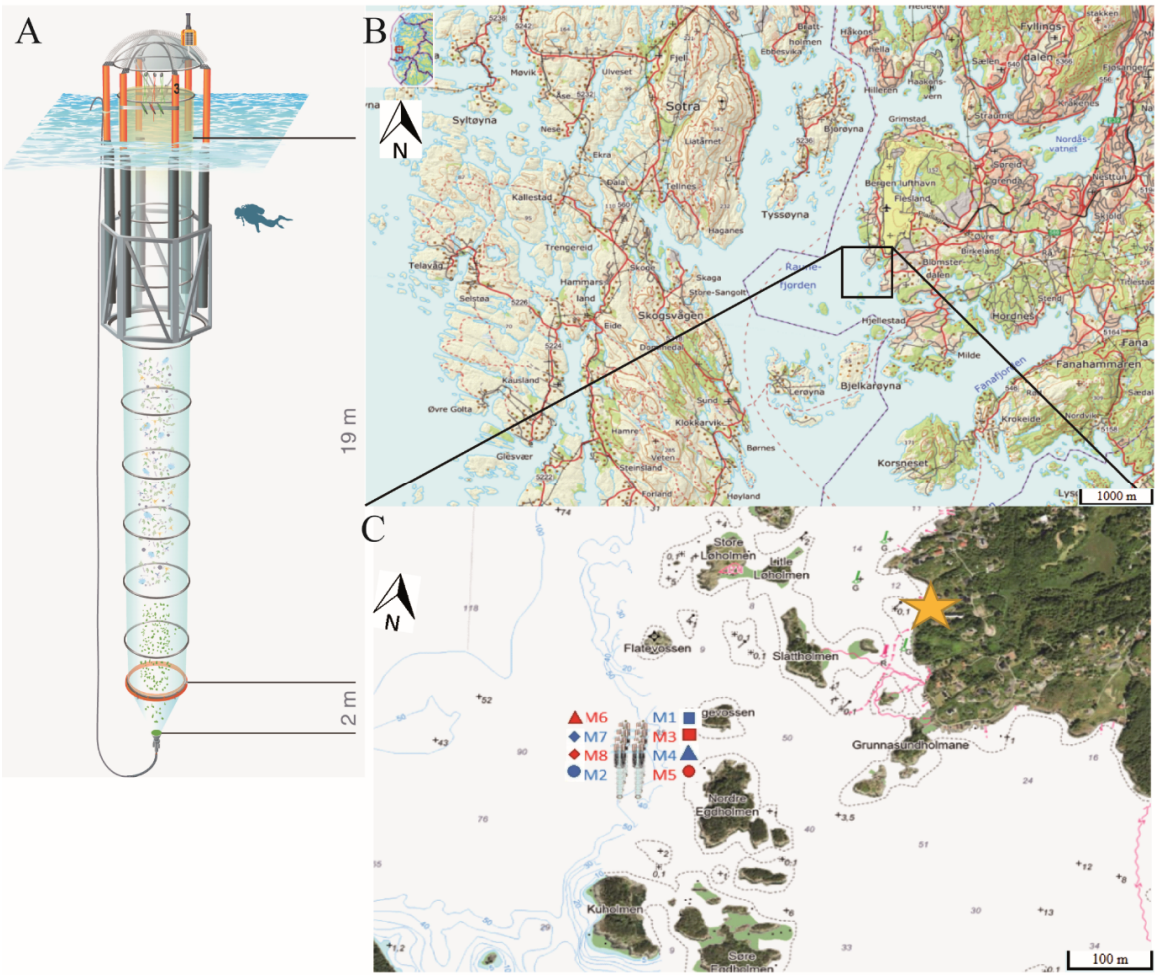

Figure 1: (A) Kiel Off-Shore Mesocosm for Ocean Simulations (KOSMOS), a pelagic mesocosm system. Blue corrugated area represents water surface. Diver for scale. Illustration of the KOSMOS unit by Rita Erven (GEOMAR) **(B)** Location of Raunefjord between the island Sotra (left) and the city of Bergen (right). Black square indicates deployment area of the mesocosms. **(C)** Position, order and corresponding symbols of the mesocosms in their deployment area in front of the Espegrend Marine Research Field Station (marked by the yellow star), Bergen (not to scale). Red mesocosm numbers indicate high pCO_2 treatments, blue ones the control treatment. **(B)** & **(C)** Map modified after: The Norwegian Mapping Authority (Kartverket, accessed 7th July 2020, http://geo.ngu.no/kart/arealisNGU/). Figure assembled and designed with Adobe Illustrator CS4 (Adobe-Inc., 2008).

MATERIAL AND METHODS

Study site

Raunefjord is a 15 km long and 4 km wide fjordlike strait on the southwest coast of Norway close to the city of Bergen (**Fig. 1B**), and is assigned to the North Sea ecoregion with microtidal and euryhaline conditions (Molvær *et al.*, 2007). Due to the wind-induced Norwegian Coastal Current, water masses are subject to a fast exchange with high salinity Atlantic deep-water. The surface layer in the fjord typically shows a salinity around 30 with

a pycnocline of up to 34.5 at depths between 100 m (winter/autumn) and 50 m (summer) (Helle, 1978; Molvær *et al.*, 2007). The mesocosms were deployed at 60°15'55"N, 5°12'21"E in the vicinity of the Espegrend Marine Research Field Station, north-west off the island of Nordre Egdholmen, where water depths ranged from 50 - 75 m.

The "KOSMOS" facility

The Kiel Off-Shore Mesocosms for Ocean Simulations (KOSMOS) are mobile, pelagic mesocosms (Riebesell *et al.*, 2013b). Each mesocosm unit consists of a floating frame with a dome-shaped hood, the mesocosm bag, and a full diameter sediment trap sealing the bottom end of the bags (**Fig. 1A**). The dimensions of the mesocosm enclosure in this study were 2 m in diameter and 21 m in length, resulting in an enclosed water volume of 56 m³ to 61m³ (**Tab. 1**). The mesocosm bags are made of a flexible thermoplastic polyurethane foil, strongly reducing UV-light, but permitting similar light intensities and depth profiles of light in the photosynthetically active radiation (PAR) spectrum inside the mesocosms as in the surrounding water masses. The hoods on top of the floating frame reduce rainfall into the enclosures and are equipped with metal spikes to impede seabirds from resting and defecating on and into the enclosures.

The bottom end of each mesocosm bag is formed by a 2 m long, cone shaped sediment trap, which is attached to lower opening of the bag. This trap is hinged and can be left open or closed with screws. The sediment trap has a steeply angled shape, minimizing adhesive friction of sinking material inside the mesocosm, and leading into a collecting cylinder of ≈ 3 L volume. A silicon tube for sampling of the accumulated material is attached to the outlet opening of the cylinder and extends to the floating frame of the mesocosm above the sea surface (Boxhammer *et al.*, 2016).

Deployment and experimental design

On the 3rd of May 2015 (Day -9, i.e. 9 days before first CO_2 manipulation), eight KOSMOS units were deployed by RV ALKOR. In this process, the mesocosms were arranged in two rows with four mesocosm units per row (M1 – M8, **Fig. 1C**).

After the mesocosms were moored, the initially folded mesocosm bags mounted 1 m below the water surface in the flotation frames were unfolded to a length of 19 m on that same day. During deployment and before mesocosm closure, nets of 3 mm mesh size covered the top and bottom openings of the bags to exclude large and heterogeneously distributed

zooplankton (e.g. large adult jellyfish) or nekton (e.g. larger fish) from the enclosures. On the 6th of May (Day -6) mesocosm hoods were installed, and sediment traps were attached by divers at the lower end of the bags. The bottom nets were removed in the morning of the 7th of May (Day -5) and the bags were sealed with the sediment traps at the bottom. Simultaneously, a boat crew pulled the mesocosm bags above the water surface and the upper net was removed, leaving the enclosed water body isolated from the surrounding sea water. The mesocosms were then monitored for 53 days, from the 9th of May (Day -3) until the 30th of June (Day 49) which marked the end of the experiment.

Table 1: Overview of the individual mesocosm numbers, symbols, volumes (Section "Volume Determination"), and average pCO_2 values over the four experiment phases (**Table 2**) and the entire study.

Symbol	Mesocosm	Average pCO_2 [µatm]					Volume [m^3]
		Phase I	Phase II	Phase III	Phase IV	Total mean	
■	1	271	274	299	341	312	58.6
●	2	261	270	299	339	309	56.1
■	3	266	989	1909	1961	1657	57.6
▲	4	266	281	304	343	314	61.0
●	5	274	1006	1912	1958	1659	60.5
▲	6	270	1024	2044	2064	1753	59.1
♦	7	272	285	306	350	319	59.2
♦	8	268	1039	2003	2044	1731	60.1
●	Fjord	271	294	293	310	298	

Blue background color indicates mesocosms belonging to the control, red background color the ones belonging to the OA treatment, and black color highlights the fjord. This color scheme and the symbols assigned to the individual mesocosms will be used in all plots throughout this paper.

Volume determination

On the 8th of May (Day -4) the volume of the enclosed water bodies was determined following Czerny *et al.* (2013). Briefly, a calibrated sodium brine solution was evenly dispersed in each mesocosm, thereby increasing the salinity by 0.2 units. This change in salinity was measured with a conductivity, temperature, density probe (CTD) before and after the addition of the brine solution. The individual mesocosm volumes were calculated from the resulting change in salinity, the amount of brine solution added to the enclosures and the individual seawater density of each mesocosm (for exact volumes see **Tab. 1**, for the exact salinity changes see **Appendix Tab. 1**).

CO_2 addition

To increase pCO_2 in the treatment mesocosms, approximately 1.4 m^3 of filtered (30 µm mesh size) fjord water was aerated with pure CO_2 gas for several hours. This CO_2-saturated water was then homogeneously injected into the water columns of the "high pCO_2" mesocosms (M3, M5, M6, M8) following procedures described in Riebesell *et al.* (2013b).

To treat all mesocosms similarly with respect to creating internal turbulences, we also moved the CO_2 injection device up and down in the water columns in the unmanipulated control mesocosms (M1, M2, M4, M7), but without the addition of any water. The four "high pCO_2" mesocosms were elevated to pCO_2 levels between 2001 µatm (M5) and 2107 µatm (M6) on Day 6 with four initial injections of CO_2-saturated seawater (Day 0, 2, 4, and 6). In the other four "ambient pCO_2" mesocosms the pCO_2 remained similar to the surrounding fjord water with a total average of ≈ 314 µatm (**Tab. 1**). During the experiment, five more CO_2 additions were conducted on Days 14, 22, 28, 40, and 46, to counteract CO_2 losses due to outgassing at the air-sea interface (**Fig. 2** and **Appendix Tab. 2**). According to these time points of the CO_2 additions, and the temporal development of chl *a* (**Fig. 4**), we divided the experiment into four phases (**Tab. 2**).

Phase I is thereby characterized as the pre-experimental phase until the first CO_2 addition (Day 0). Phase II is the transitional phase while target pCO_2 levels were established with the four initial CO_2 injections (last addition on Day 6), and the community changed from bloom to post-bloom conditions. Phases III and IV experience post-bloom conditions and were separated to distinguish between an initial temporary treatment effect on chl *a* (Days 7 to 26), and a second more steady OA effect from Day 27 onwards.

Table 2: Overview, description and duration of the four different phases of the experiment based on pCO_2 additions/manipulations and chl *a* concentration development.

Phase	Description	Duration
I	Closing of the mesocosms until first CO_2 addition	Day −3 – Day 0
II	Establishing target pCO_2 values and transition from bloom to post-bloom conditions	Day 1 – Day 6
III	First post-bloom phase with a treatment effect on chl *a* followed by a realignment	Day 7 – Day 26
IV	Second post-bloom phase with enhanced treatment differences and a continued steady decline in chl *a*	Day 27 – Day 49

Addition of organisms to the mesocosms

High pCO_2-adapted *Emiliania huxleyi*

On May 11 (Day -1), a ≈ 20 L mixture of high pCO_2-adapted (2200 µatm) and ambient pCO_2-adapted *Emiliania huxleyi* strains was injected evenly into the water column of each mesocosm. The cultures originated from an *E. huxleyi* strain that was isolated at the exact same location in Raunefjord in 2009. Since 2010, this strain was grown under

ambient (400 µatm) and high pCO_2 (2200 µatm) conditions in controlled conditions until this mesocosm experiment in 2015 (for details on culturing and the rationale for the competition experiment between high and ambient pCO_2-adapted *E. huxleyi* see Lohbeck *et al.* (2012); Schlüter *et al.* (2016); Bach *et al.* (2018). Both strains were grown in large volumes in the laboratory prior to their addition to the mesocosms. Directly after their injection into the mesocosm, their concentration was ~ 100 cells mL^{-1}. The results of the *E. huxleyi* competition experiment will be presented in a separate publication.

Atlantic herring larvae

To investigate the influence of extreme OA on higher tropic levels, on average 6364 ± 1257 eggs of the Atlantic herring *Clupea harengus* (Linneaus, 1758) were added to each mesocosm. From these eggs, on average, 2063 ± 566 larvae hatched in each mesocosm (63 m^3). This relates to a herring larval density of 32.7 ± 9.0 larvae per m^3 and ~ 650 larvae per m^2. These densities are well within the natural range for nursery grounds, with, on average, 20 larvae per m^3 and maximum 100 larvae per m^3 in the Baltic Sea (Oeberst *et al.*, 2009) and 1,000 - 10,000 larvae per m^2 along the Norwegian Coasts (ICES, 2007). Furthermore, the number of eggs was chosen to yield enough larvae to ensure sufficient survival until the end of the experiment, but still avoid the risk of a strong top-down effect on the enclosed plankton community. The herring brood stock originated from the Fens Fjord, Norway (approx. 80 km north of the study area) where they were caught at Day -7 and strip-spawned the same day. The fertilized eggs were kept on egg plates in flow-through fjord water until introduction into the mesocosms. On Day 0, the *C. harengus* eggs were transferred into egg incubators to prevent damage of the eggs, and suspended at 8 m depth in each of the eight mesocosms. From these incubators the larvae could escape freely into the mesocosms right after hatch. The introduction of herring eggs and development of larvae will be discussed in more detail in Chapter 2 of this thesis.

Cleaning of mesocosm surfaces

Inside and outside cleaning of the mesocosm walls was performed at regular intervals to prevent fouling on the mesocosm walls and thus consumption of nutrients and a decrease in light penetration depth. A specifically designed ring-shaped double-bladed wiper was used to clean the mesocosm bags from the inside, while the outside bags were cleaned by divers with scrubbers (Riebesell *et al.*, 2013b; Bach *et al.*, 2016). Only the sediment trap and the last meter of the mesocosm bags could not be cleaned from the inside due to their narrowing diameter and the fixed diameter of the cleaning ring. However, the negative influence of

this on light penetration can be considered small, as this is quite deep in the water column (~ 18 m below surface).

General sampling procedure

A variety of physical, biological, and biogeochemical parameters were measured inside the mesocosms and in the surrounding water at the mesocosm deployment site over the course of the experiment in regular intervals. Before the CO_2-manipulation, from Day -3 until Day -1, sampling was performed daily. Afterwards, samples were taken every second day until the end of the experiment (Day 49) (**Fig. 2**). Sampling lasted no longer than three hours and was always conducted between 8 and 12 am.

Sediment trap sampling and processing

Particles accumulating in the mesocosm sediment traps were removed on each sampling day (**Fig. 2**) before the water column sampling. This was done by using a gentle vacuum pump system as described in Boxhammer *et al.* (2016). Small subsamples (in total < 10%) were used for particle sinking velocity and respiration measurements as described in Stange *et al.* (2018). The bulk samples were concentrated by centrifugation, deep frozen at -30°C and then freeze dried for 72 hours. The dried bulk samples were ground in a ball mill to a homogeneous powder of 2 – 60 µm particle size and analyzed for biogenic silica (BSi_{SED}), total particulate carbon (TPC_{SED}), nitrogen (TPN_{SED}) and phosphorus (TPP_{SED}) as described by Boxhammer *et al.* (2016).

CTD casts

In order to obtain vertical profiles of temperature, salinity, pH, and photosynthetically active radiation (PAR), a hand-held self-logging CTD probe (CTD60M, Sea and Sun Technologies) was lowered down through the entire water column of each mesocosm and down to 21 m in the surrounding water on every sampling day (**Fig. 2**). Technical details on the sensors and data analysis procedures are described by Schulz and Riebesell (2013). Potentiometric measurements of pH_{NBS} (NBS scale) from the CTD were corrected to pH_T (total scale) by daily linear correlations of mean water column potentiometric pH_{NBS} to pH_T as determined from carbonate chemistry measurements (see Sect. “Dissolved inorganic carbon (DIC) and total alkalinity (TA)”).

Integrated water samples

Water samples were taken with a 5 L depth-integrating water sampler (IWS, HYDRO-BIOS, Kiel), controlled electronically via hydrostatic pressure sensors. By constantly sampling water over a defined time (50 mL s^{-1}) at each depth between 0 and 19 m, the IWS samples represent an average for the defined water column. Subsamples were taken directly from the IWS for those parameters particularly sensitive to gas exchange or contamination. These were: the inorganic nutrients nitrate + nitrite, ammonium, silicic acid, and phosphate (NO_3^-+ NO_2^-, NH_4^+, $Si(OH)_4$, and PO_4^{3-}), dissolved inorganic carbon (DIC), total alkalinity (TA), and primary production bioassays (see Sect. "Dissolved inorganic carbon (DIC) and total alkalinity (TA)" and "Inorganic nutrients"). Samples for the other parameters (see below) were transferred to 10 L plastic canisters, transported back to the laboratory and stored at *in situ* water temperature until further processing on the same day. The parameters subsampled from these canisters were: total particulate carbon (TPC), particulate organic carbon (POC), nitrogen (PON), and total particulate phosphorus (TPP), biogenic silica (BSi), chlorophyll *a* (chl *a*), phytoplankton pigments, and microscopic counts of phyto- and microzooplankton (analytical procedures described in Sect. "Phytoplankton and "Microzooplankton")

Total particulate carbon and nitrogen (TPC and TPN)

For TPC and TPN, and POC and PON measurements, three replicates of 500 to 1000 mL integrated water samples were filtered (≈ 200 mbar) through 0.7 µm pre-combusted (450°C for 6 h) GF/F filters. In case the filtration time exceeded 30 min, the vacuum was increased to ≈ 300 mbar. After filtration, two replicates for TPC and TPN measurements were directly dried at 60°C overnight, while the third filter for POC and PON analysis was fumed with hydrochloric acid (37%) for 2 h to remove any particulate inorganic carbon or nitrogen (PIC, PIN) before drying. Subsequently, all filters were packed in tin foil and stored in desiccators until analysis. Measurements were carried out using an elemental CN analyzer (EuroEA) following Sharp (1974). PIC was calculated as the difference between the TPC and POC filters. The vertical flux of TPC_{SED} and TPN_{SED} was determined from subsamples of 1 - 2 mg of the finely ground material from the sediment traps and analyzed as described above for suspended particulate matter.

Total particulate phosphorus (TPP)

For TPP, 500 to 1000 mL of IWS water were filtered through 0.7 µm GF/F filters with 200 mbar. Until analysis, the filters were stored at -20°C in glass bottles, and immediately

preceding the analysis, an oxidizing decomposition reagent (Oxisolv®, MERCK) was added to each filter. After that, the filters were cooked for 30 minutes in a pressure cooker, mixed with ascorbic acid and a mix reagent (sulfuric acid + ammonium-heptamolybdate-solution + potassium-antimonyl-tartrate solution), and centrifuged. The absorption of the supernatant was measured at 882 nm in a spectrophotometer. TPP_{SED} was analyzed from subsamples of 1 - 2 mg of the finely ground sample material following the same procedure as described for water column samples.

Biogenic Silica (BSi)

For BSi, 500 to 1000 mL of IWS water were filtered through 0.65 µm cellulose acetate filters. The filters were stored at -20°C in closed plastic bottles, and concentrations were determined spectrophotometrically in 1 cm cuvettes at 810 nm, according to Hansen and Koroleff (2007). BSi_{SED} was also determined from subsamples of 1 - 2 mg of the processed sample material as described for filters containing particulate matter from the water column.

Dissolved inorganic carbon (DIC) and total alkalinity (TA)

From a 1500 mL sample taken for carbonate chemistry, 50 mL and 100 mL subsamples were taken for measurements of DIC and TA, respectively, filtered directly after sampling (0.2 µm prefiltered by syringe, afterwards GF/F, 0.7 µm pore size) using a peristaltic pump, and stored at room temperature until measurement on the same day. Great care was taken to avoid gas exchange with the atmosphere in case of the DIC filtrations. DIC concentrations were determined by measuring infrared absorption of triplicate samples using a LI-COR LI-7000 on an AIRICA system (MARIANDA, Kiel). The overall precision was typically better than 5 µmol kg^{-1}. TA was analyzed by potentiometric titration using a Metrohm 862 Compact Titrosampler and a 907 Titrando unit with a precision < 1.5 µmol kg^{-1} following the open-cell method described in Dickson *et al.* (2003). The accuracy of DIC and TA measurements was determined by calibration against certified reference materials (CRM batch 126), supplied by A. Dickson, Scripps Institution of Oceanography (USA). DIC and TA results were used to calculate other carbonate chemistry parameters such as pCO_2, pH (on the total scale: pH_T), calcite ($\Omega_{calcite}$) and aragonite saturation state ($\Omega_{aragonite}$). For the calculation we used the Seacarb-R package (Gattuso *et al.*, 2016) with the recommended default settings for carbonate dissociation constants (K_1 and K_2) of Lueker *et al.* (2000).

Inorganic nutrients

250 mL samples for inorganic nutrients were collected in acid-cleaned (10% HCl) plastic bottles (Series 310 PETG), filtered over Whatman 0.45 µm cellulose acetate filters, and analyzed directly after sampling. A SEAL Analytical QuAAtro AutoAnalyzer connected to JASCO Model FP-2020 Intelligent Fluorescence Detector and a SEAL Analytical XY2 autosampler with AACE v.6.04 software were used to measure nitrate and nitrite (NO_3^-+ NO_2^-), dissolved silica ($Si(OH)_4$), and phosphate (PO_4^{3-}) concentrations spectrophotometrically according to Murphy and Riley (1962) and Hansen and Grasshoff (1983). Ammonium (NH_4^+) concentrations were determined fluorometrically following Holmes *et al.* (1999). Refractive index blank reagents were used (Coverly *et al.*, 2012) in order to quantify and correct for the contribution of refraction, color and turbidity on the optical reading of the samples. Instrument precision was calculated from the average standard deviation of triplicate samples (± 0.007 µmol L^{-1} for NO_3^-/ NO_2^-, ± 0.003 µmol L^{-1} for PO_4^{3-}, ± 0.011 µmol L^{-1} for $Si(OH)_4$ and ± 0.005 µmol L^{-1} for NH_4^+). Analyzer performance was controlled by monitoring baseline, calibration coefficients and slopes of the nutrient species over time. The variations observed throughout the experiment were within the analytical error of the methods.

Chl *a* and phytoplankton pigments

After vacuum filtration (< 200 mbar) of 250 to 500 mL integrated water samples for chl *a* and other phytoplankton pigments (0.7 µm GF/F, Whatman), filters were stored in cryovials at -20°C (chl *a*) and -80°C (pigments) until analysis by reverse-phase high-performance liquid chromatography (HPLC, Barlow *et al.* (1997)). For this, all pigments were extracted with acetone (100%) in plastic vials by homogenization of the filters using glass beads in a cell mill. The extract was then centrifuged (10 min, 800*g, 4°C), and the supernatant was filtered through 0.2 µm PTFE filters (VWR International). During all these steps the exposure of the samples to light was kept at a minimum. Concentration of phytoplankton pigments was determined by a Thermo Scientific HPLC Ultimate 3000 with an Eclipse XDB-C8 3.5u 4.6 x 150 column. CHEMTAX software was utilized for classifying phytoplankton based on taxon-specific pigment ratios (Mackey *et al.*, 1996) and calculating the contributions of individual phytoplankton groups to total chl *a* concentration.

Flow Cytometry

50 mL subsamples for flow cytometric analysis of phytoplankton were taken from the integrated water samples. From these subsamples, 650 µl per mesocosm were immediately analyzed within 3 hours using an Accuri C6 (BD Biosciences) flow cytometer. To verify the flow rate estimated by the Accuri C6, the volume difference of the samples before and after measurement was calculated at regular intervals by weighing. Phytoplankton populations were distinguished based on the signal strength of the forward light scatter (FSC), the red fluorescence from chl *a* light emission (FL3), and the orange fluorescence from phycoerythrin light emission (FL2) (Olson *et al.*, 1989; Bach *et al.*, 2017).

Primary production and photosynthesis irradiance response experiments

To estimate phytoplankton primary production and photophysiology, three 24 h ^{14}C-uptake primary production experiments on Days -1, 17, and 33, and six 2 h ^{14}C-uptake photosynthesis-irradiance (P-E) response experiments were conducted on Day -3, 3, 13, 23, 31, and 39 (based on techniques described in Strickland and Parsons (1972); Platt *et al.* (1980)). The 24 h primary production experiments (all mesocosms) were carried out in 1 L polycarbonate bottles, at ambient fjord temperature, and ~ 30% sunlight attenuated by neutral density screening. The P-E experiments were carried out on a subset of two ambient and two high pCO_2 mesocosms (M1, M3, M7, and M8) in a custom-made photosynthetron in 20 mL borosilicate bottles, at ambient fjord temperature, and ~ 15 - 1500 µmol quanta m^{-2} s^{-1}. All samples were filtered under dim light conditions onto 0.2 µm polycarbonate filters, acidified, measured via liquid scintillation counting (Beckman LS 6000), and dark-corrected. Daily primary production rates for the mesocosm study location were estimated from P-E experiments using 30% of MODIS-Aqua daily averaged estimated photosynthetically available radiation coupled to a daily solar position estimates (as described in Frouin *et al.* (2012)).

Phytoplankton

To determine phytoplankton abundance, a volume of 250 mL seawater sample was obtained from the IWS water, filled in brown glass bottles, and fixed with acidic Lugol's iodine (final concentration ≈ 1%). Phytoplankton counting was performed in settling chambers using an inverted microscope (ZEISS, Germany) according to Utermöhl (1931, 1958); Edler and Elbrächter (2010). Due to high abundances of diatoms at the beginning of the experiment, 50 mL settling chambers were used from Day -3 until Day 5, switching to 100 mL settling chambers thereafter to increase individual counts per species after diatom numbers

decreased. Identification was carried out to the species or genus level. See Dörner *et al.* (2020) for details.

Microzooplankton

For microzooplankton enumeration, 250 mL of seawater sample was taken every 8 days from the IWS water, fixed immediately with acidic Lugol's iodine solution (final concentration ≈ 1%), and stored in 250 mL brown glass bottles. Analysis was carried out using the Utermöhl technique (Utermöhl, 1931). See Dörner *et al.* (2020) for details.

Mesozooplankton (mesoZP)

Mesozooplankton samples were collected from Day -3 every 8 days through vertical net hauls from 19 m depth up to the surface (**Fig. 2**). On every zooplankton sampling day between 11:00 am and 1:00 pm, one net haul was conducted in every mesocosm as well as in the fjord in alternating order, to assure random sampling of the mesocosms between different sampling days. Sampling was carried out using a 100 cm long Apstein net with 55 µm mesh size and a 17 cm diameter cone-shaped opening. This resulted in a sampling volume of 431 L per net haul. The sampling interval of 8 days was chosen in order to minimize the influence on the mesozooplankton community. To get a more detailed overview of the starting conditions in the mesocosms, however, we conducted one additional mesoZP sampling one day after the first CO_2 addition (Day 1). Back in the laboratory, samples were immediately preserved in 70% EtOH. Prior to counting, the samples were split with a Folsom plankton splitter to ⅛ of the original sample. Starting with the first aliquot all organisms larger than 55 µm were counted in a Bogorov-chamber with a Leica stereomicroscope (MZ12) and specified to the lowest possible taxonomic level. Abundant taxa (> 50 individuals per aliquot) were only counted from subsamples, while less abundant taxa were counted from entire samples. Zooplankton abundance was calculated assuming 100% filtering efficiency of the net, and abundances were calculated as individuals per m^3 (ind m^{-3}).

Appendicularia

Collection of appendicularians using traditional plankton nets or pumping is too damaging to these fragile gelatinous animals. Moreover, *Oikopleura* is semelparous organism with a short life cycle, 6 days at 15°C (Bouquet *et al.*, 2009), about 11 days under the mesocosm temperature conditions (Bouquet et al. in prep). Since adult organisms die after reproduction and early stages may also be difficult to detect/identify and account for, abundance

continuously varies, between reproduction peak and rise of the next juvenile generation. Hence, to obtain more accurate abundance measurements, it is important to keep the highest sampling frequency permitted by the experimental design and overall mesocosm sampling volume limitation, using an adapted net. Consequently, in addition to the regular mesoZP sampling that also included appendicularia count, an extra net haul was conducted every 4 days (**Fig. 2**). The appendicularia net used during the experiment was designed and adapted to the scale of the mesocosm, in order to collect undamaged specimens, both for abundance quantification down to eggs, embryos and early tadpoles, and culture for parallel additional incubation experiments. The customized net was a 1 m long plankton net with a large cod-end (polycarbonate 3.8 L beaker, diameter of the beaker 17 cm). The opening of the net was 20 cm and the mesh size 55 µm. Vertical tows were manually performed, ~ 2 minutes to lower the net to 18 m and ~ 2 minutes to pull up, corresponding to a lowering and pulling rate of 0.15 m s^{-1}. For complementary information, technical description, methodology and results of parallel *O. dioica* laboratory incubation experiments under mesocosm conditions, see Bouquet et al. (in prep).

Hydrozoa

Samples for hydrozoa abundance data were obtained from the regular mesoZP net hauls preserved in 70% EtOH, the four fish larvae net hauls and the final full diameter net sampling (**Fig. 2**). Whenever mesoZP and fish larvae net hauls were conducted on the same sampling day, hydrozoa abundance data was first calculated as individuals per m^3 (ind m^{-3}) for each of the nets, and afterwards a mean was taken for calculating the final abundances. To obtain the numbers per net, always the entire net samples were scanned under a stereomicroscope (Leica MZ12). Counting of hydrozoa in the fish and final net was performed prior to preservation in 4% phosphate buffered formalin.

Atlantic herring larvae

To track the abundance of herring larvae during the experiment, two different methods were applied. First, dead larvae were manually picked out of the sediment trap samples (every second day) to monitor their mortality. Second, four net hauls with a 500 µm mesh size and 50 cm diameter net were performed after sunset on Day 13, Day 23, Day 29, and Day 37 (see **Fig. 2**). Moreover, all herring larvae that survived until the end of the experiment (Day 49) were caught with a full diameter sized net, towed through the entire water column of each mesocosm (1000 µm mesh size, 2 m diameter).

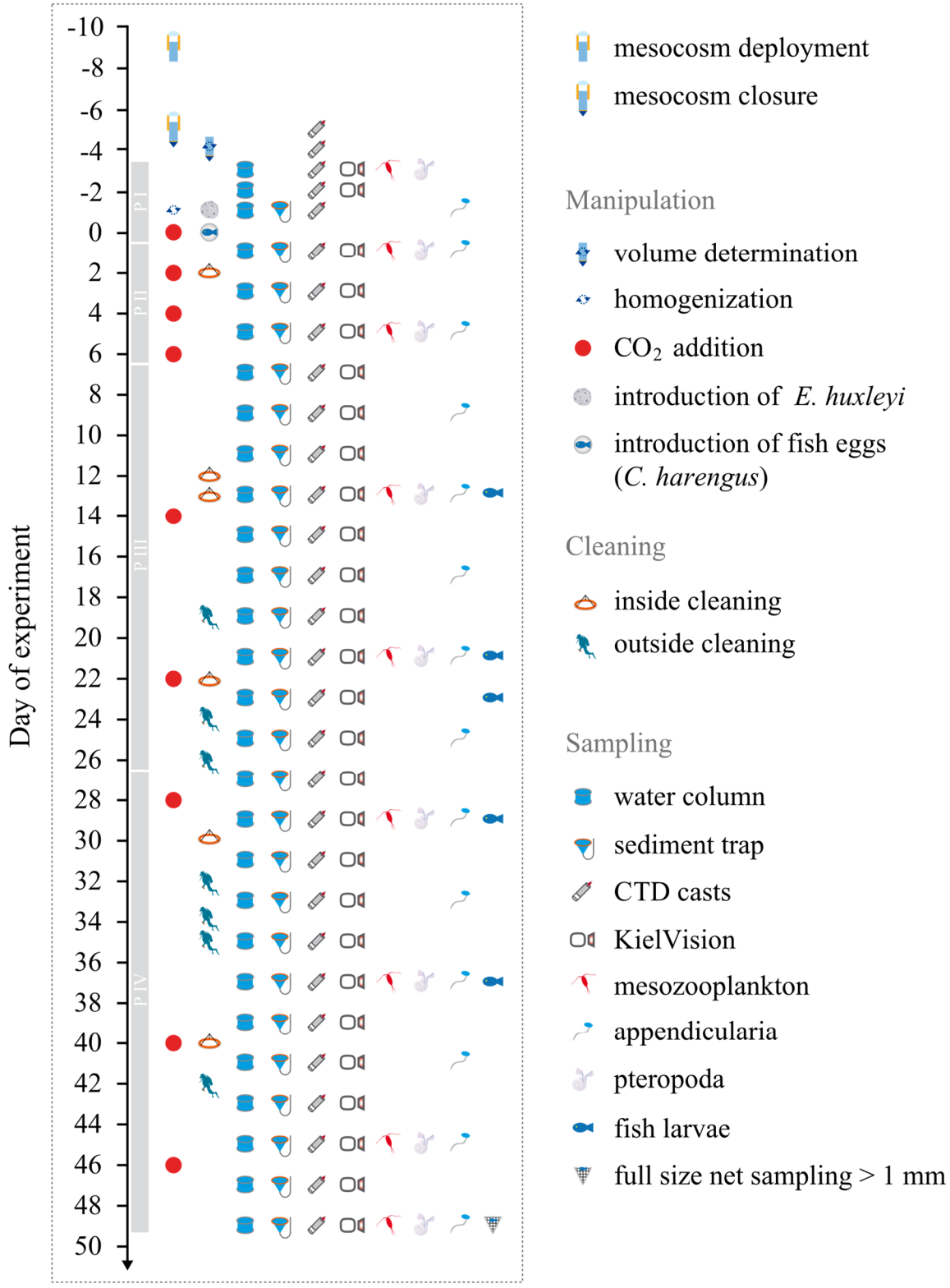

Figure 2: Overview of all sampling and maintenance activities over the course of the experiment, as described in detail in Section "Volume Determination", Section "CO_2 Addition", Section "Addition of Organisms to the Mesocosms", Section "Cleaning of Mesocosm Surfaces", and Section "General Sampling Procedure". Grey bars on the timeline represent the individual phases of the experiment as explained in **Tab. 2.** Figure assembled and designed with Adobe Illustrator CS4 (Adobe-Inc., 2008).

Data analysis

To analyze whether the OA treatment had a significant influence on the plankton community structure or on biogeochemical parameters of water column and sediment material, we conducted multivariate analyses using the "adonis" function within the 'vegan' package in R software version 3.4.2 in the RStudio environment (RStudio, 2016; Oksanen *et al.*, 2019; R Core, 2019). This function offers a directly analogous test to Permutational Multivariate Analysis of Variance (PERMANOVA) using distance matrices, and concurrently represents a robust alternative to ordination methods for describing how variation is attributed to different experimental treatments. Overall, this function was applied to plankton community data consisting of averages of the phytoplankton concentrations (µg L^{-1}, derived from pigment to chl *a* ratios from HPLC and CHEMTAX), the plankton abundances from microscopic counts of micro- (cells L^{-1}) and mesozooplankton (ind m^{-3}), as well as to the concentrations of the water column/sediment biogeochemical core parameters (µmol L^{-1}). To allow for statistical comparison of these diverse parameters with variable ranges of absolute numbers, the following function for data normalization was applied:

$$N_{norm} = \frac{N - N_{min}}{(N_{max} - N_{min})} \qquad \text{(Eq. 1)}$$

N_{norm} is the result of the individual value of the parameter N, divided by the difference between N_{max} and N_{min}, being the highest and lowest values for this certain parameter within all mesocosms on a sampling day. These normalized values were averaged according to the treatments and over time within four different phases of the experiment (for description of the phases see **Tab. 2**). Before the normalized mean data of every phase of the experiment were tested per phase in the PERMANOVA with regards to the factor pCO_2, every phase-dataset had to be pre-checked for the so called "multivariate spread" among single groups, similar to testing for variance homogeneity in univariate ANOVA. Therefore, the R function 'betadisper' as a multivariate analogue of Levene's test for homogeneity of variances was used (Anderson, 2006) and combined with an ANOVA applied to the betadisper result to check for significance. In case the ANOVA returned no significant multivariate spread between the single groups within the dataset, the PERMANOVA could be carried out based on a Bray-Curtis dissimilarity distance matrix. When a significant ($p < 0.05$) difference between the treatments of one phase was detected, a similarity percentage analysis (SIMPER) was used subsequently to reveal the contributions of the most influential species/parameters to this treatment effect.

For visualization of the results, the mean values per phase where plotted using non-metric multidimensional scaling (nMDS, performed by the metaMDS function from the vegan package in R) based on the same Bray-Curtis dissimilarity distance matrices as used for the PERMANOVA. The nMDS arranges any dissimilarities within the given parameters non-metrically onto an ordination space, where the distance between two points can be used as a hint of the degree of dissimilarity. Additionally, the standard error (SE) and the 95% confidence interval were calculated for every treatment in every phase and implemented as colored ellipsoids in the nMDS plots. The nMDS analysis was only carried out for the plankton data because with the biogeochemistry parameters the analysis provided inconclusive data output due to the low number of input parameters (too high stress values).

The univariate datasets of chl *a*, primary production, and the different inorganic nutrients were tested for treatment effects by means of a two-sample t-test performed with the R software version 3.4.2 in the RStudio environment. Thereby, a mean of the to-be-examined parameter was calculated per mesocosm per phase, or a certain time frame within a phase, grouped by high and control pCO_2, and tested for significant differences between treatment averages.

RESULTS AND DISCUSSION

Temperature and salinity

Over the course of the experiment the depth-integrated temperature in the mesocosms increased from initially 8.6°C (Day -3) to 10.4°C (Day 49) (**Fig. 3**). Temperature differences between the mesocosms were minimal, around 0.1°C. Warming of the surface layer in the second half of the experiment led to the development of a strong thermocline at about 10 m depth with a temperature decrease of ca. 2°C from 10 m to 15 m. This reflected the natural temperature development in the fjord (**Fig. 3**).

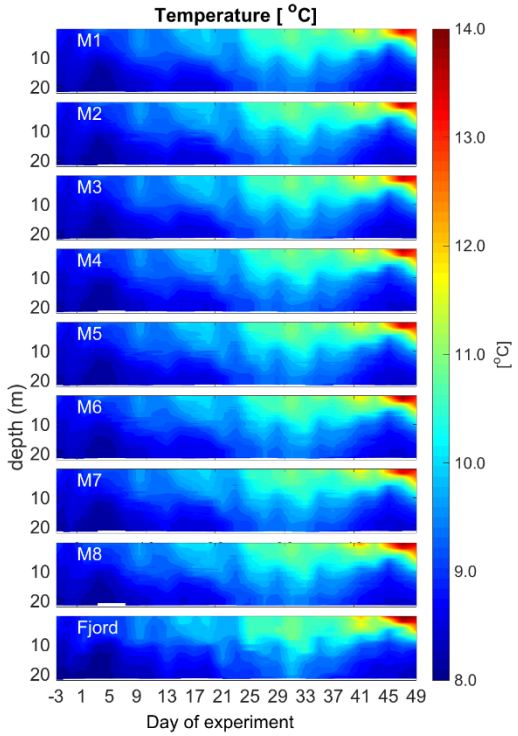

Figure 3: Overview of the CTD - depth profiles of temperature (°C) over the course of the experiment. Figure created with MATLAB (version R2013a).

Regarding salinity, there was no stratification detected inside the mesocosms. Additionally. average salinity of the enclosed water of all mesocosms was nearly constant during the experimental period, with a minor increase of 0.2 from 31.8 (Day -3) to 32 (Day 49) due to evaporation. The salinity in the surrounding water was more variable over time with an average of 31.44 and a halocline shifting between 10 m and 20 m (see **Appendix Fig. 1**).

Chlorophyll *a* and primary production

Up to the first CO_2 addition on Day 0, the mean chl *a* concentration was ≈ 2.2 µg L^{-1} (Day 1) in both treatments. It was, therefore, close to the initial values of 2.43 µg L^{-1} (± 0.24 SD) in the ambient pCO_2 and 2.44 µg L^{-1} (± 0.16 SD) in the designated high pCO_2 treatment on Day -3. During Phase II (Day 0 to Day 6) and early Phase III (up to Day 9), chl *a* decreased quickly to 0.94 µg L^{-1} (± 0.06 SD) in the ambient pCO_2, and to 0.8 µg L^{-1} (± 0.09 SD) in the high pCO_2 mesocosms. This decrease was accompanied by a reduced variance within the control and treated mesocosms (**Fig. 4**). From Day 9 onwards, the chl *a* concentration decreased constantly to 0.36 µg L^{-1} (± 0.03 SD, ambient) and 0.18 µg L^{-1} (± 0.04 SD, high) until the last day of the experiment, Day 49. Within this period of time, chl *a* concentration significantly deviated between the treatments during Phase III (t-test $p < 0.001$), and Phase IV (t-test $p = 0.03$). Overall, differences between the treatments were most pronounced on Day 17 with an average chl *a* concentration of 0.77 µg L^{-1} (± 0.1) and 0.43 µg L^{-1} (± 0.02) in the ambient and CO_2-enriched mesocosms, respectively. The difference between initial average chl *a* concentration in the mesocosms and the fjord (≈ 2.4 µg L^{-1} to ≈ 3.5 µg L^{-1}) is most likely a consequence of new water masses entering the fjord with high phytoplankton abundances between the day of mesocosm closure and the first sampling two days later (Day -3).

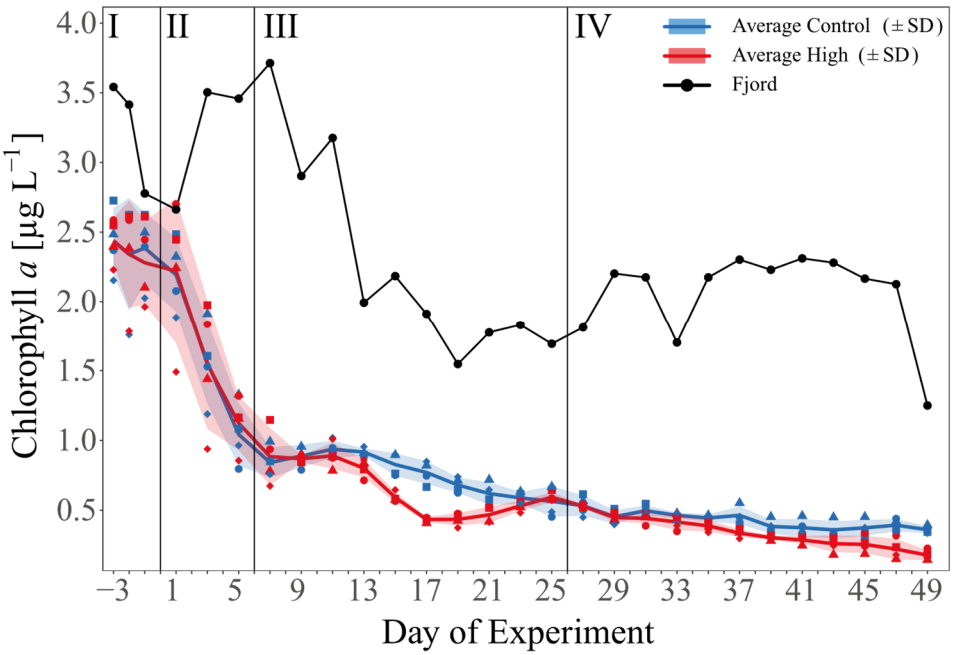

Figure 4: Temporal development of average chl *a* concentration over the course of the experiment. Blue, red, and black line indicate the respective average concentration in the control, high pCO_2 treatment, and the Fjord. The ribbons represent the standard deviations (SD). Blue symbols represent concentrations in the ambient pCO_2 mesocosms (M1, M2, M4, M7), red symbols in the high pCO_2 mesocosms (M3, M5, M6, M8), black symbols represent the fjord. For assignment of symbols to the individual mesocosms see **Tab. 1**. Roman numerals indicate the different phases of the experiment separated by vertical lines (for description of phases see **Tab. 2**). Figure created with the ggplot2 package in RStudio (RStudio, 2016; Wickham *et al.*, 2016).

Along with the decrease of chl *a*, the rate of primary production decreased from a mean of 2.01 µmol C L^{-1} d^{-1} (± 0.25 SD) in the control and 1.67 µmol C L^{-1} d^{-1} (± 0.2 SD) in treatment mesocosms on Day -1, to 0.93 µmol C L^{-1} d^{-1} (± 0.18 SD) and 0.92 µmol C L^{-1} d^{-1} (± 0.19 SD) on Day 31 (Phase IV, end of measurement), respectively. P^B_{max} (the light saturated rate of photosynthesis) also decreased, from 3.5 µg C µg chl a^{-1} h^{-1} (± 0.29 SD, control) and 3.32 µg C µg chl a^{-1} h^{-1} (± 0.07 SD, treatment) on Day -3, to 1.09 µg C µg chl a^{-1} h^{-1} (± 0.1 SD, control) and 1.29 µg C µg chl a^{-1} h^{-1} (± 0.25 SD, treatment) on Day 37 (end of measurement). Statistically, primary production and P^B_{max} measurements display only on Day 17 significantly higher mean values in the ambient mesocosms (t-test, $p < 0.05$, **Appendix Fig. 2**).

The observed decreases in chl *a*, primary production, and P^B_{max} indicate that the mesocosms were closed during or shortly after the peak of a phytoplankton bloom in the fjord and transitioned into nutrient limited post-bloom conditions, as also supported by inorganic nutrient concentrations (see results Section "Inorganic nutrients"). With that, the chl *a* response to high CO_2 is in line with experiments recently carried out in the Baltic, the

Mediterranean, and the North Sea, which suggested a more pronounced ecological impact of OA during low nutrient concentrations (Paul *et al.*, 2015; Bach *et al.*, 2016; Sala *et al.*, 2016). Furthermore, as the mesocosms exclude light in the UV range, the in this study observed negative effect on chl *a* and primary production might be further enhanced when extrapolating the results to open ocean environments. It was shown by e.g. Gao *et al.* (2019), that UV radiation can interact with OA, possibly even intensifying a negative OA effect.

Inorganic nutrients

Along with the late/ post bloom temporal development visible in the chl *a* concentrations, inorganic nutrients decreased and/ or stayed low in all mesocosms over the course of the experiment. Dissolved silica hardly exceeded the detection limit of 0.005 µmol L^{-1} with an overall mean of 0.017 µmol L^{-1} (± 0.015 SD) in the ambient and 0.009 µmol L^{-1} (± 0.006 SD) in the high pCO_2 mesocosms (**Fig. 5D**), thus indicating silicate limitation for diatoms and other silicifiers. In the bioavailable N pool, neither nitrate and nitrite nor ammonium showed any treatment differences over time. Nitrate and nitrite only took up a higher proportion of the total accessible N in Phase I of the experiment, with 0.27 µmol L^{-1} (± 0.05 SD) and 0.37 µmol L^{-1} (± 0.13 SD) in the ambient and designated high pCO_2 treatment, respectively. Afterwards they decreased until Phase IV to means of 0.08 µmol L^{-1} (± 0.03 SD) in the ambient and 0.09 µmol L^{-1} (± 0.05 SD) in the high CO_2 mesocosms. Compared to ammonium overall mean concentrations of 0.36 µmol L^{-1} (± 0.12 SD) in the ambient mesocosms and 0.41 µmol L^{-1} (± 0.18 SD) in the high pCO_2 treatment, most of the accessible N during the CO_2 enrichment and post bloom phases was provided by ammonium as a result of the predominating remineralization processes in the mesocosms. Therefore, the concentrations of nitrate, nitrite and ammonium were combined to a total N concentration ($N_{Total} = NO_3^- + NO_2^- + NH_4^+$) with an overall mean concentration of 0.47 µmol L^{-1} (± 0.14 SD) in the ambient and 0.54 µmol L^{-1} (± 0.22 SD) in the high pCO_2 mesocosms (**Fig. 5A**). The same pattern was visible in the phosphate concentrations, but the measured concentrations were low and close to the detection limit. During Phase I, PO_4^{3-} was available with 0.07 - 0.08 µmol L^{-1} in all mesocosms and decreased afterwards to 0.04 µmol L^{-1} (± 0.014 SD) in the control mesocosms and 0.05 µmol L^{-1} (± 0.006 SD) in the high pCO_2 treatment (**Fig. 5B**). Additionally, the difference in the chl *a* concentration between Days 13 and 21 (**Fig. 4**) is conversely visible in the phosphate concentration, with a higher concentration in the high pCO_2 treatment between Days 17 and 23 (difference 0.016 µmol L^{-1}, **Fig. 5B**). The lower chl *a* concentration in the high pCO_2 mesocosms during

this period indicates that a lower phytoplankton biomass led to the lower phosphate consumption compared to the ambient pCO_2 mesocosms. This is furthermore supported by the absences of a treatment separation between Days 17 and 23 in the inorganic N_{Total}, and a higher N_{Total}:P ratio in the particulate matter of the mesocosm water column of the high pCO_2 treatment during this time. The lower P consumption of the organisms thereby led to the higher N_{Total}:P ratio. Together with a steady low inorganic N_{Total} and an enhanced inorganic P concentration, this resulted in a lower inorganic N_{Total}:P ratio under high pCO_2, which is, although without statistical significance (SIMPER p = 0.288), visible between Days 13 and 21. The average N_{Total}:P ratios over the complete experimental period stayed below Redfield (16:1, Redfield *et al.* (1963)), and fluctuated around a mean of 11.91 (± 4.32 SD) in the ambient and 11.73 (± 4.51 SD) in the high pCO_2 mesocosms (**Fig. 5C**).

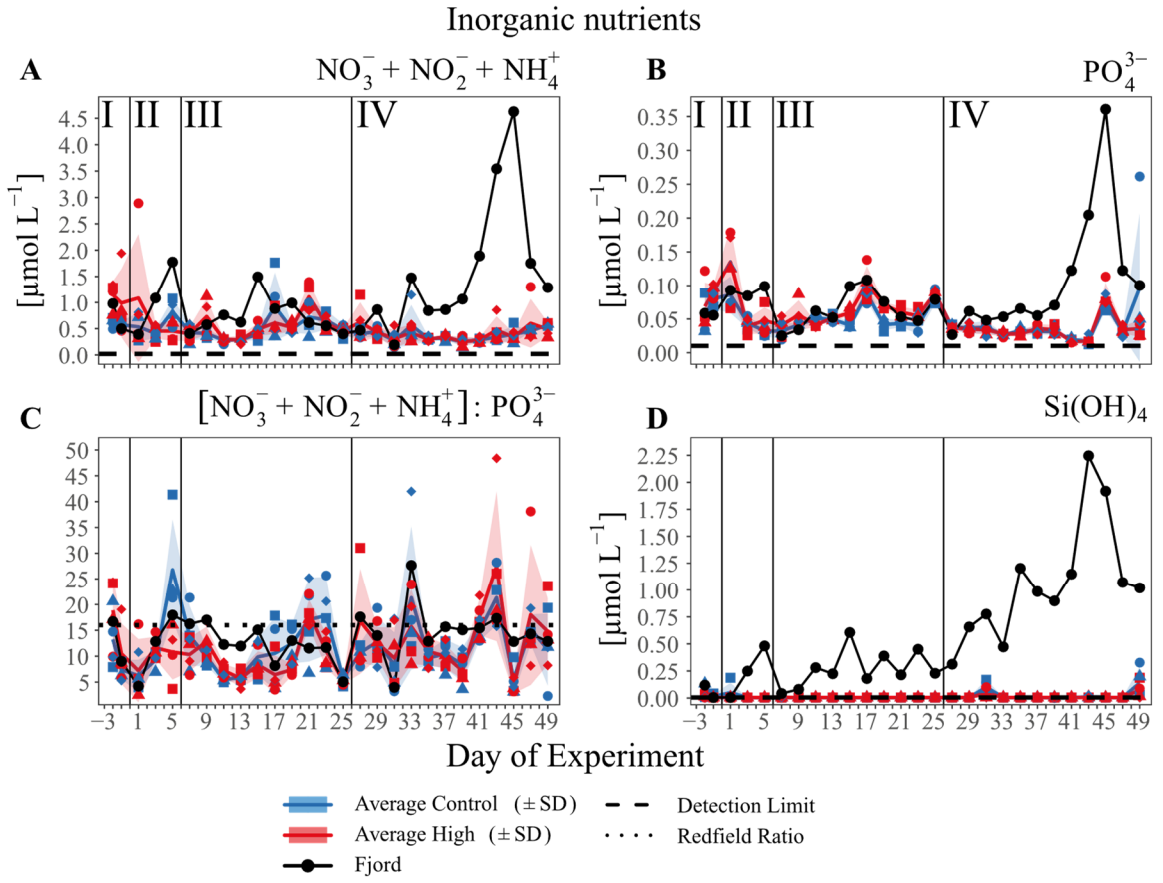

Figure 5: Nutrient concentrations of **(A)** total N = nitrate + nitrite + ammonium (NO_3^-+ NO_2^- + NH_4^+), **(B)** phosphate (PO_4^{3-}), **(C)** total N :P ratio and **(D)** dissolved silica $Si(OH)_4$ over the course of the experiment. Lines, symbols, and colors are used as described in **Fig. 4**. For assignment of symbols to the individual mesocosms see **Tab. 1**. Roman numerals label the different phases of the experiment separated by vertical lines (for description of phases see **Tab. 2**). Figure created with the ggplot2 package in RStudio (RStudio, 2016; Wickham *et al.*, 2016).

Carbonate Chemistry

Before CO_2-manipulation (Phase I), the average pCO_2 in the ambient mesocosms was 271 µatm (± 4 SD), and 272 µatm (± 4 SD) in the designated high pCO_2 treatment (**Fig. 6A**). Accordingly, average Phase I pH_T in all mesocosms was nearly identical, with 8.18 (± 0.004 SD) (**Fig. 6B**). Calcium carbonate ($CaCO_3$) saturation states of calcite ($\Omega_{calcite} \approx 3.5$) and aragonite ($\Omega_{aragonite} \approx 2.2$) exceeded the threshold of 1 in this initial phase.

From Day 0 on, the stepwise CO_2 additions increased the pCO_2 of the high treatment from initially 271 µatm to on average 553 µatm (± 20 SD) on Day 1, 821 µatm (± 30 SD) on Day 3, 1690 µatm (± 30 SD) on Day 5, and 2069 µatm (± 50 SD) on Day 7. As a result of this increase in pCO_2, the pH_T of the high pCO_2 mesocosms decreased to 7.36 (± 0.01 SD), and $\Omega_{calcite}$ and $\Omega_{aragonite}$ both dropped below 1 (≈ 0.6 and ≈ 0.4, respectively), leading to corrosive conditions for $CaCO_3$. Due to repeated CO_2 additions (see Section "CO_2 addition") the extreme pCO_2 conditions in the CO_2-enriched mesocosms were maintained througout the experiment, with Phase III and IV means of 1978 µatm (± 60 SD) and 2012 µatm (± 50 SD), respectively. In the control mesocosms, the pCO_2 increased over the course of the study due to rising water temperature and ingassing of atmospheric CO_2 from initially 271 µatm (± 4 SD, Phase I), to 365 µatm (± 5) on Day 49. Consequently, the pH_T decreased by about 0.1 unit to 8.07 (± 0.01 SD), and $\Omega_{calcite}$ and $\Omega_{aragonite}$ declined to ≈ 3.0 and ≈ 2.0, respectively. Similar changes in the carbonate chemistry were also observed in the surrounding fjord water (**Fig. 6**).

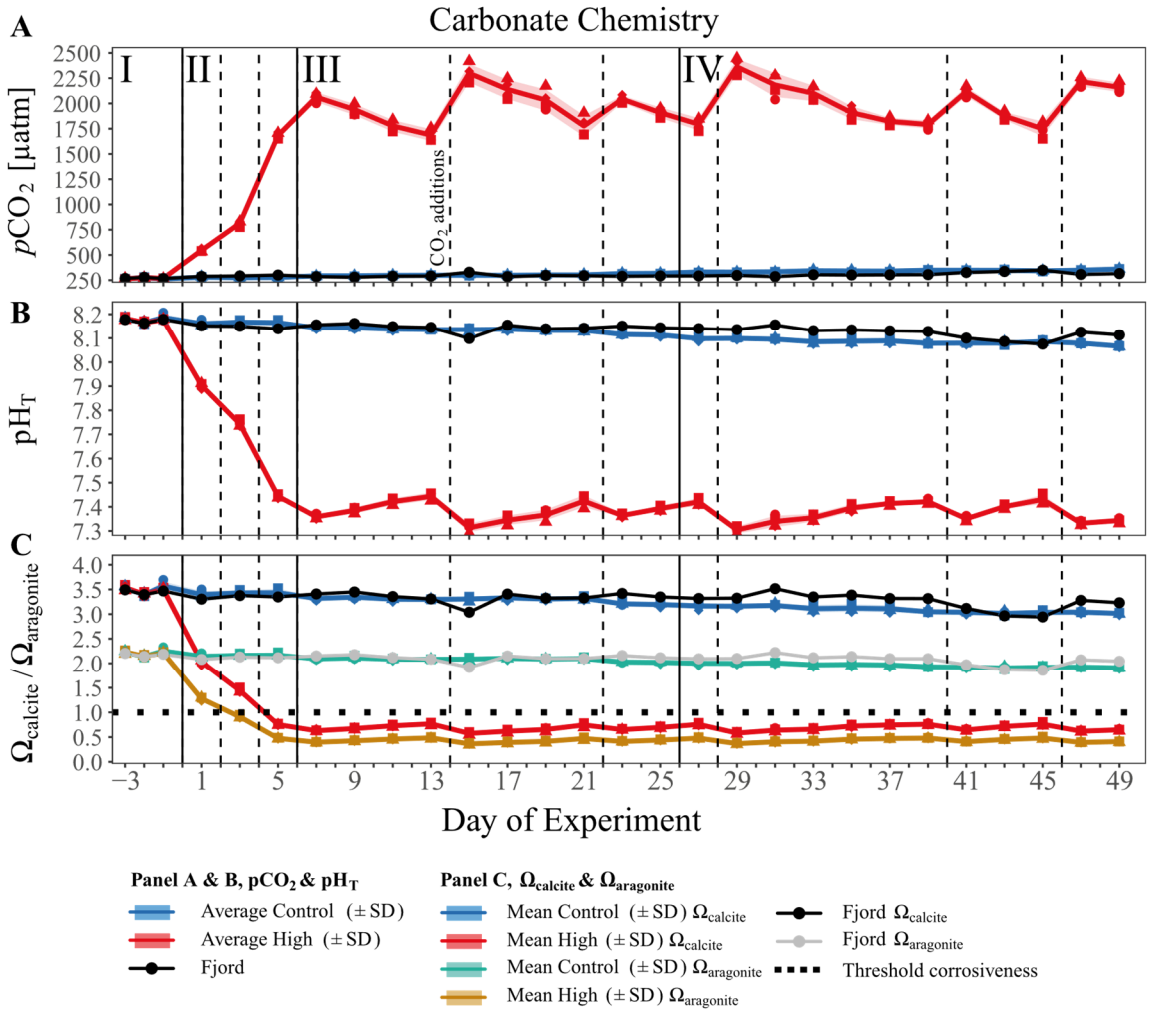

Figure 6: Overview of the carbonate system parameters. **(A)** Development of the partial pressure of CO_2 in µatm, **(B)** the pH on the total scale (pH_T), and **(C)** $\Omega_{calcite}$ (blue and red lines) and $\Omega_{aragonite}$ (green and yellow lines) over the course of the experiment. Lines, symbols, and colors are used as described in **Fig. 4**. Dashed lines indicate CO_2 additions as shown in **Fig. 2**, and described in Section "CO_2 addition". Roman numerals label the different phases of the experiment separated by vertical lines (for description of phases see **Tab. 2**). Figure created with the ggplot2 package in RStudio (RStudio, 2016; Wickham *et al.*, 2016).

Effects of high pCO_2 on the plankton community

To examine the effects of high pCO_2 levels and the related changes in seawater carbonate chemistry on the post-bloom plankton community, we analyzed the composition and succession patterns of the phytoplankton, micro-, and mesozooplankton communities during the different experimental phases. The analysis was performed from a whole-community perspective, rather than considering single-species responses. More detailed analyses of individual phyto-, microzoo-, and mesozooplankton groups and species will be provided in separate studies that are in preparation.

Phase I

During the first phase, the PERMANOVA did not reveal significant differences of the plankton community composition between the control and the high pCO_2 treatment (P(perm) = 0.113). The corresponding non-metric multidimensional scaling (nMDS) plots for Phase I supports this result (**Fig. 7 I**), and is with a stress value of 0.08 considered a reliable depiction of the multivariate dataset. Additionally, the overall small spread of data/response variables of both, high and control pCO_2 mesocosms in the chosen two-dimensional space indicates that the plankton community composition of the mesocosms was overall similar. Nevertheless, the mesocosms displayed a tendency to ordinate according to their designated treatment which can be explained by SIMPER analysis. The test identified a significantly elevated average chl *a* concentration related to increased numbers of Cyanophyceae ("Cyano", µg L^{-1}) in the high pCO_2 treatment, slightly separating the mesocosms in the two-dimensional space.

Phase II

The treatment separation indicated in Phase I developed even further during the acidification process in Phase II of the experiment, resulting in a significant split-up of the mesocosms according to their treatment (P(perm) = 0.032). However, SIMPER identified only one significant influence to this separation, being higher abundances of the appendicularian *Oikopleura dioica* ("Oiko", ind m^{-3}) in the control mesocosms. This is well illustrated by the Phase II nMDS plot (**Fig. 7 II**, stress = 0.114). Although the mesocosms are still overall close together, their "within treatment" internal variation is reduced, and in combination with the significant effect on *O. dioica*, a visible separation is caused.

Phase III

With the pCO_2 manipulation fully established in Phase III, the significant difference between the plankton communities of the control and the treatment mesocosms got more pronounced (P(perm) = 0.028, **Fig. 7 III)**. The SIMPER analysis revealed, that 7 different taxa accounted for 36.2% of the detected difference between the treated and the control mesocosms (p = 0.026). The most influential taxa in this context were Gastropoda ("Gastro", ind m^{-3}), Prymnesiophyceae ("Prym", chl *a* µg L^{-1}, mainly Coccolithophoridae, i.e. *E. huxleyi*), Dinophycaea ("Dino", chl *a* µg L^{-1}), and Echinodermata ("Echino", chl *a* µg L^{-1}), all with negative responses in abundance to the extreme OA level (see **Appendix Tab. 3**). Positive responses to OA in this phase were observed for diatoms and *Acartia* spp. copepodites. Furthermore, the significant contribution of gastropods, echinoderms, autotrophic

microplankton ("MiPl(Auto)"), and copepodites of *Acartia* spp. ("AcartiaCop") to the treatment separation emphasizes that OA did not only influence the primary producers in this study but also to a large extent the mesozooplankton community. In the corresponding nMDS plot (stress: 0.063) this becomes apparent as an obvious separation of the high pCO_2 treatment and the control in the ordination space following the effects on those taxa (see **Fig. 7 III**).

Interpretation of observed CO_2 effects during Phase III

The negative effect on calcifiers (here Gastropoda) is well in line with previous studies (Lischka *et al.*, 2011; Wittmann & Pörtner, 2013), and reflects the well-studied mechanism of lower calcification rates and/or $CaCO_3$ dissolution due to the low carbonate saturation states under high pCO_2-levels. The effects of high pCO_2 on echinoderms are variable, as studies with comparable durations and pH values revealed both negative and positive OA effects on factors like growth rate, calcification, and survival (Dupont *et al.*, 2010). This is consistent with our results, which showed an initial negative impact on echinoderms in Phase III, and no detectable effect in Phase IV (**Fig. 7 IV)**. This suggests that the treatment effect on echinoderm larvae abundances in Phase III could have been triggered indirectly via food availability and not necessarily directly by high pCO_2 impacts on the organism's physiology. The same can be assumed for the observed positive treatment effect on the abundances of *Acartia* spp. copepodites. A direct response to these OA levels would more likely be a negative one, as Zhang *et al.* (2011) found a negative response of *Acartia spinicauda* at a similar pCO_2 level of 2000 µatm, and Cripps *et al.* (2014) detected decreasing numbers of *Acartia tonsa* nauplii already at 1000 µatm. However, these experiments were carried out under controlled laboratory conditions, and did not account for complex changes in a natural food web. Nevertheless, within a natural community influenced by such an extreme level of OA, the indirect positive effect on *Acartia* spp. copepodites observed in this study is not consistent with previous findings. For example, Niehoff *et al.* (2013) (pCO_2 up to 1420 µatm) and Hildebrandt (2014) (pCO_2 up to 3000µatm) studied *Acartia* spp. under elevated pCO_2 conditions in comparatively mesocosm experiments but did not observe any significant effects. This large variability of CO_2 effects points towards the importance of food-web structure and related trophic cascades in determining the response of zooplankton to OA.

Phase IV

The nMDS plot of the second post-bloom period (Phase IV) suggests that dissimilarities between the control and treatment mesocosms (stress: 0.02) further increased during this phase. The two-dimensional space separating control and treatment from each other increased and the internal variability within the treatments decreased (**Fig. 7 IV**). Consistent with this visual impression, the PERMANOVA of Phase IV plankton data revealed a significant treatment effect (P(perm) = 0.028) and the subsequent SIMPER analysis yielded 14 planktonic taxa that accounted for ≈ 55% of the observed dissimilarities (p = 0.03). The four most influential taxa were Chlorophyceae ("Chloro"), Cyanophyceae ("Cyano"), Gastropoda ("Gastro", mostly veliger larvae), and appendicularians ("Oiko", represented by the species *Oikopleura dioica*), as also indicated by arrow orientation and length in the associated nMDS plot. Compared to Phase III, the contribution of mesozooplankton taxa to the treatment dissimilarities increased from 43% (3 out of 7) to 57% (8 of 14) in Phase IV. While we found negative effects on the abundance of calcifying organisms (Gastropoda and Bivalvia larvae), autotroph and heterotroph protists, and the koppebruder *Microsetella* spp. ("Microsetella"), positive effects of OA were visible in the abundances of all the remaining mesoZP taxa: *Oithona* spp. copepodites ("OithonaCop"), *Calanus* spp. copepodites ("CalCop"), *O. dioica*, hydrozoa, and the abundance of *Clupea harengus* larvae ("Clupea") (see **Appendix Tab. 3**).

Interpretation of observed CO_2 effects during Phase IV

The fact that elevated pCO_2 levels can alter phytoplankton communities to the advantage or disadvantage of the inherent taxa was already shown in a variety of studies (Dutkiewicz *et al.*, 2015). Furthermore, the specific response of a certain region or plankton community strongly depends on the predominant environmental conditions and community composition. Under the given complexity of the enclosed plankton community, it is challenging to distinguish between direct and indirect pCO_2 effects. An example for the possible mixture of both is the negative effect on Cyanophyceae observed in Phase IV. In a comparable mesocosm study, Bach *et al.* (2017) observed negative as well as positive effects on Cyanophyceae under elevated pCO_2 (760 µatm), and stated that it was most likely an indirect food web effect, although they could not exclude the possibility of a direct CO_2 effect. Apparently easier to determine is the here observed negative effect on Prymnesiophyceae, most likely being a direct effect on the calcifier *E. huxleyi* in this group. This direct negative effect on Prymnesiophyceae was also confirmed under different

elevated pCO_2 scenarios (ranging from 700 to 3000 µatm) in different large scale mesocosm experiments (Engel *et al.*, 2008; Hopkins *et al.*, 2010; Riebesell *et al.*, 2017) as well as at an Antarctic coastal site (Thomson *et al.*, 2016). As already discussed for the results of Phase III, positive or negative effects on copepods depend to a large degree on trophodynamic interactions and community composition. However, in contrast to the present study, most experiments do not account for indirect food web effects that may occur in natural communities. As already pointed out for the positive treatment effect on *Acartia* spp. in Phase III, a direct positive effect of OA on the mesoZP taxa in Phase IV seems unlikely. *Calanus* spp. were generally observed to be able to tolerate pCO_2 values > 3000 µatm (Weydmann *et al.*, 2012; Hildebrandt, 2014) without effects on survival, hatching success or egg production. Younger stages of *Oithona* spp. were reported to be more sensitive to OA regarding their growth rate and survival (Lewis *et al.*, 2013; Pedersen *et al.*, 2014a), but mesocosm studies by Niehoff *et al.* (2013) and Hildebrandt (2014) did not find any OA treatment effect on either of these species. On the other hand, experiments by Harris *et al.* (2000) and Søreide *et al.* (2008) revealed that diatoms and Cryptophyceae, both of which were positively influenced in Phases III and IV of our experiment, make up the main prey of *Calanus* spp. This enhanced food availability could indirectly have supported the positive responses of *Calanus* spp. and *Oithona* spp. in the high pCO_2 mesocosms, which then in turn indirectly could have triggered the positive response of Hydrozoa in the manipulated mesocosms. A direct effect on Hydrozoa in this context is unlikely, as there is currently no scientific work known to the authors that suggests the possibility of a direct positive CO_2 effect. So far, it is rather suspected that there is a direct negative CO_2 effect on the jellyfish balance sensory receptors made of basanite (Werner, 1993). The observed positive effect on *O. dioica* abundances, however, is very likely a direct OA effect. It was shown by Bouquet et al. (in prep) with parallel incubation experiments using specimens and water from the mesocosms during our study, that the fecundity of *O. dioica* was significantly higher under high pCO_2 (334 ± 140 eggs) compared to low pCO_2 (278 ± 107 eggs, ANOVA: $F_{(1,6)} = 8.60$; $p = 0.0262$). A result that already also was observed in other laboratory and mesocosms studies, although not investigated under such extreme pCO_2 conditions (Troedsson *et al.*, 2012; Winder *et al.*, 2017; Bouquet *et al.*, 2018).

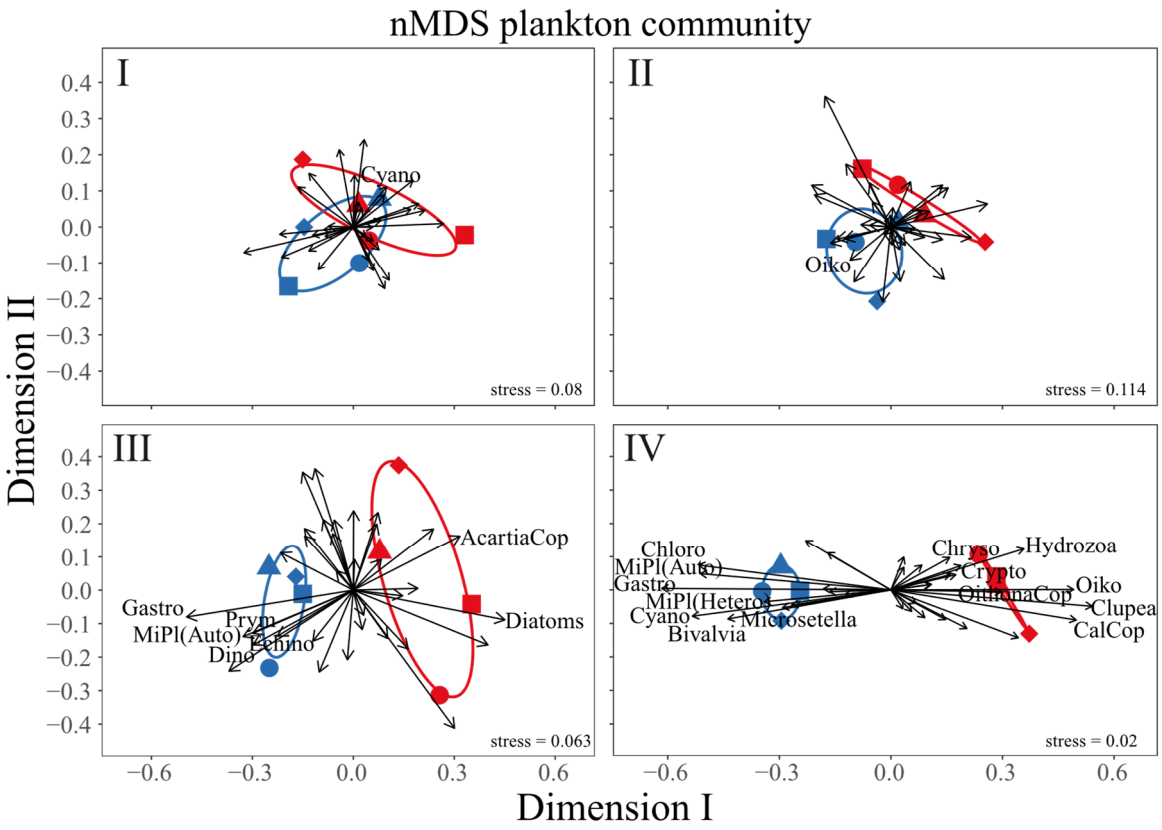

Figure 7: Non-metric dimensional scaling (nMDS) plots of range normalized mesocosm plankton community data for the different phases of the experiment. **(I)** The initial phase before CO_2 addition. **(II)** Establishing of target pCO_2 values and transition from bloom to post-bloom conditions. **(III)** First phase of post-bloom conditions and treatment effect. **(IV)** Final post-bloom phase. Stress values indicate how accurate dissimilarities among plankton communities in the mesocosms are depicted, arrows indicate the role of the various plankton groups for spatial organization of the mesocosms. **AcartiaCop** = *Acartia* spp. copepodites, **CalCop** = *Calanus* spp. copepodites, **Chloro** = Chlorophyceae, **Chryso** = Chrysophyceae, **Clupea** = *Clupea harengus* larvae, **Crypto** = Cryptophyceae, **Cyano** = Cyanophyceae, **Diatoms** = Bacillariophyceae, **Dino** = Dinophyceae, **Echino** = Echinodermata larvae, **Gastro** = Gastropoda larvae, **MiPl(Auto)** = autotrophic microplankton, **MiPl(Hetero)** = heterotrophic microplankton, **OithonaCop** = *Oithona* spp. copepodites, **Oiko** = *Oikopleura dioica*, **Prym** = Prymnesiophyceae. Figure created with the ggplot2 package in RStudio (RStudio, 2016; Wickham *et al.*, 2016).

Hypothesis (1): Plankton community composition/structure will change under extreme pH values

Our first hypothesis can be confirmed. We observed an overall restructuring of the plankton community under high pCO_2 on multiple trophic levels of the food web, ranging from primary producers to herbivorous and carnivorous consumers. Besides direct negative OA effects on calcifying organisms like Gastropoda, Bivalvia, and Prymnesiophyceae (mainly Coccolithophoridae), indirect effects via the food web were the main drivers of the significant OA treatment separation (see also **Fig. 10**). In this context, positively affected Bacillariophyceae and Cryptophyceae, inter alia, triggered higher abundances of

Calanus spp., *Oithona* spp. and *Acartia* spp., probably supporting an increase of Hydrozoa and *Clupea harengus* larvae (**Fig. 10**). Together with higher numbers of filter feeding appendicularians, this led to a substantial increase of top-down control in the food web.

Effects of high pCO_2 on biogeochemistry

In order to examine how the observed restructuring of the plankton community influenced the biogeochemical cycling in the enclosed water bodies, suspended particulate carbon, nitrogen, phosphorus and biogenic silica concentrations (µmol L^{-1}) were analyzed as well as the respective vertical flux of these elements collected in the sediment traps (µmol L^{-1} 48 h^{-1}).

Phase I & II

In Phase I as well as during the transition from bloom to post-bloom conditions in Phase II, PERMANOVA and SIMPER analysis did not uncover a significant difference between the ambient and high pCO_2 mesocosms in any of the particulate organic matter (POM) parameters in the water column (POM_{WATER}) or in the collected sediment trap samples (POM_{SED}) (Phase I: P(perm) = 1.0000, Phase II: P(perm) = 0.5966). The mean POC_{WATER} value of the designated treatment mesocosms was 19.95 µmol L^{-1} (± 1.33 SD) in Phase I, and 20.42 µmol L^{-1} (± 0.99 SD) during the acidification Phase II, while the control mesocosms had POC_{WATER} values of 20.84 µmol L^{-1} (± 1.31 SD), and 20.71 µmol L^{-1} (± 1.39 SD), respectively (**Fig. 8A, Tab. 3**). Accordingly, there was no treatment effect visible in the related POC_{WATER}:PON_{WATER} ratios in Phases I and II (**Fig. 9A**). The POC_{SED}:PON_{SED} ratio in Phase II showed a slightly increasing trend (**Fig. 9B**), and was in the high pCO_2 treatment as well as in the control, higher than the water column ratios (**Tab. 3**). This indicates that the emerging nutrient limitation lead to the preferential remineralization of N over C, as already observed for example by Stange *et al.* (2018) or Schneider *et al.* (2003). Furthermore, the stable or even slightly increasing concentrations of POC_{WATER} in combination with the decreasing POC_{SED} flux (**Fig. 8A & 8B**), and the sharp decrease of chl *a* (**Fig. 4**) and primary production in Phase II suggest that the biomass of the fading bloom was retained in the water column, i.e. being efficiently recycled by heterotrophs and/or consumed by mesozooplankton, hydrozoans or fish larvae.

Phase III

In Phase III, a significant difference between ambient and high pCO_2 mesocosms was observed in POM_{WATER} data by PERMANOVA (P(perm) = 0.031), which coincides with

the emergence of significant CO_2 effects on the plankton community composition. The similarity percentage analysis did not identify any effect on one of the POM_{SED} parameters, but revealed a significant negative effect on POC_{WATER}, TPP_{WATER}, and PON_{WATER} as major factors for the difference between the control and the treatment ($p = 0.032$). POC_{WATER} decreased further during Phase III in both ambient and high pCO_2, but in comparison concentrations stayed higher in the ambient pCO_2 mesocosms (**Fig. 8A**, **Tab. 3**). The opposite was found in the POC_{SED} flux (see **Fig. 8B**, **Tab. 3**), indicating that carbon export was temporarily enhanced under high pCO_2 conditions. POC_{WATER}:PON_{WATER} was not significantly different between the high and ambient pCO_2, but both exceeded the Redfield Ratio (6.6, **Fig. 9A**, **Tab. 3**). The PON_{WATER}:TPP_{WATER} ratio increased over time but displayed no treatment differences (**Fig. 9C**, **Tab. 3**). POC_{SED}:PON_{SED} ratio of sinking particles increased in the first half of Phase III (until Day 11, **Fig. 9B**), and then decreased sharply to 8.80 (± 0.31 SD) under ambient pCO_2 and 7.94 (± 0.28 SD) in the high pCO_2 mesocosms. Subsequently, ambient and high pCO_2 start to deviate until the end of Phase III with 7.76 (± 0.47 SD) in the high pCO_2, and 8.43 (± 0.24 SD) in the ambient pCO_2 mesocosms on Day 25. As already observed in Phase II, the POC_{SED}:PON_{SED} ratio was higher, and the PON_{SED}:TPP_{SED} lower than the respective ratios in the water column, indicating preferential remineralization of N over P and C.

Phase IV

The high pCO_2 treatment effect continued in Phase IV at a comparable scale. The PERMANOVA result was significant (P(perm) = 0.027), and SIMPER revealed the same major contributing parameters POC_{WATER}, and TPP_{WATER} ($p = 0.029$), albeit with a lower percentage contribution on the treatment differences (≈ 38% compared to ≈ 48% in Phase III). POC_{WATER} concentration in this phase was significantly higher in the ambient pCO_2 mesocosms than under high pCO_2 conditions (see **Fig. 8A**, **Tab. 3**). As in Phase III, SIMPER does not point towards any of the export flux parameters to drive the treatment differences, with a similar average POC_{SED} between ambient and high pCO_2 treatment (**Fig. 8B**, **Tab. 3**). The cumulative ΣPOC_{SED} data, however, supports the observed OA treatment effects in POM_{WATER}. In accordance with the significant negative effect on the concentration of POC_{WATER}, the cumulative mean ΣPOC_{SED} flux increased in the high pCO_2 treatment from 4.59 µmol L^{-1} (± 0.44 SD) at the beginning of Phase III to 14.38 µmol L^{-1} (± 1.08 SD) at the end of Phase IV (see **Fig 8C**). Compared to the ambient pCO_2 mesocosms, this gave a final treatment difference of 1.8 µmol L^{-1} on Day 49 (ambient pCO_2: 12.58 µmol L^{-1} ± 0.49 SD).

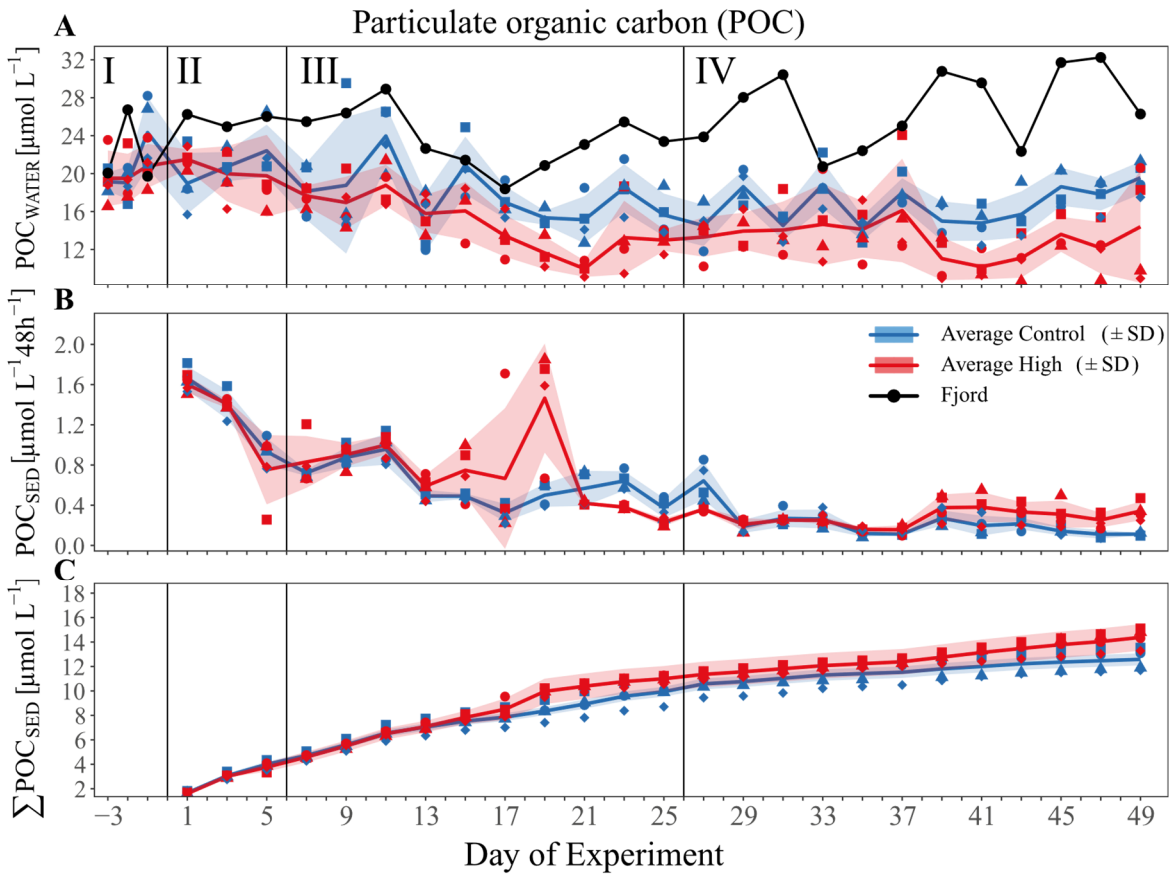

Figure 8: Overview of particulate organic carbon (POC) concentrations and vertical fluxes. Development of **(A)** POC concentration within the water column **(B)** the 48 h POC flux collected in the sediment traps, and **(C)** the cumulative vertical POC flux over the course of the experiment. Lines, symbols, and colors are used as described in **Fig. 4**. Roman numerals label the different phases of the experiment separated by vertical lines (for description of phases see **Tab. 2**). Figure created with the ggplot2 package in RStudio (RStudio, 2016; Wickham *et al.*, 2016)

Hypothesis (2): Extreme pH will accordingly (along with the plankton community changes) influence the biogeochemistry in the enclosed ecosystem

Our observations of OA effects on biogeochemical parameters in Phases III and IV along with the consistent treatment differences already observed in chl *a*, lead to the confirmation of our second hypothesis. The reduced phytoplankton biomass in the high pCO_2 treatment was also seen in POM_{WATER} concentrations. Reduced POM_{WATER}, in turn, is reflected in higher POM_{SED} export flux. This could suggest that POM was less efficiently recycled in the high pCO_2 treatment. Alternatively, when considering the already observed restructuring of the mesoZP-community, the higher mean export flux of POM_{SED} in the high pCO_2 treatment in Phases III and IV could be driven by the positive OA effects on zooplankton abundances. In this case, the lower concentrations of chl *a* and POM_{WATER} under high pCO_2 could be explained with more dominant top-down control. Indeed, grazing pressure on phytoplankton may have been sufficient to directly transfer any new production to higher trophic levels.

This hypothesis of a stronger top-down controlled community in the high pCO_2 treatment leading to higher export flux seems likely if one considers the positive development of the abundances of the two major copepod species *Calanus* spp. and *Oithona* spp. Also, higher hydrozoan and fish abundances, combined with a pronounced negative effect on the abundance and biomass of autotrophic and heterotrophic protists (see also Dörner *et al.* (2020)) points towards the interpretation of increased top-down control. Furthermore, the observed positive effect on the abundances of the appendicularian *Oikopleura dioica* in Phase IV fits in this hypothesis, as these organisms are well known to graze highly efficient on their phytoplankton prey. Additionally they create a high export potential by discarding their mucus housings filled with water column particles, thus causing the already mentioned increase in POM_{SED} export flux (Troedsson *et al.*, 2012).

Furthermore, we observed OA impacts on elemental stoichiometry of particulate matter. We found a lower C:N value under high pCO_2 conditions, which is contrary to previous studies which reported increasing C:N ratios under high pCO_2 (e.g. Riebesell et al. 2007), due to enhanced carbon overconsumption by phytoplankton under bloom conditions. One possible reason for this contradiction could be that our study was conducted during post-bloom conditions, and the observed negative C:N response reflects altered consumption (and preferential N remineralization) by secondary consumers. The PON_{WATER}:TPP_{WATER} ratio did not reveal any differences between the treatments, despite the significant effect detected in TPP_{WATER}. PON_{WATER}:TPP_{WATER} increased in both treatments during Phase IV, because of an increase in PON_{WATER}, and constant or even slightly decreasing concentrations of TPP_{WATER}. The sediment flux ratio POC_{SED}:PON_{SED} continued its decreasing trend in Phase IV, and indicates a treatment difference towards the end of the experiment with mean values of 7.61 (± 0.35 SD) under ambient pCO_2 and 7.18 (± 0.4 SD) under high pCO_2.

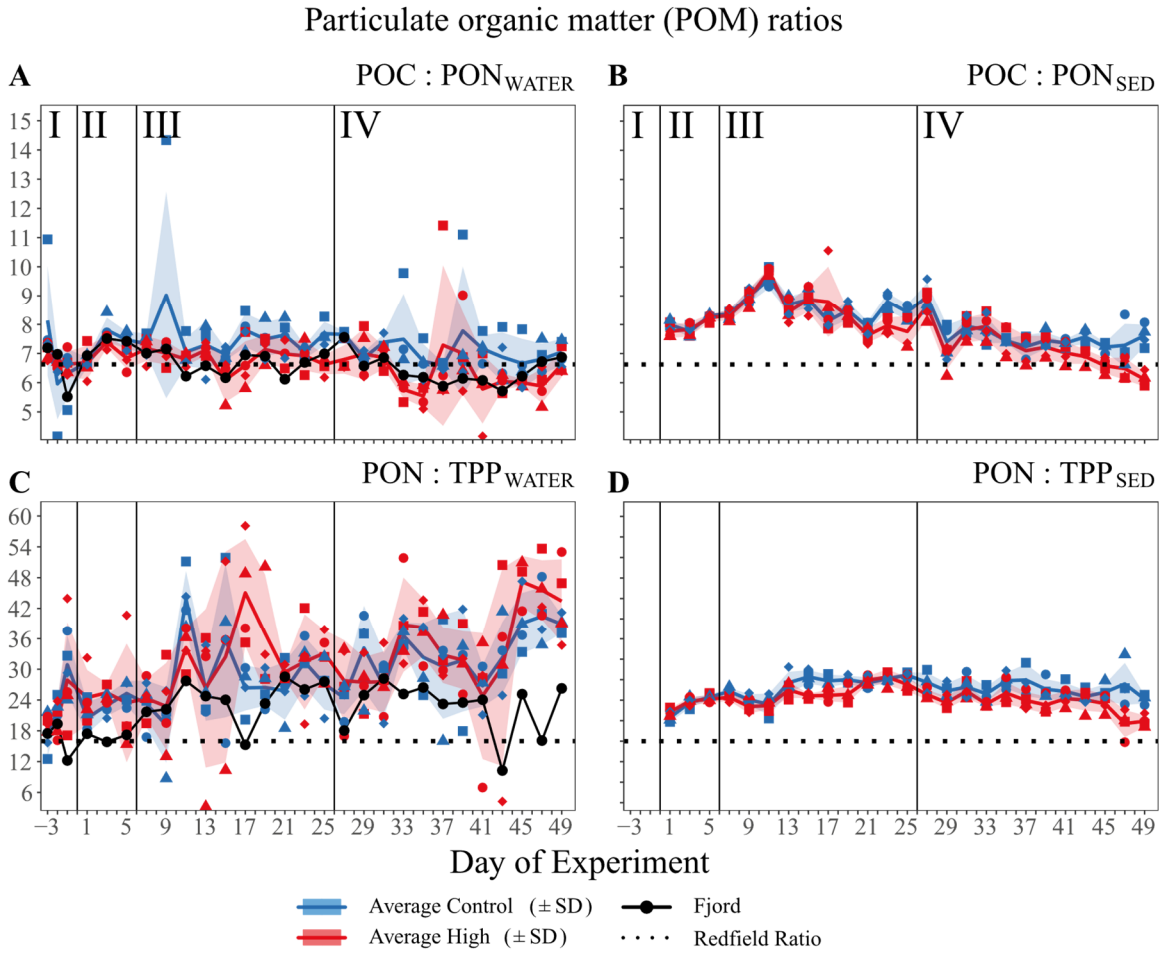

Figure 9: Organic matter ratios of **(A)** particulate organic carbon and nitrogen in the water column, **(B)** the respective flux to the sediment trap, **(C)** particulate organic nitrogen and particulate phosphorous in the water column, and **(D)** the respective flux to the sediment trap over the course of the experiment. Lines, symbols, and colors are used as described in **Fig. 4**. Roman numerals label the different phases of the experiment separated by vertical lines (for description of phases see **Tab. 2**). Figure created with the ggplot2 package in RStudio (RStudio, 2016; Wickham *et al.*, 2016).

Table 3: Summary of average POM_{WATER}, and POM_{SED} values as well as their elemental ratios under the different pCO_2 levels and the four phases of the experiment.

	Phase I		Phase II		Phase III		Phase IV	
pCO_2 level	High	Ambient	High	Ambient	High	Ambient	High	Ambient
POC_{WATER} [µmol L^{-1}]	19.95 ± 1.33	20.84 ± 1.31	20.42 ± 0.99	20.71 ± 1.39	14.61 ± 2.08	17.82 ± 2.92	13.22 ± 2.99	16.71 ± 1.87
PON_{WATER} [µmol L^{-1}]	2.95 ± 0.33	3.18 ± 0.73	2.94 ± 0.5	2.83 ± 0.35	2.16 ± 0.55	2.39 ± 0.56	2.10 ± 0.53	2.39 ± 0.47
TPP_{WATER} [µmol L^{-1}]	0.14 ± 0.03	0.14 ± 0.02	0.12 ± 0.02	0.12 ± 0.0	0.09 ± 0.1	0.09 ± 0.03	0.07 ± 0.06	0.07 ± 0.07
POC_{SED} [µmol L^{-1} 48 h^{-1}]	NA	NA	1.25 ± 0.42	1.33 ± 0.34	0.72 ± 0.22	0.59 ± 0.1	0.28 ± 0.04	0.22 ± 0.03
PON_{SED} [µmol L^{-1} 48 h^{-1}]	NA	NA	0.16 ± 0.06	0.17 ± 0.04	0.08 ± 0.05	0.07 ± 0.02	0.04 ± 0.02	0.03 ± 0.02
TPP_{SED} [µmol L^{-1} 48 h^{-1}]	NA	NA	≤DL	≤DL	≤DL	≤DL	≤DL	≤DL
$POC:PON_{WATER}$	6.77 ± 0.16	6.81 ± 0.07	6.97 ± 0.19	7.32 ± 0.19	6.84 ± 0.46	7.53 ± 0.78	6.39 ± 1.09	7.12 ± 0.94
$PON:TPP_{WATER}$	22.41 ± 7.44	23.28 ± 7.12	24.45 ± 6.79	22.91 ± 3.09	31.24 ± 9.03	28.51 ± 6.19	34.39 ± 10.75	32.75 ± 7.69
$POC:PON_{SED}$	NA	NA	7.94 ± 0.08	8.02 ± 0.03	8.49 ± 0.76	8.63 ± 0.51	7.18 ± 0.4	7.61 ± 0.35
$PON:TPP_{SED}$	NA	NA	23.24 ± 1.33	22.90 ± 1.91	25.47 ± 2.13	26.92 ± 2.17	23.42 ± 2.38	25.61 ± 4.33

The values are averaged per phase ± SD. NA, not available; DL, detection limit.

CONCLUSION AND IMPLICATION

This *in situ* mesocosm experiment was conducted to investigate how coastal plankton communities might respond to extreme ocean acidification events.

Elevated pCO_2 levels of 1987 µatm (± 57 µatm SD, average high pCO_2 mesocosms Phase III and IV) led to a restructuring of the plankton community and significantly affected biogeochemical cycling. During a nutrient-limited post-bloom situation, extreme OA conditions led to lower chl *a*, decreased primary production, lower concentrations of particulate matter, which were also linked to and enhanced export flux under high CO_2. These effects were accompanied by changes in elemental stoichiometry, e.g. lower C:N ratio of suspended particulate matter. These findings point towards a response of the entire plankton community to extreme OA, with altered consumption (and preferential N remineralization) by secondary consumers, and the establishment of a more pronounced top-down control under high pCO_2 conditions. This interpretation is also supported by pronounced CO_2 responses of various zooplankton groups. Accordingly, the enhanced top-down control reduced phytoplankton biomass (as grazing rates exceeded phytoplankton growth rate), and was reflected by higher abundances of hydrozoans, *Clupea harengus* larvae, the copepod species *Calanus* spp., *Oithona* spp. and *Acartia* spp., and filter feeding appendicularians. Reduced numbers of autotrophic and heterotrophic microplankton, and a higher POM export flux further support this interpretation.

Altogether, we found that despite their frequent exposure to low pH events already at present, coastal plankton communities display a pronounced sensitivity to future OA conditions with increasingly extreme pCO_2 fluctuations. The variety of indirect and direct OA effects led to an increase in secondary consumers and top-down control in our study. To what extent our observations are broadly applicable to coastal ecosystems, also considering extended timescales (i.e. beyond the experimental duration), or larger spatial scales, is presently uncertain. In this regard, key factors are **(a)** how will the here observed OA effects interact with other changing environmental factors like raising temperature, **(b)** whether primary production remains sufficient to sustain the increasing biomass of secondary consumers (i.e. match-mismatch situations between predators and prey), and **(c)** how competition between different consumer groups plays out, i.e. whether biomass is transferred effectively up the food web to higher trophic levels like fish, or rather transferred to “dead ends” of the food web such as jellyfish.

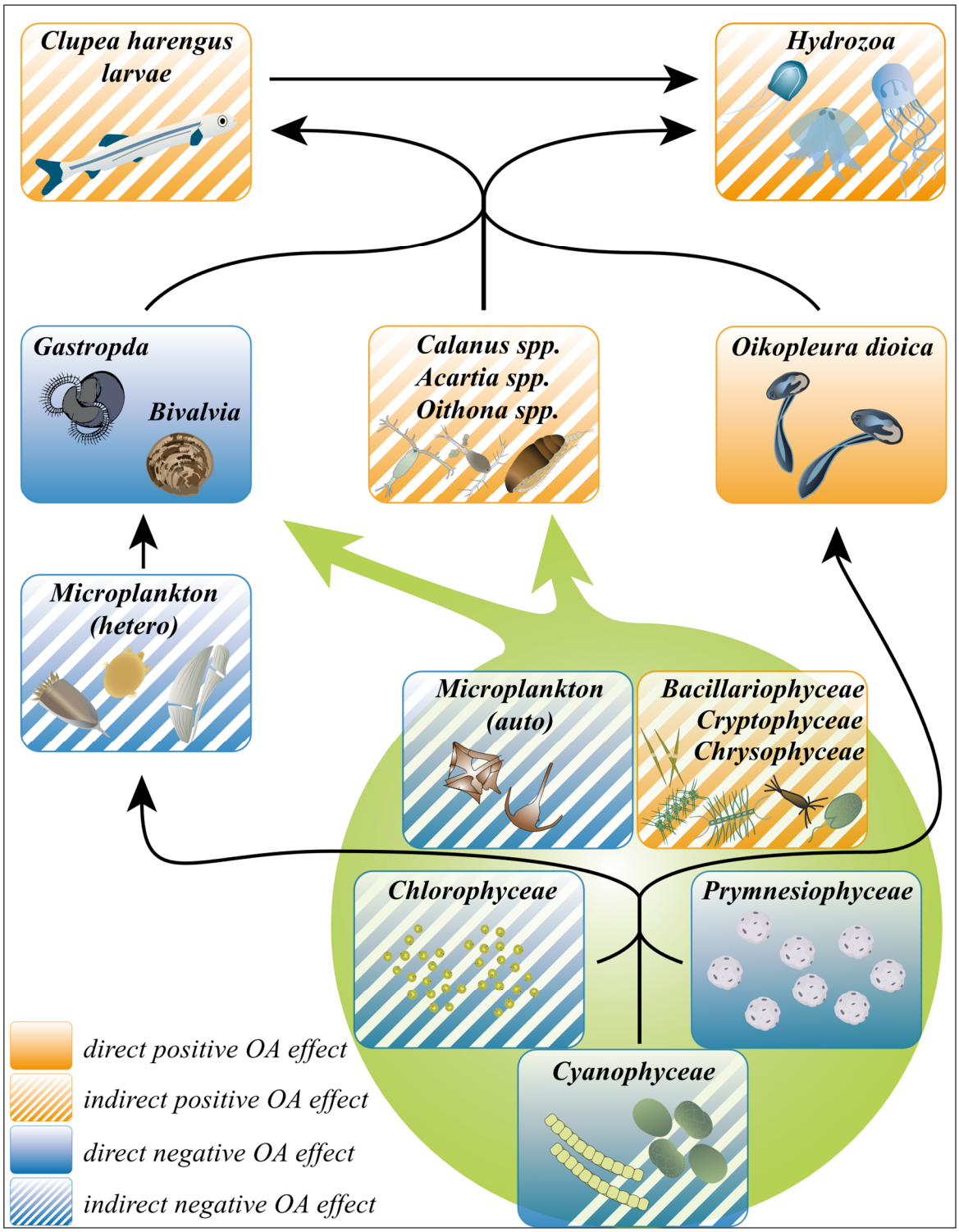

Figure 10: Overview over the positive and negative, direct and indirect OA effects within a simplified food web of our high pCO_2 treatment mesocosms. Squares containing a mixture of filled and hatched area indicate both direct and indirect OA effects on the contained taxa. Black arrows indicate the direction of biomass transfer due to the predator-prey relationships between the single taxa. Green circle summarizes all affected phytoplankton taxa. Symbols taken from "Courtesy of the Integration and Application Network, University of Maryland Center for Environmental Science (ian.umces.edu/symbols/)", accessed 25.08.2020; Figure design © Susanne Schorr, assembled and designed with Adobe Illustrator CS4 (Adobe-Inc., 2008).

ACKNOWLEDGEMENTS

We would like to thank the participants of the KOSMOS Norway 2015 experiment for maintenance and sampling of the mesocosm infrastructure over more than 55 days. A special thanks goes to all participating members of the University of Bergen for their outstanding support, especially Prof. Dr. Arild Folkvord (Department of Fisheries Ecology and Aquaculture at the University of Bergen) for the help and cooperation on introducing herring larvae to our mesocosms. We would also like to thank the staff of the Espegrend Marine Biological Station for providing excellent infrastructure and daily support, in particular Tomas Sørlie. Furthermore, we want to acknowledge the technicians for preparation and maintenance of the KOSMOS facilities. We are also grateful to the captains and crews of R/V Alkor (AL455), R/V Poseidon (POS486T) and R/V Håkon Mosby (2015627, 2015628) for the transportation and mooring of the mesocosm infrastructure.

JMB and AKL are grateful to Prof. Dr. Eric Thompson (Department of Biology at the University of Bergen) and Prof. Dr. Daniel Chourrout (SARS International Centre for Marine Molecular Biology), for approving, supporting and contributing to this collaborative opportunity with the KOSMOS group, and formalizing this work in a joint master project for AKL.

CS is thankful to the Norwegisch-Deutschen Willy-Brand Stiftung (10/2015-S) as well as the Erasmus+ project for funding of the scientific work in the framework of his master thesis.

CHAPTER 2

Ocean Acidification Alters the Predator - Prey Relationship between Hydrozoa and Fish Larvae

C. Spisla[1*], J. Taucher[1], M. Sswat[1], H. Wunderow[1], P. Kohnert[2], C. Clemmesen[1], U. Riebesell[1]

[1]GEOMAR, Helmholtz Centre for Ocean Research Kiel, Biological Oceanography, Kiel, Germany
[2]SNSB, Bavarian State Collection of Zoology, Munich, Germany

***Correspondence:**
Carsten Spisla
cspisla@geomar.de

Frontiers of Marine Science:
Submitted 8th December 2021

Abstract

Anthropogenic CO_2 emissions cause a drop in seawater pH and shift the inorganic carbon speciation. Collectively, these changes are summarized under the term ocean acidification (OA). Research of OA effects on predatory plankton, e.g. Hydrozoa and fish larvae as well as their interaction in complex natural communities remains scarce. Because Hydrozoa can be serious competitors and predators on other higher-level predators like fish, changes in their abundances may have significant consequences for marine food webs and ecosystem services. To investigate the interaction between Hydrozoa and fish larvae influenced by OA, we enclosed a natural plankton community in the Raunefjord, Norway, for 53 days in eight ≈ 58 m^3 pelagic mesocosms. CO_2 levels in four mesocosms were increased to ≈ 2000 µatm pCO_2, while the other four served as untreated controls. OA induced changes at the top of the food web were studied by following ≈ 2000 larvae of Atlantic herring (*Clupea harengus*) hatched inside each mesocosm during the first week of the experiment, and a Hydrozoa population that had already established inside the mesocosms. Under OA, we detected a 20% higher abundance of hydromedusae staged jellyfish, but a 25% lower biomass. At the same time, survival rates of Atlantic herring larvae were higher under OA (ambient pCO_2: 0.1%, high pCO_2: 1.7%) in the final phase of the study. These results indicate that higher herring larvae survival was most likely shaped by a decrease in predation pressure shortly after hatch, when hydromedusae abundance was lower in the OA treatment compared to the ambient. We conclude that the observed changes in the Hydrozoa – fish relationship were driven by indirect food-web mediated OA effects, based on significant changes in the phyto-, micro-, and mesoplankton community under high pCO_2. Ultimately, the observed immediate consequences of these changes for fish larvae survival and the balance of the Hydrozoa – fish larvae predator – prey relationship contain important implications for the functioning of oceanic food webs.

INTRODUCTION

The atmospheric CO_2 concentration is expected to have increased in 2020 to about 412 ppm (average over the year) with an annual CO_2 uptake of the world's oceans of around 2.6 Gt C y^{-1} (Friedlingstein *et al.*, 2020). The by this process caused ocean acidification (OA) already led to a decrease of open ocean surface water pH by 0.017 - 0.027 pH units per decade since the 1980s, and a further decline of around 0.136 - 0.216 by the year 2100 is predicted (Emerson & Hedges, 2008; Le Quéré *et al.*, 2009; Bindoff *et al.*, 2019). This drop in pH is expected to directly and/or indirectly affect marine organisms with advantages as well as disadvantages for the different species (Orr *et al.*, 2005; Kroeker *et al.*, 2013; Wittmann & Pörtner, 2013).

Most of OA research was, however, conducted on lower trophic levels of the food web, i.e. within bacteria, phyto-, and herbivorous zooplankton, but higher level consumers, especially within the zooplankton, remain sparsely investigated. The Cnidaria subtaxa Hydrozoa and their sister-taxa Anthozoa and Scyphozoa, were studied extensively in the context of increasing fisheries, pollution, or global warming (e.g. Purcell (2005, 2012)), but only very few studies on the possible influence of decreasing seawater pH on these animals have been conducted. In one of these few studies, Attrill *et al.* (2007) stated that higher jellyfish abundances in some areas of the North Sea correlated with lower pH levels. Although this correlation could not be confirmed by Richardson and Gibbons (2008) when they analyzed a larger dataset, both papers mention two hypothetical ways by which jellyfish could be influenced by OA: The first one is a possible direct influence, e.g. on the balance sensory receptors (statoliths) of Hydrozoa, Scyphozoa, and Cubozoa, made of calcareous basanite (Werner, 1993). Although Winans and Purcell (2010) and Knowles (2012) showed that Scyphozoa statoliths can decrease in size in an acidified environment, no obvious consequences for the studied species were shown. The second possible OA effect on jellyfish may stem from changes in the condition and/or community composition of competitors or prey organisms, therefore indirectly affecting the jellyfish population. Purcell (1997) showed, that e.g. the early life stages of ichthyoplankton are not only important prey organisms, but also competitors for food, especially for Hydrozoa and Scyphozoa. These early life stages of fish, however, were found to be susceptible to OA, also among larvae of economically important species such as Atlantic cod (*Gadus morhua*, Stiasny *et al.* (2016)), Senegalese sole (*Solea senegalensis*, Pimentel *et al.* (2014)), and Yellowfin tuna (*Thunnus albacares*, Frommel *et al.* (2016)). If future increasing OA has such severe consequences for

recruitment and fishery yield, as shown for example for Atlantic cod by Hänsel *et al.* (2020), this would result in a significant reduction of fish and fish larvae as competitors to jellyfish, and lead to a "vicious circle" for fish. As Purcell and Arai (2001) stated, competition with, and predation by Hydrozoa can be considered as one of the major ecological factors, next to prey availability, affecting fish larvae survival and thus population size. With reduced competition for food, Hydrozoa could increasingly dominate in pelagic food webs and thereby impede the recovery of fish stocks, not only through competition for food but foremost by predation (Daskalov & Mamedov, 2007). This would intensify the pressure on future fish populations and result in unforeseeable changes for the respective ecosystems.

Here we conducted a large-scale mesocosm experiment to assess how future OA might affect the interaction of fish larvae and hydrozoans in an ecosystem context. The enclosed natural plankton communities contained Atlantic herring larvae (*Clupea harengus*), that were added to the mesocosms, as well as several hydromedusae species that were already present (*Aglantha digitale*, *Clytia* spp., *Obelia* spp. and *Sarsia tubulosa*). The hatching success and the survival of *C. harengus* larvae was monitored over the course of the experiment lasting 53 days and related to the succession of the plankton community with a particular focus on the abundance and biomass of the dominant Hydrozoa.

MATERIALS AND METHODS

The mesocosm study was carried out from May 3rd, 2015 until June 30th, 2015 in the Raunefjord, a fjordlike strait on the southwest coast of Norway close to the city of Bergen (**Fig. 1B**, **C**). Specifically, the mesocosms were moored at 60°15'55'' N, 5°12'21'' E, in proximity to the Espegrend Marine Research Field Station (**Fig. 1 B**, **C**). Detailed information on the whole experimental setup, manipulation, sampling procedures, analyzed parameters, and results of the main superordinate mesocosm experiment are given in an overview paper by Spisla *et al.* (2021).

In total eight pelagic Kiel Off-Shore Mesocosms for Ocean Simulations (KOSMOS, Riebesell *et al.* (2013b)) were arranged in two rows of four mesocosm each (**Fig. 1C**). The mesocosms consist of a floating frame with a dome-shaped hood, the 21 m long mesocosm bag, a 2 m full diameter sediment trap sealing the bottom of the bags (**Fig. 1A**), and the upper opening of the mesocosm bag kept ~ 1 m above sea level. The bags are made of polyurethane foil, permeable for light in the photosynthetically active radiation (PAR) spectrum but scarcely for UV light.

Acidification treatment and measured parameters

On May 6th, 2015 the experiment was started by closing the mesocosms, thereby isolating the mesocosms water column from the surrounding fjord water and the OA treatment was started May 12th, 2015 (Day 0 of the experiment). In order to simulate pCO_2 values realistic for near future scenarios or already present especially in coastal upwelling ecosystems, target OA levels of pCO_2 around 2000 µatm were chosen for the experimental design (see Spisla *et al.* (2021)). These OA levels were achieved for the four high pCO_2 mesocosms (M3, M5, M6, M8) by injecting CO_2-saturated sea water at four time points at the beginning of the study (Day 0, 2, 4, and 6) and, to compensate for CO_2 losses due to outgassing, on Day 14, 22, 28, 40, and 46 during the experiment. Daily measurements and samples were taken over the course of the experiment from Day -3 (i.e., 3 days before first CO_2 manipulation) until Day 0 and every two days from Day 1 until the end of the study on Day 49 (see timeline Spisla *et al.* (2021)). A variety of physical, biological, and biogeochemical parameters were measured inside the mesocosms and in the surrounding fjord water at the mesocosm deployment site. Temperature, salinity, pH, and PAR was measured with a hand-held self-logging CTD probe (CTD60M, Sea and Sun Technologies, Schulz and Riebesell (2013)). Concentrations of Chlorophyll *a*/ phytoplankton pigments, inorganic nutrients (nitrate, nitrite, ammonium, dissolved silica, and phosphate), particulate organic matter (carbon, nitrogen, phosphorous), dissolved inorganic carbon (DIC), total alkalinity (TA), and microscopic as well as flow cytometric abundances of phyto-/ and microplankton were obtained from water subsamples of the water column taken with a depth-integrating water sampler (IWS, HYDRO-BIOS, Kiel).

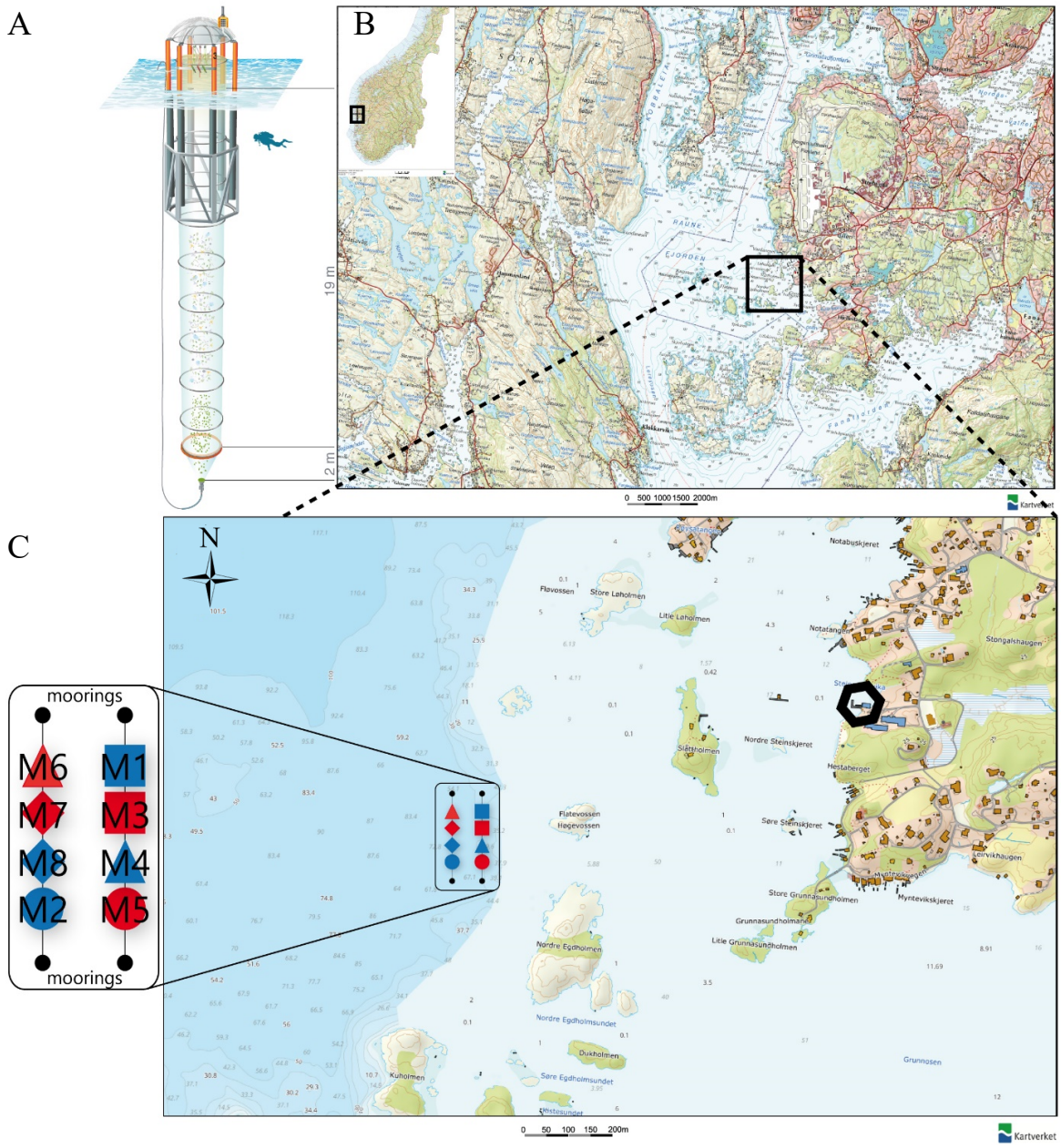

Figure 1: (A) Kiel Off-Shore Mesocosm for Ocean Simulations (KOSMOS), a pelagic mesocosm system. Blue corrugated area represents water surface. Diver for scale. Illustration of the KOSMOS unit by Rita Erven (GEOMAR), reprinted with permission from the AGU **(B)** Location of the Raunefjorden at the coast of Norway. Black square indicates deployment area of the mesocosms. **(C)** Position, order and symbols of the KOSMOS units M1 – M8 in their deployment area near the Espegrend Marine Research Field Station, Bergen (black hexagon). Red filling of the respective mesocosm symbol indicates CO_2 manipulation and blue filling the control group. Symbols and denomination of the mesocosms will be used uniformly throughout the manuscript. Small numbers in the map indicate the water depth in meter. **(B)** & **(C)** modified after: The Norwegian Mapping Authority (Kartverket, accessed February 15th 2021, http://geo.ngu.no/kart/arealisNGU/)

Herring larvae introduction and sampling

Herring eggs were obtained from adult herring caught with a gillnet (mesh size: 36 mm) in Fens Fjord (60°34`795 N, 5°0`759 E) on May 5th 2015 at a depth of ~ 6 m in cooperation with the Department of Fisheries Ecology and Aquaculture, University of Bergen. The eggs of two females were strip-spawned onto 20 plastic plates and fertilized with the sperm of three males. To allow for genetic variation every female was crossed with every male. The fertilization and early egg development took place in ambient, flow-through seawater for one week until the egg-plates were placed inside the mesocosms. Before introduction into the mesocosms the number of fertilized and developing eggs was counted for each egg plate as a proxy for hatching success. Egg plates were then combined to yield similar numbers of hatching larvae, followed by the random introduction to the mesocosms.

On May 12th, 2015 (Day 0 of the experiment), each mesocosm received on average 6364 ± 1257 fertilized eggs. To prevent damage by sampling gear the egg-plates were placed in specially designed open 'egg cages' at 8 m depth. From these cages the larvae hatched inside the mesocosms after ~ 14 days, with peak hatch (Day 0 of the days post hatching (DPH) period) estimated for May 19th (Day 7 of the experiment) by visual inspection of the egg plates (~ 50% larvae hatched = empty eggs). To maximize the number of hatched larvae, the cages were left inside the mesocosms until May 24th (5 DPH). On average, 2063 ± 566 larvae hatched in each mesocosm, calculated as the difference in egg numbers before and after hatch by counting the eggs on photographs taken of the egg plates. Dead larvae and fallen-off eggs found inside the egg cages were included into the number of non-hatched larvae.

The sampling of sediment trap material (following the protocol of Boxhammer *et al.* (2016)) gave the opportunity to directly collect dead larvae every second day during the whole experimental period. Upon arrival of the samples, the sediment material was transferred into black trays (70 cm × 50 cm × 10 cm) and visually searched for larvae. The dead (whitish) herring larvae were clearly distinguishable from the sediment trap material. The sampling of alive larvae is described in Section "Sampling of mesozooplankton".

Sampling of mesozooplankton (mesoZP)

To prevent an influence of the removed biomass through the net hauls on the plankton communities in the mesocosms, mesoZP sampling was carried out only every 8 days starting on Day -3 (May 5th) and ending with the final sampling on Day 49. Samples were collected

with a 100 cm long, 55 µm mesh size Apstein net vertically hauled from 19 m depth up to the water surface between 11:00 and 13:00 h. The opening of the net was a cone-shaped lid of 17 cm diameter, resulting in a sampled water volume of 0,431 m^3 or 431 L. Net hauls were performed in every mesocosm as well as in the fjord in alternating order to assure random sampling of the single mesocosms between different sampling days. The sample was transferred to a 500 mL Kautex bottle and filled up with 0.7 µm filtered seawater (FSW). Upon return to the laboratory the samples were immediately preserved in 70% Ethanol and later counted in a Bogorov-Chamber under a Leica stereomicroscope (MZ12).

In addition to the regular mesoZP net hauls, hydrozoan and fish larvae abundances were assessed with net hauls performed with an Apstein net of 500 µm mesh size and 0.5 m opening diameter, resulting in a sampled water volume of 3.73 m^3 or 3730 L. These net hauls started after the herring larvae hatched, from Day 13 onward, on Day 23, 29, and 37, and were taken in the evening, using a flashlight on top of the net to make use of the positive phototactic behaviour of herring larvae (Hernandez *et al.*, 2003). The samples were stored in 1 L FSW and upon arrival in the laboratory, first searched for fish larvae and then counted with respect to jellyfish. During the counting individuals of the dominant jellyfish were picked into tin capsules for carbon and nitrogen content analysis using an elemental CN analyzer (EuroEA). On Day 49 all remaining herring larvae and/or other fish that were alive in each mesocosm were sampled. For this, a net with the diameter of the mesocosms (2 m) and a mesh size of 1000 µm was hauled from the bottom to the top of every mesocosm. These final samples were again first checked for fish larvae and afterwards stored in 500 mL 4% buffered formaldehyde.

The herring larvae caught alive during and at the end of the experiment were transported in containers of 5 L to the research station, anaesthetized with MS-222 and individually prepared for further analyses. All larvae were photographed with a camera mounted on a stereomicroscope (Nikon-Leica). These pictures were used to measure larval standard length to the nearest 0.1 mm with the open-source software ImageJ (Abràmoff *et al.*, 2004). The sampled larvae were directly frozen in sea water at -80°C for later analyses of dry weight. The larval dry weight (DW) was measured after 18h of lyophilisation (Christ Alpha 1–4 freeze dryer, Martin Christ Gefriertrocknungsanlagen GmbH, Osterrode, Germany) for each individual larva on a micro balance (Sartorius SC 2 micro balance, Sartorius AG, Göttingen, Germany; precision ± 0.1 µg). The same larvae were later used for nucleic acid analysis measuring the ratio of the nucleic acids (RNA and DNA (RD), standardized to sRD = 0.92

× RD (Caldarone *et al.*, 2006) as a proxy for nutritional condition and growth (protocol described in Malzahn *et al.* (2003). In order to gain the overall biomass of herring, the individual DW of the herring larvae at the end of the study was multiplied with its abundance.

Besides the introduced *C. harengus* larvae, the final net also caught juvenile gadoid and flatfish, which were counted and measured for wet weight on a micro balance (Sartorius SC 2 micro balance, Sartorius AG, Göttingen, Germany; precision ± 0.1 µg). For a better comparison to the biomass of other members of the plankton community, wet weight of these juvenile fish was transformed into dry weight assuming a conversion factor of 0.18 (Van der Meeren *et al.*, 1994). In order to gain the overall biomass of gadoid and flatfish, the individual DW was summed up for each mesocosm.

Identification of specimen by means of mtCOI DNA sequencing

Supplementary to the visual identification of the observed Hydrozoa, individuals of the most abundant species were picked manually from the fish net haul samples and "barcoded", i.e. genetically identified, via their mitochondrial cytochrome oxidase I (mtCOI) genes. For this, the organisms were picked with as little seawater as possible, transferred to 96% Ethanol (EtOH) filled 2 mL screw cap microtubes, and stored immediately at -80°C until further analysis. In order to extract the DNA of the single organism, they were thawed, extracted from their 2 mL tubes, dried, and transferred into a 1.5 mL PCR Clean Eppendorf Safe-Lock Tube. DNA extraction was then performed according to the protocol given in 'Appendix protocol'. The subsequent PCR was carried out in a Biometra TProfessional Basic PCR Machine, following the protocol of Bucklin *et al.* (2010) with 1. Initial Step 5 min 94°C, 2. Denaturation 94°C 1 min, 3. Annealing 45°C 2 min, 4. Elongation 72°C 3 min, and 5. Final Elongation 72°C 10 min. The PCR product was purified using the ZYMO DNA Clean & Concentrator kit and analyzed on an ABI 3730 DNA sequencer (SeqGen Inc., California, USA) at the sequencing service unit Ludwig-Maximilians-University Munich (LMU, Munich, Germany).

Data Analysis

From the counts per sample and the filtered volume of the 500 µm (large) and the 55 µm (small) net, 3730 L and 431 L, respectively, abundances in individuals per m^3 (ind m^{-3}) were calculated. The abundance data of the 500 µm net was then used to obtain hydrozoan biomass by multiplying the ind m^{-3} with the measured carbon and nitrogen values. The same

procedure was applied to the calculation of copepod biomass, but in the absence of measurements, carbon and nitrogen literature values were taken to calculate biomass of the copepodite (cop.) and adult stages of the dominant species *Acartia* sp., *Calanus* sp., *Oithona* sp., and *Temora* sp. as well as copepod nauplii larvae (see **Appendix Tab. 5**).

OA effects on hydrozoan abundances (ind m^{-3}) and biomasses (µg C m^{-3}) were tested by means of a two-sample t-test. Thereby, the mean of the abundance or biomass per mesocosm per time period was calculated, grouped by high and control pCO_2, and tested for significant differences between treatment averages. Overall survival of herring larvae for each mesocosm was calculated from the initial number of hatched larvae and the survivors at the end of the experiment. For survival of herring larvae, a one-way ANOVA approach (t-test) was used to test the difference in overall survival between CO_2 treatments. The high variability in sample sizes for larval growth and nutritional condition per mesocosms over time with low survival in the ambient treatment and two mesocosms having no surviving larvae at the end of the study led to an unbalanced design, which enabled statistical analyses on treatment specific differences. Results for these parameters are therefore based on visual inspection of the data and the description of interacting factors.

All statistical calculations were performed with the R software version 3.4.2 in the RStudio environment (RStudio, 2016).

RESULTS

Chlorophyll *a* concentration

Based on the temporal development of the chl *a* concentration and the time points of the CO_2 additions, the duration of the experiment was divided into four phases (for details see Spisla *et al.* (2021)):

- Phase I (Day -3 - Day 0): Closing of the mesocosms until first CO_2 addition
- Phase II (Day 1 - Day 6): Establishing target pCO_2 values and transition from bloom to post-bloom conditions
- Phase III (Day 7 - Day 26): First post-bloom phase with a treatment effect on chl *a* followed by a realignment
- Phase IV (Day 27 - Day 49): Second post-bloom phase with enhanced treatment differences and a continued steady decline in chl *a*

In the first phase of the experiment (Day -3 to Day 0) mean chl *a* concentration decreased slightly from the initial values of 2.43 µg L^{-1} (± 0.24 SD) in the ambient pCO_2 and 2.44 µg L^{-1} (± 0.16 SD) in the designated high pCO_2 treatment, to ≈ 2.2 µg L^{-1} (Day 1) in both treatments. This decrease then became more pronounced during Phase II (Day 0 to Day 6) and early Phase III (up to Day 9) with values of 0.94 µg L^{-1} (± 0.06 SD) in the ambient pCO_2 and 0.8 µg L^{-1} (± 0.09 SD) in the high pCO_2 mesocosms (**Fig. 2**). In Phase III and IV, the chl *a* concentration decreased constantly to 0.36 µg L^{-1} (± 0.03 SD, ambient) and 0.18 µg L^{-1} (± 0.04 SD, high), and showed a significant treatment difference during Phase III (t-test $p < 0.001$), and Phase IV (t-test $p = 0.03$). This treatment effect was most pronounced on Day 17 with an average chl *a* concentration of 0.77 µg L^{-1} (± 0.1) and 0.43 µg L^{-1} (± 0.02) in the ambient and CO_2-enriched mesocosms, respectively. For more details see Spisla *et al.* (2021).

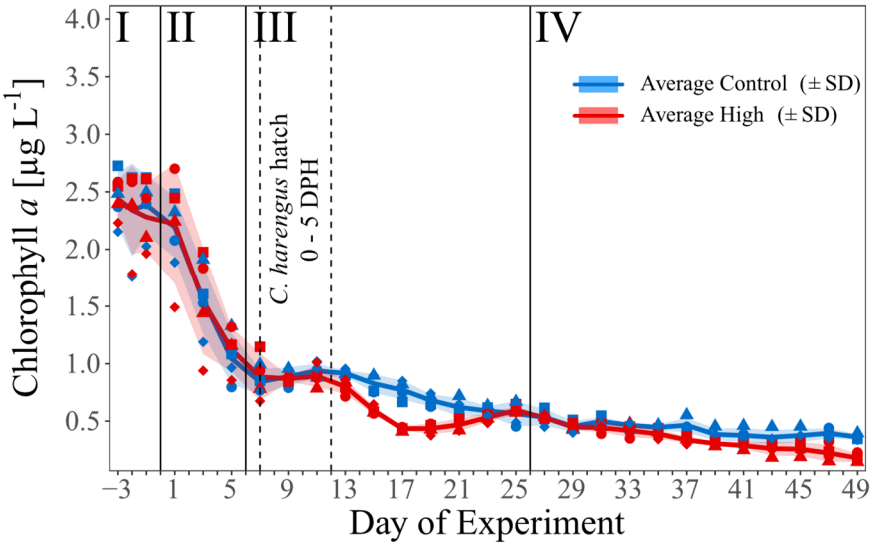

Figure 2: Temporal development of average chl *a* concentration [µg C L^{-1}] over the course of the experiment. Blue and red line indicate the respective average concentration in the control and high pCO_2 treatment. The shaded areas represent the standard deviations (SD). Blue symbols represent concentrations in the ambient pCO_2 mesocosms (M1, M2, M4, and M7), red symbols in the high pCO_2 mesocosms (M3, M5, M6, and M8), assigned as presented in **Fig. 1C**. Dashed vertical lines mark the start and peak of herring larvae (*C. harengus*) hatch as Days Post Hatching (DPH). I – IV indicate the different phases of the experiment separated by vertical lines (for details on the phases see Spisla et al. 2021).

Copepod biomass

Overall mean copepod biomass in all mesocosms was decreasing over the course of the experiment from initially about 40 mg C m^{-3} to about 13 mg C m^{-3} on Day 49 (**Fig. 3A**). After closure of the mesocosms, mean values developed a short-term peak towards the end of the acidification phase (Day 5) and decreased thereafter. The increase in biomass was

mainly due to adult and copepodite stages, and was not observed in the nauplii biomass (**Fig. 3B**, **C**). Until Day 21 no significant treatment effect in all copepods size classes was found, From Day 21 to Day 37, a significant positive OA effect in the copepods overall and copepodite biomass with 30.6 (± 6 SD) and 22.5 (± 6 SD) mg C m^{-3} in the high pCO_2 mesocosms, and 25.8 (± 2.5 SD) and 16.4 (± 4 SD) mg C m^{-3} under ambient conditions ($p = 0.02/ 0.007$) was detected. For copepod nauplii biomass a significant negative effect was observed between Day 29 and Day 37 ($p = 0.02$) with 0.47 mg C m^{-3} (± 0.2 SD, high pCO_2) and 0.72 mg C m^{-3} (± 0.2 SD, ambient).

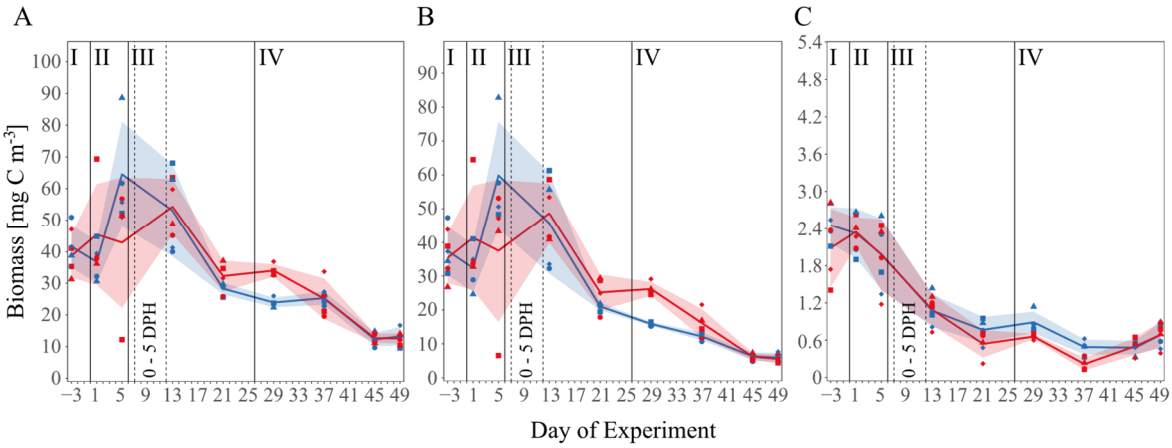

Figure 3: Biomass [µg C m^{-3}] development of all measured copepod species over the time of the experiment as **(A)** all copepod species and size classes combined (i.e. including adult, copepodite and nauplii stages), **(B)** only copepodite stages, and **(C)** only copepod nauplii larvae. Lines, symbols and colors are used as described in **Fig. 1C & 2**.

Hydrozoa abundance and biomass

Visual identification of specimen suggested that the Hydrozoa community consisted mainly of hydromedusae of the species *Aglantha* sp., *Sarsia* sp., *Clytia* sp., *Obelia* sp. and *Rathkea* sp. Subsequent sequencing of the mtCOI genes and comparison to the BLAST genbank (Altschul *et al.*, 1990) of these preidentified species confirmed the presence of *Aglantha digitale* (**Fig. 4A**), *Clytia* sp. (**Fig. 4B**), *Sarsia tubulosa* (**Fig. 4C**), and *Obelia geniculata* (**Fig. 4D**). Due to problems during sequencing, *Rathkea* sp. occurrence could not be confirmed and some unidentified hydromedusae could not be specified further.

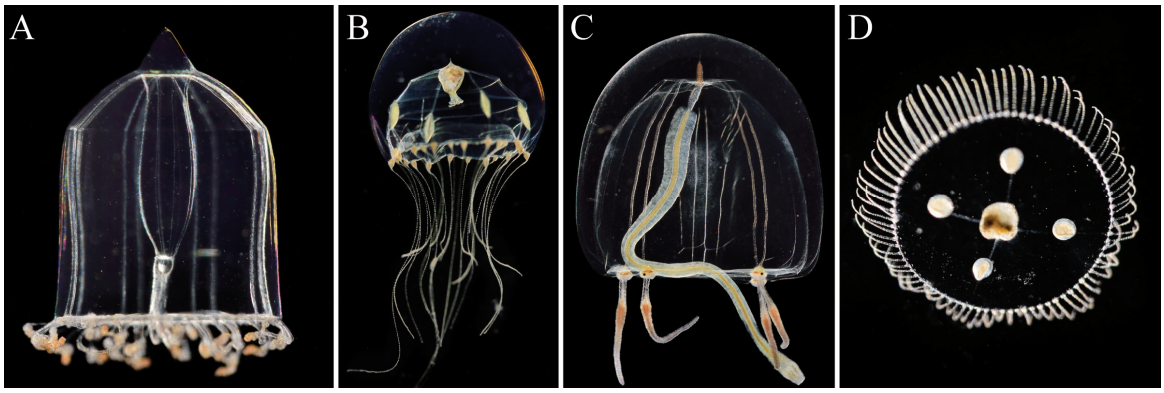

Figure 4: Main Hydrozoa species observed: **(A)** *Aglantha digitale,* **(B)** *Clytia* sp., **(C)** *Sarsia tubulosa*, and **(D)** *Obelia geniculata*. Pictures © Solvin Zanckl

These unidentified species, however, are included in the "total Hydrozoa" abundance data, given as the sum of all individuals present in the mesocosms (ind m^{-3}). Total Hydrozoa abundances in both, the 500 µm and the 55 µm net, showed decreasing mean abundances over the course of the experiment (**Fig. 5**). In the 55 µm net the mean abundance over all mesocosms decreased from initially (Day -3) 159 ind m^{-3} (± 35 SD) to 19 ind m^{-3} (± 10 SD), while in the 500 µm net the mean value went down from 69 ind m^{-3} (± 7 SD, Day 13) to 11 ind m^{-3} (± 3 SD, Day 49). These decreasing trends are reflecting the trend of hydrozoan abundances in the surrounding fjord, where abundances accessed with the 55 µm net decrease from initially 130 ind m^{-3} to 15 ind m^{-3} on Day 49. For the ambient and high pCO_2 mesocosms, respectively, the small net shows similar abundances in Phase I and II of the experiment, and except for Day 13, also in Phase III. On Day 13 hydrozoans seem to be, contrary to the remaining time of the experiment, less abundant under high pCO_2. That this decrease, however, occurred almost identically in the fjord data, and is not seen in the 500 µm net abundances could indicate a possible error in the sampling method or data collection. From Day 13 onward, and especially during Phase IV of the experiment the hydrozoan abundances of the 55 µm net are with mean values over Phase IV of 46 ind m^{-3} (± 23 SD) under high pCO_2, and 30 ind m^{-3} (± 17 SD) under ambient pCO_2, significantly higher under elevated pCO_2 conditions ($p = 0.034$). This treatment effect is also displayed in the abundance data of the 500 µm net. Although only statistically significant on Day 29 ($p = 0.003$) with 51 ind m^{-3} (± 6 SD) in the treatment mesocosms and 34 ind m^{-3} (± 4 SD) in the control group, mean Hydrozoa abundance still shows the tendency to be higher under high pCO_2 throughout Phase IV of the experiment.

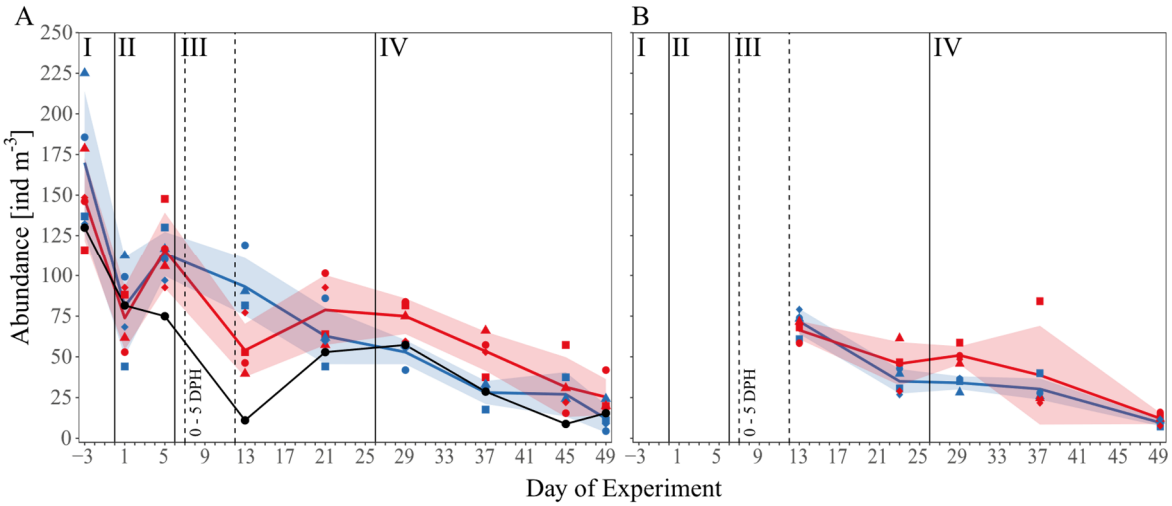

Figure 5: Abundance data [ind m^{-3}] of all observed Hydrozoa over the time of the experiment. **(A)** The small 55 µm mesh size net and **(B)** the big 500 µm mesh size net. Black line and symbols represent values measured in the surrounding ford. Other lines, symbols, and colors as described in **Fig. 1C & 2**.

Despite lower Hydrozoa abundances under ambient pCO_2 in Phase IV, total hydrozoan biomass (estimated from the 500 µm net) was elevated during this period (see **Fig. 6A** and **Tab. 1**). It amounted to 3299 µg C m^{-3} (± 1780 SD) in the ambient mesocosms compared to 1979 µg C m^{-3} (± 995 SD) in the high pCO_2 mesocosms, thereby displaying a significant treatment effect ($p = 0.035$, **Fig. 6A**). Along with the abundance data, hydrozoan biomass decreased over time in the ambient pCO_2 mesocosms from 3723 µg C m^{-3} (± 1626 SD) on Day 29 to 2139 µg C m^{-3} (± 942 SD) on Day 49, but stayed with 1698 µg C m^{-3} (± 348 SD) on Day 29 and 1754 µg C m^{-3} (± 1032 SD) on Day 49 rather stable in the high pCO_2 mesocosms (**Fig. 6B**). The majority of the biomass was comprised by the species *Aglantha digitale*, which in Phase IV made up for around 70% of the biomass in the ambient mesocosms and around 50% in the high pCO_2 ones (see **Fig. 6B**). The biomass per individual (µg C ind^{-1}) of *A. digitale*. was furthermore the driving factor of the opposing effects in hydrozoan abundance and biomass. With a mean of 227 µg C ind^{-1} (± 144 SD) under ambient compared to 73 µg C ind^{-1} (± 68 SD), the animals under high pCO_2 conditions were significantly smaller in the final phase of the experiment ($p = 0.003$, see **Fig. 6C**).

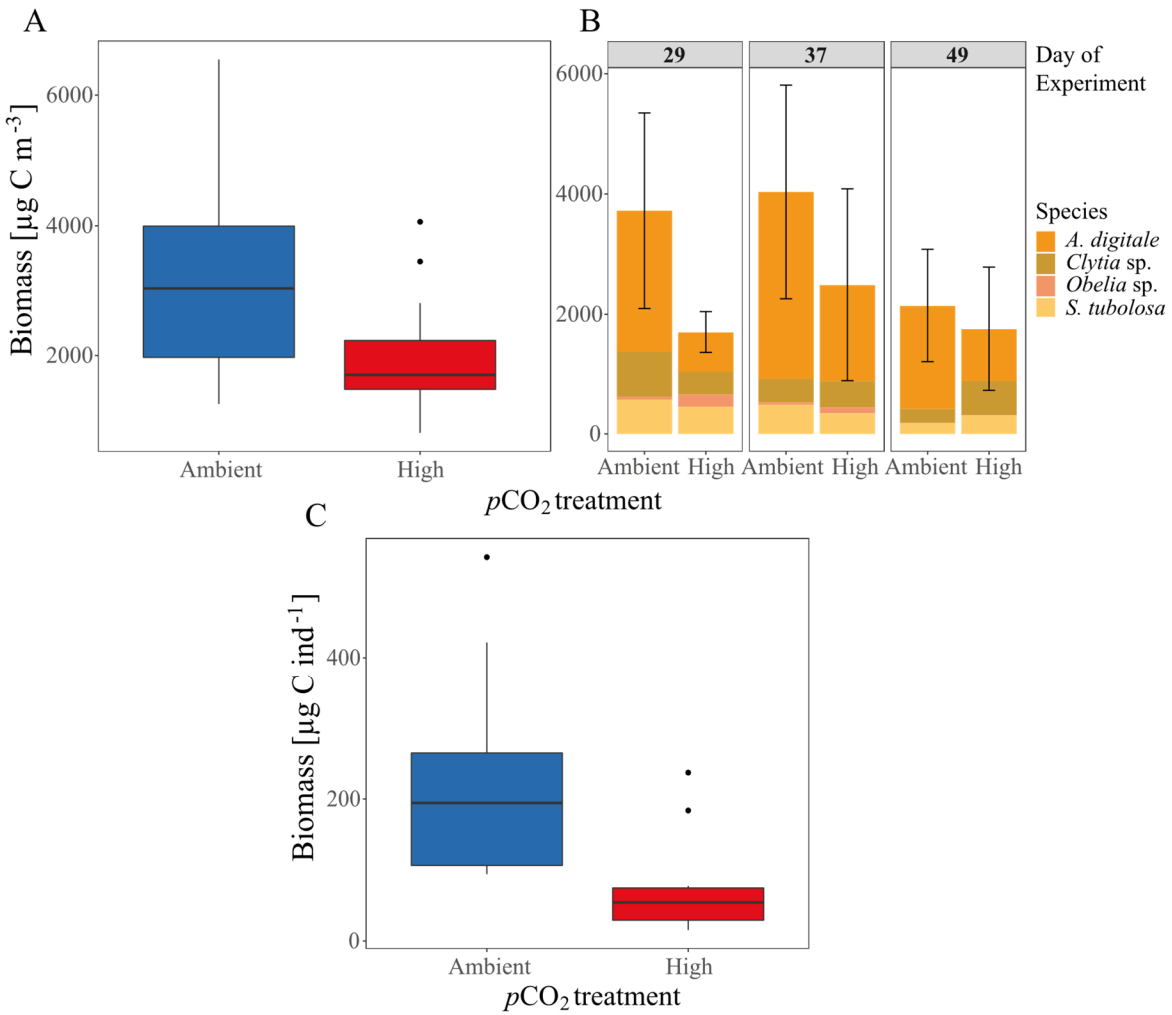

Figure 6: Hydrozoa biomass [µg C m^{-3}] development per pCO_2 treatment over Phase IV of the experiment as **(A)** combined Hydrozoa mean biomass of the four major species, and **(B)** biomass contributions of the single species (see given legend) to the overall Hydrozoa biomass per day. Error bars represent the standard deviation of the sum of all listed species, see also **Tab. 1**. **(C)** Mean biomass per pCO_2 treatment, per individual [µg C ind^{-1}] of the dominant species *Aglantha digitale*. All boxplots display the mean and the 95% confidence interval of the given data.

Table 1: Hydrozoa biomass sum (Sum µg C m^{-3}, 500 µm net samples only) per treatment on the single days (DoE) as well as the mean over Phase IV of the experiment. Standard deviations (SD) for the sums result from the calculation of µg C ind^{-1} with mean carbon (± SD) values of several measurements

pCO_2 treatment	Day of experiment	Biomass [µg C m^{-3}]	SD
Ambient	29	3723	1626
Ambient	37	4035	1776
Ambient	49	2139	942
Ambient	**Phase IV**	**3299 (mean)**	1780
High	29	1698	348
High	37	2485	1601
High	49	1754	1032
High	**Phase IV**	**1979 (mean)**	995

Herring larvae survival

Significantly more larvae were caught alive at the final sampling in the high pCO_2 treatment compared to the ambient mesocosms (ambient pCO_2: 0.1% ± 0.1 SD, high pCO_2: 1.7% ± 0.2 SD, see **Fig. 7A**). Only a small percentage of those larvae that hatched were caught alive by nets during the study (ambient pCO_2: 0.3% ± 0.2, high pCO_2: 0.8% ± 0.5). A higher percentage was found dead in the sediment trap (ambient: 16.4% ± 5.0, high: 21.2% ± 6.7, **Fig. 7B**), and the highest percentage was categorized as 'missing by predation' (ambient pCO_2: 83.3% ± 5.4, high pCO_2: 76.3% ± 6.6, **Fig. 7C**). Thus, under high pCO_2 conditions, there was on average higher survival and more larvae found dead in the sediment traps, while more larvae were 'missing by predation' in the ambient pCO_2 mesocosms indicating higher predation pressure (**Fig. 7B**, **C**). For details on the numbers of eggs that were introduced, larvae that hatched and were sampled or missing due to predation in each mesocosm and treatment, see **Appendix Tab. 6**.

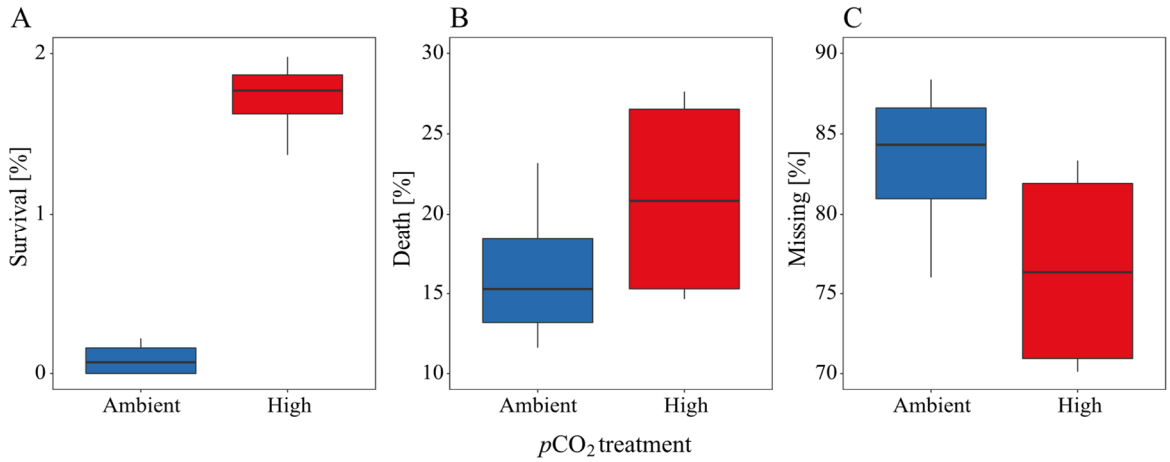

Figure 7: Percentage proportion of herring larvae at the end of the experiment from overall hatched eggs for **(A)** survival, **(B)** death, and **(C)** missing individuals. Blue color represents the ambient, red the high pCO_2 treatment. All boxplots display the mean and the 95% confidence interval of the given data.

Dry weight and nutritional condition

Due to the differences in overall survival, data on larval dry weight (DW) and nutritional condition (sRD) could only be acquired for two ambient pCO_2 mesocosms (M2, M4), but for all four high pCO_2 mesocosms (M3, M5, M6, M8; see **Appendix Fig. 4**). On average, dry weight at the end of the experiment was higher in the ambient than in the high pCO_2 mesocosms. Under ambient conditions small larvae in the range of 0.25 - 0.75 mg were missing, whereas they were present in the high CO_2 treatment. The development of the larval nutritional condition (sRD) shows a slight decline between hatch, and 12 DPH and 30 DPH,

respectively. The survivors at the end of the study show slightly higher sRD values compared to hatch. As for dry weight, the average sRD is higher in the ambient pCO_2 treatment. In general, a high variability within one pCO_2 treatment and within each mesocosm can be observed, with a higher variability in the high pCO_2 treatment, for both the dry weight as well as the nutritional condition (see **Appendix Fig. 4**).

Presence of juvenile fish and the polychaete *Tomopteris* sp.

Apart from herring larvae, also juvenile fish of the families Gadidae (cod-like) and Pleuronectidae (flatfish species) were caught alive at the end of the experiment, and were also found dead in the sediment trap over the course of the experiment. Overall, their numbers were relatively low with ≤ 4 juvenile fish per mesocosm at the end of the study, but they contributed considerably to the amount of biomass (**Fig. 8**). The biomass of cod-like juveniles, which can be considered predators of herring larvae (Reid *et al.*, 1999) was extremely high in two ambient mesocosms (M1 & M7), where no herring survived until the end of the study.

Additionally, *Tomopteris* sp., a pelagic polychaete which may potentially also feed on fish larvae (Lebour, 1927), was present over the course of the experiment. Its impact on the fish population is, however, difficult to assess as it was only measured with an overall mean of about 2 ind m^{-3} and no detectable differences between ambient and high pCO_2 mesocosms (data not shown).

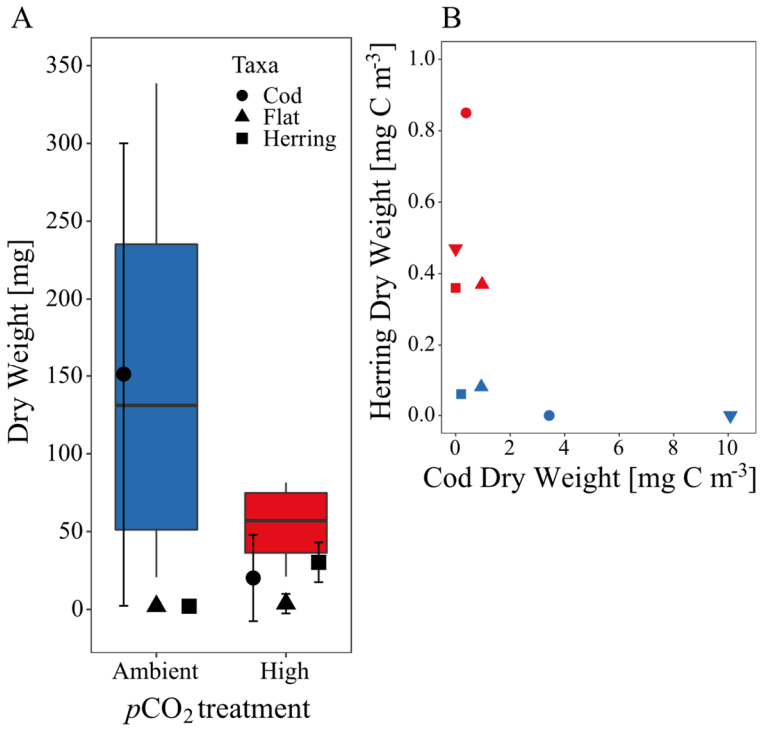

Figure 8: (A) Dry weight (DW, mg) sum and contribution of all fish larvae caught at the end of the experiment per pCO_2 treatment. Symbols according to given legend. **(B)** Comparison of herring larvae and cod DW [mg C m^{-3}] at the end of the experiment. Symbols and colors used for **(B)** are as described in **Fig. 1C & 2**.

DISCUSSION

We found significant effects of ocean acidification on all higher trophic levels of our enclosed plankton community, particularly during the post-bloom phase of this experiment. Most strikingly, we detected that Atlantic herring larvae showed a higher survival under high pCO_2, coinciding with a lower biomass of hydrozoans.

Treatment effects on Hydrozoa

The observed positive OA effect on hydrozoan abundances in the post-bloom Phase IV of the experiment is most likely not a direct, physiological CO_2 effect, but rather an indirect CO_2 effect mediated via food-web interactions. To our best knowledge, no direct positive effect of lower pH on the ecophysiological performance of jellyfish has been reported so far (Richardson & Gibbons, 2008; Winans & Purcell, 2010; Knowles, 2012). To the contrary, experiments of Winans and Purcell (2010) as well as Knowles (2012) rather suggested that a lower pH negatively influences the metabolism and statolith formation of jellyfish, yet with unknown consequences for the organisms and their ecological fitness. A possible direct negative effect on the metabolism of hydrozoans leading to increased mortality in experiments with box jellies (cubozoae) at a pH of 7.5 was shown by (Chuard *et al.*, 2019). According to the authors the lethal reduction in cubozoae metabolic rates was caused by an acidoses effect, which has already been observed for a wide range of organisms exposed to enhanced acidification (Pörtner *et al.*, 2005). In combination with an indirect OA mediated food web effect, this OA induced mechanism of decreased metabolic rates could also have played a role in the development of the hydrozoan communities observed in our experiment causing the negative effect on *Aglantha* sp. biomass per individual, and the resulting counter-intuitive pattern of higher abundance but lower biomass in the high pCO_2 treatment (see **Fig. 6** & **Tab.2)**. *Aglantha digitale*, along with the other observed Hydrozoa, is reported to feed on a broad variety of taxa and size classes (Purcell & Mills, 1988; Pagès *et al.*, 1996), making it challenging to exactly pinpoint the triggering mechanism behind the observed treatment differences in abundance, biomass and size. As a consequence of hydrozoan growth being directly inhibited by OA they might focus on small prey organisms in the range of microplankton up to early copepodite stages. As already indicated by chl *a* (**Fig. 2**) and found by Dörner *et al.* (2020), these smaller prey organisms were either substantially negative affected by OA or did not display a treatment difference until the final phase of the experiment (see **Fig. 3B, C**). Presumably, this left hydrozoans under high pCO_2 with less alternatives to compensate for a possible negative OA effect. In turn, the observed increased

biomass of copepodites in Phase IV (**Fig. 3B**) could have supported the Hydrozoa population under high pCO_2, potentially causing the observed abundance difference between enhanced OA and ambient conditions. Thus, the contrasting effects of OA on hydrozoan abundance (positive) and biomass (negative), might also reflect different temporal patterns of prey availability affecting hydrozoan populations at different stages during the life cycle of *Aglantha digitale*. On the other hand, the enhanced growth of the hydromedusae under ambient conditions might have also led to an intensified intraspecific competition for food, possibly self limiting the population and causing their abundances to decrease more rapidly than under high pCO_2.

However, as not all of our datasets cover the entire experimental period, all these possibilites have some uncertainty. The discussed Hydrozoa biomass only originates from individuals bigger than 500 µm, and consequently misses the biomass of the individuals smaller 500 µm counted in the 55 µm net samples. As we observed a positive treatment effect in the 55 µm net abundances, this "missing" biomass would have likely amplified the observed CO_2 effect on biomass during Phase IV.

Furthermore, *S. tubolosa*, *Clytia* sp., and *O. geniculata*, all include a hydroid life stage of benthic settled polyps in their lifecycle. These benthic stages were regularly removed by a every 10 day cleaning interval of the mesocosms walls, most likely mitigating the existing Phase IV treatment differences by preventing the manifestation of possible OA effects on the reproduction of these species. Additionally, it cannot be excluded that this "predation" by cleaning was one of the key drivers of the overall decreasing abundances of hydrozoans throughout the experiment. Also, it may have caused the dominance of *A. digitale* in terms of abundance and biomass in the 500 µm net samples, as this species is reproducing without a benthic life stage.

As already mentioned, these constraints in combination with the complexity of the prevailing food web and the interactions within it, make it difficult to determine the driving mechanism for the observed OA effects on hydrozoans. However, even without isolating the exact mechanism, our results demonstrate that the OA effects on the lower trophic levels of the food web, visible in the chl *a*, micro- and mesoplankton data, were propagated up the food-web and caused the pronounced treatment differences visible in the hydrozoan population.

Treatment effects on fish larval survival, growth and nutritional condition: bottom-up vs. top-down control

Similar to the OA effects on Hydrozoa the observed higher survival of fish larvae under high pCO_2 was most likely due to an indirect positive effect from the changes in the pelagic community. Such an indirect positive effect of OA on herring larvae survival was already pointed out in a previous mesocosm study, in that case indirectly triggered by a pCO_2-mediated increase in prey organisms (Sswat *et al.*, 2018). In addition to that, a direct positive OA effect becomes even more unlikely when taking into account previous laboratory experiments revealing that herring larvae can be considered either tolerant or even negatively affected by pCO_2 levels higher than 1800 µatm (Frommel *et al.*, 2014; Maneja *et al.*, 2014; Maneja *et al.*, 2015), which is similar to the CO_2 exposure in our mesocosm study.

Possible bottom-up factors

Among the indirect effects determining survival of fish larvae, one crucial factor is prey availability, especially in the "critical first feeding period" after hatching. During this critical feeding period, it is established that fish larvae rely on small mesozooplankton as a food source, e.g. copepod nauplii (Checkley, 1982). But, recent publications also show that microplankton such as ciliates and dinoflagellates, and even larger phytoplankton may be considerable prey items (Denis *et al.*, 2018; Illing *et al.*, 2018). In our experiment, the critical period for herring larvae relates to Phase III (2 - 25 DPH). In this phase combined abundances/ biomass of these potential prey organisms, although on the lower end of the ideal prey density of *C. harengus* (e.g. > 7.5 nauplii L^{-1}, see Kiørboe *et al.* (1985)), did not display sufficient treatment differences to explain the higher fish larvae survival under high pCO_2. Only the higher overall copepod biomass between Phase III and IV of the experiment (Day 21 - 37, see **Fig. 3A**), could be a possible influence contributing to the higher fish larvae survival, especially as according to Peck *et al.* (2012), it is most likely that the herring larvae at this time point after hatch already shifted their prey size spectrum to bigger prey organisms. It has to be noted, however, that it is difficult to relate herring larvae survival to prey availability in the here presented study. The low number of larvae caught alive during the time of the experiment only permitted a limited possibility of assessing herring larvae size and their size related potential prey preferences. Additionally, prey availability and the nutritional condition of the larvae (sRD), which reflects mainly prey availability, was similar between CO_2 treatments at the end of the study. The RNA/ DNA ratios determined at the

end of the experiments indicated that prey abundance about a week before was not a limiting factor (Clemmesen, 1994).

In terms of herring larval growth, we found a tendency for bigger larvae (higher individual dry weight) in the ambient pCO_2 compared to the high pCO_2 treatment. Enhanced growth could originate either from higher prey availability or size selective mortality. Since prey availability only showed minor differences, it is most likely size-selective mortality that could have acted from two sides here: Either via proportionally higher survival of those larvae with a fitness advantage under low prey conditions, or via size-selective predation by Hydrozoa on smaller larvae. Both mechanisms could explain why smaller larvae were missing as well as the tendency of less, but bigger larvae in the ambient treatment. We therefore hypothesize, that the survival and larval growth of *C. harengus* larvae were decisively influenced by size-selective mortality, which in turn is primarily controlled by the hydromedusae – herring larvae predator-prey relationship.

Possible top-down control by Hydrozoa

A comparison between the Hydrozoa data and the survival of the introduced *C. harengus* larvae indicates increased hydromedusae biomass in Phase IV under ambient pCO_2 and reduced survival data of fish larvae (**Fig. 6A/ 7A**). As it was already pointed out, the majority of herring larvae hatched in the mesocosms were neither sampled alive, nor found dead in the sediment trap over the time of the experiment. With Hydrozoa at the same time being the most abundant potential predator of these larvae in the mesocosms, it is most likely that the 'missing' larvae were preyed upon. This predatory influence can be assumed to be especially eminent during the first several days after hatching, as young herring larvae are less mobile than more developed larvae (Illing *et al.*, 2018) and thus, potentially, easier to be preyed upon by the predominating hydromedusae (Skajaa *et al.*, 2004). However, it cannot be ruled out that the jellyfish were "only" carcass-feeding on larvae that died beforehand e.g. from starvation, and it is thus not possible to disentangle how many larvae were actively preyed upon. Highest hydromedusae abundances occurred on the days before the first CO_2 enrichment and from then on decreased over time (see **Fig. 5A/ B)**. This suggests that during the

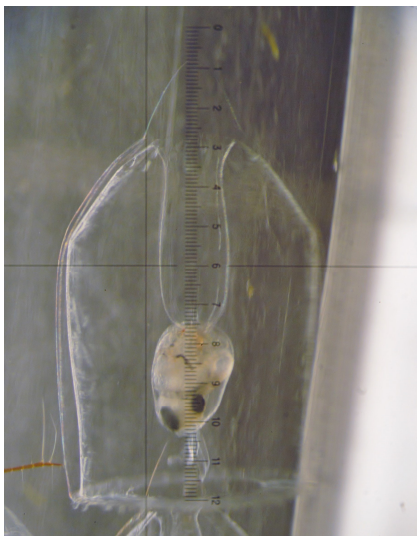

Figure 9: Microscopic observation of *Aglantha digitale* ingesting a herring larvae. Picture © Carsten Spisla

critical phase after hatching of the herring larvae, the predatory pressure by jellyfish was high, thereby potentially causing the low survival of fish larvae. Moreover, the body size of the hydromedusae was presumably a decisive factor causing the observed difference in fish larvae survival between the treatments, i.e. larger hydrozoans prey more efficicently on herring larvae. This is supported by the significantly higher Hydrozoa biomass and corresponding lower survival of herring larvae under ambient conditions in the final phase of the experiment (see **Fig. 6A/ 7A**). Additionally, as presented in the discussion Section "Treatment effects on Hydrozoa", the hydrozoans during and directly after fish larvae hatch (Phase II and III) were presumably larger in the ambient pCO_2 mesocosms. The increased body size per individual implies a larger energy demand of the hydromedusae, thus potentially leading to preferential predation of the largest and most nutritious food in the mesocosms, i.e. fish larvae. In accordance with that hypothesis, we regularly found the most abundant and "heaviest" hydromedusae of *Aglantha digitale* (see **Fig. 6B**) with herring larvae inside their stomachs as illustrated in **Fig. 9**. In addition to the predation by hydromedusae, also a possible predatory influence of the observed juvenile cods became apparent, with the lowest herring biomass (and survival) being found in those mesocosms with a high cod biomass.

CONCLUSION

Our findings revealed pronounced effects of OA on the competition between Hydrozoa and fish larvae, which are among the two major predator groups in plankton communities. In particular, we found that the strong predator-prey coupling of Hydrozoa and fish larvae, is altered by OA effects on lower trophic levels, which are mediated via the food-web and thereby substantially affected hydrozoan population dynamics and fish larvae survival.

Especially in the context of other environmental stressors, like ocean warming, that are predicted to favor jellyfish on the global scale, or fish species more sensitive to either OA and/ or other stressors, e.g. Atlantic cod, alterations in the Hydrozoa-fish relationship could also have severe consequences for important ecosystem services. This highlights the importance of studying the effects of climate change from a whole ecosystem perspective rather than focusing on particular species, since it is the response of the lower trophic levels that cascades up the food web and causes extensive changes perceptible in the high trophic level organisms.

ACKNOWLEDGEMENTS

We would like to thank the participants of the KOSMOS Norway 2015 experiment for maintenance and sampling of the mesocosm infrastructure over more than 55 days. A special thanks goes to all participating members of the University of Bergen for their outstanding support, especially Prof. Dr. Arild Folkvord and Prof. Dr. Audrey Geffen (Department of Fisheries Ecology and Aquaculture at the University of Bergen) for the help and cooperation on introducing herring larvae to our mesocosms. We would also like to thank the staff of the Espegrend Marine Biological Station for providing excellent infrastructure and daily support, in particular Tomas Sørlie. Additionally, we thank the Bavarian State Collection of Zoology in Munich, the sequencing service units at the LMU Munich, and particularly Peter Kohnert for carrying out and supporting the genetic analysis in this study. Furthermore, we want to acknowledge the technicians for preparation and maintenance of the KOSMOS facilities. We are grateful to the captains and crews of R/V Alkor (AL455), R/V Poseidon (POS486T), and R/V Håkon Mosby (2015627, 2015628) for the transportation and mooring of the mesocosm infrastructure. CS is thankful to the Norwegisch-Deutschen Willy-Brand Stiftung (10/2015-S) as well as the Erasmus+ project for funding of the scientific work in the framework of his master thesis. This study was carried out in strict accordance with the regulations applicable in Norway. The application was approved by the National Regulatory Committee on the Ethics of Animal Experiments (Permit FOTS id 7389).

CHAPTER 3

Assessing the Influence of Artificial Upwelling on Zooplankton Secondary Production and Trophic Transfer Efficiency of an Oligotrophic Plankton Community via ^{13}C Labeling

C. Spisla[1*], J. Taucher[1], M. Sswat[1], J. Ortiz[1], N. Smith-Sanchez[1], K. G. Schulz[2], U. Riebesell[1]

[1]GEOMAR, Helmholtz Centre for Ocean Research Kiel, Biological Oceanography, Kiel, Germany
[2]Centre for Coastal Biogeochemistry, Southern Cross University, Lismore, NSW, Australia

***Correspondence:**
Carsten Spisla
cspisla@geomar.de

To be submitted to:
Frontiers of Marine Science

Abstract

Nutrient-depleted areas with low biological productivity cover large parts of the world oceans and are further expanding with ongoing climate change. Technological approaches to transport nutrient rich deep-water to these "ocean deserts", termed "artificial upwelling", could help to enhance primary production and establish a shorter (more efficient) food-chain, thereby facilitating the build-up of biomass on higher trophic level such as harvestable fish. Upwelling frequency (mode) and quantity (intensity) are considered crucial factors that determine the enhancement of primary production and how it is converted into consumer production by adjacent trophic levels. In order to assess the effect of upwelling mode and intensity on the trophic transfer efficiency (TTE) of natural plankton communities in subtropical oligotrophic waters, we conducted a large scale mesocosm experiment off the coast of Gran Canaria, Spain. Artificial upwelling was simulated by adding natural deep-water (collected from about 330 m depth) to the mesocosms in two different upwelling modes: Four mesocosms received a singular water exchange, whereas another four were fertilized on a recurring basis every four days. To each upwelling mode, the four upwelling intensities 'extreme' (~ 11 µM N), 'high', 'medium', and 'low' (~ 1.5 µM N) were applied by varying the mixing ratios of mesocosm and collected deep-water. Primary (PP) and secondary production (SP) were assessed via addition and tracing of the stable isotope ^{13}C from dissolved inorganic carbon (DIC) over particulate organic carbon (POC) up to mesozooplankton (copepods), and TTE was calculated as the fraction of these two production rates (SP/PP). We found that $PO^{13}C$-based primary production was higher in the recurring than in the singular upwelling mode and increased from low to extreme upwelling intensity. In contrast, secondary production rates under singular upwelling exceeded those of the recurring upwelling mode, and TTE was found highest under extreme to high singular upwelling (10% and 16%). Our results indicate that food density and quality, as well as the size and species composition of the prevailing mesozooplankton community led to generally low SP and TTE in all mesocosms of the recurring and the medium singular upwelling treatment. These findings suggest that artificial upwelling could potentially help to revitalize "ocean deserts" if carried out with the appropriate intensity and temporal frequency, i.e. singular upwelling events with an adequate time window for zooplankton to utilize the induced phytoplankton bloom.

INTRODUCTION

In large areas of the world's oceans, a strong density gradient between warm nutrient depleted surface and colder but nutrient-rich deep-water layers is prevailing, thereby reducing nutrient supply and productivity of surface waters (Sigman & Hain, 2012; Moore *et al.*, 2013). These foremost low- and mid-latitude subtropical gyres cover the majority of all ocean basins, make up for around 40% of the earth's surface, and are generally referred to as "ocean deserts" (Polovina *et al.*, 2008). Along with increasing sea surface temperature and expanding oxygen minimum zones due to climate change, these ocean deserts are increasingly expanding and "consuming" regions with medium productivity in all major ocean basins (Polovina *et al.*, 2008; Stramma *et al.*, 2008; Irwin & Oliver, 2009).

One approach to counteract this ongoing desertification of the oceans, could be the application of "artificial upwelling" in such regions. With the appropriate technological infrastructure, the natural density boundary can be overcome by pumping nutrient rich deep-ocean water into the surface water layers, thus potentially serving two major purposes: (1) to fuel marine primary production for ecosystem-based fish production, and (2) to enhance the ocean's biological carbon pump to increase oceanic uptake and sequestration of CO_2 (Kirke, 2003; Giraud *et al.*, 2016; GESAMP, 2019). In order to convert an oligotrophic system towards sustainably harvestable amounts of fish, however, enhancing primary production (PP) via nutrient input is only a part of the solution. The primary production induced by artificial upwelling also has to create a sufficient amount of secondary production (SP), i.e. biomass of phytoplankton consumers such as copepods that serve as main prey for the different life stages of fish (Pauly & Christensen, 1995; Støttrup, 2003; Castonguay *et al.*, 2008). Furthermore, to maximize fishery yield, the plankton community created by artificial upwelling has to be capable of efficiently transferring biomass from primary production to secondary production and up to fish, i.e. in a way that minimizes the loss of biomass from one trophic level to the next as much as possible.

"Trophic transfer efficiency" (TTE) is determined as the ratio of SP and PP, in other words, the amount of primarily produced energy used for secondary production. Both PP and SP have a high variability depending on the predominant physical and chemical environment as well as the plankton community composition of the local ecosystem (Chapman & Reiss, 1998). In theory, this TTE of a system to forward energy from one trophic level to the next should be directly influenced by the intensity and temporal frequency the nutrient input fueling PP. Different application scenarios for artificial upwelling would result in different

temporal patterns of physical characteristics (e.g. mixing and advection) and nutrient fertilization, e.g. assuming either a stationary pump ("singular" upwelling event, see Fan *et al.* (2016)) or a pump drifting along with the same patch of water, suppling it on a recurring basis with nutrient rich deep-water ("recurring" upwelling event). These different environmental regimes should theoretically have different impacts on plankton communities, i.e. with varying SP and PP rates, and potentially different TTEs.

Quantifying trophic transfer efficiency is a major methodological challenge and one of the most persisting problems in experimental marine ecology due to a wide variety of constraints (Boecklen *et al.*, 2011). In theory, untangling this problem is only possible by tracing the flow of biomass and energy through the entire food web, thereby quantifying biomass production at the different trophic levels. However, measuring production rates of zooplankton is difficult and usually approximated through indirect methods (e.g. egg or fecal pellet production, molting rates or allometric scaling, see Kiørboe *et al.* (1988) or Yáñez *et al.* (2018)). Thus, common approaches to estimate TTE included measuring primary production for phytoplankton (i.e. via incubation with the radiotracer ^{14}C), and relating these numbers to the abundances and/or biomass of zooplankton grazers and higher trophic levels (Schulz *et al.*, 2004). One of the constrains of these methods is that they do not effectively account for any loss or turnover of biomass of consumers (e.g. from predation or death), and with that do not constitute quantitative rate measurements but rather approximations. In line with that, many studies reporting "trophic transfer efficiency" either use such approximations, or calculate the efficiencies by means of computer models, which include loss terms based on literature values (e.g. EcoPath, Christensen and Walters (2004)).

To overcome these uncertainties and to accurately trace the fate of primary production within the food web, stable isotope (SI) labeling constitutes a powerful tool (Boschker & Middelburg, 2002; Van den Meersche *et al.*, 2011; Middelburg, 2014). Although rarely used in the context of TTE, especially the heavier carbon isotope ^{13}C is applicable to estimate the primary and secondary production rates necessary for assessing TTE. When utilized in an enclosed experimental design, such as a mesocosm, ^{13}C can be used to enrich the natural ^{13}C dissolved inorganic carbon (DIC) pool of the respective system (see de Kluijver *et al.* (2013)). This enrichment is then traceable throughout the food web, due to the fact that the amount of ^{13}C in the organism of a consumer after a certain time reflects the combined amount of ^{13}C of its resources (Zanden & Rasmussen, 1999; Post, 2002; Middelburg, 2014). Biomass production rates can then be calculated by measuring the increase of the ^{13}C tracer

in consecutive trophic levels of the food web over time, and relating this rate of carbon enrichment to the existing biomass of the respective trophic level (Hama *et al.*, 1993). To estimate SP and TTE, this approach requires temporally resolved data of ^{13}C enrichment in different taxonomic groups of zooplankton, knowledge and correct assignment concerning their prey organisms as well as data on their ^{13}C enrichment over time.

In the here presented study, we applied this rarely utilized principle of estimating production rates and trophic transfer efficiency via ^{13}C stable isotope enrichment. In doing so, the study addresses the question if artificial upwelling can change the food web structure in oligotrophic marine areas to such an extent that trophic transfer of energy is enhanced, and formation of biomass in higher trophic levels such as fish is maximized. A large scale mesocosm experiment was conducted off Gran Canaria, Spain, studying the effect of two different upwelling modes (singular and recurring upwelling) in combination with different upwelling intensities (low, medium, high, and extreme mixing of nutrient rich deep-water). ^{13}C was added as a tracer, and TTE was quantified by measuring the gradual enrichment of ^{13}C over different trophic levels to answer the question how TTE varies under different upwelling conditions.

MATERIAL AND METHODS

We deployed nine KOSMOS (Kiel Offshore Mesocosms for Ocean Simulations) units from October 7th to December 13th 2018 in Bahía Gando, a bay located at the east coast of the island Gran Canaria, Spain (27°55.673' N, 15°21.870' W). This area predominantly covers nutrient poor oligotrophic waters influenced by the subtropical North Atlantic gyre and, to a lesser extent, the Canary Current (Barton *et al.*, 1998; Arístegui *et al.*, 2009).

The data presented in this paper only refers to the second half of the experiment, lasting from November 5th onward, because the study had to be restarted after the first half, due to the adverse environmental conditions on the experimental site. Background information about the restart as well as more details about experimental design, measured parameters and environmental data are described in an overview article by Sswat el al. (in prep).

Just framing the experiment briefly, each of our 9 KOSMOS units was dimensioned 2 m in diameter and 14 m in length, resulting in an enclosed volume of 43.8 ± 1.4 m³ of sea water and its planktonic community (details on mesocosm infrastructure, deployment and maintenance can be found in Riebesell *et al.* (2013b)). The mesocosms were split into one control (M5) and eight manipulated mesocosms, wherein four of them served as

"singular" (M1, M3, M7, M9) and the other four as "recurring" (M2, M4, M6, M8) upwelling treatments. The upwelling was simulated by replacing part of the oligotrophic mesocosm water with nutrient rich deep-water collected off the coast of Gran Canaria (see Section "Deep-water collection and addition").

Overall, a variety of samples were taken on a two-day basis over the whole course of the experiment, the most important ones for the here presented experiment being: Depth profiles of temperature, salinity, and density were assessed with a CTD equipped with additional sensors for pH, oxygen, and PAR (CTD60M Sea & Sun Technology GmbH, Trappenkamp, Germany). Integrated water samplers (IWS, HYDRO-BIOS Apparatebau GmbH, Kiel, Germany) were utilized to collect a 5 L depth integrated mesocosm water sample for the analysis of chlorophyll *a* (chl *a*), and suspended particulate organic carbon (POC). The IWS were operated as described in Taucher *et al.* (2017). See **Fig. 1** or for a full list of the assessed parameters Sswat et al. (in prep).

Deep-water collection and addition

Deep-water (DW) was collected off the coast of Gran Canaria between 28°00'N, 15°18'E and 27°57'N, 15°10'E from 330 m depth. Via an electric pump deployed from a ship, the DW was pumped from depth into a custom build synthetic bag with a volume of 100 m^3 (for technical details see Taucher *et al.* (2017)). This bag was then moored at the mesocosm study site and the water for the different DW additions was pumped from the bag into the respective mesocosm.

Due to technical issues, the DW could not be collected from around 600 m depth as planned, but had to be spiked artificially with nitrate (NO_3^-), phosphate (PO_4^{3-}) and silicic acid ($Si(OH)_4$) to simulate the nutrient concentrations predominant in this depth (see Sswat et al., in prep., for details). These concentrations were checked and adjusted accordingly prior to every deep-water addition. Overall, the "singular" treatment received one addition of deep-water in the beginning of the experiment (Day 4), while the "recurring" treatment received a comparable amount of water exchange from Day 4 onward over 28 experimental days and eight deep-water additions every four days (**Fig. 1**). The control did not receive any deep-water at all.

In addition to the different frequencies of deep-water addition, also the amount of exchanged water was varied between the four mesocosms of the singular and recurring treatment, respectively. By that, the four mixing ratios of low, medium, high, and extreme deep-water

addition were realized, all corresponding to a specific nutrient input on the basis of newly added nitrogen (N). In the singular upwelling treatment this corresponded to a new nitrogen (N) concentration of 1.62 µmol L^{-1} in the low, 3.07 µmol L^{-1} in the medium, 5.56 µmol L^{-1} in the high, and 9.8 µmol L^{-1} in the extreme mixing mesocosm on Day 4. In the recurring treatment, new N concentrations of 1.61 µmol L^{-1} (low), 3.15 µmol L^{-1} (medium), 6.16 µmol L^{-1} (high), and 10.97 µmol L^{-1} (extreme) were gradually reached until the last addition on Day 32 (see **Tab. 1**). Thus, the singular and recurring treatments received approximately the same amount of new nutrients over the course of the study, but in different temporal modes.

Table 1: Individual mesocosm numbers, symbols, upwelling mode and intensity, exchanged volumes, and total new N values added over the entire study (see also Sect. "Deep-water collection and addition"). The color scheme and the symbols assigned to the individual mesocosms will be used in all plots throughout this paper.

upwelling mode	control	singular				recurring			
upwelling intensity		low	medium	high	extreme	low	medium	high	extreme
volume exchange per addition [%]	0	6.4	12.0	22.4	39.2	0.8	1.6	3.2	6.4
total new N added [µmol L^{-1}]	0	1.6	3.1	5.6	9.8	1.6	3.1	6.2	11.0

Stable isotope labeling and sampling

11 g of ^{13}C as a mixture of 5 g labeled sodium bicarbonate and 6 g labeled sodium carbonate (99% labeled, Cambridge Isotope Laboratories and Sigma Aldrich) was added to the natural ^{13}C DIC pool of every mesocosm. Thereby, the natural DI^{13}C pool was enriched by about 110 ‰ from 1.1% to 1.21%. For addition to the mesocosms, the ^{13}C labeled material for every mesocosm was brought into solution with about 1.5 L aqua dest. (MilliQ), then diluted to 20 L, and subsequently distributed equally over the whole water column of the mesocosm. The labeling was first carried out in the singular treatment on Day 14, and afterwards in the recurring treatment on Day 16, thereby allowing to alternate the time-intensive ^{13}C sampling of zooplankton of four mesocosms (**Fig. 1**).

To obtain the standing stock ^{13}C concentrations for the different trophic levels, as required for the calculations of production rates, a sampling strategy was applied that permits to track the fate of ^{13}C to different mesozooplankton (mesoZP) size classes and key species of the food web:

From the IWS, 40 mL of mesocosm water was filtered every two days (0.2 µm prefiltered by syringe) into clear glass screw neck vials (Lab Logistics Group), and stored in the fridge until analysis for the ^{13}C baseline in the DIC. Analysis was then carried out on a GasBench - Isotope-Ratio Mass Spectrometry system (IRMS, Southern Cross University, Australia). In addition to that, between 200 and 1000 mL of IWS sea water were filtered every two days on 0.7 µm pre-combusted (450°C for 6 h) GF/F filters in order to obtain the ^{13}C concentration in all suspended POC, (including bacteria, phytoplankton, and microzooplankton). Until mass-spectrometric analysis (GEOMAR Kiel, Thermo Scientific IRMS), the filters were dried at 60°C for 24 h, packed into 8x8x15 mm tin capsules, and stored airtight and dry in desiccators.

Furthermore, defined numbers of mesozooplankton organisms were hand-picked from samples obtained with vertical net hauls with different sized Apstein nets (55/500 µm mesh size, ø 17/50 cm, HYDRO-BIOS Kiel) every four days (**Fig. 1**). Mesozooplankton organisms were categorized in different size classes (55-200 µm, 200-500 µm, > 500 µm) and separated based on their taxonomic identity and the most abundant species. After picking, the organisms were dried at about 60°C for at least 24 h, packed into tin capsules and stored dry in a desiccator until analysis (GEOMAR Kiel, Thermo Scientific IRMS). Due to the comprehensive time requirement in processing and picking the mesoZP samples (in order to obtain sufficient biomass for ^{13}C measurement of each size class and/or taxonomic group), the two upwelling treatments were sampled according to the isotopic enrichment in an alternating order. This means, mesoZP samples were taken for the singular treatment mesocosms from Day 13, and for the recurring treatment from Day 15 onward in a four-day interval, respectively.

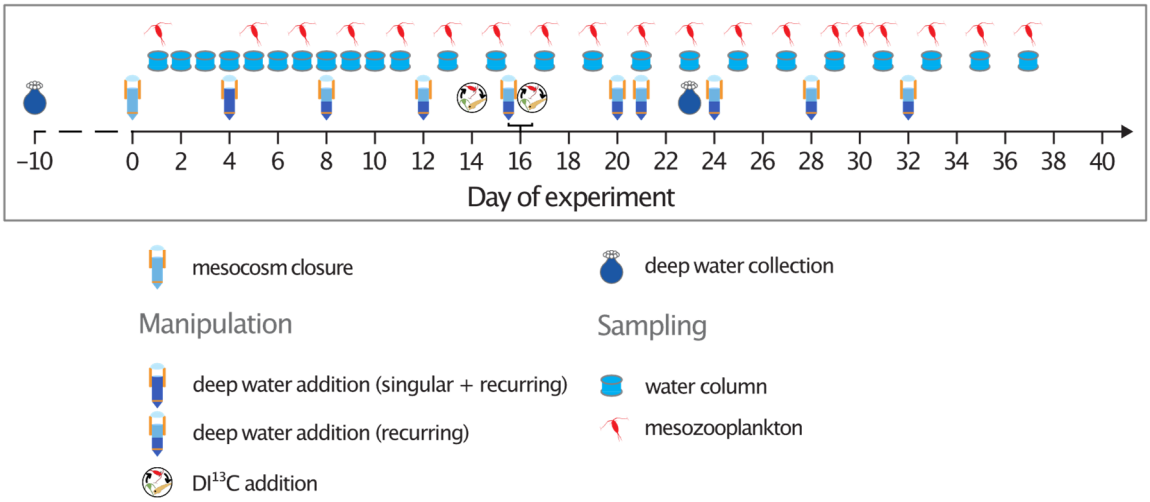

Figure 1: Timeline of relevant sampling and manipulation activities over the course of the experiment. Explanation of timeline symbols given in the legend.

Production rates and trophic transfer efficiency calculation

In general, TTE is calculated as the fraction of two biomass production rates, in our case secondary biomass production of copepods, as the most important link from primary production to higher trophic levels, divided by primary production (Eq. 1).

$$TTE = \frac{\text{secondary production}_{copepoda}}{\text{primary production}} \qquad \text{(Eq. 1)}$$

The primary and secondary production rates were calculated according to Eq. (2) as defined by Hama *et al.* (1993). With this formula, biomass production is calculated as the product of consumer's standing stock biomass ($C_{consumer}$) at the end of the incubation time (t) and the fraction of $\Delta^{13}C$ enrichment from (t-1) to (t) in the consumer ($a_{consumer} = AT\%^{13}C_{consumer}$) to the maximum possible $\Delta^{13}C$ enrichment, i.e. the difference between the ^{13}C concentration of the consumer at 't-1' and its food ($a_{food} = AT\%^{13}C_{food}$) at 't'.

$$Production = \frac{(a_{consumer(t)} - a_{consumer(t-1)})}{(a_{food(t)} - a_{consumer(t-1)})} \times \frac{C_{consumer(t)}}{t} \qquad \text{(Eq. 2)}$$

All isotopic concentrations were calculated in atomic percent (AT%) as this unit, contrary to $\delta^{13}C$, increases linearly with increasing isotopic labeling (Brenna *et al.*, 1997). For the calculation of $AT\%^{13}C$, the isotopic ratio ($^{13}C/^{12}C$) of the sample ($^{13}R_{sample}$) was derived from the blank corrected $\delta^{13}C$ output of the mass-spectrometric measurement according to Eq. (3) with $^{13}R_{VPDB}$ being the Vienna Pee Dee Belmnite (VPDB) standard of 0.0111802. $AT\%^{13}C$ was then calculated as the fraction shown in Eq. (4), and blank correction of the $\delta^{13}C$ values

was performed as shown in Eq. (5), with m_{sample}/m_{blank} being the respective carbon content in µg.

$$\delta^{13}C = \frac{^{13}R_{sample}}{^{13}R_{VPDB}} - 1 \quad \text{(Eq. 3)}$$

$$AT\%^{13}C = \left[\frac{^{13}R}{(1+^{13}R)}\right] \times 100 \quad \text{(Eq. 4)}$$

$$\delta^{13}C_{blank\ corrected} = \frac{(m_{sample} * \delta^{13}C_{sample}) - (m_{blank} * \delta^{13}C_{blank})}{m_{sample} - m_{blank}} \quad \text{(Eq. 5)}$$

Primary production rates were calculated analogously, using $AT\%^{13}C_{substrate}$ obtained from the $DI^{13}C$, and $AT\%^{13}C_{consumer}$ as well as $C_{consumer}$ [µg] from the POC filters. In line with the ^{13}C labeling of the respective treatments primary production rates were calculated from Day 15/17 in a four-day interval until Day 35/37 (singular/recurring treatment). It has to be noted that POC filters also contain carbon from non-autotrophic plankton (bacteria, microzooplankton), which may lead to slight underestimation of PP with this method (see discussion).

As already mentioned, for the calculation of secondary production, copepod biomass as well as their ^{13}C signature were given as $C_{consumer}$ [µg] and $AT\%^{13}C_{consumer}$, respectively. Copepod biomass was obtained by multiplying the abundance data from microscopy (individuals L^{-1}) with the individual carbon values [µg C] as measured by mass spectroscopy. The ^{13}C fraction of the POC filters was used as $AT\%^{13}C_{food}$.

^{14}C primary production

Since the ^{13}C tracer was added on Day 14 and 16, primary production estimates from this method are not available for the initial period. Thus, in addition to the *in situ* determination of primary production based on ^{13}C labeling, primary production was also assessed in incubations with the ^{14}C uptake method, carried out as described in Ortiz et al. For that, just to summarize briefly, 280 mL of prefiltered (250 µm mesh size) water from the IWS was distributed equally on four culture flasks (Sarstedt TC Flask d15, Nümbrecht, Germany) per mesocosm, inoculated with 80 µL of a stock solution of ^{14}C-labeled sodium bicarbonate ($NaH^{14}CO_3$, Perkin Elmer, Waltham, USA), and incubated in a climate chamber for 24 hours, simulating mesocosm water temperature and light (12 h light-dark cycle). After incubation, all samples were filtered on a circular filtration manifold (Oceomic, Fuerteventura, Spain) under low vacuum pressure (< 200 mbar), and then placed into 5 mL scintillation vials (Sarstedt HD-PE Mini-vial, Nümbrecht, Germany). Subsequently, they

were incubated for 24 hours in a desiccator with fuming hydrochloric acid (HCl 37%), in order to remove any remaining inorganic ^{14}C. Prior to the measurement on a scintillation counter (Beckman LS-6500, Brea, USA), the scintillation cocktail Ultima Gold XR (Perkin Elmer Ultima Gold, Waltham, USA) was added to all filters, and they were left in darkness overnight. While one of the sample bottles served as control, final PP rates [µg C L^{-1} h^{-1}] were calculated as a mean from the counted disintegrations per minute of the remaining three samples, using Eq. (6).

$$PP = \left[\frac{V_S}{V_F}\right] x \frac{DIC \times (DPM_S - DPM_D)}{DPM_A \times t_i} \quad \text{(Eq. 6)}$$

V_S = sample volume [L]; V_F = filtered volume [L]; DPM_S = sample disintegrations per minute; DPM_D = dark/blank disintegrations per minute; DIC = dissolved inorganic carbon [µg C L^{-1}]; DPM_A = added ^{14}C in disintegrations per minute; t_i = incubation time [h]

RESULTS

^{13}C enrichment

Dissolved inorganic ^{13}C ($DI^{13}C$)

With the first ^{13}C addition to the singular and recurring upwelling treatment on Day 14 and 16, respectively, natural ^{13}C abundance in the DIC pool of the mesocosms increased from an overall mean of AT%^{13}C = 1.1075 (± 0.0004 SD, Day 13) to AT%^{13}C = 1.2311 (± 0.008 SD, $\Delta^{13}C_{enrichment}$ = 123.6‰, Day 15, singular) and AT%^{13}C = 1.2301 (± 0.011 SD, $\Delta^{13}C_{enrichment}$ = 122.6‰, Day 17, recurring). The control was enriched in parallel with the recurring treatment on Day 16, and increased from AT%^{13}C = 1.1071 to 1.2318 ($\Delta^{13}C_{enrichment}$ = 124.7‰, Day 15 to 17, **Fig. 2A**).

Over the course of the experiment, ^{13}C DIC values of all mesocosms decreased due to the sea-air gas exchange as well as due to the repeated dilution with deep-water in case of the recurring upwelling treatment. ^{13}C DIC in the singular and control mesocosms decreased uniformly by around 0.0077 AT%^{13}C from a mean of 1.2309 (AT%, Day 17) to 1.2232 (AT%, Day 37, **Fig. 2A**). In comparison to that, mean ^{13}C DIC in the recurring treatments decreased by 0.022 AT%^{13}C from initially 1.2301 on Day 17 to 1.209 (AT%, Day 37, **Fig. 2A**). According to the amount of mesocosm water replaced by deep-water over time (mixing regime/ upwelling intensity), ^{13}C DIC in the recurring upwelling mesocosms decreased the most in M8 (extreme mixing) and least in M2 (low mixing, see **Fig. 2B**).

Particulate organic ^{13}C ($PO^{13}C$)

After the enrichment with the tracer, ^{13}C abundance on the POC filters increased almost linearly towards the end of the experiment. In the singular treatment values increased by 0.0904 AT%^{13}C from 1.0852 AT%^{13}C (± 0.001 SD, Day 13) to 1.1756 AT%^{13}C (± 0.018 SD, Day 37), and in the recurring mesocosms by 0.1016 AT%^{13}C from 1,0839 AT%^{13}C (± 0.001 SD, Day 15) to 1.1855 AT%^{13}C (± 0.005, Day 37). The control constantly stayed below the mean values of the two treatments with an increase from 1.0837 AT%^{13}C to 1.1635 AT%^{13}C (see **Fig. 2A**).

Under recurring upwelling mode, the isotopic enrichment reflected the different simulated upwelling intensities (see **Fig. 2C**). The extreme mixing regime reached with 1.1877 AT%^{13}C the highest enrichment, followed by the high (1.1853 AT%^{13}C), medium (1.1838 AT%^{13}C), and low mixing (1.1457 AT%^{13}C). The isotopic enrichment in the singular upwelling mixing ratios is almost vice versa. The singular extreme treatment reached with 1.1495 AT%^{13}C the lowest enrichment, while the medium mixing marked with 1.1963 AT%^{13}C the highest ^{13}C concentration (**Fig. 2C**).

Mesozooplankton ^{13}C

The development of the mean enrichment after addition of the ^{13}C tracer did not indicate pronounced differences between the singular and recurring upwelling treatment. Both treatments increased almost linearly, with the singular upwelling treatment increasing from 1.0842 AT%^{13}C (± 0.001 SD, Day 13) to 1.1655 AT%^{13}C (± 0.0237 SD, Day 37), and the recurring from initially 1.085 AT%^{13}C (± 0.0011 SD, Day 15) to 1.1623 AT%^{13}C (± 0.02 SD, Day 37) (**Fig. 2A**). However, analyzing the development of the tracer in the different simulated upwelling intensities reveals some deviations from the linear enrichment (see **Fig. 2D**). Most noticeable in that context is the recurring low mixing mesocosm, which from Day 21 onward revealed a significantly lower tracer enrichment rate than all other mesocosms. Furthermore, the recurring and singular extreme mixing mesocosm displayed a decreasing ^{13}C concentration from 1.1597 AT%^{13}C (Day 31, singular) and 1.156 AT%^{13}C (Day 33, recurring), to 1.1507 AT%^{13}C and 1.143 AT%^{13}C at the end of the experiment, respectively.

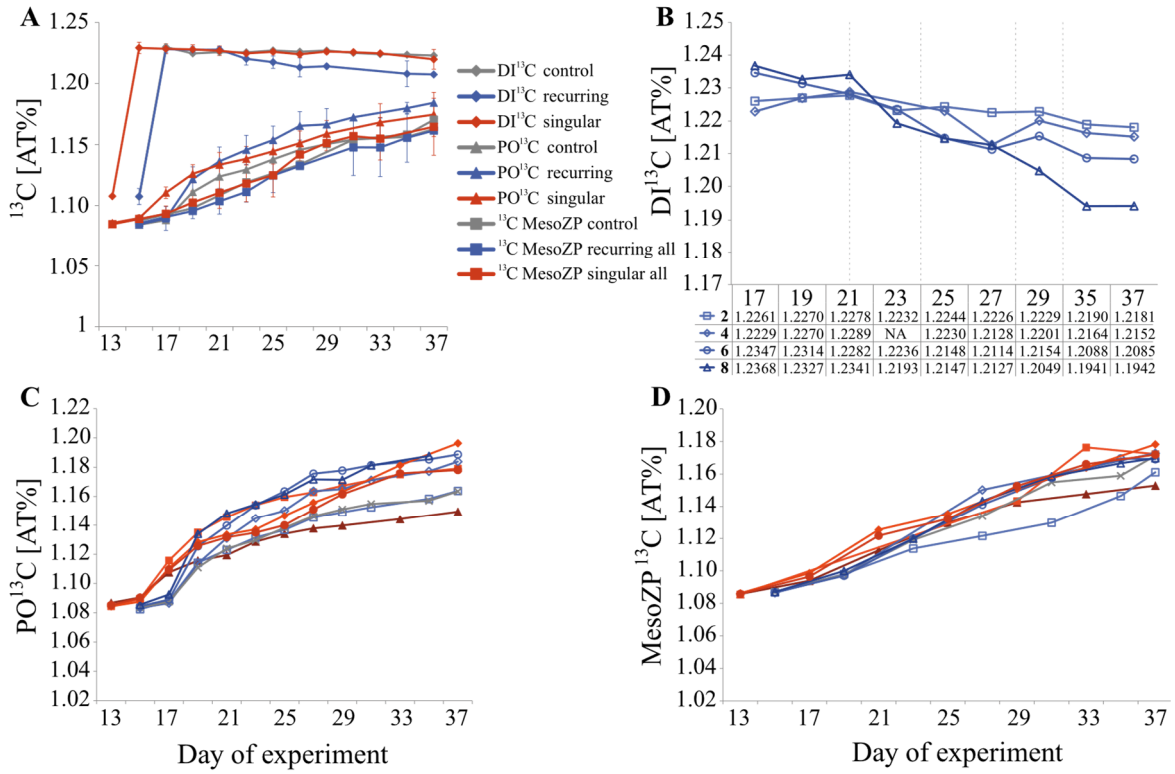

Figure 2: (A) ^{13}C tracer enrichment in DIC, POC and collected mesozooplankton organisms as mean values for the respective upwelling modes and the control over time. Respective SD given as error bar. Colors and symbols according to the given legend. **(B)** Decrease of the ^{13}C enrichment in the recurring mesocosms over time, due to deep-water addition. Exact values for each measurement are shown in the table below the figure. **(C)** ^{13}C signal per mesocosm over time for POC filters and **(D)** collected mesoZP organisms. Vertical lines depict the timepoints of deep-water additions to the mesocosms, **(B, C, D)** colors and symbols according to the overview given in **Tab.1**.

Production rates

^{13}C primary production (PP)

After the isotopic enrichment, the primary production (PP) calculated via ^{13}C was higher under recurring than under singular upwelling conditions, with an overall mean of 57.70 µg C L^{-1} d^{-1} (± 148.70 SD) compared to 12.76 µg C L^{-1} d^{-1} (± 8.44 SD), respectively, but lowest in the control with 5.32 µg C L^{-1} d^{-1} (± 3.66 SD).

The mean PP rates of the different upwelling intensities displayed a large spread in the recurring, but comparably minor variations in the singular treatment (see **Fig. 3A**). In the recurring treatment mean PP rates over the course of the isotopic measurement more than doubled under low (0.8 - 1.6 µmol N L^{-1}), medium (1.6 - 3.1 µmol N L^{-1}), and high (3.2 - 6.2 µmol N L^{-1}) nutrient input, from 6.4 µg C L^{-1} d^{-1} (± 3.1 SD) to 7.2 µg C L^{-1} d^{-1} (± 8.3 SD) to 35.1 µg C L^{-1} d^{-1} (± 19.7 SD), respectively. From recurring high to extreme mixing (6.2 - 11 µmol N L^{-1}) they almost tripled to 181.4 µg C L^{-1} d^{-1} (± 263.9 SD,

see **Fig. 3A**). In the singular upwelling treatment, the highest mean PP was calculated for the extreme mixing mesocosm with 14.3 µg C L^{-1} d^{-1} (± 13.4 SD), but with less variance to the other simulated upwelling intensities with 14.1 µg C L^{-1} d^{-1} (± 5.9 SD, high), 11.7 µg C L^{-1} d^{-1} (± 6.3 SD, medium) and 11 µg C L^{-1} d^{-1} (± 4.3 SD, low, see **Fig. 3A**). It has to be noted, however, that data coverage on ^{13}C-based primary production starts on Day 15 of the experiment, whereas the chl *a* peak in the singular treatments was already reached between Day 7 and 9 (see **Fig. 4A**).

The clear separation between singular and recurring upwelling treatment, however, is even more pronounced when comparing their cumulative sum of all calculated PP rates over the time of the isotopic enrichment. Here, the recurring upwelling mode mesocosms produced with 2424 µg C L^{-1} (sum over all recurring mesocosms) over 22 days substantially more than the singular upwelling mode with 613 µg C L^{-1} (sum over all singular mesocosms, **Fig. 3B**). Additionally, also in the cumulative PP data the extreme mixing accounted for the majority of PP in the recurring upwelling mode, while the singular upwelling mixing treatments again displayed minor variations. In numbers, the recurring extreme mixing mesocosm accounted with 1814 µg C L^{-1} for about 75% of the overall produced biomass, followed by the high mixing mesocosm with 350 µg C L^{-1} (14.4 %). In the singular upwelling treatment, however, cumulative PP only ranged from 132 µg C L^{-1} under low, to 171 µg C L^{-1} under extreme mixing conditions. The control displayed with 59 µg C L^{-1} the lowest cumulative PP (see **Fig. 3B**).

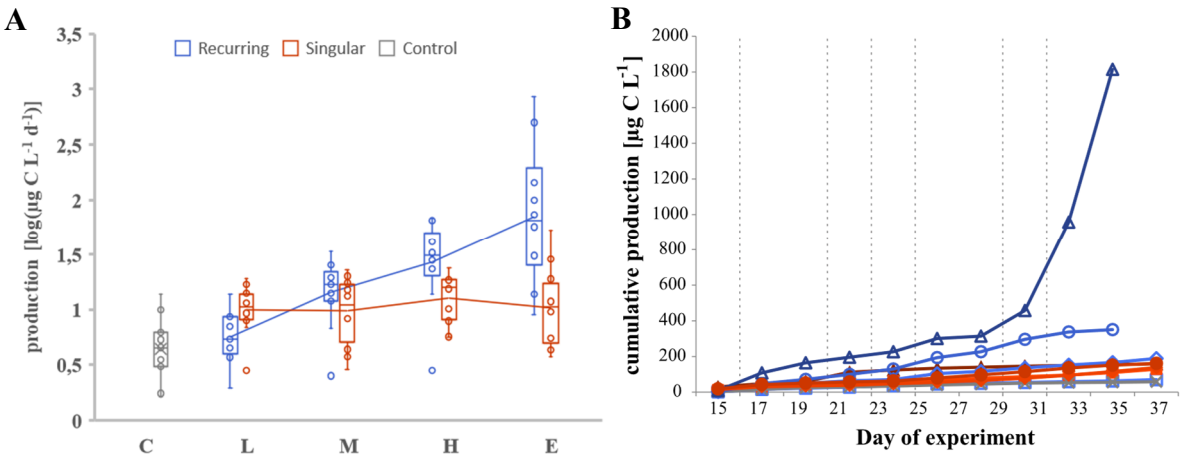

Figure 3: ^{13}C obtained primary production (PP) for the singular and recurring upwelling mode as well as the control over the time of the isotopic enrichment. **(A)** As log (base 10) transformed mean PP per upwelling intensity treatment (C = Control, L = Low, M = Medium, H = High, E = Extreme), with boxplots bounded by the minimum and maximum value of the respective dataset, and the average 50% of the remaining values within the box. Colors according to the given legend. **(B)** As cumulative PP per mesocosm, with vertical lines symbolizing deep-water additions, and colors and symbols for the single mesocosms according to **Tab. 1**.

^{14}C primary production

Mean ^{14}C PP over the whole experimental period was measured with 42 µg C L^{-1} d^{-1} under recurring, 32.6 µg C L^{-1} d^{-1} under singular upwelling conditions, and 10 µg C L^{-1} d^{-1} in the control. Note that the ^{14}C PP data in the singular treatment displays peak values from a short but intense bloom after the first deep-water addition on Day 7. Compared to the ^{13}C PP data, the treatment difference is reduced and not significant anymore, mainly due to the PP peak after the first nutrient addition (Day 7 - 11) substantially enhancing the mean PP rate, especially in the singular extreme and high upwelling treatment (cf. **Fig. 3A** and **Fig. 4A**). The mean PP in the singular extreme mesocosm was five times, and in the singular high mesocosm nearly three times higher compared to the ^{13}C PP values (59.8 µg C L^{-1} d^{-1} and 35.1 µg C L^{-1} d^{-1} compared to 14.3 µg C L^{-1} d^{-1} and 14.1 µg C L^{-1} d^{-1}), while the singular medium and low mesocosms with 22.4 µg C L^{-1} d^{-1} (vs. 11.7 µg C L^{-1} d^{-1}) and 13 µg C L^{-1} d^{-1} (vs. 11 µg C L^{-1} d^{-1}) did not deviate much (**Fig. 4A**).

The full scale of this actuated PP after the first nutrient addition is also obvious in the cumulative ^{14}C PP data, especially in the singular upwelling treatments. There, a strong increase in PP is visible directly after the nutrient addition, leading to a steep increase in cumulative PP (Day 5-9) and, similar to the recurring upwelling mesocosms, a more pronounced separation of the respective singular upwelling mixing regimes according to their nutrient input (**Fig. 4B**). As a result, the singular extreme treatment displayed a total cumulative PP of 1137 µg C L^{-1}, the singular high 667 µg C L^{-1}, and the singular medium

425 µg C L^{-1}. Under recurring upwelling conditions, the ratios between the respective mixing regimes did not change significantly compared to the ^{13}C data, however they more or less doubled in absolute values (cf. **Fig. 4B** and **Fig. 3B**). An exception to that is the recurring extreme treatment, displaying with 1732 µg C L^{-1} (^{14}C) compared to 1805 µg C L^{-1} (^{13}C), despite a different temporal development, a similar cumulative PP at the end of the experiment.

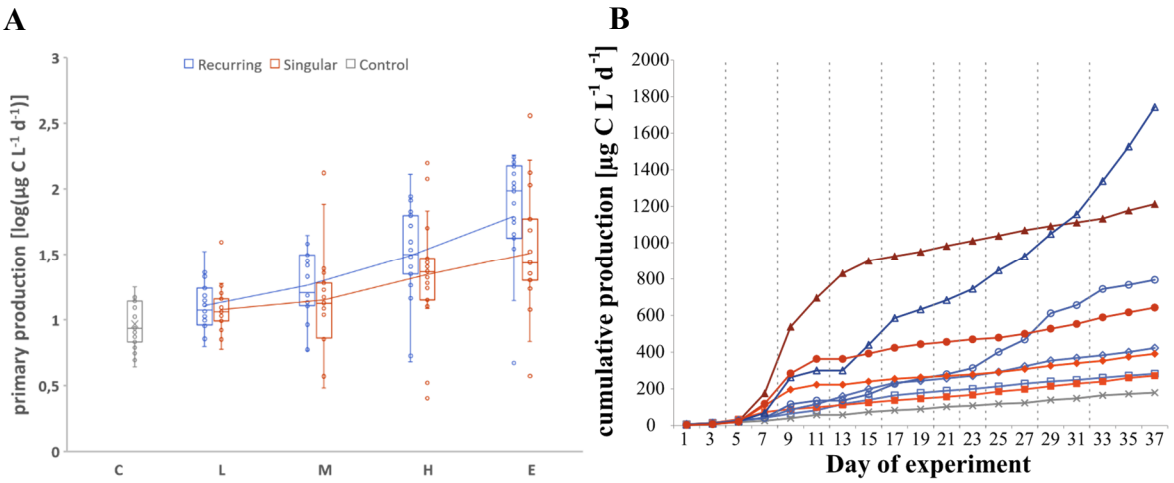

Figure 4: ^{14}C obtained primary production (PP) for the singular and recurring upwelling mode as well as the control over the whole experimental period. **(A)** As log (base 10) transformed mean PP per upwelling intensity treatment (C = Control, L = Low, M = Medium, H = High, E = Extreme), with boxplots bounded by the minimum and maximum value of the respective dataset, and the average 50% of the remaining values within the box. Colors according to the given legend. **(B)** As cumulative PP per mesocosm, with vertical lines symbolizing deep-water additions, and colors and symbols for the single mesocosms according to **Tab. 1**.

Copepods and secondary production (SP)

Copepod abundance and biomass

Overall, copepod abundance was highest in the singular upwelling treatment with a mean of 13.4 ind L^{-1} (± 6.7, SD) compared to 9.6 ind L^{-1} (± 10.3, SD) in the recurring mesocosms, and 7.7 ind L^{-1} (± 2, SD) in the control over the whole time of the experiment. Within the single upwelling treatments, abundances display an increase from low to extreme mixing. In the singular upwelling mode, this corresponds to values of 10.6 ind L^{-1} (± 3.7 SD) in the medium, 13.1 ind L^{-1} (± 6.1 SD) in the high, and 16.4 ind L^{-1} (± 8.7 SD) in the extreme mixing mesocosm (see **Fig. 5A**). The singular low upwelling mesocosm had to be removed from all copepod measurements and SP calculations, due to a massive predatory influence from unintentionally enclosed juvenile fish in the mesocosm (for details see Sswat et al., in prep.). Under recurring upwelling conditions, the positive correlation between abundance and nutrient level is reflected by an increase from 2.7 ind L^{-1} (± 0.1 SD) under low, to

5.1 ind L^{-1} (± 0.9 SD) under medium, and 20.2 ind L^{-1} (± 15.7 SD) under high mixing, however, followed by a decrease towards the extreme mixing with 10.3 ind L^{-1} (± 2.2 SD, **Fig. 5A**). The recurring high mesocosm thereby distorts the trend because of an exceptional increase of abundances towards the end of the experiment, from 6.6 ind L^{-1} on Day 25 to 46 ind L^{-1} on Day 37 (see **Fig. 5B**). Although this temporal development is similar, but more pronounced, compared to the increase in abundance in the recurring extreme mixing mesocosm, it differs substantially from the general temporal trend under singular upwelling conditions. With maximum abundances of 16 ind L^{-1}, 23.2 ind L^{-1}, and 31 ind L^{-1} the singular medium, high, and extreme mixing mesocosms rather displayed highest abundances around the middle of the isotopic enrichment period (Day 23 - 31), and decreasing values toward the end of the experiment (**Fig. 5B**).

In terms of size distribution, the majority of individuals counted in all mesocosms belonged to the smallest size class (55 - 200 µm), with an overall mean of 9.6 ind L^{-1} (± 8 SD) and a corresponding contribution of 88.3%. Individuals of the bigger size classes were present in comparably low abundances, with mean values of 1.2 ind L^{-1} (± 0.8 SD, 200 - 500 µm, 10.6%) and 0.1 ind L^{-1} (± 0.1 SD, 500+ µm, 1.1%). With respect to differences in size distribution between the two upwelling modes, individuals in the 55 - 200 µm size class contributed equally to the overall abundance per treatment, with 87% in the singular and 90% in the recurring upwelling mode. The contribution of the 200 - 500 µm and 500+ µm size class, however, displays an increased share of medium to large sized animals to the overall abundance in the singular upwelling treatment compared to the recurring upwelling mode, with 12% (200 - 500 µm) and 1.2% (500+ µm), and 9% (200 - 500 µm) and 1% (500+ µm), respectively.

Copepod biomass (based on abundances and carbon content per individual) displays comparatively similar trends as the abundance data, yet with some deviations. Under singular upwelling conditions, the overall mean biomass is with 6.33 µg C L^{-1} (± 2.61 SD) still higher than under recurring upwelling with 3.41 µg C L^{-1} (± 2.97 SD), and in the control with 3.69 µg C L^{-1} (± 0.5 SD). However, within the respective upwelling modes, biomass increases towards the high mixing mesocosms and decreases beyond that. In the singular upwelling treatment this is reflected by a mean biomass of 4.75 µg C L^{-1} (± 1.49 SD) under medium, 8.57 µg C L^{-1} (± 2.41 SD) under high, and 5.66 µg C L^{-1} (± 2.23 SD) under extreme nutrient input, while under recurring upwelling biomass increases from 0.81 µg C L^{-1} (± 0.14 SD, low) to 2 µg C L^{-1} (± 0.95 SD, medium) and slightly higher values of

6.35 µg C L^{-1} (± 4.01 SD) under high compared to the 5.64 µg C L^{-1} (± 3.33 SD) under extreme mixing ratio (**Fig 5C**). Furthermore, development of biomass over the time of the experiment does not follow the pronounced decrease visible in the abundance data towards the final sampling day. Especially the singular high (M9) and recurring extreme (M8) mesocosms in that context increased substantially in biomass with a maximum of 11.16 µg C L^{-1} on Day 33 (M9) and a steady increase from 2.39 µg C L^{-1} (Day 17) to 13.84 µg C L^{-1} on Day 37, while their abundance peaks were measured on Day 23 for M9 and Day 31 for M8 (**Fig. 5D**).

These differences between the abundance and biomass data have their major cause in the substantially different contribution of the size classes to the overall biomass of the treatments and mixing ratios. In contrast to the abundance data, the smallest size fraction 55 - 200 µm accounted only for 23% of the overall biomass, with a mean of 1.09 µg C L^{-1} (± 0.83 SD), while the 200 - 500 µm size class held 46% with 2.19 µg C L^{-1} (± 1.45 SD), and the biggest individuals 31% with 1.45 µg C L^{-1} (± 1.49 SD). Between the two upwelling modes, the smallest and biggest size classes displayed increased contributions to biomass under recurring compared to singular upwelling, with 25% (0.92 µg C L^{-1}, ± 0.92 SD) and 34% (1.25 µg C L^{-1}, ± 1.57 SD), and 22% (1.38 µg C L^{-1}, ± 0.76 SD) and 31% (1.98 µg C L^{-1}, ± 1.44 SD), respectively. The medium size class, however, had the biggest and an enhanced proportion under singular upwelling conditions with 41% (1.53 µg C L^{-1}, ± 1.31 SD) compared to 47% (2.96 µg C L^{-1}, ± 1.42 SD). The highest biomass contribution in the control mesocosm also came from the 200 - 500 µm size fraction, however with a significantly higher mean value of 63% (2.34 µg C L^{-1}, ± 0.52 SD) compared to the upwelling treatments (**Fig. 5D**).

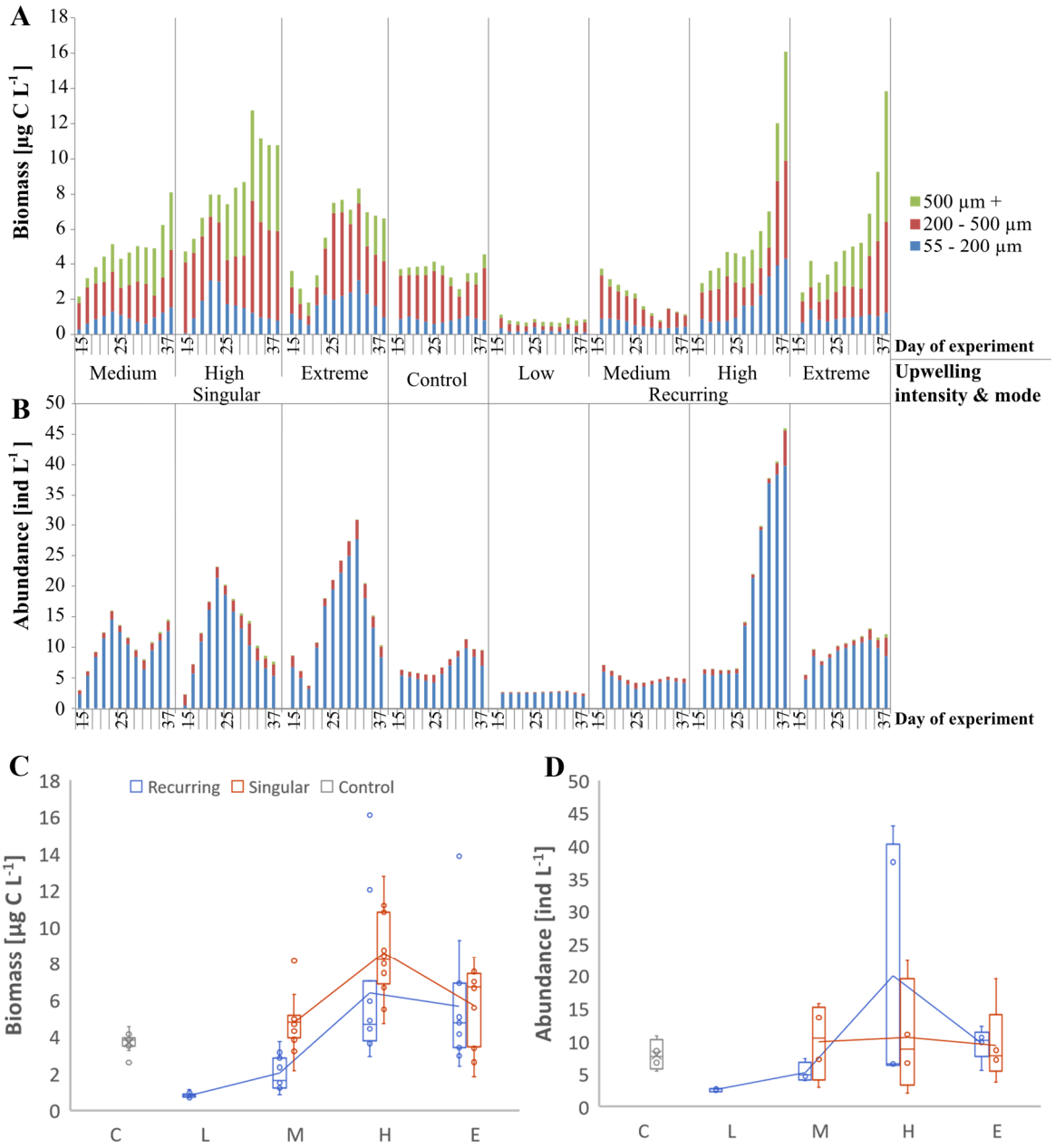

Figure 5: Distribution of **(A)** mesozooplankton biomass, and **(B)** abundances in the three size-classes 55 - 200 µm (blue), 200 - 500 µm (red), and bigger 500 µm (green) per upwelling intensity & mode, over the time of isotopic labeling. **(C)** & **(D)** Mean mesozooplankton biomass **(C)** and abundance **(D)** for singular and recurring upwelling mode as well as the control over the isotopic labeling period and per upwelling intensity treatment (C = Control, L = Low, M = Medium, H = High, E = Extreme). Boxplots bounded by the minimum and maximum value of the respective dataset, and the average 50% of the remaining values within the box. Colors according to the given legends.

Secondary Production

The secondary production calculated with the ^{13}C tracer enrichment in the copepod samples indicates an increased production rate under singular upwelling conditions, in contrast to the primary production derived from the $PO^{13}C$ filters and ^{14}C measurements (**Fig. 6A**). The mean SP rate of the singular upwelling mesocosms over the time of the isotopic enrichment

was presumably around 0.8 µg C L^{-1} d^{-1} higher than the rate calculated for the recurring upwelling treatment (1.28 µg C L^{-1} d^{-1} (± 0.77 SD) compared to 0.48 µg C L^{-1} d^{-1} ± 0.45 SD, respectively). Furthermore, results indicate that SP under singular upwelling conditions was enhanced by around 0.66 µg C L^{-1} d^{-1}, while it was slightly reduced by 0.14 µg C L^{-1} d^{-1} in the recurring treatment, compared to the control treatment with a calculated SP of 0.62 µg C L^{-1} d^{-1} (± 0.15 SD) (see **Fig. 6A**).

The mean SP rate of the different simulated upwelling intensities was highest in the singular high mixing mesocosm, followed by the singular extreme and medium mixing regimes with 1.75 µg C L^{-1} d^{-1} (± 0.80 SD), 1.30 µg C L^{-1} d^{-1} (± 0.81 SD) and 0.79 µg C L^{-1} d^{-1} (± 0.22 µg SD, see **Fig. 6A**). It has to be noted that SP for the singular extreme treatment could only be calculated until Day 27 of the experiment, due to the in the results Section "^{13}C enrichment" mentioned decreasing trend in the ^{13}C abundance (see also Section "Advantages and methodological limitations of our the ^{13}C approach"). In the recurring nutrient regimes secondary production was highest under high nutrient conditions, followed by extreme and medium, and lowest under low upwelling intensity (0.76 µg C L^{-1} d^{-1} ± 0.52 SD under high, 0.12 µg C L^{-1} d^{-1} ± 0.04 SD under low nutrients, see **Fig. 6A**). Thus, displaying lower overall values but similar patterns as the singular upwelling intensities.

These differences between and within the upwelling modes are also depicted in the cumulative SP over time. The singular upwelling produced about 7.90 µg C L^{-1} more than the recurring upwelling treatment, with a cumulative mean of 13.20 µg C L^{-1} (± 5.53 SD) compared to 5.30 µg C L^{-1} (± 3.00 SD). The singular high mesocosm was presumably the most productive treatment, with a cumulative production of 21.02 µg C L^{-1}, although the extreme mixing mesocosm displayed a comparable cumulative production on Day 27 as well as a similar increase over time (9.08 µg C L^{-1} compared to 10.15 µg C L^{-1} for singular high on Day 27, **Fig. 6B**). The high and extreme mixing mesocosms also displayed highest cumulative secondary production under recurring upwelling conditions with 8.41 µg C L^{-1} and 7.97 µg C L^{-1}, respectively. Recurring medium and low mixing, however, had the lowest overall cumulative SP with 3.57 µg C L^{-1} and 1.27 µg C L^{-1}, most likely also under the values calculated for the control mesocosm (5.60 µg C L^{-1} on Day 33, see **Fig. 6B**).

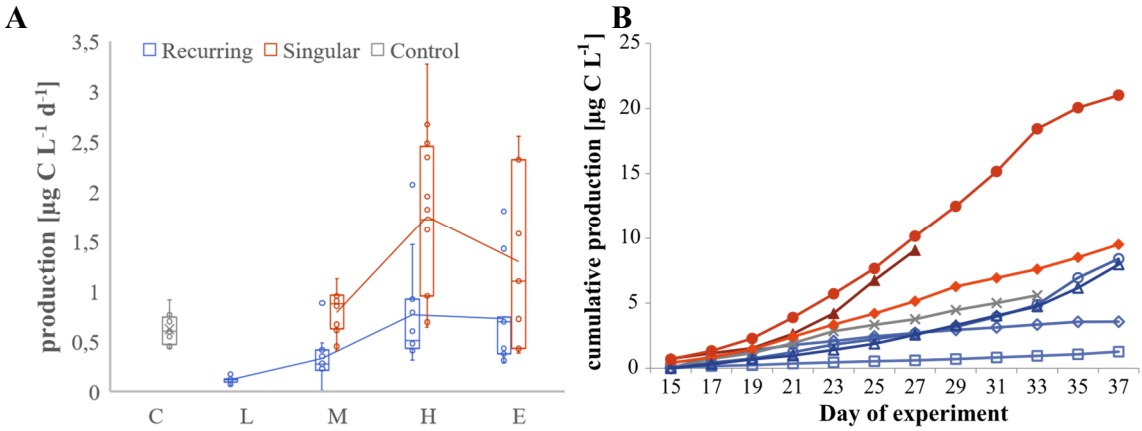

Figure 6: ^{13}C obtained secondary production (SP) for singular and recurring upwelling mode as well as the control, over the whole experimental period. **(A)** As mean SP per upwelling intensity treatment, with boxplots bounded by the minimum and maximum value of the respective dataset, and the average 50% of the remaining values within the box. Colors according to the given legend. **(B)** As cumulative SP per mesocosm, with colors and symbols for the single mesocosms according to **Tab. 1**.

Trophic transfer efficiency (TTE)

Based on our estimates for overall secondary production and primary production (cumulative PP & SP: Day 1 - 37 for ^{14}C, Day 15 - 37 for ^{13}C), trophic transfer efficiency was higher in the singular upwelling treatment, independent of the chosen carbon isotope labeling method used for PP. However, absolute values varied depending on whether ^{13}C or ^{14}C data was used. Furthermore, treatment differences in the singular upwelling displayed different patterns, as the ^{14}C primary production dataset includes the short period of highest productivity (Day 7 - 11), which was not captured by the ^{13}C tracer method. Since the biomass from this short but intense bloom was potentially also consumed by zooplankton, i.e. contributing to secondary production, we calculated TTE for both primary production datasets.

When set into relation with the cumulative ^{13}C PP, mean TTE was significantly higher in the singular than in the recurring treatment, while the control mesocosm exceeded both (8.9% ± 2.9 SD compared to 1.7% ± 0.7 SD, and 10.7%, respectively **Fig. 7A**). The mean TTE in both upwelling modes was mainly driven by the high nutrient mixing mesocosms, with 13.1% under singular and 2.4% under recurring upwelling, followed by the medium mixing with 6.9%, and the low as well as the medium mixing with 1.9% each, respectively (**Fig. 7A**). It has to be noted, however, that due to an anomaly in the ^{13}C enrichment shortly after addition of the tracer (see Day 15/ 17 **Fig. 2C**), the calculated PP for Day 15 in the singular and Day 17 in the recurring upwelling treatment had to be removed from the results, due to exceptional low values.

Overall, recalculating the TTE values with the cumulative ^{14}C PP data, including the additional PP created by the bloom after the first deep-water addition on Day 4, does not change the general treatment differences between singular and recurring modes, but scales all TTE estimates down to lower absolute values (cf. **Fig. 7A** and **Fig. 7B**). Mean TTE in the singular treatment was with 2.1% (± 0.9 SD) still significantly higher than in the recurring mesocosms with 0.7% (± 0.3 SD), and the control was with 3.2% also substantially lower compared to the ^{13}C calculated value, but still higher than both of the upwelling treatments. Additionally, also the trends within the nutrient regimes are upheld, with the two high treatments showing the largest values with 3.1% (singular) and 1.1% (recurring), followed in both upwelling modes by the medium treatment with 2.2% (singular) and 0.9% (recurring, see **Fig. 7B**). These values are, however, also systematically underestimating TTE, because no equivalent SP could be obtained for the added PP from Day 1 to Day 15, and thus Eq. (1) is decreased unequally.

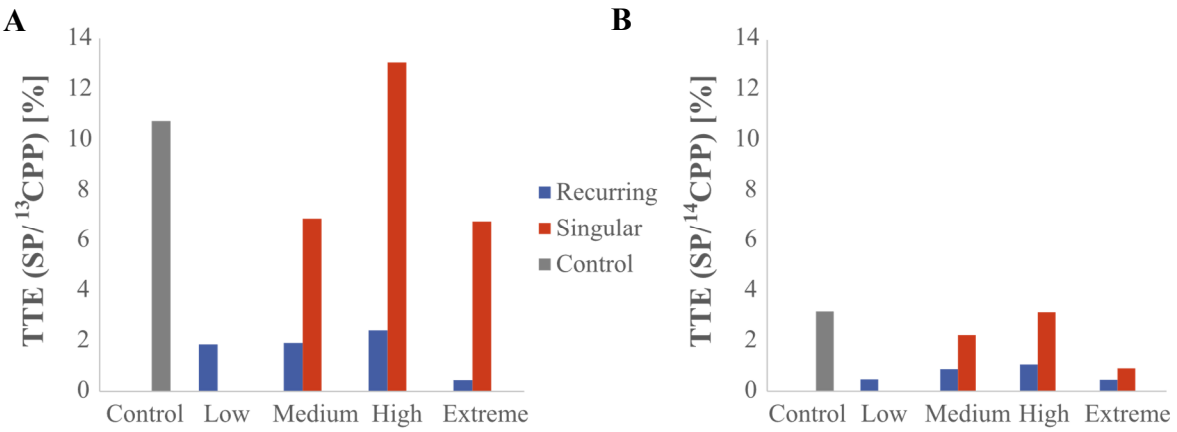

Figure 7: Trophic transfer efficiency (TTE) per upwelling intensity treatment for the singular and recurring upwelling mode as well as the control. Calculated according to Eq. (1), with cumulative ^{13}C SP and **(A)** cumulative ^{13}C PP or **(B)** cumulative ^{14}C PP. Colors according to given legend.

Summary

Overall, it became apparent that primary production was significantly enhanced under recurring as well as singular artificial upwelling conditions and any nutrient input of 2 µM N or more, compared to the control treatment. Secondary production, however, only exceeded the values in the control under singular upwelling conditions at nutrient inputs of 5.5 - 10 µM N. Finally, trophic transfer efficiency (the overall PP being converted to SP) was only found to be similar to or exceeding TTE of the control in the singular high upwelling intensity (5.5 µM N). Additionally, the singular upwelling treatment generally displayed a higher TTE than the recurring upwelling mesocosms, independent of PP being calculated from ^{13}C or ^{14}C. The commonly estimated 10% TTE (Lindeman, 1942), however,

was only exceeded by the control and the singular upwelling 5.5 µM N mixing treatment, when PP was calculated from ^{13}C.

DISCUSSION

Advantages and methodological limitations of the ^{13}C approach

This study quantified for the first time, how the transfer efficiency of biomass between trophic level can be manipulated by artificially upwelling nutrient rich deep-water to the surface, under different upwelling modes as well as different mixing intensities, i.e. nutrient input and dilution. Carbon flows within a natural plankton community were calculated via ^{13}C labeling and tracing its enrichment throughout the various compartments of the food web. This direct measurement of secondary production and TTE within a natural plankton community is a superior alternative to the use of numerical models or small-scale incubation experiments with single key species, which are commonly the basis for estimates of carbon/ biomass flows and TTE (Kiørboe *et al.*, 1988; Gómez *et al.*, 2012; Yáñez *et al.*, 2018). These methods, however, come with various assumptions of ecological parameters and can have substantial fluctuations (e.g. Yáñez *et al.* (2018)). Their major constraint lies in the difficulty of extrapolating the results to natural open ocean plankton communities and food webs. They commonly need to rely on a few, big and easy to handle key species of the examined ecosystem, and an obligatory dislocation of the experiments outside of natural *in situ* environmental conditions, especially regarding prey. In contrast to that, the SP rates in this study represent a direct measurement of biomass generated by a variety of copepod taxa in different size classes in the prevailing food webs of the simulated upwelling modes and intensities. The multi-taxonomic *in situ* quantification of SP in different size classes solitarily makes it difficult to obtain comparable results from other studies, but even more so in the context of measuring it under different artificial upwelling conditions.

Despite the advantages of ^{13}C isotopic enrichment for calculating biomass production rates of different trophic levels, the present study also revealed some constraints of this elaborate method. Foremost, it is mandatory for the PP and SP rate calculations that the ^{13}C concentration in the consumer as well as its food, increases steadily over time. While this is no problem for single taxa within the plankton community, depending on the prevailing food web dynamics it may get intricate, especially for mixed community samples taken by GF/F filters (containing microzooplankton and bacteria).

First of all, the mixture of different trophic levels on the filters utilized for primary production rates can impair the ^{13}C-based calculation of production rates. As the water samples taken for filtration were not prefiltered, the sample on the filter does include everything from bacteria to phyto-, micro- (auto-, hetero-, mixotroph), and also mesoplankton. Most critically, the largest portion of fast-growing diatoms is in the same size range as most microzooplankton (particularly ciliates), thus making it virtually impossible to separate these taxa with filtration and size-fractioning. In terms of the PP calculation, this mixing with higher, less enriched trophic levels decreases the actual ^{13}C signal of only primary producers and with that the first term of Eq. (2), i.e. the "efficiency" of the enrichment, leading to a slight underestimation of the production rate.

Secondly, changes in the dominance of species may hinder correct TTE calculation over time. For instance, a former dominant, and accordingly fast growing and ^{13}C incorporating species with a certain trophic level, can be replaced by a previously subordinate, slow growing and ^{13}C incorporating species with the same trophic position in the plankton community. When the biomass proportion of this upcoming, less enriched species then increases on the measured filter, the overall ^{13}C signal might decrease from 't-1' to 't'. This, in turn, can cause a negative outcome of Eq. (2), making the calculation of a production rate impossible.

Both factors can compromise the calculation of copepod secondary production. Although most of the lower trophic level species on the filter can be assumed to be potential food for copepods, not every size class nor species grazes on the whole prey community collected on the filters. Consequently, the denominator of Eq. (2) again is over- or underestimated in relation to the secondary production of certain species or size classes, leading to a negative value at worst. One possible solution to these inaccuracies caused by the mixed-community sample used for PP estimation could be a compound specific ^{13}C isotope analysis of fatty acids of the plankton community on the filter. This analysis would make it possible to resolve the different taxa and trophic levels to a certain degree and distinguish e.g. between bacteria, autotrophs or mixotrophs on the filters (see also de Kluijver *et al.* (2013)). This in turn, would allow for taxon-specific ^{13}C incorporation and thereby discriminating between autotrophic production and secondary production by bacteria and microzooplankton.

Production rates and trophic transfer efficiency

Primary production

The results of the ^{13}C calculated primary production rates are in accordance with the timing of the isotopic enrichment and the experimental design. As indicated by mean production rates over the whole time of the isotopic measurement, the singular upwelling treatment produced biomass with around 13 µg C L^{-1} d^{-1} on a rather low level compared to the 58 µg C L^{-1} d^{-1} of the recurring upwelling mesocosms. This is, however, due to the singular upwelling treatment having received its nutrient addition on Day 4, and with that 9 days before the isotopic enrichment of the experiment. As visible in the ^{14}C production rates, the phytoplankton bloom in the singular upwelling treatments had already faded and PP was set back to the rates prior to the singular fertilization event, while nutrient input and PP constantly increased during the time of the isotopic measurement in the mesocosms under recurring upwelling conditions (see **Fig. 4B**). This is furthermore depicted in the overall low measured cumulative ^{13}C PP and the small variation between the different singular upwelling intensities. Although the singular extreme mixing mesocosm received nearly twice as much nutrients as the high and more than triple the amount of the medium mixing regime (9.8 µM N vs. 5.6 µM N vs. 3.1 µM N), they differ with 171 µg C L^{-1} (extreme), 169 µg C L^{-1} (high), and 141 µg C L^{-1} (medium) only slightly in their ^{13}C calculated, cumulatively produced phytoplankton biomass (**Fig. 3B**).

This relation changes when considering the ^{14}C cumulative PP data, which includes the initial phytoplankton bloom after the first deep-water addition in the singular upwelling treatments. According to the nutrient input, the singular extreme mixing mesocosm doubles in PP compared to the high (1137 µg C L^{-1} d^{-1} vs. 667 µg C L^{-1} d^{-1}), and triples compared to the medium mixing treatment (1137 µg C L^{-1} d^{-1} vs. 425 µg C L^{-1} d^{-1}). Although this strong increase in singular upwelling cumulative PP reduces the overall treatment difference between singular and recurring upwelling, a distinct difference in PP remains between the extreme and high mesocosms of both upwelling modes, with 1732 µg C L^{-1} d^{-1} under extreme recurring vs. 1137 µg C L^{-1} d^{-1} under extreme singular, and 787 µg C L^{-1} d^{-1} under high recurring vs. 667 µg C L^{-1} d^{-1} under high singular upwelling mode.

Although this relation between primary production and nutrient input is not depicted in the ^{13}C calculated PP, the timing of the isotopic enrichment was scheduled after the initial deep-water addition to achieve an ideal assessment of secondary production, including a certain

delay of time to allow the zooplankton community to fully utilize the initial phytoplankton bloom.

Secondary production (SP) and trophic transfer efficiency (TTE)

From a very general point of view, the here calculated mesozooplankton SP rates (0.12 - 1.75 µg C L^{-1} d^{-1}) are well within a range of previously reported values. For instance, a metanalysis by Leandro *et al.* (2014) reported secondary production rates of the cosmopolitan copepod species *Acartia* spp. of 0.1 - 7.5 µg C L^{-1} d^{-1}. From a whole ecosystem perspective, Escribano *et al.* (2016) estimated an annual mean secondary production of 30 - 40 µg C L^{-1} d^{-1} for the Humboldt upwelling area off Chile. It is expectable that these rates exceed the SP measured in this study by far, when considering that natural upwelling regions are already adapted to their present productivity, and generally display larger population sizes, species diversity, and cover a larger body size range. Rather comparable to our SP estimates are estimated production rates by de Kluijver *et al.* (2013), a model study based on a ^{13}C stable isotope enrichment in a mesocosm study off Ny Ålesund, Svalbard. They found copepod SP rates of about 2.3 µg C L^{-1} d^{-1} under initially low nutrient, "natural" conditions in their experiment, shortly after closure of the mesocosms and prior to an artificial nutrient enrichment. These results support our observations of enhanced or more "natural" SP rates under singular compared to recurring upwelling conditions. With a calculated mean SP of 1.3 µg C L^{-1} d^{-1} in our study, the nutrient-limited singular upwelling treatment in the post-bloom period was closest to the "natural" SP rate estimated by de Kluijver *et al.* (2013).

Besides the dependency on a variety of biotic and abiotic factors, quality and availability of food for the involved secondary consumers can be considered as one of the major influences in controlling secondary biomass production in general, and growth and reproduction of several copepod taxa, as presented here, in particular (Malzahn & Boersma, 2012). In terms of food quality, diatoms (Bacillariophyceae) are generally considered to play a vital and beneficial role, especially because of their dominance in productive upwelling regions all around the world (Sarthou *et al.*, 2005). However, the beneficial role of diatoms for carbon transfer to mesozooplankton and for trophic transfer efficiency is more and more controversially discussed, due to rather negative effects of diatoms especially on copepods being proven by a variety of studies (Ianora *et al.*, 2003). In that context, a decrease in copepod nauplii hatching success and survival rates was closely linked to increased diatom abundances and thus upwelling conditions in the Humboldt upwelling region off the coast

of Chile (Vargas *et al.*, 2006). If diatoms are considered a low-quality (or unpalatable) food, their increase may negatively influence secondary production, and may thus explain the overall low SP in our study, and particularly the treatment differences in copepod biomass and SP between singular and recurring upwelling conditions. During the majority of the time period of the isotopic measurement, most of the phytoplankton biomass in all manipulated mesocosms was constituted by large chain-forming diatoms, whereas the highly productive control mesocosm displayed the lowest overall diatom contribution (Ortiz et al., in prep.). In addition to that, a higher diatom biomass was found under recurring compared to singular upwelling conditions, also scaling with upwelling intensity within the singular upwelling treatment, thereby corresponding to the lower SP and TTE in the extreme mixing compared to the medium mixing ratio (Ortiz et al., in prep.).

Adding to this difference in food quality, the food quantity could also have influenced the higher productivity of copepods in the here simulated singular upwelling mesocosms. When primary production, here as a proxy for food availability, exceeded certain thresholds, secondary production of copepods as well as trophic transfer efficiency of the whole ecosystem decreased substantially in models of different pelagic ecosystems under various nutrient regimes (Kemp *et al.*, 2001). The authors found an increase of TTE from 10% up to 30% when nutrient levels were elevated from 2 µM N to 7 µM N, but a sharp decrease back to 10% for nutrient concentration exceeding 7 µM N. Kemp *et al.* (2001) attributed this pronounced drop in secondary production and transfer efficiency primarily to the lack of herbivorous copepod taxa in the high nutrient ecosystems, leading to a faster saturation of the zooplankton community's ability to fully utilize the high food concentrations associated with enhanced nutrients. Despite the overall lower values, the scaling of TTE with nutrient input observed in our study is very similar to these results. When related to the efficiency of the singular upwelling treatment, highest TTE was observed towards the high nutrient treatment (5.6 µM N), and decreased values towards the extreme enriched mesocosm (9.8 µM N, see **Fig. 7A/ B**).

In addition to aforementioned factors related to primary production and food quantity/ quality, our findings indicate that also the species composition within the here assessed zooplankton community forms a major factor in determining SP and TTE of our enclosed ecosystem. The vast majority of the copepods analyzed for the calculation of secondary production in this study are commonly categorized as herbivores. On the one hand, this couples the here observed differences in copepod biomass to enhanced production and

transfer efficiency in the singular high compared to the singular extreme mixing regime, despite the advantage in nutrients and PP under extreme mixing. On the other side, the increased herbivorous biomass was also a decisive factor in shaping the treatment differences between the singular and recurring upwelling mode, although being counterintuitive to the beneficial conditions of constant nutrient supply and enhanced PP under recurring upwelling conditions.

Additionally, the differences in SP and TTE between singular and recurring fertilization could have been further enhanced by divergent body size of the copepod species in both treatments. High secondary production and transfer efficiencies were connected to a high proportion of small sized zooplankton in the food webs of the upwelling region off Chile, in the North Sea, and a global scale meta-analysis (Jennings *et al.*, 2002; Brun *et al.*, 2016; Escribano *et al.*, 2016). In the present study, this hypothesis would be supported by the fact that high SP and TTE were rather coupled to a high biomass contribution of smaller animals (200 - 500 µm), than to the biggest size class of copepods (> 500 µm). Compared to the recurring upwelling mesocosms, the more productive singular upwelling treatment displayed a higher proportion of biomass attributed by animals between 200 - 500 µm than from the bigger 500 µm size class (see **Fig. 5B**). In accordance with that was the biomass contribution in the control, with high mean TTE without nutrient addition, significantly decreased for the biggest size class, and increased for the 200 - 500 µm fraction compared to all other mesocosms (see **Fig. 5B**).

In general, such a size-based productivity pattern within a food web can be shaped either by top-down or bottom-up control, or a mixture of both. In the here presented experiment, however, the lack of sufficient numbers of grazers for e.g. size-selective predation on the copepod population leaves only bottom-up effects as possible explanations. In that context, the phytoplankton community structure can have a distinct influence on copepod growth, as a community with increased amounts of nano- and picoplankton, for instance, would favor the abundance of smaller copepod stages/ species (Hopcroft *et al.*, 1998). In accordance with that, nano- and picophytoplankton contributions in the here presented study were slightly elevated under singular upwelling conditions, and significantly higher in the control mesocosm (Ortiz et al., in prep), which also displayed the largest proportion of 200 - 500 µm sized copepods and the highest transfer efficiencies. It has to be noted, however, that the data from Ortiz et al. only includes information on autotrophic organisms, and at the time of this publication, no data is available on hetero- or mixotrophic nano- or picoplankton

abundances/ biomass in the mesocosms. Another explanation could stem from the low and decreasing phytoplankton numbers in the singular upwelling treatment and the control. When food becomes a limiting factor, mesozooplankton organisms like copepods run into the quandary of self-enhancing their food limitation with increasing size and the coupled higher energy demand of growth (Webber & Roff, 1995). Consequently, such an inhibition of growth could lead to the here observed accumulation of copepod biomass rather in the medium than in the larger size-fractions.

Summary

In the higher trophic levels (copepods) in the food web established in our study, higher secondary production rates and trophic transfer efficiency under singular upwelling conditions could be attributed to a prevailing zooplankton community with a smaller average size as well as an increased ability to efficiently utilize the provided primary production, presumably reinforced by more suitable concentrations, size, and higher quality of food.

CONCLUSION AND OUTLOOK

The objective of the present study was to answer the question, whether mode and intensity of artificial upwelling of nutrient rich deep to nutrient depleted oligotrophic surface waters could enhance productivity of 'ocean deserts'. Our findings indicate that, primary and secondary production as well as the trophic transfer efficiency of the enclosed communities were altered profoundly, depending on temporal mode and intensity of artificial upwelling. PP is most efficiently increased via an artificial upwelling manipulation in a recurring mode, whereas SP and TTE were higher in the singular than in the recurring treatments. The reason is likely the difference in phytoplankton community composition created by the upwelled nutrients (i.e. proportion of palatable and non-palatable food), as well as the prevailing zooplankton species and their body size distribution. In that context, the present study indicates that on the one hand a high diatom contribution to phytoplankton biomass, and on the other hand less favorable conditions for medium sized copepod species with a fast biomass turnover, could both be impairing secondary biomass production and TTE.

Nonetheless, based on the here presented results, we conclude that artificial upwelling could bear great potential to enhance the productivity in an oligotrophic ecosystem. We detected an increase in SP under singular upwelling conditions compared to the 'natural' control mesocosm, that, in case of the extreme upwelling intensity, also translated into an enhanced TTE. This effect could be further enhanced if artificial upwelling is, for instance, applied in

a “singular” upwelling mode on a recurring basis, with sufficient time periods between the upwelling events to allow for efficient utilization of/ adaption to the phytoplankton bloom by the copepod community. Furthermore, we cannot exclude that with a comparable amount of nutrients significantly higher PP in the recurring upwelling mode might have transitioned into equally higher SP and TTE, if, in contrast to this study, monitored over a longer time period after the final upwelling event. Additionally, we suggest for future studies of this kind, to test if an artificial inhibition of the dominance of diatoms in the enriched oligotrophic waters (e.g. by adjusting silicate availability in the nutrient cycle) might be capable of enhancing SP of copepods and ultimately TTE.

ACKNOWLEDGEMENTS

We would like to thank all participants of the KOSMOS Gran Canaria 2018 experiment for maintenance and sampling of the mesocosm infrastructure over the entire period of time. Here, we would like to especially thank all students involved in the zooplankton team, Alba Filella Lopez de Lamadrid and Mirian Arellano San Martin in particular. A special thanks goes to Thomas Hansen (GEOMAR), Kerstin Nachtigall (GEOMAR), and their laboratory teams for taking care of all the sample measurements. We would also like to thank the staff of the Plataforma Oceánica de Canarias (PLOCAN) for providing excellent infrastructure and outstanding support, here in particular Patricia López-García. Additionally, we would like to thank the University of Las Palmas de Gran Canaria (ULPGC) for their support, and Prof. Javier Arístegui in particular for all the scientific consultation. Furthermore, we want to acknowledge the technicians for preparation and maintenance of the KOSMOS facilities.

III. SYNTHESIS

The overarching aim of my thesis was to investigate how zooplankton communities respond to anthropogenic influences. Here, in particular to the environmental stressor ocean acidification and to the potential ocean-based climate change solution artificial upwelling. I specifically focused on the influence of both these processes on the structure, functionality, and productivity of the zooplankton community.

In terms of OA, I showed that elevated pCO_2 levels led to a pronounced restructuring of an entire plankton community, including several trophic levels of consumers. During nutrient-limited post bloom conditions, an interplay of indirect and direct OA effects thereby caused an enhanced top-down control on the base of the food web. This was reflected in decreased numbers of phytoplankton as well as autotrophic and heterotrophic microplankton, along with high abundances of various copepod species and appendicularians. Notably, this reorganization of the food web had substantial influence on the predator-prey coupling of Hydrozoa and Atlantic herring larvae, depicted in a higher survival of the larvae coinciding with lower Hydrozoa biomass.

The study on artificial upwelling did not indicate negative side effects on structure or functionality of the investigated zooplankton community. To the contrary, I observed an increased primary production in conjunction with the amount of nutrients added via deep-water, and pronounced changes in secondary production and biomass transfer efficiency in the food web. The effect size of these changes, however, was highly dependent on how the different modes and intensities of artificial upwelling influenced the phytoplankton community composition as well as the prevailing zooplankton species and their body size.

In the following, I want to set these results in context with state-of-the-art knowledge about marine community responses to OA and artificial upwelling. I will give an overview about known food web distortions due to OA, including changes in higher trophic level consumers. In addition, I will take a closer look at their possible causes as well as their interaction with ocean warming as another environmental stressor. Subsequently, I want to discuss the factors determining productive (effective) and unproductive (ineffective) food web structures, and relate them to the findings in this thesis. Finally, I want to give an outlook on the potential of artificial upwelling and how it could and should be applied in the future, also as a possible countermeasure to the direct effects of anthropogenically caused environmental stressors such as OA or warming.

1. OA effects altering food web interactions

Direct OA effects on calcifiers

The most straightforward results in terms of OA induced food web alterations are the direct negative impacts of enhanced OA on calcifiers I observed in this thesis. The underlying decrease in calcification rates and/ or intensified dissolution of $CaCO_3$ due to the low calcite and aragonite saturation states ($\Omega < 1$, **Chapter 1, Fig. 6**) is a recurring and well-known consequence of enhanced OA. These consequences are especially pronounced in colder, faster desaturating high-latitude areas of the oceans (see e.g. Dupont *et al.* (2010); Lischka *et al.* (2011); Wittmann and Pörtner (2013); Riebesell *et al.* (2017)). In these polar and subpolar ecosystems, bivalves, gastropods and prymnesiophytes are important bloom-forming species, and constitute substantial energy sources for productive food webs that reach up to higher trophic levels such as fish and marine mammals (Orr *et al.*, 2005; Lischka *et al.*, 2011; Thomson *et al.*, 2016). Thus, losing these shell forming organisms as major food web components in high latitude regions could result in less food available for previously mentioned higher trophic levels. On the other hand, there is an additional risk of harmful primary producers like dinoflagellates taking over the ecological niche of their OA affected competitors in these areas, potentially impairing the whole food web (Grandon (2020) and references within). These developments are even more eminent considering that it is most likely inevitable that polar and subpolar regions become undersaturated with regards to aragonite and calcite in the near future (IPCC, 2021).

Interplay of direct and indirect effects in the food web

Direct effects of OA are not always as easy to identify as in the case of calcifying organisms. A direct OA effect can also be covered or compensated for by indirect OA effects. This is also true for the experimental setup presented in this thesis, since direct and indirect effects coexist in the enclosed complex food webs of the mesocosms. Nonetheless, recent literature supports the formerly proposed hypothesis of direct OA effects (decreased abundance and biomass, see Chapter 1 & 2) at the bottom of the food web being decisively responsible for the alterations in the zooplankton community and higher trophic level organisms. In a comprehensive modelling study conducted by Dutkiewicz *et al.* (2015), for instance, a variety of experiments examining current and future effects of OA on phytoplankton communities were synthesized to improve predictions for near-future OA consequences. The authors detected significant intra- and interspecific OA induced shifts in the phytoplankton

community, and concluded that the indirect effects triggered by these direct effects at the ecosystem basis could have pronounced consequences for the whole food web. A similar conclusion was drawn by Taucher *et al.* (2020), who examined various large scale mesocosm experiments conducted under different OA levels. The authors also found direct OA effects restructuring large parts of the examined plankton communities, and furthermore drew the conclusion that the observed changes in the zooplankton community could be attributed to indirect OA effects originating from direct effects at the food web basis.

OA-induced decrease in food quality: The gist of the matter for the zooplankton community?

A frequently suggested explanation for this interplay of direct and indirect effects in a food web is an OA-induced decrease in food quality, which is supposed to be based on shifts in the stoichiometry or taxonomic composition of primary producers. Assuming constant food abundance, lower food quality directly caused by OA translates indirectly into a reduced energy supply for subsequent organisms in the food chain. Under low pH, higher trophic level consumers would lack this energy for the compensation of osmoregulatory stress, which could manifest in higher respiration rates as well as decreased growth, reproduction or recruitment success (Rossoll *et al.* (2012); Poore *et al.* (2013); Cripps *et al.* (2016), **Fig. 1**). The hypothesis of decreased food quality as the basis of OA alterations in food webs can, however, not always be fully confirmed. When analyzing the indirect effects of food quality on a longer time scale, Pedersen *et al.* (2014b) found a decrease in copepod recruitment and growth, but only in the parental generation of the examined animals, not within the newly hatched generation under OA. In their high pCO_2 laboratory studies, Isari *et al.* (2016) could neither detect lower food quality, nor any negative effect on respiration, growth, reproduction, or recruitment on their investigated dinoflagellate-calanoid predator-prey relationship. Nonetheless, the authors did not reject the hypothesis of OA induced low food quality, but ultimately recommended to conduct OA experiments on a longer time scale as well as under more natural and complex ecosystem conditions.

In line with these recommendations and the suspected higher probability of apparent direct and indirect OA effects, I found significant changes in the POM stoichiometry in combination with significant effects in the phytoplankton community under enhanced pCO_2 (see **Chapter 1, Fig. 7**). These changes then translated into a negative OA effect on copepod nauplii larvae (see **Chapter 2, Fig. 3C**), supporting the hypothesis that this decrease in recruitment was linked to an indirect food quality effect. In addition to that, I found evidence

in favor of the dependency of the 'low food quality effect' on the prevailing environmental conditions, as proposed by Isari *et al.* (2016): a majority of negative OA effects on the bottom of the food web (considering phyto- and microplankton responses, see **Chapter 1, Fig. 7**) coincided with distinct positive effects on either growth or abundance of copepodite stages as well as fish larvae survival (**Chapter 2, Fig. 3B & Fig. 7A**). The outcome of the direct OA effects on the basis of the food web discussed here, might be variably depending on different biotic and abiotic factors in an ecosystem. These OA effects on the primary producers are likely to be a major driver of the indirect restructuring of zooplankton communities and higher trophic levels.

Ocean warming as an additional food web stressor

Besides OA, also other environmental stressors will intensify their pressure on marine ecosystems in the near-future, a prominent one being increasing sea surface temperature (IPCC, 2021). Taking into account the pronounced food web changes caused by OA, as pointed out in this thesis, the question arises, how future ecosystems might respond to a combination of OA and warming.

Although much research has been conducted on the combined effects of sea surface warming and OA on phytoplankton (see Dutkiewicz *et al.* (2015)), insights on possible effects on zooplankton organisms and on entire food webs, including interactions between several tropic levels, are scarce. Copepods are a good example to start with, as they are the most important and wide spread species of the zooplankton community. They are poikilothermic, which makes their overall vital functions (metabolic rates, growth, reproduction etc.) sensitive to temperature changes (Mauchline *et al.*, 1998; Kjellerup *et al.*, 2012). As a consequence, ocean warming causes a distinct migration movement of many copepod species towards cooler regions around the world (Richardson, 2008). This process happens on a temporal and spatial scale, which is much faster than the majority of marine - or any terrestrial migration patterns. One consequence of this is a pronounced spatial predator-prey mismatch because many species and their recruits largely depend on the availability of copepods as food sources in their region (Pauly & Christensen, 1995; Støttrup, 2003; Castonguay *et al.*, 2008; Tommasi *et al.*, 2017). One example for such a mismatch, is the declining population of Atlantic cod in the North Sea, where recruitment is heavily limited due to the migration of copepods as their main prey (Beaugrand *et al.*, 2002; Beaugrand *et al.*, 2003). In addition to that, even if zooplankton/ copepods do not move out of a given location, warming could create a temporal predator-prey mismatch by causing annual

phytoplankton and zooplankton spring blooms to start earlier, which reduces or even impedes the period of time during which zooplankton blooms and breeding or recruitment of higher trophic levels overlap (Richardson, 2008; Durant *et al.*, 2019). For that reason, several populations of commercially important fish species are substantially altered in the North Pacific or the North Sea, most likely with reduced long-term survival chances if these species are not able to adapt to the temporal shift in zooplankton blooms (Richardson, 2008).

In addition to that, an interplay of OA and warming could further intensify these spatial and temporal predator-prey mismatches. In combination with OA, zooplankton organisms that migrate to colder regions due to warming could simply trade one environmental stressor for another. As previously noted, colder waters are more susceptible to OA and thus the direct and indirect effects of warming that organisms tried to avoid, would still be affecting them also in colder regions. Increasing levels of OA might also interact with the consequences of the aforementioned temporal predator-prey mismatches. Under the combined negative effects of OA and warming the temporally shifted zooplankton blooms could be, additionally reduced in their dimensions. This would further enhance the predator-prey mismatch, and force predators to not only adapt to the temporal shifts, but also overall lower abundances of their prey.

The increased frequency and severity of jellyfish blooms, however, is probably the most prominently perceived consequence of ocean warming for ecosystems and their services such as fisheries (see review by Purcell *et al.* (2007) or Atkinson *et al.* (2004)). In general, hydrozoans are presumed to benefit from ocean warming due to a positive correlation of their metabolic rates and temperature, leading to enhanced reproduction and growth (Purcell, 2005). In combination with increasing levels of OA, this temperature advantage of Hydrozoa and their apparent resilience to direct OA effects (as proposed in this thesis) might further contribute to their increasing dominance. This might be especially true considering the rather negative food web effects of warming, as well as the higher sensitivity of some (also commercially important) fish species to direct OA effects (Frommel *et al.*, 2014; Pimentel *et al.*, 2014; Frommel *et al.*, 2016; Stiasny *et al.*, 2016).

Food availability as an antidote to direct negative effects of OA and warming

Such scenarios purely focusing on the metabolic consequences of OA and warming may be simplified, considering that they do not account for one of the most crucial variables in determining how warming and OA will affect ecosystems. Namely changes in food quantity/

availability and/ or quality. As already pointed out, the direct effects of OA and warming, i.e. hypercapnia and hyperthermia, both lead to an increase in metabolic rates in organisms. But the outcome of this can also be beneficial if there is sufficient food available to meet the enhanced energy demand (**Fig. 1**). Connell *et al.* (2017), for instance, suggested that even the strong direct negative OA effects on calcifiers could be compensated by enhanced food availability. In addition to that, a study conducted by Goldenberg *et al.* (2017) revealed that primary production increased substantially under OA and warming as well as sufficient nutrient supply. However, not up to a sufficient rate for the subsequent zooplankton community not to run into metabolic depression and decline in abundances. Nonetheless, the authors stressed that under sufficient enhancement of PP the observed negative effects on consumers could at least be amortized, if not even converted into benefits.

Conclusion

Overall, the interaction of OA and warming is capable of strongly influencing the food webs of future ecosystems in different ways. An important factor in the context of "whole ecosystem" responses is food quality and its connection to species composition at the bottom of the food web. As I showed in this thesis, effects of OA on the quantity and quality of food produced at the base of the food web can cascade up the trophic levels. In addition to that, warming does affect higher trophic level consumers by creating distinct predator - prey mismatches via spatial or temporal separation due to the high temperature sensitivity of large parts of the zooplankton organisms. Besides these negative effects, both OA and warming have the potential to be beneficial to affected organisms to some degree. If met by a sufficient amount of energy intake (= increased food availability/ quality) the inherent increase in metabolic rates directly caused by OA and warming could be converted into enhanced growth and reproduction (see **Fig. 1**). On the one hand, this could result in an additional stressor for ecosystems, as exemplified by the case of hydrozoans in this thesis, which due to their broad spectrum of prey and the ability to adapt their food intake according to the higher energy demand could increase top-down pressure on an entire planktonic food web. On the other hand, in a more bottom-up controlled food web enhanced food or nutrient availability could also lead to an increase in primary and secondary production, which potentially would be beneficial for higher trophic levels and ecosystem services.

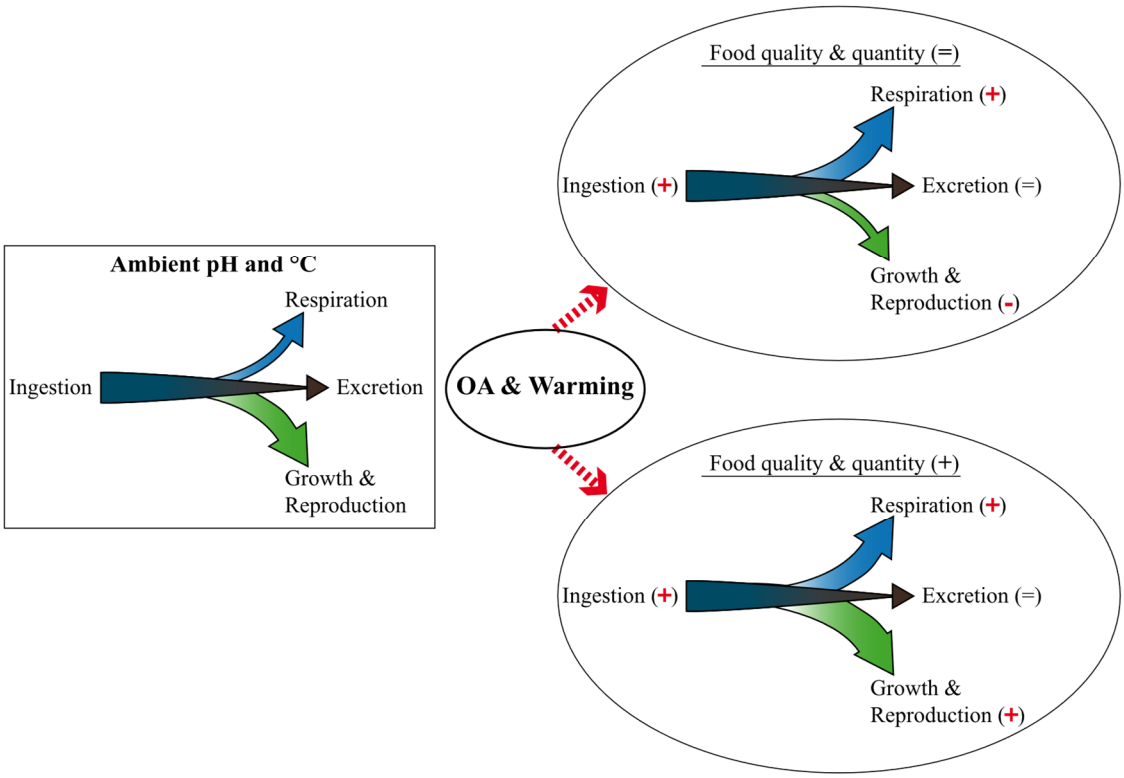

Figure 1: Change in zooplankton/ copepod metabolic rates from natural ambient pH and temperature [°C] on the left, to ocean acidification (OA) and ocean warming conditions on the right. In the light of constant (upper right) and enhanced (lower right) food quality and quantity. (+) symbolizes an increase, (-) a decrease and (=) no change in the respective metabolic rate.

2. Potential productivity enhancement under artificial upwelling

The results presented in Chapter 3 of this thesis suggest that due to a substantial increase in PP, a pronounced, but comparingly small increase in SP, and an enhanced TTE, artificial upwelling could be capable of stimulating biomass production without major negative side effects on ecosystem ecology. This could possibly lead to higher carbon export and the renaturation of expanding ocean deserts. In addition, based on aforementioned metabolic consequences of OA and warming, it might be possible that increased food availability created by artificial upwelling puts zooplankton organisms into the position of compensating for the direct effects of these intensifying environmental stressors. In order to enhance the probability of these indications it is, however, crucial to apply artificial upwelling in a way that ensures an ideal interaction of PP, SP, and TTE.

Linkage between primary and secondary production

Previous theories about the link between PP and SP generally assumed that increasing PP will also increase zooplankton biomass and SP, thereby sustaining a pronounced top-down control on primary producers (Oksanen *et al.*, 1981). In contrast to that, results presented

here indicate that beyond a certain threshold of upwelling intensity and enhanced PP, zooplankton cannot maintain top-down control, and the TTE (SP:PP ratio) starts decreasing. This also goes along well with findings from other recent studies in natural upwelling systems (e.g. Sellers *et al.* (2020)). Theoretically, one would assume that given enough time zooplankton communities would adapt to the increase in food supply and grow in population size to establish a new equilibrium, with both high PP and SP. However, results from aforementioned studies in natural upwelling systems do not support this argument. Kemp *et al.* (2001), for instance, pointed out that regardless of location and nutrient regimes, their examined pelagic ecosystems displayed substantial decreases in SP and TTE after PP exceeded certain thresholds. Although the authors related this drop in SP to community composition and size distribution in the zooplankton community, there can be various other reasons behind such a mismatch in natural upwelling systems. To analyze and comprehend these reasons is, however, important for the application of artificial upwelling, as it might give decisive hints to how it could be performed and what would have to be improved.

Influence of hydrodynamics on PP and SP and its implications

As pointed out in the review of Sellers *et al.* (2020) (and the references therein), a discrepancy between high PP (or chl *a* as a proxy) and SP can occur in coastal upwelling areas, due to the upwelled water inducing an offshore current, which could transport away zooplankton larvae. Consequently, the decoupling of zooplankton production and recruitment would remove a substantial part of SP further offshore, leaving behind only larger zooplankton species capable of resisting (e.g. swimming) or avoiding (e.g. vertical migration) such near-surface currents (**Fig. 2**). Although these species have the advantage of high food availability and quality, possibly leading to high growth rates, they cannot compensate for the loss of SP via advection (e.g. via recruitment and population growth). According to the authors, also temperature can be considered a decisive factor for defining TTE in upwelling areas (see Sellers *et al.* (2020)). As already described in the ocean warming section of this synthesis, copepods are, as the major component of zooplankton, to a certain extent sensitive to changes in water temperature. Consequently, the temperature reduction in surface waters due to cold upwelled deep-water can lead to a decrease in metabolic activity of the majority of phytoplankton grazers, resulting in lower SP. Accordingly, the so-called intermittent upwelling hypothesis (IUH, see Menge and Menge (2013)) proposes that not a continuous and strong upwelling is forming the most productive and efficient plankton communities in these areas, but an intermittent and moderate intensity upwelling is optimal

(see also Lathlean *et al.* (2019), **Fig. 2**). Inter alia, Menge and Menge (2013) based this IUH on reduced cooling of surface waters as well as a decreased offshore current generated by an intermediate upwelling. According to the authors, this leads to less inhibited metabolic rates of grazers, a closer coupling of zooplankton larvae production and recruitment, and an enhanced nutrient availability for near-shore PP due to higher residence times of nutrient rich deep-water close to shore.

Overall, the findings I presented in this thesis complement the results of these studies in a very meaningful way. In Chapter 3 I showed that a recurring supply of deep-water, especially under high advection (= exchange of mesocosm water with deep-water) led to a substantially less effective food web. It could, however, result in a higher efficiency if there was sufficient time after an upwelling event for the plankton community to adapt to and utilize the phytoplankton bloom. These insights can now be extended to artificial upwelling in terms of designing such an approach in order to minimize the negative influence of advection, i.e. drifting of the nutrient enriched water masses away from the upwelling source (= pumping device, see **Fig. 2**). Consequently, oligotrophic areas with as low currents as possible or such that prevent water masses from drifting away, e.g. cyclonic eddies, should be chosen along with a pumping device which is able to drift along with the enriched plume of water.

Biotic influence on PP and SP and its implications

Besides these hydrodynamic conditions, the artificial upwelling study also revealed that community composition of primary and secondary producers play an imminent role in shaping SP and TTE. I found evidence that the presence of diatoms as the main component of phytoplankton as well as the body size distribution and species composition of the copepod community had significant influence on secondary productivity and TTE of the ecosystem. The assumption that diatoms constitute a large proportion of the diet of copepods was established already about 100 years ago, quite similar to the theory of SP increasing constantly along with PP (Lebour, 1927). Additionally, based on observations of diatom blooms coinciding with high zooplankton SP and fishery yield in natural upwelling systems, a paradigm has emerged that these diatoms, and the blooms they are forming, have to be a major component in a food web in order for it to be highly productive (e.g. Cushing (1989)). These theories are, however, also subjected to controversial discussion. Runge and Lafontaine (1996), for instance, pointed out that zooplankton blooms are not based on the biomass produced by diatoms, but are rather sustained by the mixed protists community evolving after a diatom bloom. Evidence for this counter argumentation were accumulating

observations and experiments at that time, revealing inhibiting effects from diatoms on copepods, particularly on their reproduction and recruitment (see review by Syuhei *et al.* (1997)). As presented in Chapter 3, such negative effects have recurrently been observed until today, and the theory of diatoms as high-quality food got challenged even further during this time. Recently, the view is emerging that the decrease of reproduction rates and recruitment success of copepods is related to chemicals excreted by many diatom species (Miralto *et al.*, 1999; Russo *et al.*, 2018). The chemicals produced are so-called oxylipids, formed via oxygenation of poly-unsaturated fatty acids. Although the amount of oxylipids and hence the effect size can vary strongly between different diatom taxa, they are proven to impair embryonic development, larval growth, fitness, or alter sex ratios of copepods (Russo *et al.* (2018) and sources therein). Comparable to what was observed in the here presented thesis, with low TTE coinciding with high diatom abundances, Russo *et al.* (2018) conclude that the negative effects of diatoms' oxylipids could significantly alter carbon flows to higher trophic levels. These recent molecular insights into the diatom-copepod interaction provide a potential explanation for what I pointed out in Chapter 3 of this thesis: carbon transfer within a food web might be more effective if the contribution of diatoms would be kept minimal in an artificial upwelling scenario, e.g. by choosing deep-water with low silicate values (**Fig. 2**).

In addition to a suitable phytoplankton community the zooplankton/ copepod community establishing under artificial upwelling has to be composed in a way that enables it to utilize the given primary producer biomass most efficiently. This biomass turnover rate depends almost exclusively on the maximum possible ingestion rates and the food saturation level of the prevailing copepod taxa. Besides the dependency of these two parameters on the size distribution within the copepods (as suggested in the discussion in Chapter 3), it can be assumed that feeding mode and gender also have a substantial influence in defining the maximum possible SP (Kiorboe, 2006, 2008). Due to their sedentary diet and lifestyle, ambush feeders (e.g. Oithonidae) usually have significantly less predatory influence, energy costs, and hence food intake and SP, compared to motile active current feeders. (e.g. Temoridae) (**Fig. 2**). Considering gender, males generally show a higher ingestion rate to body size ratio and SP than females (Kiorboe, 2006; Van Someren Gréve *et al.*, 2017) (**Fig. 2**).

Clearly, it would be very challenging to actively control body size, gender, or feeding behavior of the prevailing copepod community in mesocosm experiments, and even more so

in open ocean artificial upwelling scenarios. Nonetheless, monitoring these factors in detail in such experiments (as done here) can give important insights into the capability of a zooplankton community of adapting and evolving into one that maximizes TTE and SP within a food web affected by artificial upwelling. Furthermore, it might be crucial for exploring which controlling factors are most critical in maximizing SP and TTE (e.g. phytoplankton community composition), particularly with the ultimate goal of a maximum fishery yield for the area where artificial upwelling is applied (**Fig. 2**).

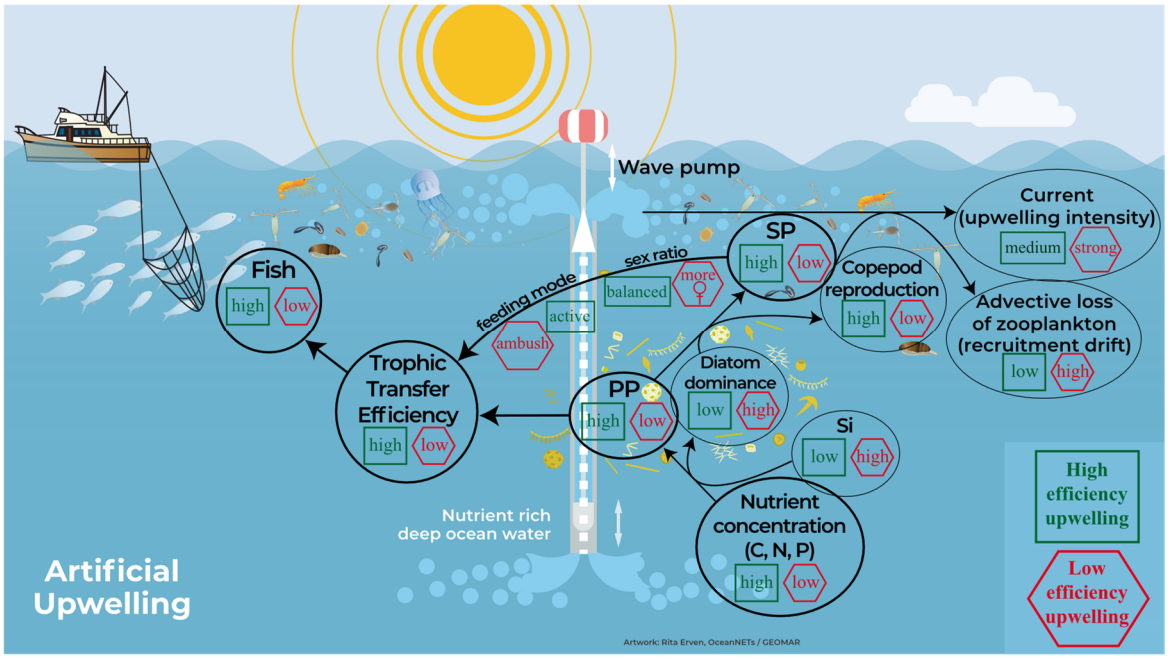

Figure 2: Conceptual overview of the potential regulating factors determining the trophic transfer efficiency and fish biomass of a food web created by artificial upwelling. Conditions to be met by the regulating factors in order to lead to a high or low TTE and fish biomass are given in green rectangles and red polygons, respectively. C = Carbon, N = Nitrogen, P = Phosphorus, Si = Silicate, PP = Primary production, SP = Secondary production. Original artwork of Rita Erven, © GEOMAR Helmholtz Centre for Ocean Research Kiel (see bottom of the figure), reworked with symbols taken from "Courtesy of the Integration and Application Network, University of Maryland Center for Environmental Science (ian.umces.edu/symbols/)", accessed 10.10.2021.

3. Future Perspectives

Based on the findings presented in this thesis, it is apparent that the alterations caused by the ocean acidification and artificial upwelling within complex natural ecosystems and food webs require an increasing need for out-of-the-box thinking. On the one hand, the observed complex and variable indirect consequences for the zooplankton community and higher trophic level consumers caused by direct OA-induced changes within primary producers, showed that a much broader view on the potential effects of OA in an ecosystem is necessary. On the other hand, long-established food web concepts should be scrutinized, e.g. the

importance of diatoms for food web efficiencies or the non-linear relationship between primary and secondary production.

As a next step in the direction of out-of-the-box thinking, we should try to improve our understanding of how artificial upwelling could enhance SP and TTE. For instance, by considering the adjustments suggested in Chapter 3 regarding upwelling mode, i.e. high intensities in a recurring mode, but with increased "resting" times between upwelling events. In addition, implementing a manipulation of the inherent phytoplankton community towards less diatoms might be beneficial. Furthermore, building on the insight that artificial upwelling achieves substantial enhancement of PP (Chapter 3), the scope of such experiments could be extended to also include OA and/ or ocean warming. This would allow for a further evaluation of the hypothesis whether higher food availability or cooling of surface waters is a decisive factor in mitigating direct negative effects caused by environmental stressors like OA and warming. In the course of that, it could also be further elucidated if potential negative ecological effects of artificial upwelling might counteract such a mitigation. As cold deep-water is enriched with CO_2, it could further acidify surface waters instead of mitigating effects of OA. In addition to that, high zooplankton biomasses consume oxygen and produce CO_2 via respiration, which could reinforce the acidification effect as well as add another process of CO_2 emissions to the atmosphere. Evaluating how all these possible effects come together in an open ocean plankton community will be vital in order to assess if artificial upwelling could not only serve as a carbon dioxide removal method, but possibly help in directly alleviating negative (and already occurring) impacts of climate change.

Although mesocosm experiments like the ones performed in this thesis have proven as a valuable tool for such studies, I also see the necessity to take the next step and carry out large scale field tests in order to understand the general effects of artificial upwelling on ecosystems. Even large-scale mesocosm experiments have the constraint of truncating a community by excluding bigger zooplankton organisms (e.g. everything above 3 mm in the experiments presented here), and thus also releasing the food web to a certain extent from predation pressure. Additionally, due to the limitation of space, mesocosms do not allow for diel vertical migration of zooplankton/ copepods. This might affect the individuals habituated to it, yet with unknown consequences, and potentially favor the dominance of species that do not vertically migrate. Moreover, the enclosed ecosystem of the mesocosms

does prevent organisms from migrating in or out of the system as well as removes the vast majority of hydrodynamics these organisms would be exposed to in natural habitats.

In order to overcome these constraints, field tests could be carried out with already established technical realizations of artificial upwelling (e.g. a wave or propeller pump), and could be performed not only in oligotrophic 'ocean deserts', but also in areas strongly influenced by OA and/ or warming. These could be, for instance, areas with low or ideally no currents and low abundance or biomass of certain zooplankton species, e.g. due to migration or direct OA effects on calcifiers. In such areas it could then be evaluated whether long-term enhancement of PP and food availability provided by artificial upwelling translates into recovering biomass of species affected by climate change, compared to surrounding areas with high exposure to OA or/ and warming. Additionally, also SP and TTE could be calculated for the artificial upwelling area via an assessment of copepod abundances and biomass as well as under ideal circumstances (no or low drifting of water masses) a possible stabile isotope enrichment. In a field study more comprehensive methods could be added to the ones presented in this thesis in order to determine which plankton community composition leads to the most productive food web and/ or if this food web is possibly bottom-up or top-down restricted by environmental stressors. In this context, genetic identification of single animals via DNA sequencing has already been proven to be a valuable tool to confirm microscopic classification (Chapter 3), and allow for the implementation of ecological traits of the various zooplankton species into a trait-based food web analysis. Furthermore, this technique could be combined with "Next Generation" high throughput parallel DNA sequencing, which is capable of identifying the totality of genetic material present in mixed samples, e.g. different plankton species within a water sample, on a filter, or in the gut of a grazer. If applied to a plankton community, this technique could add valuable information to the microscopic species identification data as well as be an efficient replacement or improvement of classical gut content analysis, enabling a profound next step towards the solution of "who eats whom" in complex food webs.

Although conducting a field study of the above described scale would require a tremendous amount of work and very detailed planning, I would argue that it is a necessary step for advancing from assessing possible impacts of artificial upwelling in a regulated, experimental setup, to gaining new insights into the actual effect size and practicability of applying artificial upwelling. Not only as a carbon dioxide removal approach or method to revitalize expanding ocean deserts, but also as a potential countermeasure against direct

effects of future ocean change in form of OA, warming or other environmental stressors to plankton communities. Under the given circumstances of the increasing speed of global climate change and the pressing issue of taking measures against it, there is urgent need for conducting such proof-of-concept field studies to evaluate long term durability, efficacy and possible side effects of ocean-based climate change solutions like artificial upwelling within natural open ocean conditions. This includes a mandatory change of focus, away from assessing single species responses to ocean change under laboratory conditions, and towards pilot-field studies of reasonable scales, with the aim of taking active measures against climate change instead of continuing to theoretically evaluate its present and future consequence to marine life.

APPENDIX

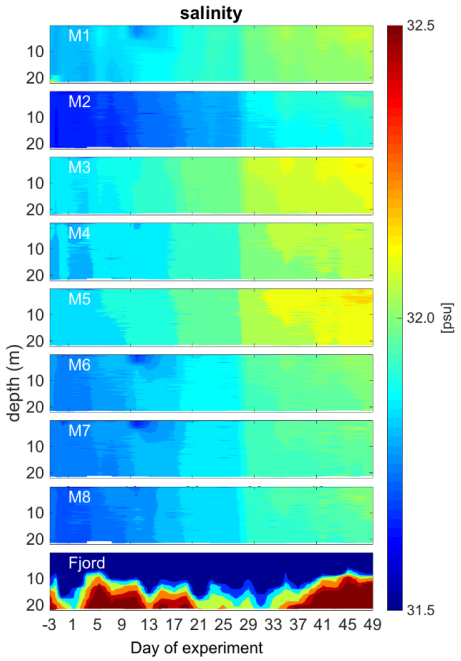

Appendix Fig. 1: Overview of the CTD - depth profiles of salinity over the course of the experiment. Figure created with MATLAB (version R2013a).

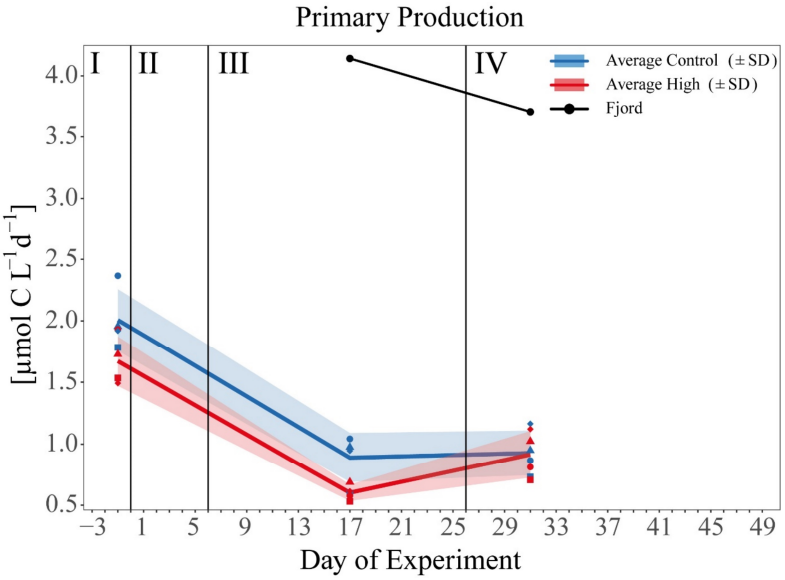

Appendix Fig. 2: Temporal development of average primary production (PP, µg C L^{-1} d^{-1}) over the course of the experiment. Blue, red, and black line indicate the respective average concentration in the control, high pCO_2 treatment, and the Fjord. The ribbons represent the standard deviations (SD). Blue symbols represent concentrations in the ambient pCO_2 mesocosms (M1, M2, M4, M7), red symbols in the high pCO_2 mesocosms (M3, M5, M6, M8), black symbols represent the fjord. For assignment of symbols to the individual mesocosms see **Chapter 1, Tab. 1**. Roman numerals indicate the different phases of the experiment separated by vertical lines (for description of phases see **Chapter 1, Tab. 2**). Figure created with the ggplot2 package in RStudio (RStudio, 2016; Wickham *et al.*, 2016).

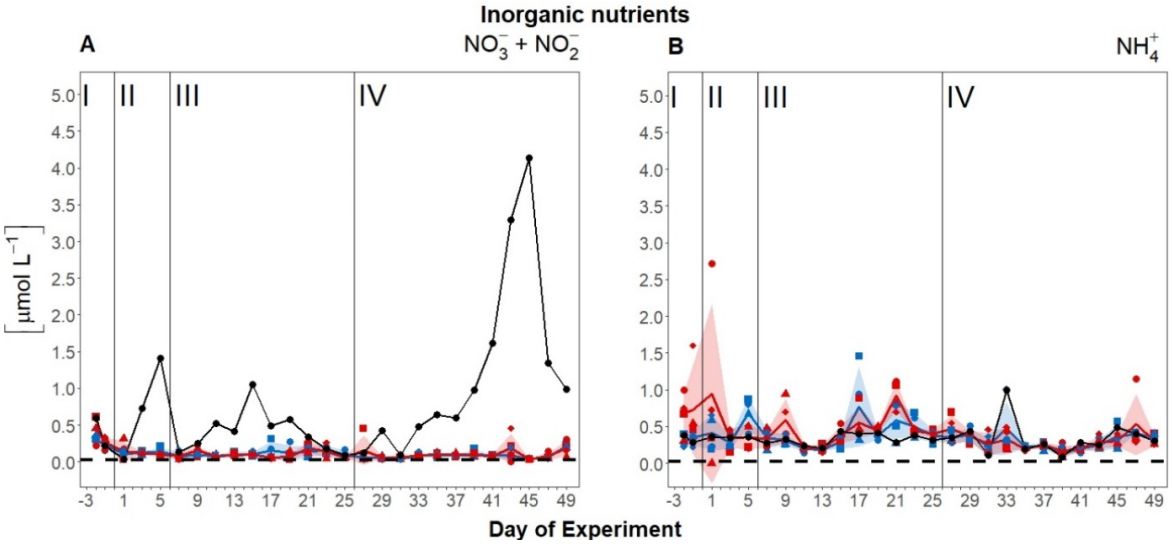

Appendix Fig. 3: Nutrient concentrations of **(A)** Nitrate + nitrite (NO_3^-+ NO_2^- +), and **(B)** ammonium (NH_4^+) over the course of the experiment. Lines, symbols, and colors are used as described in **Chapter 1, Fig. 5**. For assignment of symbols to the individual mesocosms see **Chapter 1, Tab. 1.** Roman numerals label the different phases of the experiment separated by vertical lines (for description of phases see **Chapter 1, Tab. 2**). Figure created with the ggplot2 package in RStudio (RStudio, 2016; Wickham *et al.*, 2016).

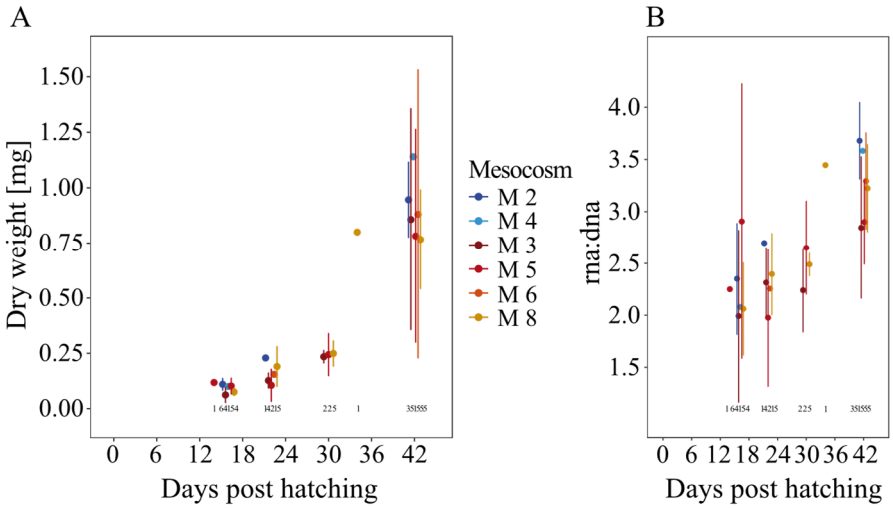

Appendix Fig. 4: (A) Herring larvae dry weight [mg] and **(B)** RNA:DNA ratio (nutritional condition sRD) per mesocosm over the time after hatching. Small numbers in the plots correspond to the number of animals measured for this mesocosm and day. Error bars within the plots represent standard deviation (SD). Symbols and colors according to the given legend.

Appendix Tab. 1: Summary of the mesocosm volume determination by means of saturated NaCl addition (see **Chapter 1, Section "Volume determination"**)

Mesocosm	Salinity before addition	δsal	Salinity after addition	Calculated mesocosm-volume [L]
M1	31,616	0,196	31,812	58578
M2	31,461	0,206	31,667	56138
M3	31,662	0,200	31,862	57563
M4	31,660	0,188	31,848	61010
M5	31,683	0,189	31,872	60463
M6	31,584	0,194	31,778	59139
M7	31,573	0,194	31,766	59210
M8	31,544	0,191	31,735	60084

Appendix Tab. 2: Overview of the added volumes of CO_2 enriched seawater [L] to every mesocosm (see **Chapter 1, Section "CO_2 addition"**)

Day of experiment	M1	M2	M3	M4	M5	M6	M7	M8
05/12/15 (Day 0)	0	0	150	0	150	150	0	150
05/14/15 (Day 2)	0	0	100	0	100	100	0	100
05/16/15 (Day 4)	0	0	150	0	150	150	0	150
05/18/15 (Day 6)	0	0	50	0	50	50	0	50
05/26/15 (Day 14)	0	0	75	0	75	75	0	75
06/03/15 (Day 22)	0	0	45	0	50	30	0	43
06/09/15 (Day 28)	0	0	75	0	75	75	0	75
06/21/15 (Day 40)	0	0	50	0	54	46	0	46
06/27/15 (Day 46)	0	0	50	0	50	50	0	50

Appendix Tab. 3: Summary of the significant treatment effects detected by similarity percentage analysis (SIMPER) performed on the normalized abundance/concentration data. Significant negative impacts indicated with red, significant positive effects with green background color.

	Phase I	Phase II	Phase III	Phase IV
Biogeochemistry				
TPC_{WATER}			p = 0.029	p = 0.031
TPN_{WATER}				
POC_{WATER}			p = 0.029	p = 0.007
PON_{WATER}			p = 0.029	
TPP_{WATER}			p = 0.029	p = 0.031
BSi_{WATER}				
$POC:PON_{WATER}$				
$PON:TPP_{WATER}$				
$POC:TPP_{WATER}$				
TPC_{SED}	NA			
TPN_{SED}	NA			
POC_{SED}	NA			
PON_{SED}	NA			
TPP_{SED}	NA			
BSi_{SED}	NA			
Phytoplankton				
Chlorophyceae				p = 0.029
Chrysophyceae				p = 0.029
Cryptophyceae				p = 0.029
Cyanophyceae	p = 0.026			p = 0.029
Bacillariophyceae			p = 0.029	
Dinophyceae			p = 0.029	
Prasinophyceae				
Prymnesiophyceae			p = 0.029	
Microzooplankton				
Autotrophic			p = 0.029	p = 0.029
Heterotrophic				p = 0.029
Mesozooplankton				
Acartia spp. copepodites			p = 0.029	
Bivalvia				p = 0.029
Bryozoa				
Calanus spp. adults				
Calanus spp. copepodites				p = 0.029
Centropages spp. adults				
Centropages spp. copepodites				
Cirripedia				
Clupea harengus larvae				p = 0.029
Echinodermata			p = 0.029	
Gastropoda			p = 0.029	p = 0.029
Hydrozoa				p = 0.029
Microsetella spp.				p = 0.029
Para-/Clausocalanus adults				
Para-/Clausocalanaus copepodites				
Copepod nauplii				
Oikopleura dioica		p = 0.031		p = 0.029
Oithona spp. adults				
Oithona spp. copepodites				p = 0.029
Oncaea spp. adults				
Polychaeta				
Temora spp. adults				
Temora spp. copepodites				

Appendix Tab. 4: Summary of statistical analysis

A Plankton nMDS	**Phase I**	**Phase II**	**Phase III**	**Phase IV**
Distance	Bray-Curtis	Bray-Curtis	Bray-Curtis	Bray-Curtis
Dimensions	2	2	2	2
Stress	0.1066	0.1203	0.0916	0.0197
B Betadisper on vegdist + ANOVA				
F-value	0.1481	0.6613	0.5023	0.1442
Pr (> F)	0.7136	0.4472	0.5051	0.7172
C PERMANOVA				
F model	1.2028	1.5240	3.7741	7.4774
R^2	0.1670	0.2026	0.3861	0.5548
Pr (> F)	0.1133	0.1463	0.0302	0.0289

Appendix Tab. 5: Carbon content per individual [µg C ind^{-1}] used as conversion factor for the biomass calculation of the respective species, and the literature source they originated from.

Species	**Biomass conversion factor [µg C ind^{-1}]**	**Sources**
Acartia sp. copepodite	1,5	Hay *et al.* (1991)
Acartia sp. adult	4,5	
Calanus sp. cop.	55	Blachowiak-Samolyk *et al.* (2008)
Calanus sp. adult	100	
Oithona spp. cop.	0,5	Hay *et al.* (1991); Sabatini and Kiørboe (1994)
Oithona spp. adult	0,8	
Temora spp. cop.	2,5	Hay *et al.* (1991)
Temora spp. adult	6,0	
Copepod nauplii	0,4	mean of above

Appendix Tab. 6: Number of eggs and fish larvae introduced and sampled over the course of the mesocosm study.

Treatment - Mesocosm	Eggs before hatch	Unhatched eggs	Larvae hatched	Alive larvae sampled	Dead larvae in sediment	Surviving larvae	Missing larvae
Ambient – Mesocosm 1	4140	2753	1387	4	211	0	1172
Ambient - Mesocosm 2	6710	4357	2354	13	521	5	1815
High - Mesocosm 3	7972	5008	2964	17	742	57	2148
Ambient - Mesocosm 4	7081	4833	2248	8	360	3	1877
High - Mesocosm 5	5966	3883	2083	17	563	29	1474
High - Mesocosm 6	5183	4035	1148	4	206	24	914
Ambient - Mesocosm 7	6342	4196	2146	0	292	0	1854
High - Mesocosm 8	7519	5347	2173	29	337	37	1771

Appendix protocol: DNA extraction for mtCOI DNA sequencing

The single organisms were mixed with 400 µl CTAB + ß-mercaptoethanol (1 ml CTAB : 20 µl ß-mercaptoEtOH mixture) and 20 µl Proteinase K, briefly vortexed (VELP Scientifica Classic Advanced dVortex Mixer) and centrifuged (Eppendorf Centrifuge 5417R), and afterwards stored overnight in a BioShake iQ thermal mixer (56°C, 900 rpm). On the next day, all samples were briefly centrifuged again, mixed with 1 µl RNaseA (20mg/ml), and went back to incubation in the water bath for 30 min at 37°C. Next, 400 µl of chloroform:isoamyl alcohol mixture (24:1) was added, the samples were vortexed for 10 sec, and centrifuged at 4°C, 14000 rpm, for 5 min. As a result of the chloroform:isoamyl alcohol mixture, 3 different phases developed in the microtubes after centrifuging. Out of these phases, the upper aqueous one, containing the extracted DNA, was removed by carefully pipetting it into a new 1.5 ml microfuge tube. This step of extraction with chloroform:isoamyl alcohol (addition of 400 µl, vortexing, centrifuging, pipetting) was done twice to get the DNA as clean as possible. To then concentrate, and further clean the extracted DNA, all samples were mixed with 40 µl 3M sodium acetate and 833 µl 96% EtOH, inverted several times, and were once more centrifuged at 4°C, 14000 rpm for 10 min. Afterwards, the sodium acetate and EtOH mixture containing the now created DNA pellet, was removed without touching or resuspending the pellet, and was replaced with 200 µl of 70% EtOH. Centrifuging and removing the alcohol then was repeated, and the DNA pellet was dried in a thermoblock between 40°C – 56°C until all the remaining EtOH evaporated. Finally, the pellet was resuspended in 100 µl warm Elution Buffer Macherey-Nagel (Buffer AE), briefly vortexed and centrifuged, and let to rest at room temperature for one hour. The so extracted DNA was subsequently split in two halfs. One as stock DNA, permanently frozen at -20°C, and one as working aliquots, also stored at -20°C but for further use in PCRs.

REFERENCES

Abràmoff, M.D., Magalhães, P.J. & Ram, S.J. (2004): Image processing with ImageJ. *Biophotonics international*, **11**, 36-42.

Adobe-Inc. (2008): *Adobe Illustrator*.

Algueró-Muñiz, M., Horn, H.G., Alvarez-Fernandez, S., Spisla, C., Aberle, N., Bach, L.T., Guan, W., Achterberg, E.P., Riebesell, U. & Boersma, M. (2019): Analyzing the Impacts of Elevated-CO_2 Levels on the Development of a Subtropical Zooplankton Community During Oligotrophic Conditions and Simulated Upwelling. *Frontiers in Marine Science*, **6**. 10.3389/fmars.2019.00061

Altschul, S.F., Gish, W., Miller, W., Myers, E.W. & Lipman, D.J. (1990): Basic local alignment search tool. *J Mol Biol*, **215**, 403-10. 10.1016/s0022-2836(05)80360-2

Anderson, M.J. (2006): Distance-Based Tests for Homogeneity of Multivariate Dispersions. *Biometrics*, **62**, 245-253. 10.1111/j.1541-0420.2005.00440.x

Arístegui, J., Barton, E.D., Álvarez-Salgado, X.A., Santos, A.M.P., Figueiras, F.G., Kifani, S., Hernández-León, S., Mason, E., Machú, E. & Demarcq, H. (2009): Sub-regional ecosystem variability in the Canary Current upwelling. *Progress in Oceanography*, **83**, 33-48. 10.1016/j.pocean.2009.07.031

Atkinson, A., Siegel, V., Pakhomov, E. & Rothery, P. (2004): Long-term decline in krill stock and increase in salps within the Southern Ocean. *Nature*, **432**, 100-103. 10.1038/nature02996

Attrill, M.J., Wright, J. & Edwards, M. (2007): Climate-related increases in jellyfish frequency suggest a more gelatinous future for the North Sea. *Limnology and Oceanography*, **52**, 480-485. 10.4319/lo.2007.52.1.0480

Bach, L.T., Lohbeck, K.T., Reusch, T.B.H. & Riebesell, U. (2018): Rapid evolution of highly variable competitive abilities in a key phytoplankton species. *Nature Ecology & Evolution*, **2**, 611-613. 10.1038/s41559-018-0474-x

Bach, L.T., Alvarez-Fernandez, S., Hornick, T., Stuhr, A. & Riebesell, U. (2017): Simulated ocean acidification reveals winners and losers in coastal phytoplankton. *PLoS One*, **12**, e188198. 10.1371/journal.pone.0188198

Bach, L.T., Taucher, J., Boxhammer, T., Ludwig, A., Kristineberg, K.C., Achterberg, E.P., Alguero-Muniz, M., Anderson, L.G., Bellworthy, J., Budenbender, J., Czerny, J., Ericson, Y., Esposito, M., Fischer, M., Haunost, M., Hellemann, D., Horn, H.G., Hornick, T., Meyer, J., Sswat, M., Zark, M. & Riebesell, U. (2016): Influence of Ocean Acidification on a Natural Winter-to-Summer Plankton Succession: First Insights from a Long-Term Mesocosm Study Draw Attention to Periods of Low Nutrient Concentrations. *PLoS One*, **11**, e159068. 10.1371/journal.pone.0159068

Barlow, R.G., Cummings, D.G. & Gibb, S.W. (1997): Improved resolution of mono- and divinyl chlorophylls a and b and zeaxanthin and lutein in phytoplankton extracts using reverse phase C-8 HPLC. *Marine Ecology Progress Series*, **161**, 303-307. 10.3354/meps161303

Barton, E.D., Arístegui, J., Tett, P., Cantón, M., García-Braun, J., Hernández-León, S., Nykjaer, L., Almeida, C., Almunia, J., Ballesteros, S., Basterretxea, G., Escánez, J., García-Weill, L., Hernández-Guerra, A., López-Laatzen, F., Molina, R., Montero, M.F., Navarro-Pérez, E., Rodríguez, J.M., van Lenning, K., Vélez, H. & Wild, K. (1998): The transition zone of the Canary Current upwelling region. *Progress in Oceanography*, **41**, 455-504. 10.1016/S0079-6611(98)00023-8

Beaugrand, G., Reid, P.C., Ibañez, F., Lindley, J.A. & Edwards, M. (2002): Reorganization of North Atlantic Marine Copepod Biodiversity and Climate. *Science*, **296**, 1692-1964. 10.1126/science.1071329

Beaugrand, G., Brander, K.M., Alistair Lindley, J., Souissi, S. & Reid, P.C. (2003): Plankton effect on cod recruitment in the North Sea. *Nature*, **426**, 661-664. 10.1038/nature02164

Berge, T., Daugbjerg, N., Andersen, B. & Hansen, P. (2010): Effect of lowered pH on marine phytoplankton growth rates. *Marine Ecology Progress Series*, **416**, 79-91. 10.3354/meps08780

Bindoff, N.L., Cheung, W.W.L., Kairo, J.G., Arístegui, J., Guinder, V.A., Hallberg, R., Hilmi, N., Jiao, N., Karim, M.S., Levin, L.A., O´Donoghue, S., Purca Cuicapusa, S.R., Rinkevich, B., Suga, T., Tagliabue, A. & Williamson, P. (2019): Changing Ocean, Marine Ecosystems, and Dependent Communities. *IPCC Special Report on the Ocean and Cryosphere in a Changing Climate* (ed. by H.-O. Pörtner, D.C. Roberts, V. Masson-Delmotte, P. Zhai, M. Tignor, E. Poloczanska, K. Mintenbeck, A. Alegría, M. Nicolai, A. Okem, J. Petzold, B. Rama and N.M. Weyer), Vol: In press.

Blachowiak-Samolyk, K., Søreide, J.E., Kwasniewski, S., Sundfjord, A., Hop, H., Falk-Petersen, S. & Nøst Hegseth, E. (2008): Hydrodynamic control of mesozooplankton abundance and biomass in northern Svalbard waters (79–81°N). *Deep Sea Research Part II: Topical Studies in Oceanography*, **55**, 2210-2224. 10.1016/j.dsr2.2008.05.018

Boecklen, W.J., Yarnes, C.T., Cook, B.A. & James, A.C. (2011): On the use of stable isotopes in trophic ecology. *Annual review of ecology, evolution, and systematics*, **42**, 411-440. 10.1146/annurev-ecolsys-102209-144726

Boschker, H.T.S. & Middelburg, J.J. (2002): Stable isotopes and biomarkers in microbial ecology. *FEMS Microbiology Ecology*, **40**, 85-95. 10.1111/j.1574-6941.2002.tb00940.x

Bouquet, J.-M., Spriet, E., Troedsson, C., Ottera, H., Chourrout, D. & Thompson, E.M. (2009): Culture optimization for the emergent zooplanktonic model organism *Oikopleura dioica*. *Journal of Plankton Research*, **31**, 359-370. 10.1093/plankt/fbn132

Bouquet, J.M., Troedsson, C., Novac, A., Reeve, M., Lechtenborger, A.K., Massart, W., Skaar, K.S., Aasjord, A., Dupont, S. & Thompson, E.M. (2018): Increased fitness of a key appendicularian zooplankton species under warmer, acidified seawater conditions. *PLoS One*, **13**, e0190625. 10.1371/journal.pone.0190625

Boxhammer, T., Bach, L.T., Czerny, J. & Riebesell, U. (2016): Technical note: Sampling and processing of mesocosm sediment trap material for quantitative biogeochemical analysis. *Biogeosciences*, **13**, 2849-2858. 10.5194/bg-13-2849-2016

Brenna, J.T., Corso, T.N., Tobias, H.J. & Caimi, R.J. (1997): High-precision continuous-flow isotope ratio mass spectrometry. *Mass Spectrometry Reviews*, **16**, 227-258. 10.1002/(SICI)1098-2787(1997)16:5<227::AID-MAS1>3.0.CO;2-J

Brun, P., Payne, M.R. & Kiørboe, T. (2016): Trait biogeography of marine copepods – an analysis across scales. *Ecology Letters*, **19**, 1403-1413. doi.org/10.1111/ele.12688

Bucklin, A., Ortman, B.D., Jennings, R.M., Nigro, L.M., Sweetman, C.J., Copley, N., Sutton, T. & Wiebe, P.H. (2010): A "Rosetta Stone" for metazoan zooplankton: DNA barcode analysis of species diversity of the Sargasso Sea (Northwest Atlantic Ocean). *Deep-Sea Research II*, **57**, 2234-2247. 10.1016/j.dsr2.2010.09.025

Calbet, A., Sazhin, A.F., Nejstgaard, J.C., Berger, S.A., Tait, Z.S., Olmos, L., Sousoni, D., Isari, S., Martinez, R.A., Bouquet, J.M., Thompson, E.M., Bamstedt, U. & Jakobsen, H.H. (2014): Future climate scenarios for a coastal productive planktonic food web resulting in microplankton phenology changes and decreased trophic transfer efficiency. *PLoS One*, **9**, e94388. 10.1371/journal.pone.0094388

Caldarone, E.M., Clemmesen, C.M., Berdalet, E., Miller, T.J., Folkvord, A., Holt, G.J., Olivar, M.P. & Suthers, I.M. (2006): Intercalibration of four spectrofluorometric protocols for measuring RNA/DNA ratios in larval and juvenile fish. *Limnology and Oceanography: Methods*, **4**, 153-163. 10.4319/lom.2006.4.153

Caldeira, K. & Wickett, M.E. (2003): Anthropogenic carbon and ocean pH. *Nature*, **425**, 365. 10.1038/425365a

Castonguay, M., Plourde, S., Robert, D., Runge, J.A. & Fortier, L. (2008): Copepod production drives recruitment in a marine fish. *Canadian Journal of Fisheries and Aquatic Sciences*, **65**, 1528-1531. 10.1139/F08-126

Chapman, J.L. & Reiss, M.J. (1998): *Ecology: principles and applications*. Cambridge University Press.

Chavez, F.P. & Messié, M. (2009): A comparison of Eastern Boundary Upwelling Ecosystems. *Progress in Oceanography*, **83**, 80-96. 10.1016/j.pocean.2009.07.032

Checkley, D.M. (1982): Selective Feeding by Atlantic Herring (*Clupea harengus*) Larvae on Zooplankton in Natural Assemblages. *Marine Ecology Progress Series*, **9**, 245-253. http://www.jstor.org/stable/24814536

Christensen, V. & Walters, C.J. (2004): Ecopath with Ecosim: methods, capabilities and limitations. *Ecological Modelling*, **172**, 109-139. 10.1016/j.ecolmodel.2003.09.003

Chuard, P.J.C., Johnson, M.D. & Guichard, F. (2019): Ocean acidification causes mortality in the medusa stage of the cubozoan Carybdea xaymacana. *Scientific Reports*, **9**, 5622. 10.1038/s41598-019-42121-0

Clemmesen, C. (1994): The effect of food availability, age or size on the RNA/DNA ratio of individually measured herring larvae: laboratory calibration. *Marine Biology*, **118**, 377-382. 10.1007/BF00350294

Connell, S.D., Doubleday, Z.A., Hamlyn, S.B., Foster, N.R., Harley, C.D.G., Helmuth, B., Kelaher, B.P., Nagelkerken, I., Sarà, G. & Russell, B.D. (2017): How ocean acidification can benefit calcifiers. *Current Biology*, **27**, R95-R96. 10.1016/j.cub.2016.12.004

Coverly, S., Kerouel, R. & Aminot, A. (2012): A re-examination of matrix effects in the segmented-flow analysis of nutrients in sea and estuarine water. *Analytica Chimica Acta*, **712**, 94-100. 10.1016/j.aca.2011.11.008

Cripps, G., Lindeque, P. & Flynn, K. (2014): Parental exposure to elevated pCO_2 influences the reproductive success of copepods. *Journal of Plankton Research*, **36**, 1165-1174. 10.1093/plankt/fbu052

Cripps, G., Flynn, K.J. & Lindeque, P.K. (2016): Ocean Acidification Affects the Phyto-Zoo Plankton Trophic Transfer Efficiency. *PLoS One*, **11**, e0151739. 10.1371/journal.pone.0151739

Cushing, D.H. (1989): A difference in structure between ecosystems in strongly stratified waters and in those that are only weakly stratified. *Journal of Plankton Research*, **11**, 1-13. 10.1093/plankt/11.1.1

Czerny, J., Schulz, K.G., Krug, S.A., Ludwig, A. & Riebesell, U. (2013): Technical Note: The determination of enclosed water volume in large flexible-wall mesocosms "KOSMOS". *Biogeosciences*, **10**, 1937-1941. 10.5194/bg-10-1937-2013

Daskalov, G.M. & Mamedov, E.V. (2007): Integrated fisheries assessment and possible causes for the collapse of anchovy kilka in the Caspian Sea. *ICES Journal of Marine Science*, **64**, 503-511. 10.1093/icesjms/fsl047

de Kluijver, A., Soetaert, K., Czerny, J., Schulz, K.G., Boxhammer, T., Riebesell, U. & Middelburg, J.J. (2013): A ^{13}C labelling study on carbon fluxes in Arctic plankton communities under elevated CO_2 levels. *Biogeosciences*, **10**, 1425-1440. 10.5194/bg-10-1425-2013

Denis, J., Vincent, D., Antajan, E., Vallet, C., Mestre, J., Lefebvre, V., Caboche, J., Cordier, R., Marchal, P. & Loots, C. (2018): Gut fluorescence technique to quantify pigment feeding in Downs herring larvae. *Marine Ecology Progress Series*, **607**, 129-142. 10.3354/meps12775

Dickson, A.G., Afghan, J.D. & Anderson, G.C. (2003): Reference materials for oceanic CO_2 analysis: a method for the certification of total alkalinity. *Marine Chemistry*, **80**, 185-197. 10.1016/s0304-4203(02)00133-0

Dörner, I., Hauss, H., Aberle, N., Lohbeck, K., Spisla, C., Riebesell, U. & Ismar-Rebitz, S.M.H. (2020): Ocean acidification impacts on biomass and fatty acid composition of a post-bloom marine plankton community. *Marine Ecology Progress Series*, **647**, 49-64. 10.3354/meps13390

Dupont, S., Ortega-Martínez, O. & Thorndyke, M. (2010): Impact of near-future ocean acidification on echinoderms. *Ecotoxicology*, **19**, 449-462. 10.1007/s10646-010-0463-6

Durant, J.M., Molinero, J.-C., Ottersen, G., Reygondeau, G., Stige, L.C. & Langangen, Ø. (2019): Contrasting effects of rising temperatures on trophic interactions in marine ecosystems. *Scientific Reports*, **9**, 15213. 10.1038/s41598-019-51607-w

Dutkiewicz, S., Morris, J.J., Follows, M.J., Scott, J., Levitan, O., Dyhrman, S.T. & Berman-Frank, I. (2015): Impact of ocean acidification on the structure of future phytoplankton communities. *Nature Climate Change*, **5**, 1002-1006. 10.1038/nclimate2722

Edler, L. & Elbrächter, M. (2010): The Utermöhl method for quantitative phytoplankton analysis. *Microscopic and molecular methods for quantitative phytoplankton analysis* (ed. by B. Karlson, C. Cusack and E. Bresnan), Vol: 55, pp. 13-20. UNESCO, Paris.

Emerson, S.R. & Hedges, J.I. (2008): The Marine Carbonate System. *Chemical Oceanography and the Marine Carbon Cycle* (ed. by S.R. Emerson and J.I. Hedges), Vol: pp. 101-150. Cambridge University Press, New York, United States of America.

Engel, A., Schulz, K.G., Riebesell, U., Bellerby, R., Delille, B. & Schartau, M. (2008): Effects of CO_2 on particle size distribution and phytoplankton abundance during a mesocosm bloom experiment (PeECE II). *Biogeosciences*, **5**, 509-521. 10.5194/bg-5-509-2008

Escribano, R., Bustos-Rios, E., Hidalgo, P. & Morales, C.E. (2016): Non-limiting food conditions for growth and production of the copepod community in a highly productive upwelling zone. *Continental Shelf Research*, **126**, 1-14. 10.1016/j.csr.2016.07.018

Fabricius, K.E., Langdon, C., Uthicke, S., Humphrey, C., Noonan, S., De'ath, G., Okazaki, R., Muehllehner, N., Glas, M.S. & Lough, J.M. (2011): Losers and winners in coral reefs acclimatized to elevated carbon dioxide concentrations. *Nature Climate Change*, **1**, 165-169. 10.1038/nclimate1122

Fan, W., Pan, Y., Zhang, D., Xu, C., Qiang, Y. & Chen, Y. (2016): Experimental study on the performance of a wave pump for artificial upwelling. *Ocean Engineering*, **113**, 191-200. 10.1016/j.oceaneng.2015.12.056

Fassbender, A.J., Sabine, C.L., Feely, R.A., Langdon, C. & Mordy, C.W. (2011): Inorganic carbon dynamics during northern California coastal upwelling. *Continental Shelf Research*, **31**, 1180-1192. 10.1016/j.csr.2011.04.006

Feely, R.A., Sabine, C.L., Hernandez-Ayon, J.M., Ianson, D. & Hales, B. (2008): Evidence for Upwelling of Corrosive "Acidified" Water onto the Continental Shelf. *Science*, **320**, 1490-1492. 10.1126/science.1155676

Friedlingstein, P., Bopp, L., Ciais, P., Dufresne, J.-L., Fairhead, L., LeTreut, H., Monfray, P. & Orr, J. (2001): Positive feedback between future climate change and the carbon cycle. *Geophysical Research Letters*, **28**, 1543-1546. 10.1029/2000GL012015

Friedlingstein, P., Jones, M.W., O'Sullivan, M., Andrew, R.M., Hauck, J., Peters, G.P., Peters, W., Pongratz, J., Sitch, S., Le Quéré, C., Bakker, D.C.E., Canadell, J.G., Ciais, P., Jackson, R.B., Anthoni, P., Barbero, L., Bastos, A., Bastrikov, V., Becker, M., Bopp, L., Buitenhuis, E., Chandra, N., Chevallier, F., Chini, L.P., Currie, K.I., Feely, R.A., Gehlen, M., Gilfillan, D., Gkritzalis, T., Goll, D.S., Gruber, N., Gutekunst, S., Harris, I., Haverd, V., Houghton, R.A., Hurtt, G., Ilyina, T., Jain, A.K., Joetzjer, E., Kaplan, J.O., Kato, E., Klein Goldewijk, K., Korsbakken, J.I., Landschützer, P., Lauvset, S.K., Lefèvre, N., Lenton, A., Lienert, S., Lombardozzi, D., Marland, G., McGuire, P.C., Melton, J.R., Metzl, N., Munro, D.R., Nabel, J.E.M.S., Nakaoka, S.-I., Neill, C., Omar, A.M., Ono, T., Peregon, A., Pierrot, D., Poulter, B., Rehder, G., Resplandy, L., Robertson, E., Rödenbeck, C., Séférian, R., Schwinger, J., Smith, N., Tans, P.P., Tian, H., Tilbrook, B., Tubiello, F.N., van der Werf, G.R., Wiltshire, A.J. & Zaehle, S. (2019): Global Carbon Budget 2019. *Earth System Science Data*, **11**, 1783-1838. 10.5194/essd-11-1783-2019

Friedlingstein, P., O'Sullivan, M., Jones, M.W., Andrew, R.M., Hauck, J., Olsen, A., Peters, G.P., Peters, W., Pongratz, J., Sitch, S., Le Quéré, C., Canadell, J.G., Ciais, P., Jackson, R.B., Alin, S., Aragão, L.E.O.C., Arneth, A., Arora, V., Bates, N.R., Becker, M., Benoit-Cattin, A., Bittig, H.C., Bopp, L., Bultan, S., Chandra, N., Chevallier, F., Chini, L.P., Evans, W., Florentie, L., Forster, P.M., Gasser, T., Gehlen, M., Gilfillan, D., Gkritzalis, T., Gregor, L., Gruber, N., Harris, I., Hartung, K., Haverd, V., Houghton, R.A., Ilyina, T., Jain, A.K., Joetzjer, E., Kadono, K., Kato, E., Kitidis, V., Korsbakken, J.I., Landschützer, P., Lefèvre, N., Lenton, A., Lienert, S., Liu, Z., Lombardozzi, D., Marland, G., Metzl, N., Munro, D.R., Nabel, J.E.M.S., Nakaoka, S.I., Niwa, Y., O'Brien, K., Ono, T., Palmer, P.I., Pierrot, D., Poulter, B., Resplandy, L., Robertson, E., Rödenbeck, C., Schwinger, J., Séférian, R., Skjelvan, I., Smith, A.J.P., Sutton, A.J., Tanhua, T., Tans, P.P., Tian, H., Tilbrook, B., van der Werf, G., Vuichard, N., Walker, A.P., Wanninkhof, R., Watson, A.J., Willis, D., Wiltshire, A.J., Yuan, W., Yue, X. & Zaehle, S. (2020): Global Carbon Budget 2020. *Earth Syst. Sci. Data*, **12**, 3269-3340. 10.5194/essd-12-3269-2020

Frommel, A.Y., Maneja, R., Lowe, D., Pascoe, C.K., Geffen, A.J., Folkvord, A., Piatkowski, U. & Clemmesen, C. (2014): Organ damage in Atlantic herring larvae as a result of ocean acidification. *Ecological Applications*, **24**, 1131-1143. 10.1890/13-0297.1

Frommel, A.Y., Maneja, R., Lowe, D., Malzahn, A.M., Geffen, A.J., Folkvord, A., Piatkowski, U., Reusch, T.B.H. & Clemmesen, C. (2012): Severe tissue damage in Atlantic cod larvae under increasing ocean acidification. *Nature Climate Change*, **2**, 42-46. 10.1038/nclimate1324

Frommel, A.Y., Margulies, D., Wexler, J.B., Stein, M.S., Scholey, V.P., Williamson, J.E., Bromhead, D., Nicol, S. & Havenhand, J. (2016): Ocean acidification has lethal and sub-lethal effects on larval development of yellowfin tuna, *Thunnus albacares*. *Journal of Experimental Marine Biology and Ecology*, **482**, 18-24. 10.1016/j.jembe.2016.04.008

Frouin, R., McPherson, J., Ueyoshi, K. & Franz, B.A. (2012): A time series of photosynthetically available radiation at the ocean surface from SeaWiFS and MODIS data. Proceedings SPIE 8525, *Remote Sensing of the Marine Environment II*. Kyoto, Japan.

Gao, K., Beardall, J., Häder, D.-P., Hall-Spencer, J.M., Gao, G. & Hutchins, D.A. (2019): Effects of Ocean Acidification on Marine Photosynthetic Organisms Under the Concurrent Influences of Warming, UV Radiation, and Deoxygenation. *Frontiers in Marine Science*, **6**. 10.3389/fmars.2019.00322

Gattuso, J.-P. & Hansson, L. (2011): Ocean acidification: background and history. *Ocean acidification* (ed. by J.-P. Gattuso and L. Hansson), Vol: pp. 1-20. Oxford University Press, Oxford.

Gazeau, F., Sallon, A., Maugendre, L., Louis, J., Dellisanti, W., Gaubert, M., Lejeune, P., Gobert, S., Borges, A.V., Harlay, J., Champenois, W., Alliouane, S., Taillandier, V., Louis, F., Obolensky, G., Grisoni, J.M. & Guieu, C. (2017): First mesocosm experiments to study the impacts of ocean acidification on plankton communities in the NW Mediterranean Sea (MedSeA project). *Estuarine, Coastal and Shelf Science*, **186**, 11-29. 10.1016/j.ecss.2016.05.014

GESAMP (2019): High level review of a wide range of proposed marine geoengineering techniques. In: *GESAMP Reports & Studies Series* (eds. P. Boyd, C. Vivian and C.M.G.), p. 144,

Giraud, M., Boye, M., Garçon, V., Donval, A. & de la Broise, D. (2016): Simulation of an artificial upwelling using immersed in situ phytoplankton microcosms. *Journal of Experimental Marine Biology and Ecology*, **475**, 80-88. 10.1016/j.jembe.2015.11.006

Goldenberg, S.U., Nagelkerken, I., Ferreira, C.M., Ullah, H. & Connell, S.D. (2017): Boosted food web productivity through ocean acidification collapses under warming. *Global Change Biology*, **23**, 4177-4184. 10.1111/gcb.13699

Gómez, M., Martinez, I., Mayo, I., Morales, J., Santana-del-Pino, A. & Packard, T. (2012): Testing zooplankton secondary production models against Daphnia magna growth. *ICES Journal of Marine Science*, **69**, 421-428. 10.1093/icesjms/fsr193

Grandon, N. (2020): *Effects of Ocean Acidification on Species Composition and Biodiversity in the Region of Kongsfjord (Svalbard)*. Student thesis. http://urn.kb.se/resolve?urn=urn:nbn:se:hh:diva-42347

Gruber, N., Clement, D., Carter, B.R., Feely, R.A., van Heuven, S., Hoppema, M., Ishii, M., Key, R.M., Kozyr, A., Lauvset, S.K., Lo Monaco, C., Mathis, J.T., Murata, A., Olsen, A., Perez, F.F., Sabine, C.L., Tanhua, T. & Wanninkhof, R. (2019): The oceanic sink for anthropogenic CO_2 from 1994 to 2007. *Science*, **363**, 1193-1199. 10.1126/science.aau5153

Hama, T., Hama, J. & Handa, N. (1993): ^{13}C Tracer Methodology in Microbial Ecology with Special Reference to Primary Production Processes in Aquatic Environments. *Advances in Microbial Ecology* (ed. by J.G. Jones), Vol: pp. 39-83. Springer US, Boston, MA. 10.1007/978-1-4615-2858-6_2

Hänsel, M.C., Schmidt, J.O., Stiasny, M.H., Stöven, M.T., Voss, R. & Quaas, M.F. (2020): Ocean warming and acidification may drag down the commercial Arctic cod fishery by 2100. *PLOS ONE*, **15**, e0231589. 10.1371/journal.pone.0231589

Hansen, H.P. & Grasshoff, K. (1983): Automated chemical analysis. *Methods of Seawater Analysis* (ed. by K. Grasshoff, M. Ehrhardt and K. Kremling), Vol: pp. 347-379. Verlag Chemie GmbH, Weinheim.

Hansen, H.P. & Koroleff, F. (2007): Determination of nutrients. *Methods of Seawater Analysis* (ed. by K. Grasshoff, K. Kremling and M. Ehrhardt), Vol: pp. 159-228. Wiley-VCH Verlag GmbH. 10.1002/9783527613984.ch10

Harris, R.P., Irigoien, X., Head, R.N., Rey, C., Hygum, B.H., Hansen, B.W., Niehoff, B., Meyer-Harms, B. & Carlotti, F. (2000): Feeding, growth, and reproduction in the genus Calanus. *ICES Journal of Marine Science*, **57**, 1708-1726. 10.1006/jmsc.2000.0959

Hay, S.J., Kiørboe, T. & Matthews, A. (1991): Zooplankton biomass and production in the North Sea during the Autumn Circulation experiment, October 1987–March 1988. *Continental Shelf Research*, **11**, 1453-1476. 10.1016/0278-4343(91)90021-W

Helle, H.B. (1978): Summer Replacement of Deep Water in Byfjord, Western Norway: Mass Exchange Across the Sill Induced by Coastal Upwelling. *Hydrodynamics of Estuaries and Fjords*, **23**, 441-464. 10.1016/s0422-9894(08)71293-5

Hernandez, F., Shaw, R., Cope, J., Ditty, J., Farooqi, T. & Benfield, M. (2003): The across-shelf larval, postlarval, and juvenile fish assemblages collected at offshore oil and gas platforms west of the Mississippi River delta. *Fisheries, Reefs, and Offshore Development* (ed. by D.R. Stanley and A. Scarborough-Bull), Vol: 36, pp. 39-72. American Fisheries Society Symposium, Bethesda, Maryland.

Hildebrandt, N. (2014): *The response of three dominant Arctic copepod species to elevated CO_2 concentrations and water temperatures*. Dissertation, University of Bremen, Bremerhaven.

Hofmann, G.E., Smith, J.E., Johnson, K.S., Send, U., Levin, L.A., Micheli, F., Paytan, A., Price, N.N., Peterson, B., Takeshita, Y., Matson, P.G., Crook, E.D., Kroeker, K.J., Gambi, M.C., Rivest, E.B., Frieder, C.A., Yu, P.C. & Martz, T.R. (2011): High-Frequency Dynamics of

Ocean pH: A Multi-Ecosystem Comparison. *PLoS ONE*, **6**, e28983. 10.1371/journal.pone.0028983

Holmes, R.M., Aminot, A., Kérouel, R., Hooker, B.A. & Peterson, B.J. (1999): A simple and precise method for measuring ammonium in marine and freshwater ecosystems. *Canadian Journal of Fisheries and Aquatic Sciences*, **56**, 1801-1808. 10.1139/f99-128

Hopcroft, R.R., Roff, J.C. & Lombard, D. (1998): Production of tropical copepods in Kingston Harbour, Jamaica: the importance of small species. *Marine Biology*, **130**, 593-604. 10.1007/s002270050281

Hopkins, F.E., Turner, S.M., Nightingale, P.D., Steinke, M., Bakker, D. & Liss, P.S. (2010): Ocean acidification and marine trace gas emissions. *Proceedings of the National Academy of Sciences*, **107**, 760-765. 10.1073/pnas.0907163107

Huntley, M.E. & Lopez, M.D. (1992): Temperature-dependent production of marine copepods: a global synthesis. *Am Nat*, **140**, 201-42. 10.1086/285410

Ianora, A., Poulet, S.A. & Miralto, A. (2003): The effects of diatoms on copepod reproduction: a review. *Phycologia*, **42**, 351-363. 10.2216/i0031-8884-42-4-351.1

ICES (2007): Report of the Working Group on Northern Pelagic and Blue Whiting Fisheries (WGNPBW). In, p. 229, I.C.F.T.E.O.T. Sea, Vigo, Spain

Illing, B., Moyano, M., Berg, J., Hufnagl, M. & Peck, M.A. (2018): Behavioral and physiological responses to prey match-mismatch in larval herring. *Estuarine, Coastal and Shelf Science*, **201**, 82-94. 10.1016/j.ecss.2016.01.003

IPCC (2014): Climate Change 2014: Impacts, Adaption, and Vulnerability. Part A: Global and Sectoral Aspects. In: *Contribution of Working Group II to the Fifth Assessment Report of the Intergovernmental Panel on Climate Change* (eds. C.B. Field, V. Barros, D.J. Dokken, K.J. Mach, M.D. Mastrandrea, T.E. Bilir, M. Chatterjee, K.L. Ebi, Y.O. Estrada, R.C. Genova, B. Girma, E.S. Kissel, A.N. Levy, S. Maccracken, P.R. Mastrandrea and L.L. White), p. 1132, C.U. Press, Cambridge, United Kingdom and New York, NY, USA

IPCC (2021): Summary for Policymakers. In: *Climate Change 2021: The Physical Science Basis. Contribution of Working Group I to the Sixth Assessment Report of the Intergovernmental Panel on Climate Change* (eds. V. Masson-Delmotte, P. Zhai, A. Pirani, S.L. Connors, C. Péan, S. Berger, N. Caud, Y. Chen, L. Goldfarb, M.I. Gomis, M. Huang, K. Leitzell, E. Lonnoy, J.B.R. Matthews, T.K. Maycock, T. Waterfield, O. Yelekci, R. Yu and B. Zhou), p. 42, C.U. Press, Cambridge, United Kingdom and New York, NY, USA

Irwin, A.J. & Oliver, M.J. (2009): Are ocean deserts getting larger? *Geophysical Research Letters*, **36**. 10.1029/2009GL039883

Isari, S., Zervoudaki, S., Peters, J., Papantoniou, G., Pelejero, C. & Saiz, E. (2016): Lack of evidence for elevated CO_2-induced bottom-up effects on marine copepods: a dinoflagellate–calanoid prey–predator pair. *ICES Journal of Marine Science*, **73**, 650-658. 10.1093/icesjms/fsv078

Jennings, S., Warr, K.J. & Mackinson, S. (2002): Use of size-based production and stable isotope analyses to predict trophic transfer efficiencies and predator-prey body mass ratios in food webs. *Marine Ecology Progress Series*, **240**, 11-20. 10.3354/meps240011

Kämpf, J. & Chapman, P. (2016): *Upwelling systems of the world*. Springer.

Kemp, W.M., Brooks, M.T. & Hood, R.R. (2001): Nutrient enrichment, habitat variability and trophic transfer efficiency in simple models of pelagic ecosystems. *Marine Ecology Progress Series*, **223**, 73-87. 10.3354/meps223073

Kiorboe, T. (2006): Sex, sex-ratios, and the dynamics of pelagic copepod populations. *Oecologia*, **148**, 40-50. 10.1007/s00442-005-0346-3

Kiorboe, T. (2008): Optimal swimming strategies in mate-searching pelagic copepods. *Oecologia*, **155**, 179-192. 10.1007/s00442-007-0893-x

Kiørboe, T., Munk, P. & Støttrup, J.G. (1985): First feeding by larval herring *Clupea harengus* L. *Dana*, **5**, 95-107.

Kiørboe, T., Møhlenberg, F. & Tiselius, P. (1988): Propagation of planktonic copepods: production and mortality of eggs. *Hydrobiologia*, **167**, 219-225. 10.1007/BF00026308

Kirke, B. (2003): Enhancing fish stocks with wave-powered artificial upwelling. *Ocean & Coastal Management*, **46**, 901-915. 10.1016/S0964-5691(03)00067-X

Kjellerup, S., Dunweber, M., Swalethorp, R., Nielsen, T.G., Moller, E.F., Markager, S. & Hansen, B.W. (2012): Effects of a future warmer ocean on the coexisting copepods Calanus finmarchicus and C-glacialis in Disko Bay, western Greenland. *Marine Ecology Progress Series*, **447**, 87-U132. 10.3354/meps09551

Knowles, T.S. (2012): *Effects of Acidified Seawater on Asexual Reproduction and Statolith Size in the Scyphozoan Chrysaora colorata*. Masters Thesis, California State University, Monterey Bay. https://hdl.handle.net/11028/610

Kroeker, K.J., Kordas, R.L., Crim, R.N. & Singh, G.G. (2010): Meta-analysis reveals negative yet variable effects of ocean acidification on marine organisms. *Ecol Lett*, **13**, 1419-34. 10.1111/j.1461-0248.2010.01518.x

Kroeker, K.J., Kordas, R.L., Crim, R., Hendriks, I.E., Ramajo, L., Singh, G.S., Duarte, C.M. & Gattuso, J.P. (2013): Impacts of ocean acidification on marine organisms: quantifying sensitivities and interaction with warming. *Global Change Biology*, **19**, 1884-96. 10.1111/gcb.12179

Lathlean, J.A., Trassierra, J.A., Everett, J.D. & McQuaid, C.D. (2019): Testing the intermittent upwelling hypothesis: Intercontinental comparisons of barnacle recruitment between South Africa and Australia. *Estuarine, Coastal and Shelf Science*, **224**, 197-208. 10.1016/j.ecss.2019.04.040

Le Quéré, C., Raupach, M.R., Canadell, J.G., Marland, G., Bopp, L., Ciais, P., Conway, T.J., Doney, S.C., Feely, R.A., Foster, P., Friedlingstein, P., Gurney, K., Houghton, R.A., House, J.I.,

Huntingford, C., Levy, P.E., Lomas, M.R., Majkut, J., Metzl, N., Ometto, J.P., Peters, G.P., Prentice, I.C., Randerson, J.T., Running, S.W., Sarmiento, J.L., Schuster, U., Sitch, S., Takahashi, T., Viovy, N., van der Werf, G.R. & Woodward, F.I. (2009): Trends in the sources and sinks of carbon dioxide. *Nature Geoscience*, **2**, 831-836. 10.1038/ngeo689

Leandro, S.M., Tiselius, P., Marques, S.C., Avelelas, F., Correia, C., Sá, P. & Queiroga, H. (2014): Copepod production estimated by combining in situ data and specific temperature-dependent somatic growth models. *Hydrobiologia*, **741**, 139-152. 10.1007/s10750-014-1833-5

Lebour, M.V. (1927): The Food of Plankton Organisms, II. *Journal of the Marine Biological Association of the United Kingdom*, **13**, 70-92.

Lewis, C.N., Brown, K.A., Edwards, L.A., Cooper, G. & Findlay, H.S. (2013): Sensitivity to ocean acidification parallels natural pCO_2 gradients experienced by Arctic copepods under winter sea ice. *Proceedings of the National Academy of Sciences*, **110**, E4960-E4967. 10.1073/pnas.1315162110

Li, G., Cheng, L., Zhu, J., Trenberth, K.E., Mann, M.E. & Abraham, J.P. (2020): Increasing ocean stratification over the past half-century. *Nature Climate Change*, **10**, 1116-1123. 10.1038/s41558-020-00918-2

Lindeman, R.L. (1942): The trophic-dynamic aspect of ecology. *Ecology*, **23**, 399-417. 10.2307/1930126

Lischka, S., Büdenbender, J., Boxhammer, T. & Riebesell, U. (2011): Impact of ocean acidification and elevated temperatures on early juveniles of the polar shelled pteropod *Limacina helicina*: mortality, shell degradation, and shell growth. *Biogeosciences*, **8**, 919-932. 10.5194/bg-8-919-2011

Lischka, S., Bach, L.T., Schulz, K.G. & Riebesell, U. (2017): Ciliate and mesozooplankton community response to increasing CO_2 levels in the Baltic Sea: insights from a large-scale mesocosm experiment. *Biogeosciences*, **14**, 447-466. 10.5194/bg-14-447-2017

Lohbeck, K.T., Riebesell, U. & Reusch, T.B.H. (2012): Adaptive evolution of a key phytoplankton species to ocean acidification. *Nature Geoscience*, **5**, 346. 10.1038/ngeo1441

Lovelock, J.E. & Rapley, C.G. (2007): Ocean pipes could help the Earth to cure itself. *Nature*, **449**, 403-403. 10.1038/449403a

Lueker, T.J., Dickson, A.G. & Keeling, C.D. (2000): Ocean pCO_2 calculated from dissolved inorganic carbon, alkalinity, and equations for K1 and K2: Validation based on laboratory measurements of CO_2 in gas and seawater at equilibrium. *Marine Chemistry*, **70**, 105-119. 10.1016/s0304-4203(00)00022-0

Mackey, M.D., Mackey, D.J., Higgins, H.W. & Wright, S.W. (1996): CHEMTAX - A program for estimating class abundances from chemical markers: Application to HPLC measurements of phytoplankton. *Marine Ecology Progress Series*, **144**, 265-283. 10.3354/meps144265

Malzahn, A.M. & Boersma, M. (2012): Effects of poor food quality on copepod growth are dose dependent and non-reversible. *Oikos*, **121**, 1408-1416. 10.1111/j.1600-0706.2011.20186.x

Malzahn, A.M., Clemmesen, C. & Rosenthal, H. (2003): Temperature effects on growth and nucleic acids in laboratory-reared larval coregonid fish. *Marine Ecology Progress Series*, **259**, 285-293. 10.3354/meps259285

Maneja, R.H., Dineshram, R., Thiyagarajan, V., Skiftesvik, A.B., Frommel, A.Y., Clemmesen, C., Geffen, A.J. & Browman, H.I. (2014): The proteome of Atlantic herring (*Clupea harengus* L.) larvae is resistant to elevated pCO_2. *Marine Pollution Bulletin*, **86**, 154-160. http://dx.doi.org/10.1016/j.marpolbul.2014.07.030

Maneja, R.H., Frommel, A.Y., Browman, H.I., Geffen, A.J., Folkvord, A., Piatkowski, U., Durif, C.M.F., Bjelland, R., Skiftesvik, A.B. & Clemmesen, C. (2015): The swimming kinematics and foraging behavior of larval Atlantic herring (*Clupea harengus* L.) are unaffected by elevated pCO_2. *Journal of Experimental Marine Biology and Ecology*, **466**, 42-48. 10.1016/j.jembe.2015.02.008

Maruyama, S., Yabuki, T., Sato, T., Tsubaki, K., Komiya, A., Watanabe, M., Kawamura, H. & Tsukamoto, K. (2011): Evidences of increasing primary production in the ocean by Stommel's perpetual salt fountain. *Deep Sea Research Part I: Oceanographic Research Papers*, **58**, 567-574. 10.1016/j.dsr.2011.02.012

Masuda, T., Furuya, K., Kohashi, N., Sato, M., Takeda, S., Uchiyama, M., Horimoto, N. & Ishimaru, T. (2010): Lagrangian observation of phytoplankton dynamics at an artificially enriched subsurface water in Sagami Bay, Japan. *Journal of Oceanography*, **66**, 801-813. 10.1007/s10872-010-0065-1

Mauchline, J., Blaxter, J.H.S., Southward, A.J. & Tyler, P.A. (1998): The biology of calanoid copepods. *Advances in Marine Biology* (ed. by J. Mauchline), Vol: 33, pp. 1-710. Academic Press Ltd-Elsevier Science Ltd, London. <Go to ISI>://WOS:000082359200001

McNeil, B.I. & Sasse, T.P. (2016): Future ocean hypercapnia driven by anthropogenic amplification of the natural CO_2 cycle. *Nature*, **529**, 383-395. 10.1038/nature16156

McNeil, B.I., Sweeney, C. & Gibson, J.A.E. (2011): Short Note: Natural seasonal variability of aragonite saturation state within two Antarctic coastal ocean sites. *Antarctic Science*, **23**, 411-412. 10.1017/S0954102011000204

Medellín-Mora, J., Atkinson, A. & Escribano, R. (2019): Community structured production of zooplankton in the eastern boundary upwelling system off central/southern Chile (2003–2012). *ICES Journal of Marine Science*, **77**, 419-435. 10.1093/icesjms/fsz193

Menge, B.A. & Menge, D.N.L. (2013): Dynamics of coastal meta-ecosystems: the intermittent upwelling hypothesis and a test in rocky intertidal regions. *Ecological Monographs*, **83**, 283-310. 10.1890/12-1706.1

Middelburg, J.J. (2014): Stable isotopes dissect aquatic food webs from the top to the bottom. *Biogeosciences*, **11**, 2357-2371. 10.5194/bg-11-2357-2014

Miralto, A., Barone, G., Romano, G., Poulet, S.A., Ianora, A., Russo, G.L., Buttino, I., Mazzarella, G., Laabir, M., Cabrini, M. & Giacobbe, M.G. (1999): The insidious effect of diatoms on copepod reproduction. *Nature*, **402**, 173-176. 10.1038/46023

Molvær, J., Eikrem, W., Magnusson, J., Pedersen, A. & Tjomsland, T. (2007): The OSPAR Comprehensive Procedure for the Norwegian West Coast – Eutrophication Status. In, p. 86,

Moore, C.M., Mills, M.M., Arrigo, K.R., Berman-Frank, I., Bopp, L., Boyd, P.W., Galbraith, E.D., Geider, R.J., Guieu, C., Jaccard, S.L., Jickells, T.D., La Roche, J., Lenton, T.M., Mahowald, N.M., Marañón, E., Marinov, I., Moore, J.K., Nakatsuka, T., Oschlies, A., Saito, M.A., Thingstad, T.F., Tsuda, A. & Ulloa, O. (2013): Processes and patterns of oceanic nutrient limitation. *Nature Geoscience*, **6**, 701-710. 10.1038/ngeo1765

Murphy, J. & Riley, J.P. (1962): A modified single solution method for the determination of phosphate in natural waters. *Analytica Chimica Acta*, **27**, 31-36. 10.1016/S0003-2670(00)88444-5

Niehoff, B., Schmithüsen, T., Knüppel, N., Daase, M., Czerny, J. & Boxhammer, T. (2013): Mesozooplankton community development at elevated CO_2 concentrations: results from a mesocosm experiment in an Arctic fjord. *Biogeosciences*, **10**, 1391-1406. 10.5194/bg-10-1391-2013

Nielsen, L.T., Jakobsen, H.H. & Hansen, P.J. (2010): High resilience of two coastal plankton communities to twenty-first century seawater acidification: Evidence from microcosm studies. *Marine Biology Research*, **6**, 542-555. 10.1080/17451000903476941

Oeberst, R., Dickey-Collas, M. & Nash, R.D.M. (2009): Mean daily growth of herring larvae in relation to temperature over a range of 5–20°C, based on weekly repeated cruises in the Greifswalder Bodden. *ICES Journal of Marine Science*, **66**, 1696-1701. 10.1093/icesjms/fsp193

Oksanen, J., Blanchet, F.G., Friendly, M., Kindt, R., Legendre, P., McGlinn, D., Minchin, P.R., O'Hara, R.B., Simpson, G.L., Solymos, P., Stevens, M.H.H., Szoecs, E. & Wagner, H. (2019): *Vegan: Community Ecology Package*.

Oksanen, L., Fretwell, S.D., Arruda, J. & Niemela, P. (1981): Exploitation Ecosystems in Gradients of Primary Productivity. *The American Naturalist*, **118**, 240-261. 10.1086/283817

Olson, R.J., Zettler, E.R. & Anderson, O.K. (1989): Discrimination of eukaryotic phytoplankton cell types from light scatter and autofluorescence properties measured by flow cytometry. *Cytometry*, **10**, 636-643. 10.1002/cyto.990100520

Orr, J.C., Fabry, V.J., Aumont, O., Bopp, L., Doney, S.C., Feely, R.A., Gnanadesikan, A., Gruber, N., Ishida, A., Joos, F., Key, R.M., Lindsay, K., Maier-Reimer, E., Matear, R., Monfray, P., Mouchet, A., Najjar, R.G., Plattner, G.-K., Rodgers, K.B., Sabine, C.L., Sarmiento, J.L.,

Schlitzer, R., Slater, R.D., Totterdell, I.J., Weirig, M.-F., Yamanaka, Y. & Yool, A. (2005): Anthropogenic ocean acidification over the twenty-first century and its impact on calcifying organisms. *Nature*, **437**, 681-686. 10.1038/nature04095

Oschlies, A., Pahlow, M., Yool, A. & Matear, R.J. (2010): Climate engineering by artificial ocean upwelling: Channelling the sorcerer's apprentice. *Geophysical Research Letters*, **37**. 10.1029/2009GL041961

Otero, J., Álvarez-Salgado, X.A. & Bode, A. (2020): Phytoplankton Diversity Effect on Ecosystem Functioning in a Coastal Upwelling System. *Frontiers in Marine Science*, **7**. 10.3389/fmars.2020.592255

Pagès, F., Gonzàlez, H.E. & Gonzàles, S.R. (1996): Diet of the gelatinous zooplankton in Hardangerfjord (Norway) and potential predatory impact by *Aglantha digitale* (Trachymedusae). *Marine Ecology Progress Series*, **139**, 69-77. https://www.jstor.org/stable/24857095

Pan, Y., Li, Y., Fan, W., Zhang, D., Qiang, Y., Jiang, Z.-P. & Chen, Y. (2019): A Sea Trial of Air-Lift Concept Artificial Upwelling in the East China Sea. *Journal of Atmospheric and Oceanic Technology*, **36**, 2191-2204. 10.1175/jtech-d-18-0238.1

Pan, Y., Fan, W., Zhang, D., Chen, J., Huang, H., Liu, S., Jiang, Z., Di, Y., Tong, M. & Chen, Y. (2016): Research progress in artificial upwelling and its potential environmental effects. *Science China Earth Sciences*, **59**, 236-248. 10.1007/s11430-015-5195-2

Paul, A.J., Bach, L.T., Schulz, K.G., Boxhammer, T., Czerny, J., Achterberg, E.P., Hellemann, D., Trense, Y., Nausch, M., Sswat, M. & Riebesell, U. (2015): Effect of elevated CO_2 on organic matter pools and fluxes in a summer Baltic Sea plankton community. *Biogeosciences*, **12**, 6181-6203. 10.5194/bg-12-6181-2015

Pauly, D. & Christensen, V. (1995): Primary production required to sustain global fisheries. *Nature*, **374**, 255. 10.1038/374255a0

Peck, M.A., Kanstinger, P., Holste, L. & Martin, M. (2012): Thermal windows supporting survival of the earliest life stages of Baltic herring (*Clupea harengus*). *ICES Journal of Marine Science*, **69**, 529-536. 10.1093/icesjms/fss038

Pedersen, S.A., Vage, V.T., Olsen, A.J., Hammer, K.M. & Altin, D. (2014a): Effects of elevated carbon dioxide (CO_2) concentrations on early developmental stages of the marine copepod *Calanus finmarchicus* Gunnerus (Copepoda: Calanoidae). *Journal of Toxicology and Environmental Health, Part A*, **77**, 535-49. 10.1080/15287394.2014.887421

Pedersen, S.A., Håkedal, O.J., Salaberria, I., Tagliati, A., Gustavson, L.M., Jenssen, B.M., Olsen, A.J. & Altin, D. (2014b): Multigenerational Exposure to Ocean Acidification during Food Limitation Reveals Consequences for Copepod Scope for Growth and Vital Rates. *Environmental Science & Technology*, **48**, 12275-12284. 10.1021/es501581j

Peterson, W.T., Tiselius, P. & Kiørboe, T. (1991): Copepod egg production, moulting and growth rates, and secondary production, in the Skagerrak in August 1988. *Journal of Plankton Research*, **13**, 131-154. 10.1093/plankt/13.1.131

Pimentel, M.S., Faleiro, F., Dionisio, G., Repolho, T., Pousao-Ferreira, P., Machado, J. & Rosa, R. (2014): Defective skeletogenesis and oversized otoliths in fish early stages in a changing ocean. *J Exp Biol*, **217**, 2062-70. 10.1242/jeb.092635

Platt, T., Gallegos, C.L. & Harrison, W.G. (1980): Photoinhibition of photosynthesis in natural assemblages of marine phytoplankton. *Journal of Marine Research*, **38**, 687-701.

Polovina, J.J., Howell, E.A. & Abecassis, M. (2008): Ocean's least productive waters are expanding. *Geophysical Research Letters*, **35**. 10.1029/2007GL031745

Poore, A.G.B., Graba-Landry, A., Favret, M., Sheppard Brennand, H., Byrne, M. & Dworjanyn, S.A. (2013): Direct and indirect effects of ocean acidification and warming on a marine plant–herbivore interaction. *Oecologia*, **173**, 1113-1124. 10.1007/s00442-013-2683-y

Pörtner, H.-O., Karl, D.M., Boyd, P.W., Cheung, W.W.L., Lluch-Cota, S.E., Nojiri, Y., Schmidt, D.N. & Zavialov, P.O. (2014): Ocean Systems. *Climate Change 2014: Impacts, Adaption, and Vulnerability. Part A: Global and Sectoral Aspects. Contribution of Working Group II to the Fifth Assessment Report of the Intergovernmental Panel on Climate Change* (ed. by C.B. Field, V.R. Barros, D.J. Dokken, K.J. Mach, M.D. Mastrandrea, T.E. Bilir, M. Chatterjee, K.L. Ebi, Y.O. Estrada, R.C. Genova, B. Girma, E.S. Kissel, A.N. Levy, S. Maccracken, P.R. Mastrandrea and L.L. White), Vol: pp. 411-484. Cambridge University Press, Cambridge, United Kingdom, and New York, NY, USA.

Pörtner, H.O., Langenbuch, M. & Michaelidis, B. (2005): Synergistic effects of temperature extremes, hypoxia, and increases in CO_2 on marine animals: From Earth history to global change. *Journal of Geophysical Research: Oceans*, **110**. 10.1029/2004JC002561

Post, D.M. (2002): Using Stable Isotopes To Estimate Trophic Position: Models, Methods, and Assumptions. *Ecology*, **83**, 703-718. 10.1890/0012-9658(2002)083[0703:USITET]2.0.CO;2

Purcell, J.E. (1997): Pelagic cnidarians and ctenophores as predators: Selective predation, feeding rates and effects on prey populations. *Annales de l'Institute Oceanographieque*, **73**, 125-137.

Purcell, J.E. (2005): Climate effects on formation of jellyfish and ctenophore blooms: a review. *Journal of the Marine Biological Association of the UK*, **85**, 461-476. 10.1017/s0025315405011409

Purcell, J.E. (2012): Jellyfish and Ctenophore Blooms Coincide with Human Proliferations and Environmental Perturbations. *Annual Review of Marine Science*, **4**, 209-235. 10.1146/annurev-marine-120709-142751

Purcell, J.E. & Mills, C.E. (1988): The correlation of nematocyst types to diets in pelagic Hydrozoa. *The biology of nematocysts* (ed. by D. Hessinger and H. Lenhoff), Vol: pp. 463-485. Academic Press, San Diego.

Purcell, J.E. & Arai, M.N. (2001): Interactions of pelagic cnidarians and ctenophores with fish: a review. 27-44. 10.1007/978-94-010-0722-1_4

Purcell, J.E., Uye, S. & Lo, W. (2007): Anthropogenic causes of jellyfish blooms and their direct consequences for humans: a review. *Marine Ecology Progress Series*, **350**, 153-174. 10.3354/meps07093

R Core, T. (2019): *R: A language and environment for statistical computing*. R Foundation for Statistical Computing.

Raven, J., Caldeira, K., Elderfield, H., Hoegh-Guldberg, O., Liss, P., Riebesell, U., Shepherd, J., Turley, C. & Watson, A. (2005): Ocean acidification due to increasing atmospheric carbon dioxide. In, T.R. Society,

Redfield, A.C., Ketchum, B.H. & Richards, F.A. (1963): The influence of organisms on the composition of sea water. *The sea* (ed. by M.N. Hill), Vol: pp. 26-77. Interscience.

Reid, R.N., Cargnelli, L.M., Griesbach, S.J., Packer, D.B., Johnson, D.L., Zetlin, C.A., Morse, W.W. & Berrien, P.L. (1999): Atlantic herring, Clupea harengus, life history and habitat characteristics. *NOAA Technical Memorandum NMFS-NE*, **126**, 48.

Richardson, A.J. (2008): In hot water: zooplankton and climate change. *ICES Journal of Marine Science*, **65**, 279-295. 10.1093/icesjms/fsn028

Richardson, A.J. & Gibbons, M.J. (2008): Are jellyfish increasing in response to ocean acidification? *Limnology and Oceanography*, **53**, 2040-2045.

Riebesell, U., Gattuso, J.P., Thingstad, T.F. & Middelburg, J.J. (2013a): Preface "Arctic ocean acidification: pelagic ecosystem and biogeochemical responses during a mesocosm study". *Biogeosciences*, **10**, 5619-5626. 10.5194/bg-10-5619-2013

Riebesell, U., Bach, L.T., Bellerby, R.G.J., Monsalve, J.R.B., Boxhammer, T., Czerny, J., Larsen, A., Ludwig, A. & Schulz, K.G. (2017): Competitive fitness of a predominant pelagic calcifier impaired by ocean acidification. *Nature Geoscience*, **10**, 19-23. 10.1038/ngeo2854

Riebesell, U., Czerny, J., von Bröckel, K., Boxhammer, T., Büdenbender, J., Deckelnick, M., Fischer, M., Hoffmann, D., Krug, S.A., Lentz, U., Ludwig, A., Muche, R. & Schulz, K.G. (2013b): Technical Note: A mobile sea-going mesocosm system – new opportunities for ocean change research. *Biogeosciences*, **10**, 1835-1847. 10.5194/bg-10-1835-2013

Ritchie, H. & Roser, M. (2020): CO_2 and Greenhouse Gas Emissions. *Our World in Data*. https://ourworldindata.org/co2-and-other-greenhouse-gas-emissions

Roberts, J.M. (2015): The response of reef framework-forming cold-water corals to ocean acidification. *Sailing through Changing Oceans: Ocean and Polar Life and Environmental Sciences on a Warming Planet* (ed. by J.-P. Henriet, L. De Santis, E. Ramirez-Llodra, P. Campus and R. Azzolini), Vol. European Science Foundation.

Rogelj, J., den Elzen, M., Höhne, N., Fransen, T., Fekete, H., Winkler, H., Schaeffer, R., Sha, F., Riahi, K. & Meinshausen, M. (2016): Paris Agreement climate proposals need a boost to keep warming well below 2 °C. *Nature*, **534**, 631-639. 10.1038/nature18307

Rossoll, D., Sommer, U. & Winder, M. (2013): Community interactions dampen acidification effects in a coastal plankton system. *Marine Ecology Progress Series*, **486**, 37-46. 10.3354/meps10352

Rossoll, D., Bermúdez, R., Hauss, H., Schulz, K.G., Riebesell, U., Sommer, U. & Winder, M. (2012): Ocean Acidification-Induced Food Quality Deterioration Constrains Trophic Transfer. *PLoS ONE*, **7**, e34737. 10.1371/journal.pone.0034737

RStudio, T. (2016): *RStudio: Integrated Development for R*. RStudio, Inc.

Runge, J.A. & Lafontaine, Y.d. (1996): Characterization of the pelagic ecosystem in surface waters of the northern Gulf of St, Lawrence in early summer: the larval redfish-Calanus-microplankton interaction. *Fisheries Oceanography*, **5**, 21-37. 10.1111/j.1365-2419.1996.tb00014.x

Russo, E., Ianora, A. & Carotenuto, Y. (2018): Re-shaping marine plankton communities: effects of diatom oxylipins on copepods and beyond. *Marine Biology*, **166**, 9. 10.1007/s00227-018-3456-2

Sabatini, M. & Kiørboe, T. (1994): Egg production, growth and development of the cyclopoid copepod *Oithona similis*. *Journal of Plankton Research*, **16**, 1329-1351. 10.1093/plankt/16.10.1329

Sakka Hlaili, A., Chikhaoui, M.A., El Grami, B. & Hadj Mabrouk, H. (2006): Effects of N and P supply on phytoplankton in Bizerte Lagoon (western Mediterranean). *Journal of Experimental Marine Biology and Ecology*, **333**, 79-96. 10.1016/j.jembe.2005.12.049

Sala, M.M., Aparicio, F.L., Balagué, V., Boras, J.A., Borrull, E., Cardelús, C., Cros, L., Gomes, A., López-Sanz, A., Malits, A., Martínez, R.A., Mestre, M., Movilla, J., Sarmento, H., Vázquez-Domínguez, E., Vaqué, D., Pinhassi, J., Calbet, A., Calvo, E., Gasol, J.M., Pelejero, C. & Marrasé, C. (2016): Contrasting effects of ocean acidification on the microbial food web under different trophic conditions. *ICES Journal of Marine Science: Journal du Conseil*, **73**, 670-679. 10.1093/icesjms/fsv130

Sarthou, G., Timmermans, K.R., Blain, S. & Tréguer, P. (2005): Growth physiology and fate of diatoms in the ocean: a review. *Journal of Sea Research*, **53**, 25-42. 10.1016/j.seares.2004.01.007

Sastri, A.R. & Roff, J.C. (2000): Rate of chitobiase degradation as a measure of development rate in planktonic Crustacea. *Canadian Journal of Fisheries and Aquatic Sciences*, **57**, 1965-1968. 10.1139/f00-174

Schlüter, L., Lohbeck, K.T., Gröger, J.P., Riebesell, U. & Reusch, T.B.H. (2016): Long-term dynamics of adaptive evolution in a globally important phytoplankton species to ocean acidification. *Science Advances*, **2**. 10.1126/sciadv.1501660

Schneider, B., Schlitzer, R., Fischer, G. & NöThig, E.-M. (2003): Depth-dependent elemental compositions of particulate organic matter (POM) in the ocean. *Global Biogeochemical Cycles*, **17**. 10.1029/2002GB001871

Schulz, K.G. & Riebesell, U. (2013): Diurnal changes in seawater carbonate chemistry speciation at increasing atmospheric carbon dioxide. *Marine Biology*, **160**, 1889-1899. 10.1007/s00227-012-1965-y

Schulz, M., Koschel, R., Reese, C. & Mehner, T. (2004): Pelagic trophic transfer efficiency in an oligotrophic, dimictic deep lake (Lake Stechlin, Germany) and its relation to fisheries yield. *Limnologica*, **34**, 264-273. 10.1016/S0075-9511(04)80050-1

Sekiguchi, H., McLaren, I.A. & Corkett, C.J. (1980): Relationship between growth rate and egg production in the copepod Acartia clausi hudsonica. *Marine Biology*, **58**, 133-138. 10.1007/BF00396124

Sellers, A.J., Leung, B. & Torchin, M.E. (2020): Global meta-analysis of how marine upwelling affects herbivory. *Global Ecology and Biogeography*, **29**, 370-383. 10.1111/geb.13023

Sharp, J.H. (1974): Improved analysis for "particulate" organic carbon and nitrogen from seawater. *Limnology and Oceanography*, **19**, 984-989. 10.4319/lo.1974.19.6.0984

Sigman, D.M. & Hain, M.P. (2012): The Biological Productivity of the Ocean. *Nature Education*, **3**, 1-16.

Skajaa, K., Fernö, A. & Folkvord, A. (2004): Ontogenetic- and condition-related effects of starvation on responsiveness in herring larvae (*Clupea harengus* L.) during repeated attacks by a model predator. *Journal of Experimental Marine Biology and Ecology*, **312**, 253-269. 10.1016/j.jembe.2004.06.012

Smith, P., Adams, J., Beerling, D.J., Beringer, T., Calvin, K.V., Fuss, S., Griscom, B., Hagemann, N., Kammann, C., Kraxner, F., Minx, J.C., Popp, A., Renforth, P., Vicente Vicente, J.L. & Keesstra, S. (2019): Land-Management Options for Greenhouse Gas Removal and Their Impacts on Ecosystem Services and the Sustainable Development Goals. *Annual Review of Environment and Resources*, **44**, 255-286. 10.1146/annurev-environ-101718-033129

Søreide, J.E., Falk-Petersen, S., Hegseth, E.N., Hop, H., Carroll, M.L., Hobson, K.A. & Blachowiak-Samolyk, K. (2008): Seasonal feeding strategies of Calanus in the high-Arctic Svalbard region. *Deep Sea Research Part II: Topical Studies in Oceanography*, **55**, 2225-2244. 10.1016/j.dsr2.2008.05.024

Spisla, C., Taucher, J., Bach, L.T., Haunost, M., Boxhammer, T., King, A.L., Jenkins, B.D., Wallace, J.R., Ludwig, A., Meyer, J., Stange, P., Minutolo, F., Lohbeck, K.T., Nauendorf, A., Kalter, V., Lischka, S., Sswat, M., Dörner, I., Ismar-Rebitz, S.M.H., Aberle, N., Yong, J.C.,

Bouquet, J.-M., Lechtenbörger, A.K., Kohnert, P., Krudewig, M. & Riebesell, U. (2021): Extreme Levels of Ocean Acidification Restructure the Plankton Community and Biogeochemistry of a Temperate Coastal Ecosystem: A Mesocosm Study. *Frontiers in Marine Science*, **7**. 10.3389/fmars.2020.611157

Sswat, M., Stiasny, M.H., Jutfelt, F., Riebesell, U. & Clemmesen, C. (2018): Growth performance and survival of larval Atlantic herring, under the combined effects of elevated temperatures and CO_2. *PLoS One*, **13**, e0191947. 10.1371/journal.pone.0191947

Stange, P., Taucher, J., Bach, L.T., Alguero-Muniz, M., Horn, H.G., Krebs, L., Boxhammer, T., Nauendorf, A.K. & Riebesell, U. (2018): Ocean Acidification-Induced Restructuring of the Plankton Food Web Can Influence the Degradation of Sinking Particles. *Frontiers in Marine Science*, **5**, 13. 10.3389/fmars.2018.00140

Stiasny, M.H., Mittermayer, F.H., Sswat, M., Voss, R., Jutfelt, F., Chierici, M., Puvanendran, V., Mortensen, A., Reusch, T.B. & Clemmesen, C. (2016): Ocean Acidification Effects on Atlantic Cod Larval Survival and Recruitment to the Fished Population. *PLoS One*, **11**, e0155448. 10.1371/journal.pone.0155448

Støttrup, J.G. (2003): Production and Nutritional Value of Copepods. *Live Feeds in Marine Aquaculture*, Vol: pp. 145-205. 10.1002/9780470995143.ch5

Stramma, L., Johnson, G.C., Sprintall, J. & Mohrholz, V. (2008): Expanding Oxygen-Minimum Zones in the Tropical Oceans. *Science*, **320**, 655-658. 10.1126/science.1153847

Strickland, J.D.H. & Parsons, T.R. (1972): *A Practical Handbook of Seawater Analysis*, 2 edn. Fisheries Research Board of Canada, Ottawa, Canada.

Sunday, J.M., Fabricius, K.E., Kroeker, K.J., Anderson, K.M., Brown, N.E., Barry, J.P., Connell, S.D., Dupont, S., Gaylord, B., Hall-Spencer, J.M., Klinger, T., Milazzo, M., Munday, P.L., Russell, B.D., Sanford, E., Thiyagarajan, V., Vaughan, M.L.H., Widdicombe, S. & Harley, C.D.G. (2017): Ocean acidification can mediate biodiversity shifts by changing biogenic habitat. *Nature Climate Change*, **7**, 81-85. 10.1038/nclimate3161

Sydeman, W.J., Garcia-Reyes, M., Schoeman, D.S., Rykaczewski, R.R., Thompson, S.A., Black, B.A. & Bograd, S.J. (2014): Climate change and wind intensification in coastal upwelling ecosystems. *Science*, **345**, 77-80. 10.1126/science.1251635

Syuhei, B., Carolyn, B., Jacques, C., Yannick, C., Epaminondas, C., Ruben, E., Serena Fonda, U., Stephane, G., Francisco Guerrero, R., Monica, H., Adrianna, I., Hyung-Ku, K., Mohamed, L., Arnaud, L., Antonio, M., Xiuren, N., Serge Poulet, V.R., Jeffrey, R., Junxian, S., Michel, S., Shin-ichi, U. & Yijun, W. (1997): The paradox of diatom-copepod interactions. *Marine Ecology Progress Series*, **157**, 287-293. https://www.jstor.org/stable/24858372

Taucher, J., Boxhammer, T., Bach, L.T., Paul, A.J., Schartau, M., Stange, P. & Riebesell, U. (2020): Changing carbon-to-nitrogen ratios of organic-matter export under ocean acidification. *Nature Climate Change*, **11**, 52-57. 10.1038/s41558-020-00915-5

Taucher, J., Bach, L.T., Boxhammer, T., Nauendorf, A., Consortium, T.G.C.K., Achterberg, E.P., Alguero-Muniz, M., Arístegui, J., Czerny, J., Esposito, M., Guan, W., Haunost, M., Horn, H.G., Ludwig, A., Meyer, J., Spisla, C., Sswat, M., Stange, P. & Riebesell, U. (2017): Influence of Ocean Acidification and Deep Water Upwelling on Oligothrophic Plankton Communities in the subtropical North Atlantic: Insights from an *In situ* Mesocosm Study. *Frontiers in Marine Science*, **4**, 1-18. 10.3389/fmars.2017.00085

Thomsen, J., Gutowska, M.A., Saphörster, J., Heinemann, A., Trübenbach, K., Fietzke, J., Hiebenthal, C., Eisenhauer, A., Körtzinger, A., Wahl, M. & Melzner, F. (2010): Calcifying invertebrates succeed in a naturally CO_2-rich coastal habitat but are threatened by high levels of future acidification. *Biogeosciences*, **7**, 3879-3891. 10.5194/bg-7-3879-2010

Thomson, P.G., Davidson, A.T. & Maher, L. (2016): Increasing CO_2 changes community composition of pico- and nano-sized protists and prokaryotes at a coastal Antarctic site. *Marine Ecology Progress Series*, **554**, 51-69. 10.3354/meps11803

Thor, P. & Oliva, E.O. (2015): Ocean acidification elicits different energetic responses in an Arctic and a boreal population of the copepod *Pseudocalanus acuspes*. *Marine Biology*, **162**, 799-807. 10.1007/s00227-015-2625-9

Tommasi, D., Stock, C.A., Pegion, K., Vecchi, G.A., Methot, R.D., Alexander, M.A. & Checkley Jr., D.M. (2017): Improved management of small pelagic fisheries through seasonal climate prediction. *Ecological Applications*, **27**, 378-388. 10.1002/eap.1458

Troedsson, C., Bouquet, J.-M., Lobon, C.M., Novac, A., Nejstgaard, J.C., Dupont, S., Bosak, S., Jakobsen, H.H., Romanova, N., Pankoke, L.M., Isla, A., Dutz, J., Sazhin, A.F. & Thompson, E.M. (2012): Effects of ocean acidification, temperature and nutrient regimes on the appendicularian *Oikopleura dioica*: a mesocosm study. *Marine Biology*, **160**, 2175-2187. 10.1007/s00227-012-2137-9

Turner, J.T. (2004): The Importance of Small Planktonic Copepods and Their Roles in Pelagic Marine Food Webs. *Zoological Studies*, **43**, 255-266.

Utermöhl, H. (1931): Neue Wege in der quantitativen Erfassung des Planktons (mit besonderer Berücksichtigung des Ultraplanktons). *Mitteilungen Internationale Vereinigung für Theoretische und Angewandte Limnologie*, **5**, 567-596.

Utermöhl, H. (1958): Zur Vervollkommnung der quantitativen Phytoplankton-Methodik. *Mitteilungen Internationale Vereinigung für Theoretische und Angewandte Limnologie*, **9**, 1-38.

Valdés, V., Escribano, R. & Vergara, O. (2017): Scaling copepod grazing in a coastal upwelling system: the importance of community size structure for phytoplankton C flux. *Latin american journal of aquatic research*, **45**, 41-54. http://www.scielo.cl/scielo.php?script=sci_arttext&pid=S0718-560X2017000100005&nrm=iso

Van den Meersche, K., Soetaert, K. & Middelburg, J.J. (2011): Plankton dynamics in an estuarine plume: a mesocosm ^{13}C and ^{15}N tracer study. *Marine Ecology Progress Series*, **429**, 29-43. 10.3354/meps09097

Van der Meeren, T., Jørstad, K.E., Solemdal, P. & Kjesbu, O.S. (1994): Growth and survival of cod larvae (*Gadus morhua* L.): comparative enclosure studies of Northeast Arctic cod and coastal cod from western Norway. 198, *ICES Mar. Sci. Symp*, pp. 633-645.

Van Someren Gréve, H., Almeda, R., Lindegren, M. & Kiørboe, T. (2017): Gender-specific feeding rates in planktonic copepods with different feeding behavior. *Journal of Plankton Research*, **39**, 631-644. 10.1093/plankt/fbx033

Vargas, C.A., Escribano, R. & Poulet, S. (2006): Phytoplankton food quality determines time windows for successful zooplankton reproductive pulses. *Ecology*, **87**, 2992-2999. 10.1890/0012-9658(2006)87[2992:pfqdtw]2.0.co;2

Webber, M.K. & Roff, J.C. (1995): Annual biomass and production of the oceanic copepod community off Discovery Bay, Jamaica. *Marine Biology*, **123**, 481-495. 10.1007/BF00349227

Werner, B. (1993): Stamm Cnidaria, Nesseltiere. *Lehrbuch der speziellen Zoologie* (ed. by A. Kästner), Vol: I/2, pp. 11-305. Fischer, Stuttgart.

Weydmann, A., Søreide, J.E., Kwasniewski, S. & Widdicombe, S. (2012): Influence of CO_2-induced acidification on the reproduction of a key Arctic copepod *Calanus glacialis*. *Journal of Experimental Marine Biology and Ecology*, **428**, 39-42. 10.1016/j.jembe.2012.06.002

Wickham, H., Chang, W., Henry, L., Pedersen, L.T., Takahashi, K., Wilke, C., Woo, K., Yutani, H. & Dunnington, D. (2016): *ggplot2: Elegant Graphics for Data Analysis*. Springer-Verlag New York.

Winans, A.K. & Purcell, J.E. (2010): Effects of pH on asexual reproduction and statolith formation of the scyphozoan, *Aurelia labiata*. *Hydrobiologia*, **645**, 39-52. 10.1007/s10750-010-0224-9

Winder, M., Bouquet, J.-M., Bermúdez, R.J., Berger, S.A., Hansen, T., Brandes, J., Sazhin, A.F., Nejstgaard, J.C., Båmstedt, U., Jakobsen, H.H., Dutz, J., Frischer, M.E., Troedsson, C. & Thompson, E.M. (2017): Increased appendicularian zooplankton alter carbon cycling under warmer more acidified ocean conditions. *Limnology and Oceanography*, **62**, 1541-1551. 10.1002/lno.10516

Wittmann, A.C. & Pörtner, H.-O. (2013): Sensitivities of extant animal taxa to ocean acidification. *Nature Climate Change*, **3**, 995-1001. 10.1038/nclimate1982

Yáñez, S., Hidalgo, P., Ruz, P. & Tang, K.W. (2018): Copepod secondary production in the sea: Errors due to uneven molting and growth patterns and incidence of carcasses. *Progress in Oceanography*, **165**, 257-267. 10.1016/j.pocean.2018.06.008

Zanden, M.J.V. & Rasmussen, J.B. (1999): Primary Consumer $\delta^{13}C$ and $\delta^{15}N$ and the Trophic Position of Aquatic Consumers. *Ecology*, **80**, 1395-1404. 10.1890/0012-9658(1999)080[1395:PCCANA]2.0.CO;2

Zhang, D., Li, S., Wang, G. & Guo, D. (2011): Impacts of CO_2-driven seawater acidification on survival, egg production rate and hatching success of four marine copepods. *Acta Oceanologica Sinica*, **30**, 86-94. 10.1007/s13131-011-0165-9

DANKSAGUNG

Vorrangig möchte ich mich bei Ulf Riebesell bedanken, ohne den ich niemals die Gelegenheit gehabt hätte, diese Arbeit anzufertigen. Dabei möchte ich ihm nicht nur dafür danken, dass ich die wunderbare Möglichkeit hatte all die inspirierenden KOSMOS Studien mitmachen zu dürfen, sondern auch, dass er mich bis zur Fertigstellung dieser Arbeit und darüber hinaus immer unterstützt und beraten hat.

Im Zuge dessen möchte ich mich auch sehr bei allen Post-Docs der AG Riebesell bedanken, die mich auf meinem Weg als Doktorand immer mehr als tatkräftig unterstützt, beraten und angeleitet haben. Dabei gilt mein besonderer Dank Micha, Lennart, Allanah, Judith und vor allem Jan Taucher, ohne den diese Arbeit niemals das geworden wäre, was sie jetzt ist. Aber auch allen nicht namentlich genannten möchte ich ganz herzlich für ihre Unterstützung danken.

Weiterhin möchte ich meinen restlichen Kollegen am GEOMAR danken, dass sie mir bei sämtlichen Angelegenheiten und Fragen immer mit Rat und Tat zur Seite standen und mich über die Jahre an so einem angenehmen Arbeitsklima teilhaben ließen. Hier insbesondere Kerstin Nachtigall, Kai Schulz und Thomas Hansen, die meine unendliche Flut an nicht immer leichten Organismenproben so bravourös analysiert und mich mit ihrem Wissen in vielen Bereichen der Probenanalytik bereichert haben. Außerdem danke ich natürlich meinem lieben Bürokollegen Moritz, für eine wunderbar unbeschwerte und angenehme Arbeitsatmosphäre, sowie unserem Nachbarbüro mit Leila, Nico und Joaquin für die geradezu unendlichen Fluten an Kaffee.

Natürlich bedanke ich mich aber auch ganz herzlich bei allen nationalen und internationalen Studierenden, die mich auf meinem Weg immer wieder begleitet und mich während aller Feldstudien so tatkräftig und mit Begeisterung unterstützt haben. Hier möchte ich insbesondere Dana, Henni, Mirian, Nico und Alba danken, für die unzähligen, langen Arbeitstage und -nächte im Labor und ohne die ich diese unglaubliche Menge an Zooplankton-Daten niemals hätte erheben können.

Auch möchte ich mich bei dem Team KOSMOS Technik/Tauchen bedanken, für ihre Freundschaft, ihre Unterstützung bei jeglichen Probenahmen und die viele Gelegenheiten auch mal aus dem Labor zu kommen. Hierbei danke ich insbesondere Micha K., Pete, Christus, Sidney und Jan H.

Davon abgesehen möchte ich auch allen danken, die ich den letzten Jahren über meine Arbeit kennenlernen durfte und von denen viele mittlerweile zu guten Freunden und einem festen Bestandteil meines Lebens geworden sind. Hierbei vor allen anderen Marie, bei der ich mich ganz besonders für ihre Unterstützung und liebevolle Fürsorge bedanken möchte.

Ein großer Dank auch an Philip, für seine Freundschaft, Unterstützung und Empathie, derer ich mir über die letzten Jahre immer sicher sein konnte.

Zu guter Letzt möchte ich ganz herzlich meiner Familie danken, dafür, dass sie es mir ermöglicht hat, dahin zu kommen wo ich jetzt stehe und mir immer mit Rat und Tat zur Seite gestanden hat.

EIDESSTAATLICHE ERKLÄRUNG

Hiermit versichere ich, dass ich die vorliegende Dissertation mit dem Titel:

„Marine Zooplankton Community Responses to Anthropogenic Influences",

abgesehen von der Beratung durch meinen Betreuer, eigenständig und ohne unerlaubte Hilfe angefertigt habe. Es wurden keine anderen als die von mir angegebenen Quellen und Hilfsmittel verwendet.

Die Dissertation ist unter Einhaltung der Regeln guter wissenschaftliche Praxis der Deutschen Forschungsgemeinschaft entstanden und wurde weder ganz noch zum Teil an anderer Stelle im Rahmen eines Prüfungsverfahrens vorgelegt oder veröffentlicht. Veröffentlichte oder zur Veröffentlichung eingereichte Manuskripte wurden kenntlich gemacht.

Ich erkläre mich einverstanden, dass diese Arbeit an die Bibliothek des GEOMAR Helmholtz-Zentrum für Ozeanforschung Kiel und die Universitätsbibliothek der Christian-Albrechts-Universität zu Kiel weitergeleitet wird.

Kiel, den 21.12.2021

(Carsten Spisla)